Integral Projection Models and analysis of patch dynamics of the reef building coral *Monstastraea annularis*.

Submitted by

Heather Rachel Burgess

to the University of Exeter as a thesis for the degree of Doctor of Philosophy in

Mathematics, December 2011.

This thesis is available for Library use on the understanding that it is copyright material and that no quotation from the thesis may be published without proper acknowledgement.

I certify that all material in this thesis which is not my own work has been identified and that no material has previously been submitted and approved for the award of a degree by this or any other University.

. . . .

Heather Rachel Burgess

Abstract

Over the past 40 years, coral cover has reduced by as much as 80%. At the same time, Coral Reefs are coming under increasing threat from hurricanes, as climate change is expected to increase the intensity of hurricanes. Therefore, it has become increasingly important to understand the effect of hurricanes on a coral population.

This Thesis focuses on the reef-building coral *Montastraea annularis*. This species once dominated Caribbean Coral Reefs, but is fast being replaced by faster growing more opportunistic species. It is important that the underlying dynamics of the decline is understood, if managers stand any chance of reversing this decline.

The aim of this Thesis is to investigate the effect of hurricane activity on the dynamics of the reef-building coral *Montastraea annularis*. To achieve this the Integral Projection Model (IPM) method was adopted and the results compared to those produced using the more traditional method of Population Projection Matrix (PPM) method.

The models were fitted using census data from June 1998 to January 2003, which described the area of individual coral patches on a sample of ramets on Glovers Reef, Belize. Glovers Reef is a marine reserve that lies 30km off the coast of Belize and 15km east of the main barrier reef. Three hurricanes struck Glovers Reef during the study: Hurricane Mitch (October 1998), Hurricane Keith (September 2000) and Hurricane Iris (October 2001).

The data have been divided by two different methods in order to test two research questions, firstly if the initial trauma following a hurricane affects the long term dynamics of a population and, secondly, if the dynamics exhibited during a hurricane varied with hurricane strength.

In this Thesis five main results are shown:

1. All models for all divisions of data are in long term decline.

2. As initial trauma increased, the long term growth rates decreased, conversely the short term extremes increased.

3. Fragmentation is more likely as patch size increased and more likely under stronger hurricanes.

4. Integral Projection Modelling painted a similar picture to Population Projection Matrix models and should be a preferred method of analysis.

5. Interaction of the IPMs can be used to model the changing occurrence of hurricanes under climate change. It is shown that with increased intensity, the population could become extinct 6.3 years sooner.

This research is the first step in modelling coral patch populations by the IPM method. It suggests possible functional forms and compares the results with the PPM method. Further research is required into the biological functions which drive fragmentation, the method by which large patches divide into groups of smaller patches. The conclusions from this Thesis add to the growing body of knowledge concerning the response of coral species to hurricanes, focusing on the importance of understanding patch dynamics, in order to understand colonial dynamics.

Acknowledgements

'I can do all this through him who gives me strength' Philippians 4:13.

I would like to thank my Supervisors Prof. Stuart Townley and Prof. Peter Cox for their support and input into my PhD.

I would like to thank my parents, Keith and Jackie Burgess and my brother, Rob Burgess. Without their constant support and encouragement I would not have got this far. Thank you.

Finally I would like to thank my friends. To the 301 guys (Alex, Kieran, Paul, James, Dan and Maria), thanks for the fun times in the office and the Thursday night drinks down at the Rusty Bike, its been good! To Anne Zschiegner, Sam Connor, Hannah Raines, Sarah and Luke Hanney, Ali Barker, Beckie Coyle and Hugh and Kate Ledger, at different times over the last four years you have picked me up after bad days and celebrated with me on the good. Thank you. Finally to Charlotte Davies and Charlotte Hewlett for your constant prayer and support over the last eight years. I could not have done this without you.

Contents

II   Should Population Projection Matrices or Integral Projection Models be used to model *Montastraea annularis*? 105

List of Figures

List of Tables

Part I

Introduction and Mathematical Background

Chapter 1

Introduction

1.1 Research Background

1.1.1 Coral Reefs

Coral Reefs are diverse and complex ecosystems (Knowlton, 2001) that occupy under 1% of the world's oceans (VanOppen and Gates, 2006). They are formed through the excretion of calcium carbonate from reef-building corals, which provides the structure that other species can live off of (Spalding et al., 2001).

To exist coral reefs require a sea surface temperature of between 18 and 36^oC, with an optimum range of 26 to 28^oC (Hubbard, 1997). This means that most coral reefs are located between the Tropics of Cancer and Capricorn (Sheppard et al., 2009) (see Figure 1.1). Most coral reefs are located on the eastern shores of continents, due to the upwelling of cold water on the western sides of continents (Glynn and D'Croz, 1990).

It is estimated that for every square kilometre of a coral reef the economic value is between $100,000$ and $600,000$ every year (UNEP-WCMC, 2006). This comes from the value of commercial fisheries, tourism and other benefits from the reefs. The value of tourism to the reefs can make up over $\frac{1}{3}$ of the foreign earnings of small countries like the Seychelles and the Maldives (Sheppard et al., 2009). In the USA it was estimated that commercial fisheries contribute $100 million dollars per year to the American economy, whilst tourism in the Florida Keys from the
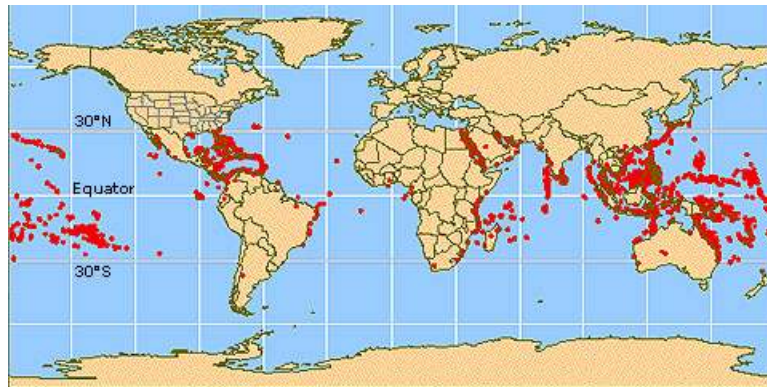
Figure 1.1: The global locations of coral reefs, where a red dot indicates a coral reef. Source: NOAA

visitors to the reefs is estimated to be $1.2 billion per year (NOAA, 2011). As well as this obvious economic contribution, reefs also provide a vital source of food to millions of people (Birkeland, 1997). A coral reef may provide natural breakwaters to coastal communities from storms such as hurricanes.

Between 1 and 9 million species live in association with coral reefs, making coral reefs as diverse as terrestrial rainforests (Knowlton, 2001). This means that coral reefs contribute substantially to global diversity (Sheppard et al., 2009), despite only occupying 1% of the worlds oceans (VanOppen and Gates, 2006). However much of this diversity does not come from the corals themselves but instead from the species that are living in association with them (Knowlton, 2001).

1.1.2 *Montastraea annularis*

Montastraea annularis is a reef-building coral, which once dominated the Caribbean reefs (Jackson, 2001). This species has been in decline, being replaced by faster growing opportunistic species (Jackson, 2001). This decline is significant as reef-building species are more resistant to hurricanes, but reef-building corals have low recruitment and low growth rates (Hughes, 1994). As a reef-building coral *Montastraea annularis* has contributed to the reef-framework over the past 20 million years (Szmant, 1991).

A **colony** of *M. annularis* is made up of columnar structures known as **ramets**

Figure 1.2: A colony of *Montastraea annularis*, circled is an individual ramet. Source: Nicola Foster.

(Graus and Macintyre, 1982) (Figure 1.2). These ramets vary in size and range from 2 to $763cm^2$ in this data set, with the mean size of $37.7cm^2$. Live tissue is restricted to the upper surface of these ramets, known as **coral patches**. On the upper surface coral patches compete with algal patches for both space and light (Nugues and Bak, 2006).

1.1.3 Hurricanes

Hurricanes are intense tropical storms, where strong winds rotate around an inner 'eye'. If wind speeds exceed $33ms^{-1}$ then the tropical storm is classified as a hurricane (Eichler, 1996). Hurricanes are classified according to the Saffir-Simpson scale by the maximum wind strength. This ranges from a Category 1 hurricane for wind speeds between 33 and $42ms^{-1}$, to a Category 5 hurricane for wind speeds greater than $70ms^{-1}$. Hurricanes can last for between 7 and 10 days (Lugo et al., 2000) and can move between 16 and 24 km per hour (Barry and Chorley, 2003).

Each year there are around 80 tropical storms of which 10 are found in the North Atlantic basin (Lugo et al., 2000). Of these 10 on average 6 develop into hurricanes (Lugo et al., 2000). Over 80% of hurricanes in the Caribbean occur

Figure 1.3: The location of Glovers Reef (Wildlife Conservation Society, 2011).

between August and October.

Hurricanes form where there are sustained sea surface temperatures of over 26^oC (Lugo et al., 2000). This means that hurricanes form near the equator, and recurl poleward (Lugo et al., 2000). This means that the location of hurricanes and coral reefs directly intersect.

1.1.4 Data Set

Glovers Reef is one of seven marine reserves on the Belize Barrier Reef. Glovers Reef lies 30km off the coast of Belize and 15km east of the main Barrier Reef (Figure 1.3). The Belize Barrier Reef extends from Mexico in the North to Guatemala in the South (United Nations Educational and Organisation, 2011) and it is dominated by the coral *Montastraea annularis*.

Between June 1998 and January 2003, three hurricanes passed close to Glovers Reef. Namely Hurricanes Mitch, Keith and Iris. Hurricane Mitch which occurred in October 1998, was the strongest as a Category 5 hurricane which left 2.7 million people homeless and a death toll of 19,325. Hurricanes Keith and Iris were Categories 3 and 4 respectively which occurred in September 2000 and October 2001.

Time Step	Date
1	June 1998
2	October 1998
3	December 1998
4	June 1999
5	June 2000
6	May 2001
7	May 2002
8	January 2003

Table 1.1: The dates at which the colonies were monitored on Glovers Reef.

An alternative measure of hurricanes is the Hurricane Index (HI) (Allison et al., 2003). This is a measure of the maximum wind speed alongside the distance that it passes from a given location, in this case Glovers Reef, where W is the mean wind speed and d the distance from Glovers Reef then the HI is calculated as:

$$HI = \sum \frac{W^2}{\ln(d)}. \tag{1.1}$$

The measures for Glovers Reef were given in Mumby et al. (2005) for the total hurricane activity for each year of the study. This resulted in a HI for Hurricane Mitch of 2781, Keith of 2678 and Iris of 1557. In comparison in 1999 the HI was 69 and for both 2002 and 2003 of 0.

The data set was collected by the Marine Spatial Ecology Lab at the University of Exeter in particular Prof. Peter Mumby and Dr. Nicola Foster. They monitored two sites at Glovers Reef, Long Cay and Middle Cay, where 20 colonies were selected at random and they monitored growth, fragmentation and extinction of patches on existing, upright colonies of *M. annularis*. They were sampled at 8 non-uniformly spaced times over a 4.5 year period (Table 1.1). At each time step the colonies were videoed and analysed to determine the live area of coral and algal patches (see Mumby et al. (2005)). In this Thesis, 262 ramets were randomly selected from a total of 30 colonies, whilst the majority came from 3 colonies this did not significantly alter the results.

1.2   Aims and Objectives of Thesis

The aim of this Thesis is to investigate the effect of hurricane activity on the dynamics of the reef-building coral *Montastraea annularis*. In order to achieve this, three research objectives were determined. Firstly, to develop the modelling techniques which are used to model coral populations and apply these to the given data set. Secondly to analyse these models in order to investigate two questions:

1. If the initial trauma following a hurricane determines the long-term dynamics of a coral patch population.

2. If the dynamics exhibited during a hurricane varied with strength.

The final objective aimed at investigating the impact of climate change on the projection models, in particular investigating the impact of changing hurricane activity due to climate change. These three objectives were selected as they investigated both the modelling techniques as well as the future behaviour that could be exhibited on the reef. Each objective is further broken down into a total of ten research questions which will be answered in this Thesis (see Figure 1.4).
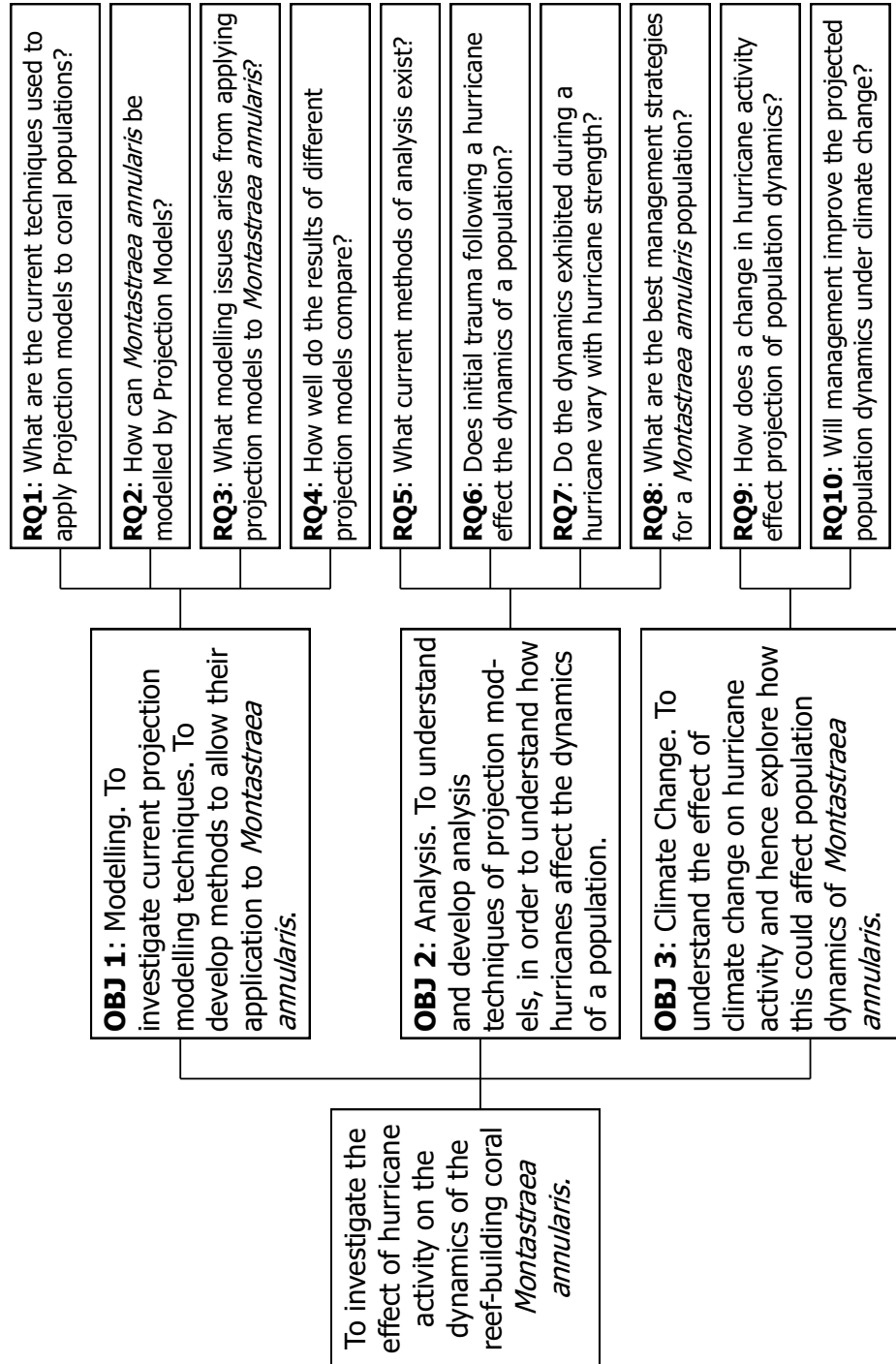
Figure 1.4: The research aims, objectives and research questions investigated in this Thesis.

Research Question	Chapters answering the question
RQ1: What are the current techniques used to apply projection models to coral populations	2, 3, 4 and 7
RQ2: How can *Montastraea annularis* be modelled by projection models?	2, 3, 4, 5 and 7
RQ3: What modelling issues arise from applying projection models to *Montastraea annularis*	2, 3, 4, 5, 6 and 7
RQ4: How well do the results of different projection models compare?	3, 5 and 6
RQ5: What current methods of analysis exist?	3
RQ6: Does initial trauma following a hurricane effect the dynamics of a population?	4, 5 and 6
RQ7: Do the dynamics exhibited during a hurricane vary with hurricane strength?	7 and 10
RQ8: What are the best management strategies for a *Montastraea annularis* population	8 and 10
RQ9: How does a change in hurricane activity effect projection of population dynamics?	9 and 10
RQ10: Will management improve the projected population dynamics under climate change?	9 and 10

Table 1.2: A summary of the research questions tackled in this Thesis and the Chapters that tackle each question.

1.3 Structure of Thesis

This Thesis is broken down into four main parts. Part I, which contains the first three Chapters, include this introduction, a literature review and the mathematical background to the models built in this Thesis. In Part II of this Thesis, the question of whether Population Projection Matrices or Integral Projection Models are better at modelling the *M. annularis* data set is answered. In Part III, three Integral Projection Models are built in order to investigate the impact of changing hurricane activity on the reef as a result of climate change. The final part draws conclusions on the research carried out in Parts I, II and III in order to answer the research questions set out in Figure 1.4.

Table 1.2 shows which chapters tackle the different research questions asked in Figure 1.4. Each Chapter in this thesis contributes in a different way to investigate the research aims.

A literature review was carried out to motivate this Thesis and its research aims. It is divided into three sections reflecting the three different research objectives of this thesis. It investigates the current analysis of coral populations in response to hurricanes and will introduce two types of projection models: The Integral Projection Model (IPM) and the Population Projection Matrix (PPM). Whilst the literature review motivates the need for this research, Chapter 3 gives the mathematical background to the models and their methods of analysis, which underpin the rest of the Thesis. The methods for parameterizing the models are described in this chapter, alongside a discussion of methods of analysis. These techniques will be used in Chapters 4, 5 and 7.

The aim of Chapter 4 was to investigate if initial trauma following a hurricane affected the dynamics of a coral population (RQ6). This chapter builds on work started in a MMath project (Burgess, 2008) and although the same hypothesis is tested, the PPMs have been re-parameterized using more sophisticated techniques and re-analyzed. The PPMs parameterized in Chapter 4 are used in Chapter 5 to compare the results with parameterized IPMs. The data were divided according to the relative decline following Hurricane Mitch (Figure 1.5). In this case three PPMs (Chapter 4) and three IPMs (Chapter 5) were built for three selections of data (I_{Severe}, I_{Weak} and I_{Mild}) to compare the dynamics for different levels of decline. A discussion of the results and of the different methods used is found in Chapter 6. In this it is concluded that, where possible, Integral Projection Models should be used to model *M. annularis* populations.
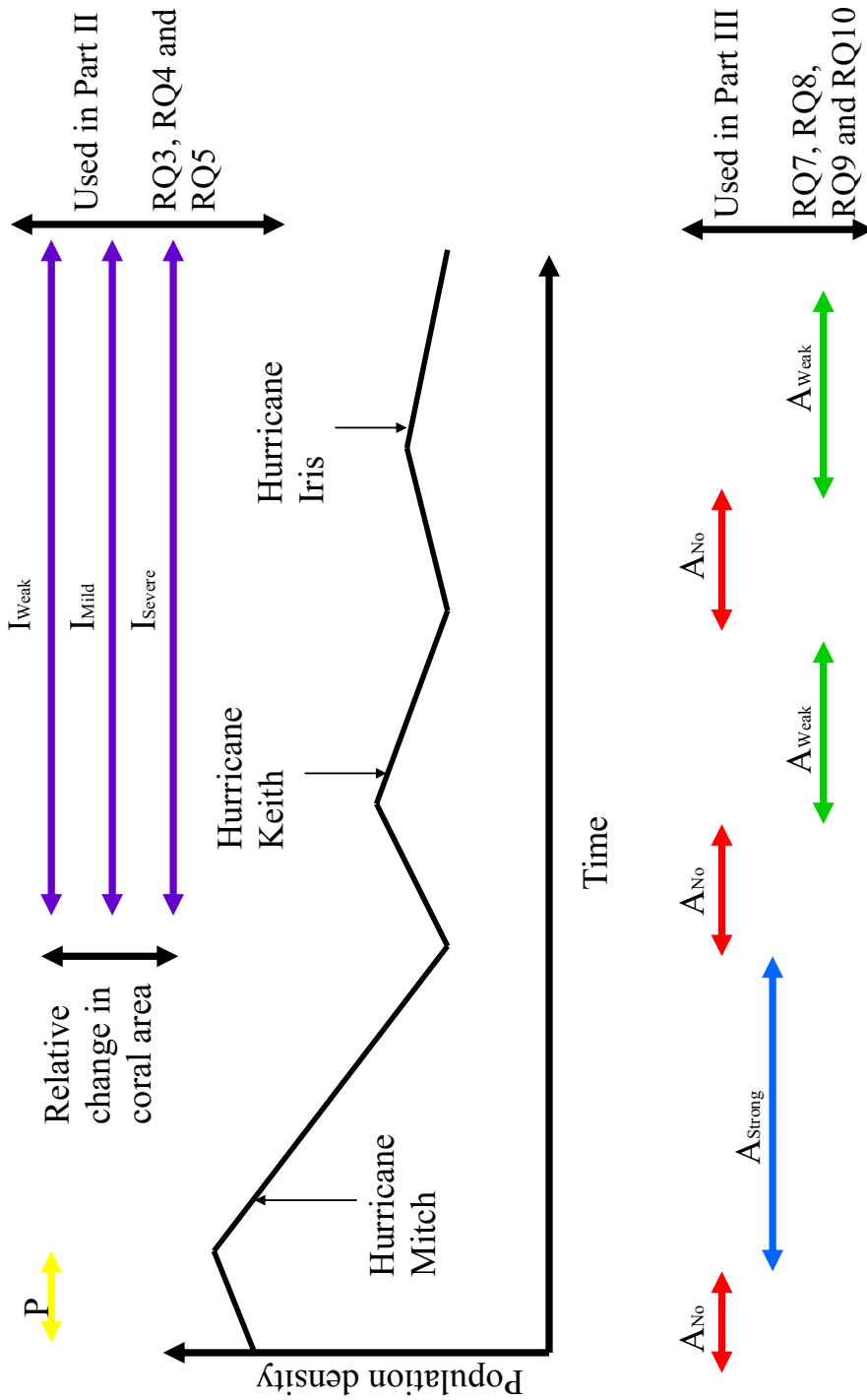
Figure 1.5: A schematic showing how the data are divided in order to answer the different research questions.

The aim of Part III is to investigate the impacts of climate change on the frequency and intensity of hurricanes. This required three IPMs to be built, Chapter 7 gives the behaviour of the coral patches over different hurricane periods found between October 1998 and January 2003 (A_{Strong}, A_{Weak} and A_{No}) (Figure 1.5). It was not possible to use the IPMs parameterized in Chapter 5, as these take an average of the behaviour from the five time steps post Hurricane Mitch. Instead, this alternative method of dividing the data allows the projection of the population under differing hurricane scenarios in Chapter 9.

In addition to building three IPMs in Chapter 7 in order for them to be used in Chapter 9, this chapter also investigates RQ7. This investigates if the dynamics exhibited during a hurricane is different when the strength of the hurricanes vary.

In Chapter 8, the Integral Projection Models built in Chapter 7 are used to suggest possible management strategies, which could be used to increase the growth rate of coral patches on the reef in periods when there are no hurricane activity. This is in order to investigate RQ8 on what the best management strategies are for *M. annularis*.

It is important to understand the effect that climate change could have upon a coral population. Chapter 9 investigates how a change in hurricane activity could directly impact the reef. This is achieved through the use of the Integral Projection Models built in Chapter 7. The second part of Chapter 9 combines the projections from the first part of the chapter with the management strategies suggested in Chapter 8 in order to investigate RQ10, whether under management the forecasted effect of climate change on the population would change. Chapter 10 discusses these results, giving possible ways in which these management strategies could be achieved, and the implications of the extinction times on the reef.

Finally Chapter 11 concludes this thesis by answering all ten research questions from Figure 1.4, as well as highlighting the main research contributions.

Chapter 2

Literature Review

2.1 Introduction

This chapter contains a literature review that motivates the research aim of this Thesis, namely:

To investigate the effect of hurricane activity on the dynamics of the reef-building coral - Montastraea annularis.

It is broken down into two main sections, the first section looks at coral reefs and hurricanes and the second section investigates the current methods of analysis adopted to look at the impacts of hurricanes on coral populations. It then goes on to introduce the Population Projection Matrix (PPM) and Integral Projection Model (IPM) methods. This chapter concludes by showing how this leads to the three research aims given in Figure 1.4.

2.2 Coral Reefs and Hurricanes

2.2.1 *Montastraea annularis*

Montastraea annularis is a reef-building massive coral consisting of large dome-shaped colonies that are often over 1 m in diameter. Each of these colonies consist of large columnar shaped branches known as ramets. The live tissue on these

ramets is restricted to the upper surface, known as coral patches. *M. annularis* is a slow-growing coral with colony growth rates estimates varying from 0.37cm/year to 1.6cm/year (Foster et al., 2007). The majority of studies focus on the dynamics of colonies of this species (for example Hughes (1984) and Edmunds and Elahi (2007)). The reason for this is because with any large scale destruction of these colonies, as in disturbances like hurricanes, it may take decades for the colonies to recover as a result of their slow growth rate. The live coral exists on the upper surface of the ramets, if there is no live coral located on top of the ramet there is no way for that ramet or indeed the colony to grow. Therefore, it is vital to gain an understanding of these small-scale dynamics, as understanding the dynamics on a patch scale will give a better understanding of the long-term health of a colony.

It is at the patch scale where there is interaction between coral and algal patches. Coral and algal patches compete on ramets for space and light (Nugues and Bak, 2006). When coral is healthy and unstressed it inhibits the growth of algae and coral is the dominant species on the reef (McCook et al., 2001). However, when coral is unhealthy and stressed it cannot inhibit algae growth and reefs are instead increasingly being dominated by algae (Mumby et al., 2007). There has been a documented change from reefs being coral-dominated to being algae-dominated (Hughes, 1994). It is unclear if left untreated what long-term effect this would have on a reef.

An abundance of colonies of *M. annularis* is vital to the healthiness of reefs, but with increasing intensity and frequency of disturbances these colonies are being replaced by quicker growing branching corals (Jackson, 2001). This decline is significant to the long-term structure of the reef. Particularly as these reef builders have low recruitment and low growth rates meaning it could take many decades for *M. annularis* colonies to recover to its abundance of 40 years ago (Hughes, 1994).

2.2.2 Coral Reefs

Over the past 40 years, coral cover on worldwide reefs has reduced by up to 80% (Gardner et al., 2005). It is now thought that 20% of reefs have been destroyed and

not recovered (Spalding et al., 2001) a further 24% are under immediate threat and 26% under long-term threat (VanOppen and Gates, 2006). It is vital to understand both the reasons behind this decline and also to be able to forecast behaviour over the next few decades. The decline has slowed, compared to the rate in the 1980s, but there is still significant decline on already depleted reefs (Gardner et al., 2003).

The decline in coral reefs has been attributed to the increasing stress that they face, for example from overfishing (Hawkins and Roberts, 2004; Hughes et al., 2003); the *Diadema antillirum* die-off (Lessios et al., 1984; Lessios, 1988; Mumby et al., 2006b); coral bleaching (Muller and D'Elia, 1997) and hurricanes (Hughes, 1984, 1994). Coral reefs are important to local communities as they provide both a source of food as well as economic provision (Johannes, 1997; McManus et al., 2000). However, since the 18th and 19th century, reefs have been overfished as the demand for food sources have increased and, more recently, as the ability to export food sources has improved (Hughes, 1994; Jackson, 1997; Pandolfi et al., 2003). By removing key grazers from the reef it increases the growth of algal patches (Mumby et al., 2006a), which can cause algal blooms and ultimately result in algal-dominated reefs (Hughes et al., 2007; Szmant, 2002).

A key transition on Caribbean reefs occurred during the *Diadema antillirum* die off in 1983. *D. antillirum* is a herbivorous sea urchin that inhabits coral reefs (Lessios et al., 1984) and played a critical role in keeping algal cover low (Carpenter, 1988; Ogden et al., 1973; Sammarco, 1982). From January 1983, more than 93% of the Caribbean population died in 13 months (Lessios, 1988). The result was an increase over the next four years in algal cover on Jamaican reefs by 95% and a coral cover decline of 60% (Hughes et al., 1987). It is said to have played a key role in reducing the ability of reefs to remain healthy and coral dominated (McManus and Polsenberg, 2004).

Coral bleaching, caused by an increase in sea surface temperatures of $1 - 2^o C$ above the seasonal average (Brown, 1997), is the releasing of the symbiotic zooxan-thallae by the host coral. This leaves the white calcium carbonate structure visible, hence the name attributed to it (Brown, 1997; Glynn, 1993; Hughes et al., 2003;

Lesser, 1997). Corals can survive for weeks and sometimes months when bleached, but it affects the structure of the reef (Muller and D'Elia, 1997). Bleaching events have been observed since the early 1900's (Edmunds, 1994), but climate change is believed to have increased the intensity, frequency and distribution of these events (Brown, 1997; Edmunds, 1994; Hoegh-Guldberg, 1999, 2004).

Coral reefs are now under constant stress from coral bleaching; the *D. antillirum* die off and overfishing to name a few. When a reef is then struck by a further disturbance, like a hurricane, the already present stresses described above inhibit the ability of the reef to recover following this disturbance.

2.2.3 Hurricanes and Climate Change

Hurricanes are an intense tropical storms formed in areas where the sea surface temperature (SST) rises above 26^oC for at least the upper 50m of the sea surface (Lugo et al., 2000). They are low pressure systems with central pressures of between 980mb and 920mb. They generally form between 5° and 30° from the equator with 87% forming no further than 20° from the equator (Henderson-Sellers et al., 1998). This area gives SSTs high and far enough from the equator so that the Coriolis force is non-zero and hurricanes can form (NOAA, 2011).

A tropical storm is classified as a hurricane when wind speeds peak above $33ms^{-1}$ (Simpson and Riehl, 1981). A hurricane is classified by the Saffir-Simpson scale according to the maximum wind speeds. Category 1 hurricanes have a peak wind speed of between 33 and $42ms^{-1}$, whilst Category 5 hurricanes have maximum wind speeds above $70ms^{-1}$.

In the North Atlantic there are on average 9-10 tropical storms annually, with 5-6 of these reaching hurricane status (Henderson-Sellers et al., 1998). The main hurricane season lies between August and October with the peak activity between late August and September (Neumann et al., 1985) when sea surface temperatures are at their peak.

Over the past 35 years there has been an observed increase in the proportion and number of strong hurricanes (Webster et al., 2005, 2006). In fact since 1970 there

has been a 75% increase in the number of Category 4 and Category 5 hurricanes (IPCC, 2007). Climate scientists forecast that this trend of increasing intensity will continue (IPCC, 2007), with an increase in mean maximum wind speed expected to be between +2% and +11% globally (Knutson et al., 2010). Although there is some disagreement in the effect of climate change on the frequency of hurricanes. It is mainly accepted that the global hurricane frequency will remain the same (Webster et al., 2005), but there are some who believe that the overall frequency will decrease (IPCC, 2007). Oouchi *et al.* (2006) predict that there will be an overall decrease in global frequency of 30%, but with an increase of 34% in the North Atlantic, whilst Knutson *et al.* (2010) believe there is evidence for between a −3% and −34% change in frequency globally.

An accepted effect of climate change is that hurricane intensity will increase (Webster et al., 2005). This is seen in the observed increase in the Power Dissipation Index (PDI) since the mid 1970s (Emanuel, 2005). This is equivalent to the increase in duration and peak intensity of hurricanes. If the frequency of hurricanes remain the same alongside the increase in intensity this is equivalent to an increase in frequency of strong hurricanes balanced by a decrease in frequency of weaker less intense hurricanes (IPCC, 2007).

2.2.4 Hurricane Impacts on Coral Reefs

For thousands of years coral reefs and hurricanes have co-existed (Glynn, 1993). The presence of modern day reefs suggest that the impacts as a result of a hurricane have not always led to decline (Gardner et al., 2005). Instead hurricanes have helped build these diverse ecosystems (Connell, 1997), by removing abundant species at regular intervals from reefs, creating space for colonization by different species aiding diversity (Bythell et al., 1993; Connell, 1978; Hughes and Connell, 1999).

The damage which hurricanes can cause to coral reefs fall into two categories: mechanical and biological. Primarily there is mechanical damage, where waves caused by hurricanes break off pieces of coral causing partial or colonial mortality

(Adey, 1978; Darwin, 1842). Sedimentation of material dislocated by a hurricane can bury colonies blocking their light source or can abrade the upper surface of these colonies (Brown, 1997). The increase in rainfall reduces salinity near the reef, which can also damage the reef (Harmelin-Vivien, 1994), as well as increasing the number of nutrients in the water encouraging algal growth resulting in eutrophication (McCook, 1999). The majority of mechanical damage will effect branching corals, who are particularly vulnerable due to their structure (Woodley et al., 1981; Lugo et al., 2000), with reef building corals like *M. annularis* less likely to experience this fragmentation of colonies (Woodley et al., 1981). As always there are some extreme cases with large areas of reef building corals destroyed by this mechanical action (Hubbard et al., 1991).

The biological effects of hurricanes include the disruption of reef structures (Woodley et al., 1981; Dollar, 1982; Grauss et al., 1984). The main damage comes through the coral cover reduction, with the reefs instead being dominated by algae. The transition from coral-dominated to algal-dominated reefs has been particularly observed on Caribbean reefs (Done, 1992; Hughes, 1994; Knowlton, 1992). This may occur following a hurricane, but the roots of this phase shift comes from the degradation of a reef prior to a hurricane (Hughes, 1994; Lugo et al., 2000; Knowlton et al., 1981, 1990).

The more recent decline change following a disturbance has been attributed to an increase in other stressors on the reef (Knowlton et al., 1981, 1990). Meaning coral cover cannot recover prior to the next disturbance. This additional stress is thought to come mainly from human induced sources such as: overfishing, eutrophication and sedimentation (Aronson and Precht, 2006; Hughes and Connell, 1999; Nystrom et al., 2006). These can reduce the ability of a reef to regenerate and recover from more frequent and intense storms (Gardner et al., 2005; Rogers et al., 1997, 1991).

There are some benefits for corals during a hurricane. Coral bleaching, the release of the symbiotic algae due to increased sea surface temperatures, is negated by the passage of a hurricane, with documented cases of recovery from coral bleach-

ing alongside hurricane damage (Manzanello et al., 2007). Another benefit comes from the release of resources, in particular space on the reef for growth and recruitment (Rogers, 1993; Treml et al., 1997; Hughes and Connell, 1999). This also prevents the monopolization of the reef by one particular species (Hughes and Connell, 1999), with undisturbed reefs suffering from overcrowding. This reduces recruitment rates when there is limited free space, due to pre-emption or shading from other species (Hughes and Jackson, 1985; Fisk and Harriott, 1993).

The damage of a hurricane on a coral reef is not always felt immediately. For example, there is an increased incidence of disease on damaged corals (Knowlton et al., 1981, 1990). Damaged corals are also more likely to be eroded and further damaged, which can result in delayed mortality (Knowlton et al., 1981, 1990). Also the community structure on a reef can change after a hurricane due to the differing speeds of recovery. For example, branching corals can recover in as little as five years, due to their high growth rates (Shinn, 1972; Rogers et al., 1979), whilst reef building corals can take between 10 and 25 years (Gardner et al., 2005).

Coral reefs and hurricanes have existed alongside each other for about 5000-6000 years (Glynn, 1973; Donnelly and Woodruff, 2007). This indicates that reefs are able to recover following a hurricane (Lugo-Fernandez and Gravois, 2010). However, this recovery is becoming less common, with many studies of interaction between coral reefs and hurricanes reporting decline (Knowlton et al., 1981, 1990; Hughes, 1989, 1994; Liddell and Ohlhorst, 1993). In fact the main study that indicates recovery is of a branching coral (Shinn, 1972), rather than a reef-building coral. Recovery rates are indicated to lie somewhere between 10 and 25 years, but there are some studies that claim recovery could take as long as a century (Glynn, 1973; Woodley, 1992; Sorokin, 1995; Pandolfi and Jackson, 2007; Gardner et al., 2005; Grauss et al., 1984; Harmelin-Vivien, 1994).

Recovery occurs when surviving corals can grow, both through the attachment and growth of new fragments of partially damaged corals, and through colonization of new corals (Lugo et al., 2000). Historical recovery of coral reefs has shown that conditions experienced on reefs following a hurricane should be conducive

to re-growth and recovery (Lugo et al., 2000) and yet most studies now record an increased decline following a hurricane. The reasons suggested for this surround the issue that there has been an increase in chronic disturbances from anthropogenic factors. This compromises the ability of the reef to recover (Lugo et al., 2000). In Jamaica the overfishing of the reefs and then the *D. antillirum* die-off in 1983, lead to a lack of recovery following Hurricane Allen (Hughes, 1994; Hughes and Connell, 1987; Hughes, 1994). This lack of recovery resulted in an increase in phase shifts to an algal-dominated reef (Bellwood et al., 2004; Done, 1992; Hughes, 1994; Knowlton, 1992). It is not known how stable this alternative state is and if coral reefs can again be dominated by coral (Knowlton, 1992; Scheffer et al., 2001; Petraitis and Dudgeon, 2004).

2.3 Adopted Modelling Techniques

Despite the introduction of Population Projection Matrices (PPMs) to coral colony population modelling in 1984 (Hughes, 1984), an abundance of models still use coral cover as the measure of population dynamics (Gardner et al., 2003, 2005; Graham et al., 2011; Hughes and Connell, 1987). Coral cover is measured as the percentage of a reef which contains coral as opposed to algae, sponges or free space. Coral cover is used to model the response of populations to hurricane events by looking at the percentage change of cover (Gardner et al., 2005). It is claimed that, following a hurricane, populations will follow one of four trajectories according to their percentage growth rate (Gardner et al., 2005). The reliance on coral cover percentages does not give the underlying dynamics of the observed results. It is also only possible to carry this analysis out retrospectively, and does not allow the forecast of behaviour.

Coral cover models have also been used to calculate the recovery rates following tropical storms, bleaching events or crown-of-thorns outbreaks (Graham et al., 2011; Sheppard et al., 2008; Naim et al., 2000; Halford et al., 2004), but the definition of recovery in these studies is unclear. The clearest definition takes into account all dynamics following a disturbance. Normally the term 'recovery'

is restricted to either the time until at least half the amount of cover lost in the disturbance is restored (Naim et al., 2000), or by a positive growth rate, which takes the population back to the position is would have been in if the disturbance had not occurred (Gardner et al., 2005).

Coral cover studies provide a simplistic description of the behaviour seen on a reef, they fail to take into account the underlying dynamics that explain these observations. In fact it must be questioned whether coral cover is even the best metric to measure healthiness of the reef. If, for example, there was an abundance of small colonies following a disturbance, coral cover percentages could mask the loss of large colonies that are required if a population is going to withstand future disturbances. These models contribute understanding to the behaviour observed, but fail to project the population into the future to try and explain what future behaviour may occur.

A better alternative to the percentage coral cover models are the size-frequency distribution models. In these models the structure of the populations are observed over time to understand the changing structures of the reefs (Hughes and Jackson, 1985; Gilmour, 2004). These models can be used to monitor the relative abundance of small or large colonies (Hughes and Jackson, 1985) or the structure of reefs following disturbances (Gilmour, 2004). They provide a greater understanding of the dynamics than percentage coral cover models can provide. However, they fail to account for the processes, which link these censuses through time. They are useful, like coral cover, for historical analysis in relation to particular events, but they fail to provide information about future population structures beyond broad statements about what may occur.

Over time populations change, sometimes for the good of the population and other times to the detriment of the population. The focus for management of populations is to understand past behaviour and to predict future behaviour (Caswell, 2001). Understanding the behaviour of one individual can give vital insight into a population, but often it is more beneficial to get an overview of the complete population (Caswell, 2001). This is achieved through population modelling, taking

data describing the behaviour of the population and transforming it into a coherent model that takes into account how the population changes over time (Caswell, 2001). This allows projection into the future and understanding of the past.

Population models, like the Population Projection Matrix (PPM) and Integral Projection Model (IPM), are used in a range of settings from pest control (Smith and Trout, 1994; Shea and Kelly, 1998; Hastings et al., 2006; Dudas et al., 2007; Miller et al., 2009) to harvesting (Cropper Jr. and Di Resta, 1999; Souza and Martins, 2006), from conservation (Price and Kelly, 1994; Esparza-Olguin et al., 2002; Linares et al., 2007) to understanding the effect of disturbances (Hughes, 1984). They can be used to understand the behaviour of endangered species (Easterling et al., 2000) and to understand evolutionary strategies adopted by populations (Hesse et al., 2008; Kuss et al., 2008; Rees and Rose, 2002). This makes them an ideal fit to model coral patch dynamics.

2.3.1 The Population Projection Matrix

The PPM was first conceived by Leslie in 1945 . PPMs have been used in population modelling ever since (Caswell, 2001). Since the seminal paper by Leslie, methods to analyze and parameterize PPM models have been well developed (for an excellent summary see Caswell (2001)). The PPM describes the transition of a population from one time step to another. It does this by dividing the population into a given number of groups and calculating the transition probabilities of moving from one group to another. Initially PPMs were only used in modelling populations characterised by age, but the PPM structure has now been developed to include models determined by developmental stage (Lefkovitch, 1965) and size (Hughes, 1984). For a mathematical introduction to these models see Chapter 3.

Population Projection Matrices for coral populations were first used in 1984 (Hughes, 1984), where a size-structured PPM was introduced as an adapted Leslie matrix (Leslie, 1945). This was to allow not only additional stasis entries, but also all growth and shrinkage entries. In Hughes (1984) paper a population of *Agaricia agaricites* was modelled over time to capture the effect of storms on the dynamics

of the population. This was achieved through creating a 'storm' matrix and a 'calm' matrix from the data. These PPMs were projected with varying storm occurrence rates to investigate extinction time under differing scenarios.

Caribbean coral reefs have declined dramatically in the past three decades with a decline of nearly 80% coral cover (Gardner et al., 2005). As a result, PPMs have been applied to coral populations in the Caribbean with the aim to understand this decline (Lasker, 1991; Hughes and Tanner, 2000; Edmunds and Elahi, 2007).

2.3.2 Benefits of Using the Population Projection Matrix on Coral Populations

In order to fully understand the dynamics on a reef, projection models must be used, because not only do they explain what was observed in the data, they also project future behaviour (Caswell, 2001). By assuming current conditions will remain unchanged, the population structure and size can be calculated (Hughes and Tanner, 2000). However, coral populations are subject to repeated disturbances and so these projections are often unrealistic. In Hughes (1984) the use of two different matrices for two different environmental years (Storm and Calm) allows projection over time with varying storm occurrences in order to compare recovery rates and population sizes. This interweaving of environments is a more realistic projection for coral populations. PPMs have also been used to project populations under differing strategies of recruitment (Edmunds and Elahi, 2007). In this case three different recruitment strategies were used in order to compare overall population size 50 years into the future. This can aid understanding about a particular aspect of a population and can also fill gaps in missing data providing a range of possible responses.

The main benefit of the PPM is the intuitive nature by which the life cycle of a population can be turned into a PPM. Why is it intuitive? Because each connection of the life-cycle is directly transferable to an entry in the PPM (Caswell, 2001). For example, growth transitions are placed on the lower triangle of the PPM, stasis entries on the diagonal and shrinkage and reproduction are on the upper triangle

(Leslie, 1945; Lefkovitch, 1965; Hughes, 1984). This makes it easy to interpret the significance of different types of behaviour in the PPM.

The PPM is mathematically simple (Caswell, 2001). Not only is it relatively easy to approximate probability estimates from data, but the standard analysis tools are relatively simple to calculate using matrix analysis (Caswell, 2001). This makes them attractive to ecological modellers and makes the PPMs very popular with hundreds published in literature (Stott et al., 2010b).

2.3.3 Drawbacks of the Population Projection Matrix

There are issues surrounding the selection of size class boundaries (van der Meer, 1978; Moloney, 1986). When a PPM is created using age or stage classes these boundaries are biologically motivated (for example (Leslie, 1945; Lefkovitch, 1965), but when the PPM is created using size classes there is no biological relevance to these size class boundaries (for example (Edmunds and Elahi, 2007)). Instead they are selected through the application of an algorithm (van der Meer, 1978; Moloney, 1986). This creates a weakness in the analysis and the dynamics within the size classes are not accounted for. This issue is known as the problem of discretization of the size class boundaries.

The PPMs created for coral populations (Hughes and Tanner, 2000; Edmunds and Elahi, 2007; Lasker, 1991; Hughes, 1984) often choose size class boundaries somewhat arbitrarily. For example, in Lasker (1991) and Hughes and Tanner (2000) small, medium and large classes are used whilst in Edmunds and Elahi (2007) they are in 50cm intervals. However, there are often no biological reasons for these boundaries and so these can break the assumption that all individuals within a given size class will exhibit the same behaviour. To correct this, the van der Meer and Moloney algorithms (van der Meer, 1978; Moloney, 1986) (see Section 3.1.3) need to be used in order to minimize the errors that are created by this discretization.

Coral populations are often best described by size (Hughes, 1984). However, there is some discussion on the need to include age within size classes, (Hughes

and Jackson, 1985) as small old colonies will behave differently from small young colonies. As was stated in their paper, in order to calculate the age of coral, damage to the coral is necessary. Hence many data sets provide only size as an indicator (Hughes and Jackson, 1985).

The success of size-determined plant populations being modelled by IPMs (Easterling et al., 2000; Childs et al., 2003, 2004; Rose et al., 2005; Ellner and Rees, 2006; Hesse et al., 2008; Kuss et al., 2008) should encourage the use of IPMs in coral populations. As far as I am aware, there are currently no coral populations modelled using the Integral Projection Model despite the obvious advantage of the model being continuous in size.

A secondary flaw of the PPM is that when the state-classes are poorly selected this can lead to issues of missing transitions, either due to the data being missing in the data sets or due to poorly selected boundaries. This issue is discussed in more detail in Section 3.1.3.

2.3.4   The Integral Projection Model

The IPM was first introduced into ecological modelling by Easterling et al. in 2000. Following just over 10 years of development these models have been developed to include a wide range of applications. The IPM is a form of integrodifference equation and was introduced to population modelling in order to deal with the problem of discretization of size (Easterling et al., 2000). For a mathematical background to the IPM see Chapter 3.

The main focus of the original IPM for *Aconium noveboracense* was to model a given set of data and show how methods of analysis for a PPM can be transferred to IPMs, particularly focusing on sensitivity analysis (Easterling et al., 2000). Sensitivity is an area considered vital in population ecology in the analysis of PPMs as it captures the contribution of each entry to population growth (Caswell, 2001). The ease with which IPMs deal with delayed reproduction was shown by population models of *Oenothera glazionviana* (Rees and Rose, 2002) and *Campanula thyrsoides* (Kuss et al., 2008). Stochastic variation in parameters due to environ-

mental variations was introduced for a *Carlina vulgaris* IPM (Rose et al., 2002), which was then further developed by Childs et al. (2003; 2004) and for *Carduus nutans* by Jongejans et al. (2011) as a method for measuring spacial spread. The theory behind stochastic IPMs was laid out in two papers by Ellner and Rees (Ellner and Rees, 2007; Rees and Ellner, 2009). Invasion of a species was modelled by a *Cirsium canescens* IPM (Rose et al., 2005), as well as being used to measure the effect of an invasive species on the growth rate of a native species (Williams and Crone, 2009).

A population is said to experience complex demography when the population dynamics are determined by two or more biological factors. For example the dynamics of *Onopordum illyricum* were determined by both age and size (Ellner and Rees, 2006). Complex demography could also include quality of offspring or flowering probabilities as well as any other factors that affect the population (Ellner and Rees, 2006). This shows the ability of an IPM to accommodate both discrete and continuous state factors.

The majority of models in literature are density independent. This is not normally a problem as many populations modelled are decreasing or are at densities well below carrying capacity. However, IPMs have been developed to include density dependence, for example, when modelling an invasive species or when certain parameters are restricted by density (Ellner and Rees, 2006). The effect of different habitats on a population can be modelled as in the case of *Veratrum album* (Hesse et al., 2008); this paper also promoted the ease with which two or more IPMs can be compared.

The modelling of tree populations by IPMs overcame some of the problems of fitting PPM models to these populations caused by high sensitivity of the growth rate to size-class width. By eradicating the need to select size classes the IPM resolved this issue (Zuidema et al., 2010). However Zuidema et al. (2010) claim that the numerical integration method adopted by the majority of IPMs for plant populations cannot be directly transferred to tree populations, this is in spite of the use of the mid-point rule by Metcalf et al. (2009). Instead of the mid-point rule,

for numerical integration, they suggest the use of the 'Integration' method. This method assumes a uniform size distribution in each mesh point instead of assuming all individuals lie at the mid-point of the mesh. The cost of additional complexity is out-weighed by the additional benefits of using this method for slow-growing populations as the integration method prevents individuals from passing through size-class unrealistically quickly (Zuidema et al., 2010).

The interaction between a tree Cholla cactus (*Opuntia imbricata*) and herbivore attacks were modelled by Miller (2009). This was achieved by a comparison between a control population and one under attack. This is a popular method in population modelling to quantify the effect of predators on a population and shows the ability of the IPM to facilitate this analysis. Environmental factors, other than herbivore attacks, can affect the parameters fitted in an IPM and thus in turn, the population growth rates (Dahlgren and Ehrlen, 2009).

Transient analysis is a relatively new phenomena to the Integral Projection Model, but is becoming increasingly popular in Population Projection Matrices (Stott et al., 2010a; Townley et al., 2007; Townley and Hodgson, 2008). However, it is thought that the ability to capture transients is determined by the dimensions of the models (Stott et al., 2010a; Tenhumberg et al., 2009), the IPM should be better at capturing the transients (Eager et al., In Press). Eager et al. (In Press) have begun a discussion of possible transient methods by comparing population structures at each time step to the previous time step in order to measure attenuation and amplification.

Whilst most developments in Integral Projection Modelling have occurred due to a need to model a particular population, there are a few papers which give theoretical background and understanding to the methods employed. This is particularly the case in the application of stochastic IPMs (Ellner and Rees, 2007; Rees and Ellner, 2009), where a theoretical underpinning to the stochastic IPMs produced was given. These papers present both the theory for analyzing IPMs and further details on how they are parameterized. These details for deterministic IPMs were restricted to Appendices in Easterling et al. (2000) and Ellner and Rees

(2006).

2.3.5 How the Integral Projection Model Solves the Problems of the Population Projection Matrix

The IPM is continuous in state. This makes IPMs ideally suited to modelling populations whose state is determined by size (Easterling et al., 2000; Ellner and Rees, 2006). The IPM does not require discretization of sizes to form size classes and the errors introduced by these methods in PPMs are not introduced to IPMs (van der Meer, 1978; Moloney, 1986). By avoiding discretization, IPMs have greater realism, whilst analysis methods are simple enough not to prevent usage.

The estimation of parameters in an IPM is carried out through statistical curve fitting, that is taking a range of possible parameters and selecting the parameters with the best fit (Easterling et al., 2000). In comparison, estimation of probabilities in the PPM does not use this best fit technique. Instead, probabilities are estimated directly from data (Caswell, 2001). There has been some effort to correct this (Gross et al., 2006), but the complexity of these methods suggests that the IPM should be used ahead of the PPM.

Construction of a PPM from data requires a trade-off between biological realism and uncertainty in estimation of the parameters (Doak et al., 2005). Especially if the data set is sparse or if the population is complex or if a stochastic model is being fitted. An analysis of the data requirements to accurately estimate parameters was completed by Fiske, Bruna and Bulker (2008). With a lack of data, estimates may be biased, which in turn biases the analysis of the matrices (Doak et al., 2005). For a PPM of size $n \times n$ there are up to n^2 parameters to be fitted. If the PPM is stochastic and is calculated for m different years then there are up to n^2m parameters to be fitted. PPM models, especially stochastic PPMs are data hungry. In comparison an IPM may be fitted by much fewer parameters (Ramula et al., 2009) and stochasticity may be included with the addition of only a few extra parameters (Rees and Ellner, 2009). However, an analysis of the minimum data amounts required to accurately fit an IPM has not yet been carried out.

Only recently has the discussion on the effect of data limitations on both parameter estimates and their analysis been carried out (Fiske et al., 2008; Doak et al., 2005; Ludwig, 1999; Ellner et al., 2002; Fieburg and Ellner, 2001). Doak et al. (2005) state that if data has less that 5 sampling points in time it is best to produce a deterministic PPM rather than a stochastic one. This is because the benefits of a more complex model are out-weighed by parameter uncertainty.

A drawback of IPMs compared to PPMs is that the transfer from the life-cycle to the model is not as easily achieved in the IPM. In an IPM the life-cycle influences the selection of functions to be fitted (Rose et al., 2002). However, instead of a direct translation, all growth must be grouped together, along with all survival and all reproduction. These functions must then be further broken down into factors that influence them. This makes the IPM less easily interpretable.

2.3.6 The Issues Surrounding Analysis of Projection Models

The main measure of population dynamics is the population growth rate (Caswell, 2001; Godfray and Rees, 2002). The calculation of this rate is easy for PPMs with standard code available in R or Matlab, with the growth rate being calculated as the dominant eigenvalue of the system (Caswell, 2001). However, for large numerical approximations of the IPM, this can be costly and often only the dominant eigenvalue is calculated rather than the entire spectrum of eigenvalues (Easterling et al., 2000). This makes the convergence to asymptotic dynamics difficult to calculate for IPMs.

The growth rate is useful as it gives a single measure for the population which takes into account all the parameters that build the model. As parameters change the measure changes in response to this, this one measure can then be compared for a variety of parameter values (Lasker, 1991). However, questions about the suitability of relying on this indicator are being asked (Godfray and Rees, 2002; Townley et al., 2007; Townley and Hodgson, 2008). This is especially the case when populations are disturbed (Townley and Hodgson, 2008). It is now thought that it

is more important to understand these **transient** dynamics as populations often do not reach the **asymptotic** dynamics because populations are periodically hit by disturbances. For PPMs, these methods are well developed to include maximum amplification and attenuation (Townley et al., 2007), Kreiss bounds (Kreiss, 1962), Reactivity (Caswell and Neubert, 2007) and transient time bounds (Townley and Hodgson, 2008). These bounds help create an overall picture of the possible dynamics which a population may experience. Transient bounds for IPMs are in their infancy, with methods still in development (Eager et al., In Press).

2.4 Conclusion

In this chapter, the benefits of both the PPM and IPMs have been discussed. Also discussed has been the application of these models to coral populations. It has been shown that PPMs are a tool used in coral colony modelling, but their use is not widespread. Instead, the use of percentage coral cover models is preferred. However the benefits in understanding the dynamics underlying the population mean that where the data exists, projection models should be fitted to this data. Although the data is of patch dynamics, many of the processes described in PPM modelling for colonies should be readily transferable.

The application of Integral Projection Modelling to coral populations is yet to be explored. It is believed that coral populations are ideal candidates for use in IPMs as the best descriptors of dynamics is size. It is thought current frameworks should be adaptable to ensure accurate fits of the population.

Projection of PPMs (and IPMs) with data from hurricane and non-hurricane years has been carried out previously. These methods, once adapted, will be carried out to the data in order to determine what would happen under varying hurricane occurrences.

Transient analysis is becoming commonplace in PPM modelling as this allows understanding of the dynamics following disturbances. Transient analysis in IPMs is relatively new, with many of the techniques not yet transfered from the PPM methods.

This chapter has highlighted the need to investigate the effects of hurricanes on coral populations. It has highlighted the increased decline in coral cover in the Caribbean and climate change only increases the urgency of understanding the underlying dynamics. Where coral cover percentages have previously been used, the benefits of using projection modelling have been shown, in particular the benefits of using the IPM have been highlighted. This chapter has helped develop the aim of this Thesis into three different areas, namely:

OBJ 1. **Modelling**. To investigate current projection modelling techniques. To develop methods to allow their application to *Montastraea annularis*.

OBJ 2. **Analysis**. To understand and develop analysis techniques of projection models, in order to understand how hurricanes affect the dynamics of a population.

OBJ 3. **Climate Change**. To understand the effect of climate change on hurricane activity and hence explore how this could affect population dynamics of *Montastraea annularis*.

These objectives will be investigated through the remaining chapters of this Thesis.

Chapter 3

An Introduction to Projection Modelling

Population models can be derived from two different sources; data and biological processes. The first rely completely upon data to look at the dynamics of the population, for example percentage coral cover models (Gardner et al., 2003, 2005; Graham et al., 2011; Hughes and Connell, 1987). These models do not account explicitly for the biological reasons for these changes. In contrast, there are models defined by biological processes, which do not include any data, but instead attempt to understand the dynamics of populations purely from what is expected to occur. For example, differential equation models can be analysed to understand the dynamics without the application of data. These two types of models require different frameworks; one needs a biology-defined state and the other a data-defined state.

Where data and biological processes meet is Projection Modelling. They take known biological information about the population to form the skeleton of a model and then require the application of data to parameterize the populations' dynamics. Two projection models, which model discrete time populations, are the Population Projection Matrix (PPM) model and the Integral Projection Model (IPM) (Caswell, 2001; Easterling et al., 2000). In this chapter, methods for formulation and analysis of these models are discussed. The methods for analysis are broadly similar, therefore this chapter will firstly describe the parameterization of each model, followed

by a discussion of Asymptotic and Transient Analysis of these models.

3.1 The Population Projection Matrix

The Population Projection Matrix (PPM) describes the behaviour of a population over time (Caswell, 2001). They are discrete in both time and state and capture the transition probabilities between states over two time periods (t and $t + 1$). Specifically, given a population at time t, the population at time $t+1$ is determined by the projection equation (3.1) (Leslie, 1945),

$$\mathbf{x}\left(t+1\right) = \mathbf{A}\mathbf{x}\left(t\right). \tag{3.1}$$

The vector $\mathbf{x}\left(t\right)$ is a population vector whose components describe the number of members in each state class at a given time t. The PPM $\mathbf{A} = (a_{ij})$, is a matrix containing the transition probabilities the population is subject to between two time steps, where:

$$a_{j,i} = \text{number of individuals in } j \text{ at time } t+1 \mid \text{one unit is in } i \text{ at time } t+1. \tag{3.2}$$

If there are n state classes then $\mathbf{x}\left(t\right) \in \mathbb{R}^{n\times 1}$ and $\mathbf{A} \in \mathbb{R}^{n\times n}$.

The state classes of a population can be defined by age, stage, size or a combination of these. The state class boundaries of a PPM are determined by this and classes are divided accordingly. The PPM $\mathbf{A}$ can be analyzed using matrix algebra techniques giving asymptotic and transient results, e.g. asymptotic growth rate (Caswell, 2001) or transient time bounds (Townley et al., 2007; Townley and Hodgson, 2008).

3.1.1 Assumptions Used in Constructing a Population Projection Matrix

The fitting of data to a prescribed model, such as the PPM, requires a number of assumptions to be made. Some of these are necessary for the model to reflect the

data, whilst some are necessary due to data collection methods. These assumptions are:

1. **Members of a population that begin within the same state class exhibit the same behaviour throughout the entire time period studied** (Caswell, 2001).

   This can also be stated as within size class information is irrelevant. The results from a PPM are often sensitive to the width of the state classes selected, due to this assumption. This assumption is reasonable when state classes are defined by natural biological processes, for example age or stage. However, a populations' dynamics are often described by size meaning that discrete size class boundaries are artificial (van der Meer, 1978; Moloney, 1986). These boundaries are determined from data by a reduction in errors, both sampling and distributive, rather than by biological processes. A numerical solution to this problem was suggested by Van der Meer (1978) and developed by Moloney (1986) to minimize both types of error (See Section 3.1.3 for further detail). However, this method can only reduce modelling errors, not eradicate them. It can result in two individuals being placed in the same state class which exhibits very different behaviour, and this may skew the results.

   Another consequence of this assumption is that if too few size classes are used, then individuals are able to pass through the size classes at an unrealistic speed. This is not the case for age or stage classes, where individuals will pass through at their natural speed.

2. **For deterministic PPMs the parameters estimated are time-invariant** (Caswell, 2001).

   This means that the parameters do not change with time and is a necessary assumption for parameterizing the probability transitions. This assumption is of particular importance when calculating and analyzing asymptotic results. For example, this is a key assumption when the PPM is projected over time to calculate the population's asymptotic rate of geometric growth, the

expected population size and state-structure (Caswell, 2001). If this assumption is broken then a stochastic PPM must be parameterized.

3. **A sample of a population is sufficient to describe the dynamics of an entire population** (Fiske et al., 2008).

   Often a PPM is calculated with a relatively small amount of data, so that parameter estimates are fitted using only a sampled population rather than the entire population, due to experimental costs and restrictions. Through the re-sampling of data, a confidence interval can be calculated for each of these estimates. There has also been analysis carried out to determine the minimum required data for confidence in these parameters (Fiske et al., 2008).

These assumptions are necessary in order to fit a PPM, but some of these assumptions are not biologically realistic or can introduce errors into the model. For example, the size-class boundaries are artificially determined and can introduce distribution errors to the model. This can be corrected through the use of IPMs.

3.1.2 Parameterization of a PPM

Prior to parameterization of a PPM, the biological structure of the model must be determined. This is achieved firstly by selecting the type of state classes; secondly the number of state classes must be decided; thirdly the boundaries of these state classes are chosen and only then can the generic matrix structure be selected according to the known behaviour of a population. Once the structure of the PPM is determined, then the parameters can be estimated. In the following sections each of these steps are described.

Biological information of a population must be used in order to determine which state-classes should be used to model a given population. Traditionally there are 3 main types of state-classes used: age, developmental stage and size. It is possible to use a combination of these, however the simplest PPMs use just one.

If a population's dynamics are determined by age or stage then there are natural biological boundaries to the age or stage-classes. In the case of age the bound-

aries are yearly, whilst for developmental stage they may, for example, be: pre-reproduction, reproduction and post-reproduction stage classes. If a population's dynamics are determined by size then the boundaries must be estimated from data. This can be achieved by following the Van der Meer (1978) algorithm, which was updated by Moloney (1986).

The Role of the Generic Population Projection Matrix

The dynamics of different species are often determined by different biological factors. In animal populations age is often the main factor used in describing the dynamics, for example as in the case of a Cheetah (Crooks et al., 1998), Chinook Salmon (Kareiva et al., 2000) and Peregrine Falcon (Wootton and Bell, 1992). Some species are best modelled by stages in its life cycle, for example reproductive stages. This is the case for the Loggerhead Turtle (Crouse et al., 1987) and the Desert Tortoise (Doak et al., 1994), as well as for some tree populations, like Californian Conifers (Van Mantgem and Stephenson, 2005). Finally, size can also describe a population, as in the case of Coral (McFadden, 1991), Savannah Grasses (O'Connor, 1993) and Herbs (Valverde and Silvertown, 1998). It is vital that the structure of these populations is reflected in the PPM that is used to model them. This forces the PPM into a particular generic structure with some entries being forced to zero if that transition is impossible. These structures are called the Generic PPMs (Table 3.1), which inform which parameters need to be fitted. It is often found that in addition to those entries biologically forced to zero there are some other entries that are numerically zero, as in this Thesis. This could be due to missing data where that transition is not occurring in the time period of the study.

PPM Type	State Classes	PPM	Examples of uses
Leslie	Age	$\begin{pmatrix} F & F & F & F & F \\ G & 0 & 0 & 0 & 0 \\ 0 & G & 0 & 0 & 0 \\ 0 & 0 & G & 0 & 0 \\ 0 & 0 & 0 & G & 0 \end{pmatrix}$	Chinook Salmon (Kareiva et al., 2000)
Leslie+	Age	$\begin{pmatrix} F & F & F & F & F \\ G & 0 & 0 & 0 & 0 \\ 0 & G & 0 & 0 & 0 \\ 0 & 0 & G & 0 & 0 \\ 0 & 0 & 0 & G & S \end{pmatrix}$	Cheetah (Crooks et al., 1998) Peregrine Falcon (Wootton and Bell, 1992)
Progression	Stage	$\begin{pmatrix} F & F & F & F & F \\ G & S & 0 & 0 & 0 \\ 0 & G & S & 0 & 0 \\ 0 & 0 & G & S & 0 \\ 0 & 0 & 0 & G & S \end{pmatrix}$	Desert Tortoise (Doak et al., 1994) Loggerhead Turtle (Crouse et al., 1987) Californian Conifers (Van Mantgem and Stephenson, 2005)
Growth	Size	$\begin{pmatrix} F & F & F & F & F \\ G & S & 0 & 0 & 0 \\ G & G & S & 0 & 0 \\ G & G & G & S & 0 \\ G & G & G & G & S \end{pmatrix}$	Vipers Bugloss (Klemow and Raynal, 1985) Western Gorse (Stokes et al., 2004)
Lefkovitch	Size	$\begin{pmatrix} F & F & F & F & F \\ G & S & R & R & R \\ G & G & S & R & R \\ G & G & G & S & R \\ G & G & G & G & S \end{pmatrix}$	Soft coral (McFadden, 1991) Savannah Grasses (O'Connor, 1993) Herbs (Valverde and Silvertown, 1998)

Table 3.1: Different generic PPMs, where G is where an individual grows from one state-class to another, S is where an individual remains in the same state-class or stasis, F is fecundity or reproduction, where an adult individual produces one or more new individuals, and R reflects the shrinkage of an individual. Finally zero entries in the generic PPMs represent transitions which are biologically impossible. As an example, the PPMs are assumed to have 5 state-classes, but this number can vary.

Parameter Estimation

There are a variety of methods, which can be applied in order to estimate the parameters of a PPM (Caswell, 2001; Gross et al., 2006). In this Thesis, the method suggested by Caswell (2001) is followed. The following assumes size classes are used, but this method could be used for stage or age classes as well. This method uses the following steps:

1. Data is divided into different transitions.

2. Each individual at time t is labelled by their size class i and each individual at time $t + 1$ is labelled by their size class j.

3. Label the nature of each transition:

    (a) if the individual has formed new individuals label as $F_{j,i}$,

    (b) if $i > j$ the individual has shrunk $(R_{j,i})$,

    (c) if $i < j$ the individual has grown $(G_{j,i})$,

    (d) if $i = j$ the individual has remained the same $(S_{i,i})$.

4. Collate data and sum the total number of all types of transitions.

5. Sum how many individuals are in each size class i at time t.

6. Calculate the transition probability by:

$$\text{p}(X_{j,i}) = \frac{\text{total number of } X_{j,i}}{\text{total number of individuals in size class } i}.$$

7. Enter these probabilities into the generic matrix.

3.1.3 Parameterization for *Montastraea annularis*

To demonstrate the parameterization of a PPM, this following section fits a model for one transition in the data set. Transition 4 (June 1999 to June 2000) was

selected as a variety of behaviour was exhibited in this transition and it will test the ability of a PPM to accommodate this in the model.

Biological Processes

The life cycle for $M.$ $annularis$ is given in Figure 3.1. With each increment in time a coral patch will undergo one of a number of processes, a patch can either:

1. Remain in the same size class, i, (Stasis) represented by $S_{i,i}$. These entries are found on the diagonal of the generic PPM (3.3).

2. Grow from stage class i to size class j where $j > i$ (Growth). This is represented by $G_{j,i}$ in the generic PPM (3.3), these entries are found on the lower diagonal.

3. Shrink from size class i to size class j where $j < i$ (Shrinkage). These entries are found in the upper triangle of the generic PPM (3.3) and are represented by $R_{j,i}$.

4. Fragment into more than one patch, where the original patch is of size i and the new patches formed are size j. These are represented by $D_{j,i}$ and are found on the upper triangle and diagonal.

5. Become extinct.

It was decided to use a Lefkovitch, matrix (Lefkovitch, 1965) as the generic matrix in order to incorporate all the possible processes (Table 3.1). This resulted in the generic matrix of the form:

$$\mathbf{A} = \begin{pmatrix} S_{1,1} + D_{1,1} & D_{1,2} + R_{1,2} & D_{1,3} + R_{1,3} & D_{1,4} + R_{1,4} & D_{1,5} + R_{1,5} \\ G_{2,1} & S_{2,2} + D_{2,2} & D_{2,3} + R_{2,3} & D_{2,4} + R_{2,4} & D_{2,5} + R_{2,5} \\ G_{3,1} & G_{3,2} & S_{3,3} + D_{3,3} & D_{3,4} + R_{3,4} & D_{3,5} + R_{3,5} \\ G_{4,1} & G_{4,2} & G_{4,3} & S_{4,4} + D_{4,4} & D_{4,5} + R_{4,5} \\ G_{5,1} & G_{5,2} & G_{5,3} & G_{5,4} & S_{5,5} + D_{5,5} \end{pmatrix}. \quad (3.3)$$
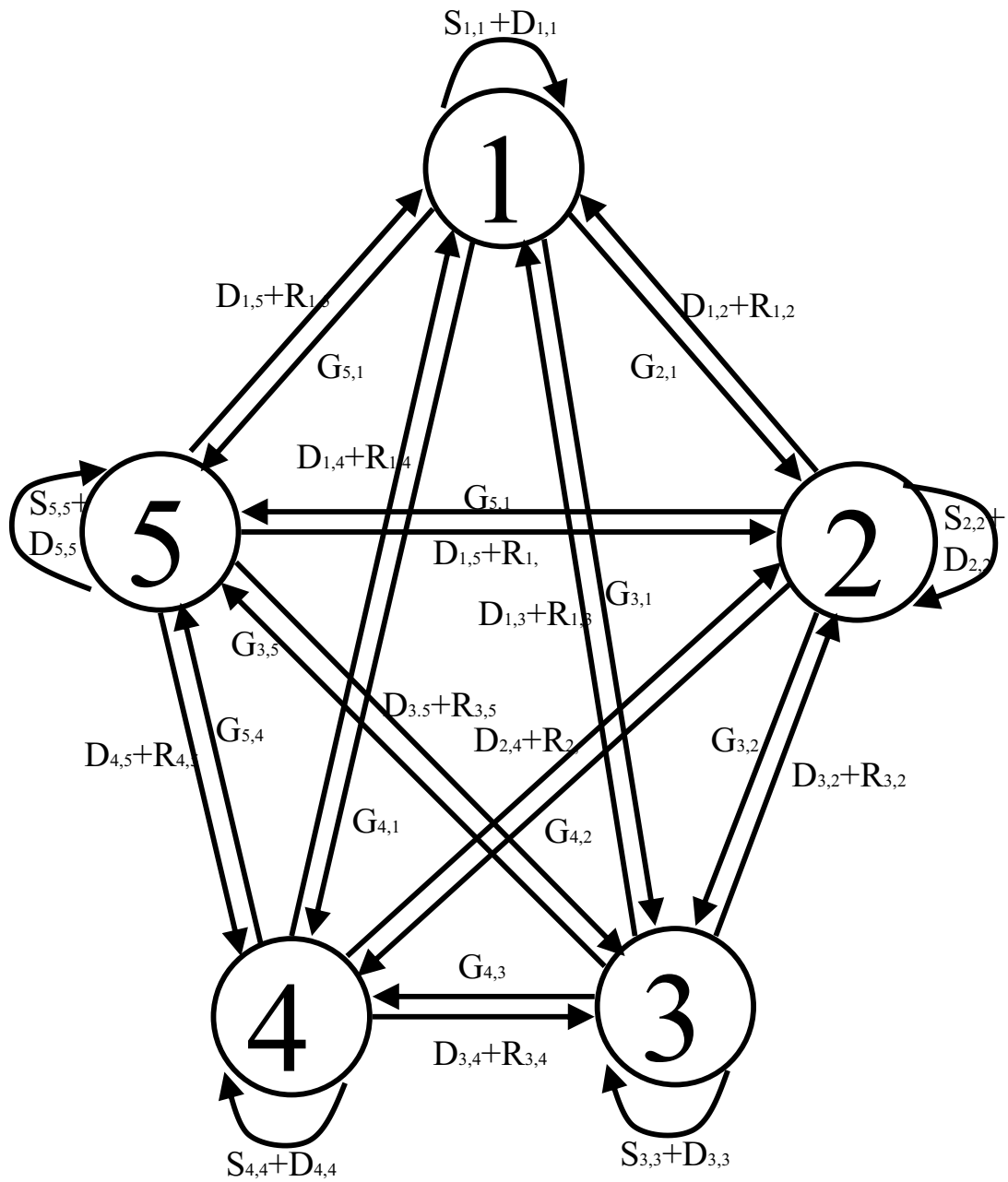
Figure 3.1: The life-cycle of *Montastraea annularis*. The circles, or nodes, define a size class and the arrows the possible transitions. $G_{j,i}$ represents growth, $D_{j,i}$ fragmentation, $S_{j,i}$ stasis and $R_{j,i}$ shrinkage, where j is the size class the arrow points towards and i where is originates.

This is an adapted Lefkovitch matrix, due to the inclusion of fragmentation rather than fecundity. Under fragmentation, a patch can produce fragments of any size smaller than itself. It is not restricted to producing patches in the first size class. Therefore $D_{j,i}$ is located in all upper triangular and diagonal entries. This generic matrix is for a PPM with 5 size classes, but it can easily be expanded for a greater number of size classes. In order to calculate the fragmentation transitions, $D_{j,i}$, the total number of fragments in size class j at time $t + 1$ were divided by the number of patches in size class i that are fragmenting at time t (Renken et al., 2010). Following a fragmentation event the resulting coral patches were treated independently. All estimates of $G_{j,i}$, $R_{j,i}$ and $S_{j,i}$ are probability estimates, based on a sample of the population, and therefore lie between zero and one. If there was no fragmentation each column of the matrix would sum to a maximum of one; if there was no mortality then the columns would sum to exactly one. Reproduction of *M. annularis* occurs at the colonial scale and not at the patch scale (Szmant, 1991), therefore reproduction was not included in the PPM.

Size Class Selection

In this section a varying number of size classes will be selected in order to demonstrate the issues surrounding selection of the correct boundaries. Between June 1999 and June 2000 there are 272 pieces of data, of which there are 16 growth events, 91 stasis events, 15 fragmentation and 107 shrinkage events. Coral patches in June 1999 ranged from $1cm^2$ to $426cm^2$. Three examples are given below which demonstrate the problems and the benefits of different methods.

The first method is to create a PPM with 2 size classes. The boundary of these size classes were chosen so that there was approximately an equal number of patches in each size class in June 1999, but ensured all patches of the same size were placed in the same size class, this method is the same used by Gardner et al. (2005). This gave the size classes: (I) $1 - 14cm^2$ and (II) $15 - 426cm^2$, resulting in the PPM:

$$\mathbf{A}_1 = \begin{pmatrix} 0.874 & 0.154 \\ 0.016 & 0.955 \end{pmatrix}. \tag{3.4}$$

This PPM over-estimates the stasis values, whilst underestimating growth and shrinkage. Only 2 growth events and 6 shrinkage events were captured by the model, compared to 16 and 107 observed in the data. The benefit of this model is the low sampling error in the parameter estimation, with 272 pieces of data used to fit 4 parameters.

As a PPM with a small number of size classes under-estimated growth and shrinkage events, a larger number of size classes will be used in the second model to try and capture these transitions. In this case, 10 size classes will be used and are chosen by dividing the entire range of sizes into 10 equal size classes to the nearest cm^2, as suggested by Edmunds and Elahi (2007). This gave the size classes: (I)$1 - 43cm^2$ (II)$44 - 86cm^2$ (III)$87 - 129cm^2$ (IV)$130 - 172cm^2$ (V)$173 - 215cm^2$ (VI)$216 - 258cm^2$ (VII)$259 - 301cm^2$ (VIII)$302 - 344cm^2$ (IX)$345 - 387cm^2$ (X)$388 - 426cm^2$, which forms the PPM:

$$
\mathbf{A}_2 = \begin{pmatrix}
0.933 & 0.375 & 0.409 & 0 & 0 & 0 & 0 & 0 & 4 & 0 \\
0 & 0.708 & 0.136 & 0 & 0 & 0 & 0 & 0 & 0 & 0 \\
0 & 0 & 0.727 & 0.167 & 0 & 0 & 0 & 0 & 0 & 0 \\
0 & 0 & 0 & 0.833 & 1 & 0 & 0 & 0 & 0 & 0 \\
0 & 0 & 0 & 0 & 0 & 0 & 0 & 0 & 0 & 0 \\
0 & 0 & 0 & 0 & 0 & 1 & 0 & 0 & 0 & 0 \\
0 & 0 & 0 & 0 & 0 & 0 & 1 & 0 & 0 & 0 \\
0 & 0 & 0 & 0 & 0 & 0 & 0 & 0 & 0 & 0 \\
0 & 0 & 0 & 0 & 0 & 0 & 0 & 0 & 0 & 0 \\
0 & 0 & 0 & 0 & 0 & 0 & 0 & 0 & 0 & 1
\end{pmatrix}. \tag{3.5}
$$

The abundance of zero-entries in this PPM shows the problem of choosing too many size classes as well as bad selection of size class boundaries. The increase in the number of size classes failed to capture the growth transitions as growth has been classified as stasis in this case, due to the poor selection of size class boundaries. The presence of $a_{i,j} = 1$ entries showed that the sampling error is high in estimating these parameters. Only one piece of data approximates each of these

transitions and therefore skews the parameter estimates. This example showed the problem of too many size class boundaries and the problem of selecting size classes failing to take into account the initial structure of the data.

In comparison a 10×10 PPM is created using a different method to select the size class boundaries. In this case, the method suggested by Gardner et al. (2005) is used. The size classes were selected to contain a similar number of data in June 1999, in this example approximately 25 coral patches. This resulted in the size classes: (I)$1 - 2cm^2$ (II) $3 - 5cm^2$(III)$6 - 7cm^2$ (IV)$8 - 9cm^2$ (V)$10 - 14cm^2$ (VI)$15 - 21cm^2$ (VII)$22 - 31cm^2$ (VIII)$32 - 56cm^2$ (IX)$57 - 106cm^2$ (X)$107 - 426cm^2$ and the PPM:

$$
\mathbf{A}_3 =
\begin{pmatrix}
0.63 & 0.09 & 0 & 0 & 0.04 & 0 & 0 & 0.08 & 0 & 0 \\
0 & 0.68 & 0.10 & 0.07 & 0.15 & 0 & 0.04 & 0 & 0.04 & 0.08 \\
0 & 0.05 & 0.81 & 0.27 & 0.04 & 0.04 & 0 & 0.04 & 0 & 0 \\
0 & 0 & 0.05 & 0.7 & 0.07 & 0.13 & 0 & 0.04 & 0 & 0.04 \\
0 & 0 & 0 & 0 & 0.63 & 0.08 & 0 & 0.08 & 0 & 0.08 \\
0 & 0 & 0 & 0 & 0.07 & 0.71 & 0.25 & 0.08 & 0.04 & 0.21 \\
0 & 0 & 0 & 0 & 0 & 0.04 & 0.63 & 0.2 & 0.12 & 0.04 \\
0 & 0 & 0 & 0 & 0 & 0 & 0.04 & 0.56 & 0.08 & 0.04 \\
0 & 0 & 0 & 0 & 0 & 0 & 0 & 0 & 0.81 & 0.13 \\
0 & 0 & 0 & 0 & 0 & 0 & 0 & 0 & 0 & 0.75
\end{pmatrix}. \tag{3.6}
$$

In this case, selecting the size classes differently captured more growth and stasis events than $\mathbf{A}_2$. This showed the benefit that can come from a greater number of size classes, however there are still some transitions missing which are biologically probable, in particular $G_{2,1}$, $G_{5,4}$, $G_{9,8}$ and $G_{10,9}$. This shows that these transitions may be missing in the data set or that a greater number of size classes are needed to capture these in the model. This model also shows the problem of a high sampling error, there is low confidence in these parameter estimates as 272 pieces of data has been used to fit at most 100 parameters. In fact only 45 entries were non-zero in this model, but this is still only on average 6 pieces of data per parameter, this

could lead to high inaccuracies in parameter estimation.

These three examples show the problems of selecting too few or too many size classes as well as the issue of selecting the wrong method to determine the size class boundaries. It is for this reason that the Van der Meer and Moloney algorithm described in the following section is used. This balances the width of the size classes against the amount of data to estimate the parameters.

Selection of Size Classes - the Van der Meer and Moloney Method

To select size class boundaries two errors are minimized. In doing this errors in the predicted dynamics due to the selection of boundaries is reduced. The two errors of interest are:

1. Sampling Error (SE): caused by a lack of data in each size class. In reducing the sampling error, size classes are restricted to a width that ensures sufficient data is present to accurately estimate parameters.

2. Distribution Error (DE): caused when size classes are too wide and information on movement between size classes is lost. Through narrowing the width of the size classes this error is reduced.

The widths of the size classes are optimized to reduce both the sampling and distribution errors. This is achieved by the minimization of the total error (TE) given by

$$TE = SE + DE. \tag{3.7}$$

It is assumed that the two errors, SE and DE, are equally important to minimize, but one could be weighted in the analysis if it is more important.

To calculate these two errors we first need to define some variables. The data are sampled at times $t = 1, ..., T$, for individuals $i = 1, ..., N$ where N is the total number of individuals. The size of an individual i at time t is $m_i(t)$, and the change in size from time t to $t + 1$ is given by $d_i = m_i(t + 1) - m_i(t)$. The size interval, Ω, of a given size-class, is defined as $\Omega = [M_{min}, M_{max}]$, where M_{min} is the lower

boundary of size-class Ω and M_{max} is the upper boundary of Ω. The mid-point of this interval is $M_{mid} = \frac{M_{min}+M_{max}}{2}$.

Two indicators are calculated; firstly for each $i \in N$ to determine if an individual i starts in Ω, $s_i(t)$, and secondly if an individual which starts in Ω remains in Ω, $r_i(t)$:

$$s_i(t) = \begin{cases} 1 & \text{if } m_i(t) \in \Omega \\ 0 & \text{otherwise} \end{cases}, \tag{3.8}$$

$$r_i(t) = \begin{cases} 1 & \text{if } s_i(t) = 1 \text{ and } m_i(t+1) \in \Omega \\ 0 & \text{otherwise} \end{cases} \tag{3.9}$$

The probability, P, that an individual starts in Ω and remains in Ω is $\widehat{P}$ (Moloney, 1986):

$$\widehat{P} = \frac{\sum_t \sum_i r_i(t)}{\sum_t \sum_i s_i(t)}, \tag{3.10}$$

and the probability of an individual starting in Ω and then leaving Ω is $\widehat{Q} = 1 - \widehat{P}$. When the distribution error is zero, $\widehat{P}$ is independent of Ω.

If it is assumed that all individuals in Ω begin at size M_{mid}, then an individual i at time $t+1$ will have size $m_i^*(t+1) = M_{mid} + d_i(t)$. In this case indicator (3.9) is re-defined to be:

$$r_i^*(t) = \begin{cases} 1 & \text{if } s_i(t) = 1 \text{ and } m_i^*(t+1) \in \Omega \\ 0 & \text{otherwise} \end{cases}, \tag{3.11}$$

and the probability of an individual starting at M_{mid} and remaining in Ω is:

$$\widehat{P}_{mid}(t) = \frac{\sum_i r_i^*(t)}{\sum_i s_i(t)}. \tag{3.12}$$

Again the probability that an individual starts at M_{mid} and leaves Ω is $\widehat{Q}_{mid}(t) = 1 - \widehat{P}_{mid}(t)$.

Given (3.10) and (3.12), Moloney (1986) states that the Distribution Error is calculated as:

$$DE = \frac{1}{T-1} \sum_t \frac{1}{2} \left(\left(\frac{\widehat{P}_{mid}(t) - \widehat{P}}{\widehat{P}} \right)^2 + \left(\frac{\widehat{Q}_{mid}(t) - \widehat{Q}}{\widehat{Q}} \right)^2 \right). \qquad (3.13)$$

The calculation of the Sampling Error is more involved. It requires a random sample of individuals with replacement to be taken from those individuals which start in Ω, *i.e.* for those individuals where $s_i(t) = 1$. Then the size of an individual, i, from the kth random sample at time $t+1$ is $m_{ik}^{\dagger}(t+1)$. Then $r_{ik}^{\dagger}(t)$ is those which remain in Ω at time $t+1$ from the sample k:

$$r_{ik}^{\dagger}(t) = \begin{cases} 1 & \text{if } s_i(t) = 1 \text{ and } m_{ik}^{\dagger}(t+1) \in \Omega \\ 0 & \text{otherwise} \end{cases} \qquad (3.14)$$

For sample k, the probability that a patch starts and remains in Ω, is defined as:

$$\widehat{P}_k^{\dagger}(t) = \frac{\sum\limits_i r_{ik}^{\dagger}(t)}{\sum\limits_i s_i(t)}, \qquad (3.15)$$

and $\widehat{Q}_k^{\dagger}(t) = 1 - \widehat{P}_k^{\dagger}(t)$. The Sampling Error is then defined by Moloney (1986) as:

$$SE = \frac{1}{K(T-1)} \sum_{t=1}^{T-1} \sum_{k=1}^{K} \frac{1}{2} \left(\left(\frac{\widehat{P}_k^{\dagger}(t) - \widehat{P}}{\widehat{P}} \right)^2 + \left(\frac{\widehat{Q}_k^{\dagger}(t) - \widehat{Q}}{\widehat{Q}} \right)^2 \right). \qquad (3.16)$$

In calculating both the Distribution Error (3.13) and Sampling Error (3.16) the Total Error is calculated. As the width of Ω decreases the DE will approach zero and the SE will increase. As the width of Ω increases the SE will approach zero and the DE will increase. To calculate the size-class boundaries, the minimum size in a size class is selected, M_{min}, and the TE is calculated for all possible M_{max} values and the M_{max} which minimizes the TE is chosen. The algorithm is then re-run with a new M_{min} which is slightly larger than the previous M_{max} in order to determine the next size class. This method is used whilst creating a PPM for the reef-building coral *Montastraea annularis* in Chapter 4.

The van der Meer and Moloney algorithm was applied to all data from June 1998 to January 2003. For the most accurate parameterization of PPMs this analysis should be carried out for each PPM created, as this would ensure the capturing of as many growth and shrinkage transitions as possible. However, this would not allow the comparison of results between PPMs, which is the focus of the analysis in Chapters 4 and 5. Therefore, it was decided to choose one set of size classes to be used in the parameterization of all PPMs in this Thesis. Five size classes were selected through the minimization of errors and are used in all PPMs in this Thesis (Table 3.2).

Size Class	Boundaries (cm^2)
I	1-3
II	4-12
III	13-48
IV	49-153
V	≥ 154

Table 3.2: Size Classes for the PPMs, as determined by the van der Meer and Moloney algorithm.

Using the size class boundaries selected by the van der Meer and Moloney algorithm, for data between June 1999 and June 2000, leads to the PPM:

$$\mathbf{A}_4 = \begin{pmatrix} 0.658 & 0.062 & 0.039 & 0.042 & 0 \\ 0.026 & 0.901 & 0.158 & 0.083 & 0 \\ 0 & 0.012 & 0.852 & 0.188 & 0.571 \\ 0 & 0 & 0 & 0.833 & 0 \\ 0 & 0 & 0 & 0.021 & 0.857 \end{pmatrix}. \qquad (3.17)$$

This PPM captures 3 of the growth transitions, but confidence in the parameters is higher than in $\mathbf{A}_3$, as only 25 parameters were fitted as opposed to 100. There are some missing transition estimates, which could be because of a lack of data on these transitions or because of the selected boundaries. There are two solutions to this problem. Firstly, a PPM of size 426x426 could be estimated with $1cm^2$ size classes, but a lack of data would result in uncertain parameter estimates. The

second solution is to use an Integral Projection Model. In this latter method, fewer parameters need to be estimated and statistical curve fitting can solve the problem of missing transitions. This method is described in more detail in the next section.

3.2 Integral Projection Models

The PPM is a popular modelling tool in population ecology with at least 171 species modelled in this way by 652 PPMs (Stott et al., 2010b). There are many problems in their formulation and parameterization, especially for species where size determines their dynamics. The primary problem is in the discretization of size classes and the selection of boundaries. These problems were shown in the parameterization of a PPM for *M. annularis*. The selection is a balancing act reducing sampling and distribution errors. There is also a problem in the assumption that, within size class dynamics is irrelevant. This allows some individuals to pass through multiple size classes unrealistically quickly, ignoring differences in individuals at either end of the size class. The PPM also cannot deal with missing transitions, this can be from missing data or through discretization. All of these problems can be solved through the fitting of an Integral Projection Model. In the following sections the IPM will be defined and modelling techniques will be discussed. Finally an example of fitting an IPM will be given.

The Integral Projection Model (IPM) is a continuous-state, discrete-time model that is an alternative to the PPM (Easterling et al., 2000). The IPM is particularly used where populations are determined by size (Easterling et al., 2000) or by a combination of discrete and continuous factors (Childs et al., 2003, 2004; Ellner and Rees, 2006). In this Thesis, the population is determined by size (Chapter 1). Hence, from here on it is assumed the IPM is a size-determined IPM.

Between time t and $t+1$ a population undergoes a number of transitions in size. These may include growth, survival, fecundity or fragmentation. In an IPM each of these biological processes are individually estimated, as opposed to a PPM where all biological processes in each PPM entry are estimated together. In an IPM a function $\mathbf{p}(y,x)$ describes both the growth and survival of individuals in a

population, which were size x at time t, and are now size y at time $t+1$, whilst a function $\mathbf{f}(y, x)$ describes the fecundity or the creation of new individuals. Thus the equivalent projection equation of (3.1) for an IPM is:

$$\mathbf{n}(y, t+1) = \int_\Omega \left[\mathbf{p}(y, x) + \mathbf{f}(y, x) \right] \mathbf{n}(x, t) \, dx, \tag{3.18}$$

this is more generally stated as:

$$\mathbf{n}(y, t+1) = \int_\Omega \mathbf{k}(y, x) \mathbf{n}(x, t) \, dx. \tag{3.19}$$

Here the non-negative probability density function $\mathbf{k}(y, x)$ is the kernel of the integral describing all transitions between sizes x at time t and y at time $t+1$. The range of possible sizes of the population is given by Ω and $\mathbf{n}(x, t)$ is a density function describing the distribution of population size at time t. The number of individuals between sizes x and $x + dx$ at time t is $\mathbf{n}(x, t)dx$.

The IPM is a form of an integrodifference equation. These, unlike the IPM, have a long history in Mathematics. They are not only studied for their own sake but also have applications in spatial ecology (Caswell, 2001; Kot and Schaffer, 1986; Kot, 1992; Kot et al., 1996; Neubert et al., 1995). In the case of spatial spread the model is firstly divided into the difference equation describing the spread of each individual member, and secondly the integration of these difference equations over the entire spatial area. These model the dispersion of a population over a given area (Neubert et al., 1995). The IPM is the discrete time form of the continuous-time integrodifference equation where the spatial re-distribution is replaced by size re-distribution.

3.2.1 Assumptions of the Integral Projection Model

Many of the assumptions required to model populations with an IPM are similar to those required in modelling PPMs: vital rates are assumed to be time-invariant and samples are assumed to accurately model an entire population (Easterling et al., 2000). Some assumptions need to be tighter for an IPM than a PPM, for example

it is assumed that two individuals that start at the same state will exhibit the same behaviour throughout the study (Easterling et al., 2000). This is a more realistic assumption than the PPM, where two individuals in the same state class exhibit the same behaviour, but it still fails to account for genetic differences between two individuals.

3.2.2 Parameterization of an IPM

The life-cycle of a population determines the functional forms of $\mathbf{k}(y, x)$. These functions are then fitted using well accepted statistical methods (Easterling et al., 2000). Prior to fitting, assumptions about the error structure in the data must be made. Each of these functions are fitted and combined in a pre-selected form to parameterize the IPM. Each stage of this process is described in the following sections.

Functional Forms

The kernel, $\mathbf{k}(y, x)$ is divided primarily into $\mathbf{p}(y, x)$, the survival-growth element of the populations dynamics, and $\mathbf{f}(y, x)$, the function which describes how new individuals are formed, such that $\mathbf{k}(y, x) = \mathbf{p}(y, x) + \mathbf{f}(y, x)$. They describe how an individual x at time t becomes size y at time $t + 1$.

These functions in turn are further subdivided. How this is achieved varies from population to population. Often there are some similarities in the forms that these functions take. In the case of the survival-growth function it is common (Easterling et al., 2000; Ellner and Rees, 2006; Kuss et al., 2008) to state that:

$$\mathbf{p}(y, x) = s(x)\mathbf{g}(y, x), \tag{3.20}$$

where $s(x)$ is a probability density function describing the survival of individuals, the probability that an individual of size x at time t will survive to time $t + 1$. The change in size of an individual is described by the growth function $\mathbf{g}(y, x)$, this takes an individual of size x at time t and gives the size y at time $t + 1$. This function

does not only take into account growth of individuals (where $y > x$) but also the negative growth of individuals (where $y < x$). As an individual that survives must have a size then $\int_{\Omega} \mathbf{g}(y, x) dx = 1$. Alternatively, if reproduction is fatal:

$$\mathbf{p}(y, x) = s(x)(1 - p_f(x))\mathbf{g}(y, x), \qquad (3.21)$$

is a popular selection (Hesse et al., 2008), where $p_f(x)$ is a probability density function describing the probability that an individual of size x at time t will reproduce.

There is a greater variety in the functional forms of $\mathbf{f}(y, x)$ due to the differing strategies used by species to produce new individuals (Table 3.3 summarizes the published forms). Although there are some differences in structure, many contain similar elements, for example the probability that a new offspring is produced, the number of offspring produced and the distribution of these offspring occur in all models. This can help inform the structure of the function for a population, but it must be noted that these are for varying plant populations and other species, like coral, may require further functions to be fitted.

Parameter Estimation

Assumptions on the shape of the selected functions can aid parameter estimation. These assumptions come from the data structure alongside information from previous studies where certain functions typically follow particular probability density functions. Estimation of parameters is achieved through the following steps:

1. Select which function needs to be estimated.

2. Make assumptions about error structure, both from data and from traditional forms.

3. Fit the model using statistical analysis by:

    (a) Testing for non-linearities against linear terms, as well as against different models with different error structures.

	$\mathbf{f}(y,x)$	Functions
1	$f_1(x)f_2(x,y)$	$f_1(x)$: Mean number of offspring $f_2(y,x)$: Offspring sizes
2	$p_e s(x) p_f(x) f_n(x) f_d(y,x)$	p_e: Probability of establishment $s(x)$: Probability of survival $p_f(x)$: Probability of flowering $f_n(x)$: Number of seeds produced $f_d(y,x)$: Offspring distributions
3	$f_n(x)c(f_n)f_d(y,x)$	$f_n(x)$: Number of flowers produced $c(f_n)$: Relationship between flowering and recruits $f_d(y,x)$: Offspring distribution
4	$p_s(x)p_f(x)f_v(x)f_{vd}(y)$	$p_s(x)$: Probability of survival $p_f(x)$: Probability of flowering $f_v(x)$: Number of offspring $f_{vd}(y)$: Offspring sizes
5	$p_e s(x) p_f(x) f_n(x) f_d(y)$	p_e: Probability of establishment $s(x)$: Probability of survival $p_f(x)$: Probability of flowering $f_n(x)$: Number of flowers $f_d(y)$: Offspring distribution
6	$s(x)f_n(x)p_E f_d(y)$	$s(x)$: Probability of survival $f_n(x)$: Number of flowers p_E: Number of seeds becoming seedlings $f_d(y)$: Offspring distribution
7	$f_p(x)f_n(x)s_e f_d(y)$	$f_p(x)$: Probability of flowering $f_n(x)$: Number of flowers s_e: Seedling establishment $f_d(y)$: Offspring distribution

Table 3.3: The varying forms which the function $\mathbf{f}(y,x)$ can take. 1. Easterling et al. (2000) 2. Childs et al. (2003; 2004) 3. Williams and Crone (2009) 4. Hesse et al. (2008) 5. Kuss et al. (2008) 6. Miller et al. (2009) 7. Ramula et al. (2009)

(b) Selecting the model through the application of the χ^2 test using 95% significance.

4. Repeat for all functions.

Numerical Integration of an Integral Projection Model Kernel.

The IPM is an infinite-dimensional model, which requires numerical integration in order to gain results. This creates a 'giant' matrix which can be analyzed using slightly adapted methods for PPMs. In order to achieve this, the eigenvalue equation (3.22) must be solved:

$$\int_L^U \mathbf{k}(y,x)\mathbf{n}(y)dy = \lambda\mathbf{n}(x), \tag{3.22}$$

by the numerical solution:

$$\sum_{j=0}^m w_j k(y_i, y_j)\overline{n}(y_j) = \overline{\lambda}\overline{n}(y_i), \tag{3.23}$$

for $i = 1, ..., m$. This can be summarized by:

$$\mathbf{KD}\overline{n} = \overline{\lambda}\overline{n}, \tag{3.24}$$

where $K_{ij} = k(y_i, y_j)$, $\mathbf{D} = diag(w_0, w_1, ..., w_n)$ and $\overline{n} = (\overline{n}(y_0), ..., \overline{n}(y_m))^T$. This method is known as the quadrature method, where y_i are the quadrature mesh points and w_j the quadrature weights. Given the range of values $\Omega = [L, U]$, the boundaries of the mesh points, β_i are:

$$\beta_i = L + \frac{i}{n}(U - L), \tag{3.25}$$

where $i = 0, 1, ..., n$, with the corresponding mid-points:

$$y_i = \frac{\beta_{i-1} + \beta_i}{2}. \tag{3.26}$$

If $\mathbf{M} = \mathbf{KD}$ then $M_{ij} = \frac{(U-L)k(y_i, y_j)}{n}$, for $i = 1, ..., n$.

To calculate the numerical approximation of the IPM the upper and lower boundaries [L,U] must be determined. The boundaries are determined by the size of the observed data, where the smallest value observed is l and the largest value observed is u. The two main methods which have been adopted are:

1. $[L, U] = [0.9l, 1.1u]$, this allows for both shrinkage and growth of individuals. The restriction comes for growing populations where some larger individuals will ultimately be larger than $1.1u$ (Rees and Rose, 2002).

2. $[L, U] = [l - 3\sigma, u + 3\sigma]$, where σ is the standard deviation of the sizes at the beginning of the study (Easterling et al., 2000).

Another issue of numerical integration is the number of mesh points used to integrate the kernel. This requires a balance between using a large number of mesh points to ensure accuracy and the computational cost of a large mesh size. In order to decide on the number of mesh points a particular asymptotic indicator is selected, normally the population growth rate (see Section 3.3), and calculated for varying mesh sizes. When the indicator converges to a predetermined accuracy level then the mesh size where this is first achieved is used in the 'giant' matrix approximation.

The determination of these boundaries of integration and the number of mesh points required can lead to very different asymptotic results. These issues are discussed in Section 7.3.1 using the example of the IPM created in the following section.

3.2.3   Parameterization of an IPM for *Montastraea annularis*.

To illustrate the issues surrounding parameterization of an IPM, one is created for *M. annularis*. This is created for all transitions where a hurricane did not occur, known as the non-hurricane IPM A_{No}.

Biological Processes

Between two time steps, t and $t + 1$, a coral patch can experience:

Function	Biological Relevance
$s(x)$	Probability of survival
$\mathbf{g}(y, x)$	Growth (and shrinkage) of patches
$p_f(x)$	Probability of fragmentation
$n_f(x)$	Number of fragments
$\mathbf{f}_d(y, x)$	Fragment distribution
$f_s(x)$	Family size of fragments
$\mathbf{f}_d(y, \frac{x}{n})$	Fragment distribution
$\mathbf{f}_d(y, x, n)$	Fragment distribution

Table 3.4: The functions used in the construction of an IPM for *M. annularis*.

- Survival (A patch of size x survives between 2 time periods),

- Mortality (A coral patch of size x dies before time $t + 1$),

- Growth (A patch of size x grows to size y at time $t + 1$),

- Shrinkage (A patch of size x shrinks to size y at time $t + 1$),

- Fragmentation (A patch of size x fragments into 2 or more patches sizes y_1, y_2, ...),

- There is no fecundity at the patch scale, instead this occurs at the colonial scale (Szmant, 1991).

These biological processes can be grouped together in order to form the skeleton for the IPM. This is shown in Figure 3.2. and the functions that need to be parameterized are given in Table 3.4.

Possible Functional Forms of the IPM

Integral Projection Models have not previously been used on coral populations, instead they have been applied to plant and tree populations. As a result some of the functional forms in literature (Table 3.3) are not applicable to coral populations. As coral populations have never been fitted with an IPM five different models will be tested and reviewed to decide which model will be used in this Thesis. These different forms are:
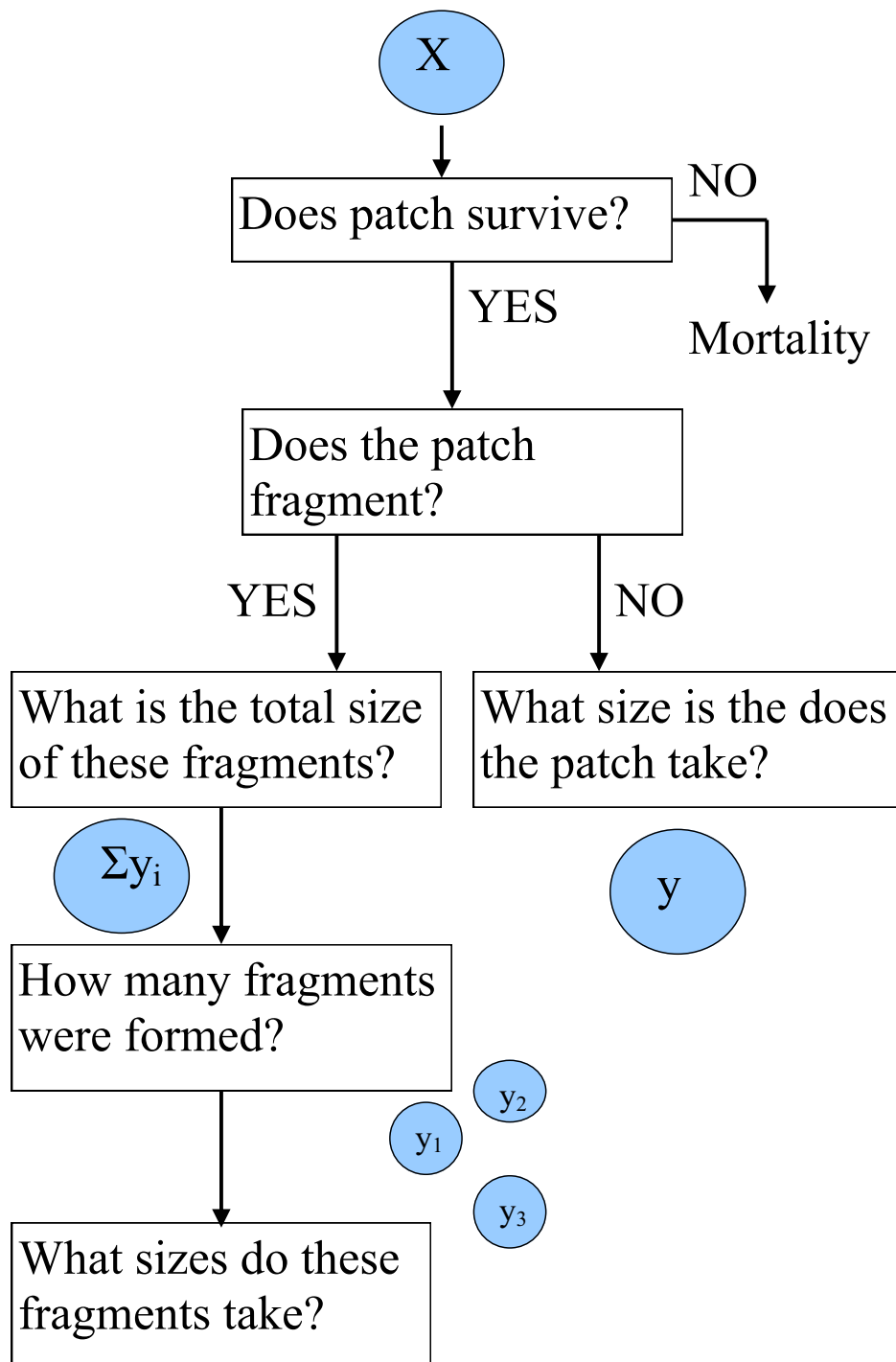
Figure 3.2: A decision tree showing the differing paths a *M. annularis* patch could take between two time steps.

I. $s(x)\mathbf{g}(y,x) + p_f(x)n_f(x)\mathbf{f}_d(y,x)$

   A form similar to that for plant populations both in the survival-growth and fragmentation form.

II. $s(x)\mathbf{g}(y,x) + f_s(x)p_f(x)n_f(x)\mathbf{f}_d(y,x)$

   As method I, but with the inclusion that the family size of the fragments is important in determining the contribution of fragmentation to the kernel.

III. $(1 - p_f(x))s(x)\mathbf{g}(y,x) + s(x)f_s(x)p_f(x)n_f(x)\mathbf{f}_d(y,x)$

   Assumes that a patch must not fragment in order to either grow or shrink and also that a patch must survive if it is going to fragment.

IV. $(1 - p_f(x))s(x)\mathbf{g}(y,x) + s(x)f_s(x)p_f(x)n_f(x)\mathbf{f}_d(y,\frac{x}{n})$

   A change in the fragment distribution from method III, where the size of new fragments does not just depend on the size of the 'parent' patch but on the average size of the 'parent' patch, when divided into the number of fragments produced.

V. $(1 - p_f(x))s(x)\mathbf{g}(y,x) + s(x)f_s(x)p_f(x)n_f(x)\mathbf{f}_d(y,x,n)$

   The fragments distribution is changed so that it is dependent on both the parent patch size and the number of patches produced.

Parameter Estimation

Before the functions can be combined to form the kernel, each individual function must be fitted. Below follows a description of how these functions are fitted, with parameter estimates given in Table 3.5. It must be noted that the size of coral patches approximately follows a log-normal distribution, as a result the statistical models were fitted to the log-size of the coral patch.

Survival. The probability that a patch survives is estimated by a logistic regression. In order to fit the model each coral patch was assigned a value of 1 if the patch survived to time $t + 1$ and a value of 0 was assigned if the patch died. If a patch fragmented the 'parent' patch was assumed to have survived and assigned a value of 1. The fitted linear model is then $\log\left(\frac{s(x)}{1+s(x)}\right) = a + bx$, with quadratic

terms being rejected ($P = 0.7042$). This fitted model (Figure 3.3 and Table 3.5) gives the probability that a patch of size x at time t will survive.

Growth. The relationship between size at time t and size $t + 1$ needs to be determined. The data are plotted (Figure 3.5) and show a near linear relationship. This shows that there is only small scale change in size. The relationship was fitted with a Gaussian assumption as the residuals followed a log-normal distribution (Figure 3.7). The fitted mean was linear (quadratic terms were rejected (P=0.344)) such that $\mu(x) = a + bx$. The variance, fitted such that $\sigma^2 = c + dx$, was dependent on the patches size at time t, but was not dependent on quadratic terms (P=0.8827, Figure 3.6). The combination of the mean and variance in the Gaussian distribution gives: $g(y, x) = \frac{1}{\sqrt{2\pi\sigma^2(x)}} exp\left(\frac{-(y-\mu(x))^2}{2\sigma^2(x)}\right)$.

Probability of Fragmentation. Each coral patch at time t was assigned a value of 0 if the patch did not fragment or 1 if the patch did fragment. This was estimated by a logistic regression and is of the form $\log\left(\frac{p_f(x)}{1+p_f(x)}\right) = a + bx$, with quadratic terms rejected (P=0.054). Fragmentation is rare (Figure 3.4 and Table 3.5) and so the fitted probability function is very small.

Number of Fragments. Of those patches which fragment, the number of fragments X produced is fitted. The mean number of fragments was $E(X) = 2.4$, with variance $VAR(X) = 0.67$. As $E(X) > VAR(X)$, the number of fragments is instead fitted using a Poisson distribution for a transformed variable $Y = X - 2$, giving mean $E(Y) = 0.4$ and $VAR(Y) = 0.67$. Although $VAR(Y) > E(X)$ the over-dispersion is assumed to not be a problem. This gives the fitted function $n_f(Y) = exp(a+bY)$ for the transformed variable. In this case the linear terms are not significant (P=0.07) and so the fitted function is of the form: $n_f(Y) = exp(a)$ or $n_f(x) = 2 + exp(a)$ and is independent of the size of the patch which fragments (Figure 3.8 and Table 3.5).

Function	Fitted Model
$s(x)$	$0.2392(0.2844) + 1.0669(0.1474)x$
$\mathbf{g}(y, x)$	$-0.1198(0.0242) + 1.0129(0.0076)x$
σ^2	$exp(-3.3197(0.1543) - 0.6000(0.0482)x)$
$p_f(x)$	$-5.9059(0.7673) + 0.6730(0.1867)x$
$n_f(x)$	$-0.9163(0.3536)$
$\mathbf{f}_d(y, x)$	$-0.1527(0.5772) + 0.6439(0.1383)x$
σ^2	1.2683
$\mathbf{f}_d(y, \frac{x}{n})$	$0.5721(0.4612) + 1.1439(0.2665)(x/n)$
$\mathbf{f}_d(y, x, n)$	$0.2423(0.5519) + 0.8079(0.1399)x - 0.3977(0.1361)n$
$f_s(x)$	$0.2102(0.3682) + 0.8592(0.0905)x$

Table 3.5: A list of the fitted parameters for A_{No}, standard errors are given in brackets.

Family Size. The total area of the fragments produced from one 'parent' patch is related to the size of the patch (Figure 3.9). As the 'parent' patch size increases so does the total area of the fragments. This is fitted assuming a Gaussian error structure such that $f_s(x) = a + bx$, with quadratic terms rejected (P=0.20).

Fragment Size Distribution. The distribution of fragments could take three different forms: The size of the fragments could depend completely on the patch size of the 'parent' patch; they could depend on the size of the 'parent' patch divided by the number of fragments it produced; or finally they could depend on the number of fragments and the 'parent' patch size. All of these were assumed to follow a Gaussian distribution, with the variance taken to be the variance in fragment sizes at time $t+1$ (Table 3.5). However the size of the fragments increases as the size of the parent patch increases, therefore three separate mean functions were fitted for each of these cases (Figure 3.10). This gives the functions of the forms: $\mu(x) = a + bx$, with quadratic terms rejected (P=0.22), $\mu(\frac{x}{n}) = c + d(\frac{x}{n})$, with quadratic terms rejected (P=0.72) and finally $\mu(x, n) = e + fx + gn$. Each of these can be inserted into the fragment distribution: $f_d(y, .) = \frac{1}{\sqrt{2\pi\sigma^2}}exp(\frac{-(y-\mu(.))^2}{2\sigma^2})$ (Table 3.5).

In order to select the functional form used in this Thesis, asymptotic indicators
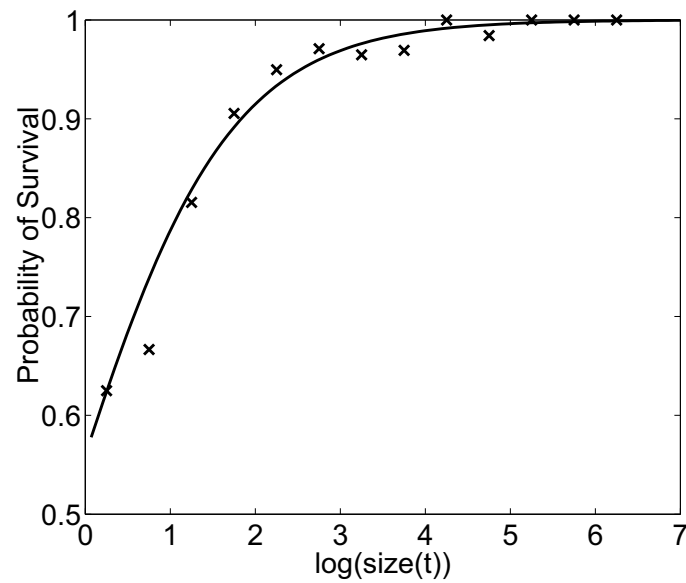
Figure 3.3: The fitted probability of survival $s(x)$ model for the IPM A_{No}. Crosses mark points from data, whilst the solid lines denote the models fitted to the data.
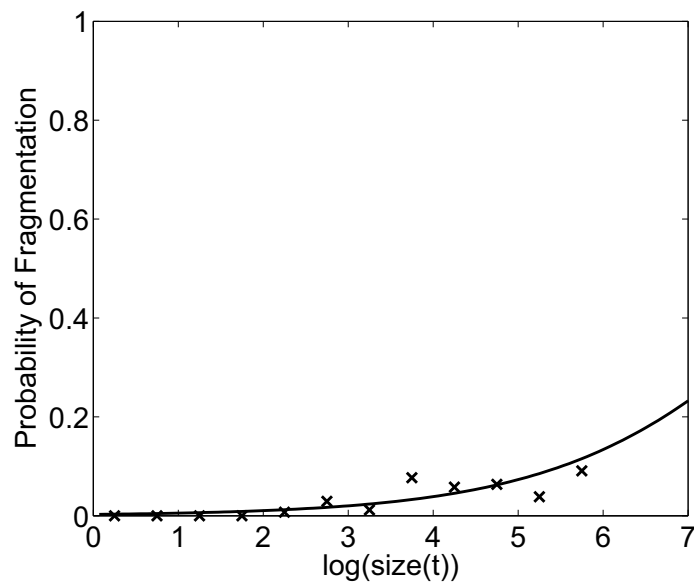
Figure 3.4: The fitted probability of fragmentation model $p_f(x)$ for the IPM A_{No}. Crosses mark points from data, whilst the solid lines denote the models fitted to the data.
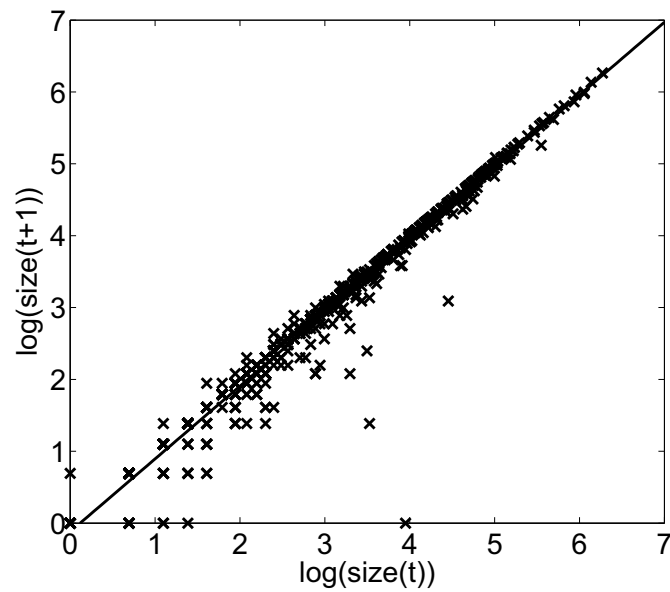
Figure 3.5: The fitted mean growth model $\overline{\mathbf{g}(y, x)}$ for the IPM A_{No}. Crosses mark points from data, whilst the solid lines denote the models fitted to the data.
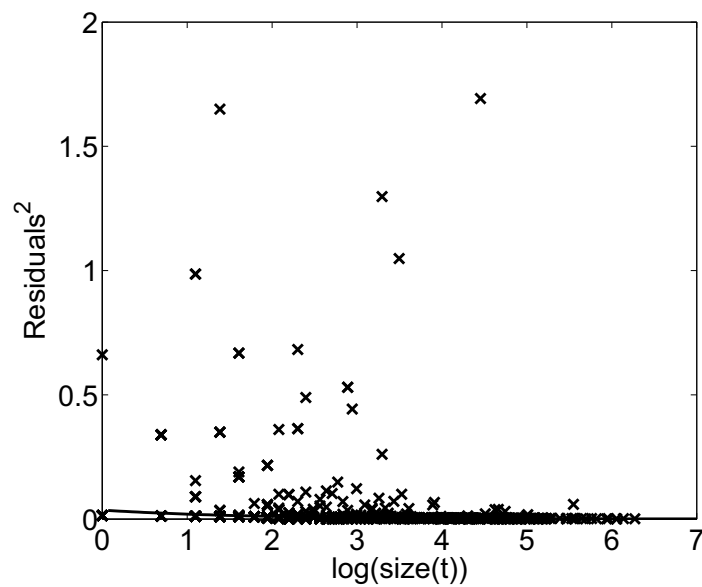
Figure 3.6: The fitted variance of growth model, $\log(\sigma^2(\mathbf{g}(y, x)))$ for the IPM A_{No}. Crosses mark points from data, whilst the solid lines denote the models fitted to the data.
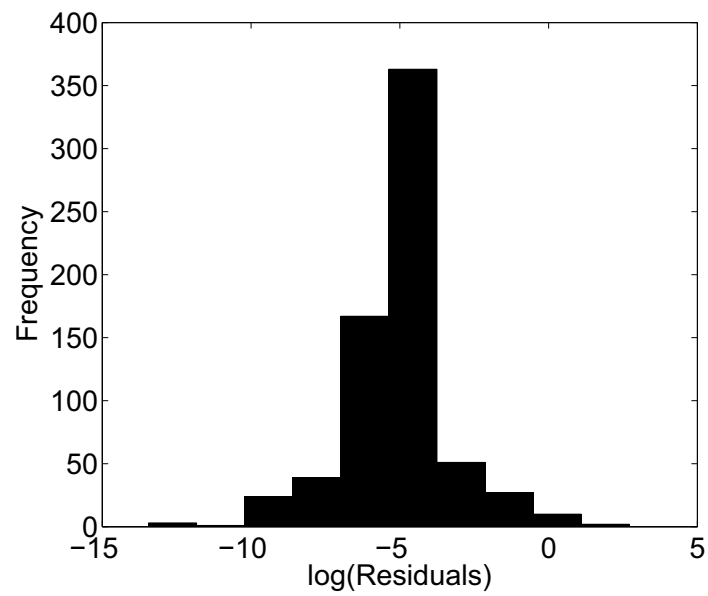
Figure 3.7: The log-residuals from the fitted mean growth model for the IPM A_{No}.
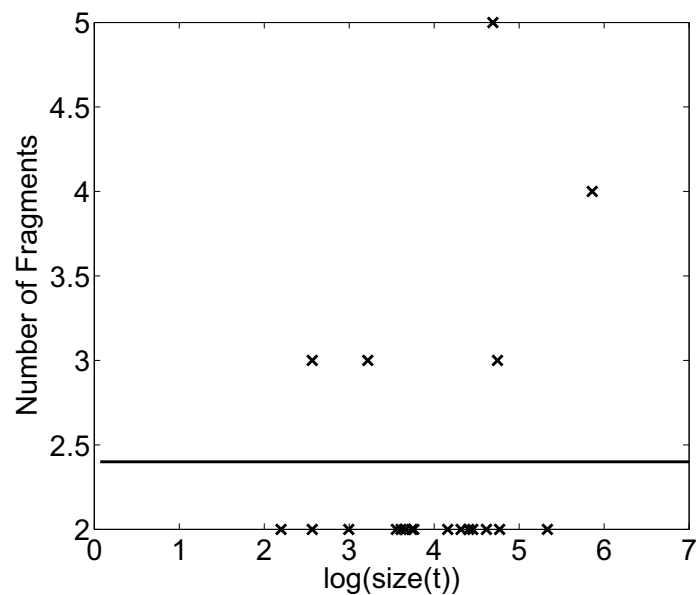
Figure 3.8: The fitted number of fragments model $n_f(x)$ for the IPM A_{No}. Crosses mark points from data, whilst the solid lines denote the models fitted to the data.
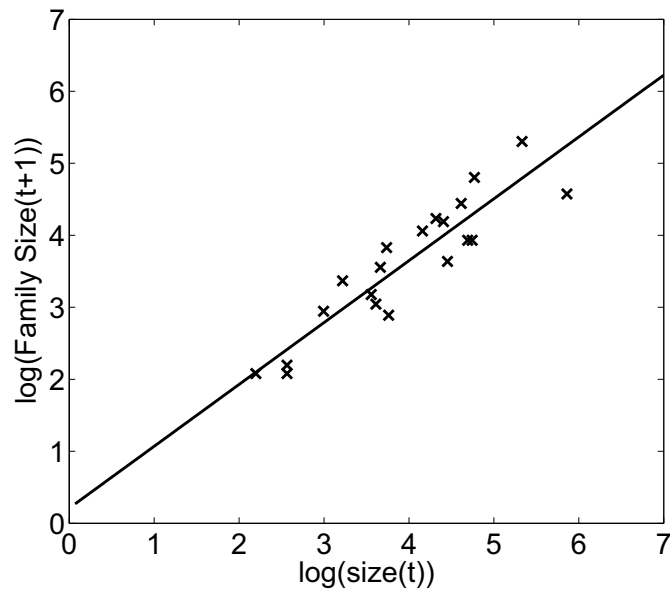
Figure 3.9: The fitted family size model $f_s(x)$ for the IPM A_{No}. Crosses mark points from data, whilst the solid lines denote the models fitted to the data.
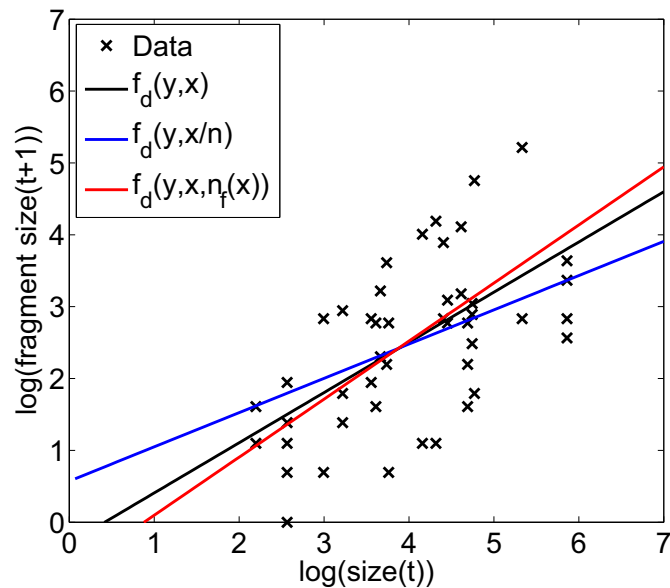
Figure 3.10: The three possible fitted fragment size models, where crosses mark data points.

will be used to select the model which gives the most realistic results. The asymptotic indicators are described in the next section and IPM selection is discussed in Section 3.5.

3.3 Asymptotic Behaviour

Asymptotic dynamics are a particularly useful method of analysis as they are independent of the initial conditions. The asymptotic, or long-term, behaviour of a population is observed when a population is not disturbed for a long period of time and the vital rates are time-invariant. In analysing projection models, the most common indicators are:

1. The population growth rate, λ_1 (Section 3.3.3),

2. The stable size distribution, $\mathbf{w}_1$ (Section 3.3.4),

3. The reproductive value, $\mathbf{v}_1$ (Section 3.3.5),

4. Perturbation analysis of the vital rate (Section 3.3.10).

The combination of these gives an overall view of the long term dynamics, which could be skewed by using only one indicator. Firstly, two other indicators will be explained, these are the population size and the projection of the population. These are not asymptotic indicators as they depend on the initial conditions, even so they help describe the transition from transient to asymptotic dynamics.

3.3.1 Population Size

The structure of the population at time t for a PPM is given by the vector $\mathbf{x}(t) \in \mathbb{R}^{1 \times n}$ and gives the number of individuals in each size class. In the case of the IPM $\mathbf{n}(x, t)$, gives the distribution of sizes at time t. These size structures are used to calculate the total size of the population. In the case of the PPM the 1-norm of the size structure is taken, which is calculated as the sum of all the entries, written

as $|\mathbf{x}(t)|_1 = |\mathbf{x}(t)|$. In the case of the IPM the L_1-norm is used and calculated as:

$$\int_\Omega \mathbf{n}(x,t)dx. \tag{3.27}$$

3.3.2   Projection of the Population

Projecting the population over time shows the dynamics of the population assuming that the vital rates are time-invariant. Projection is clearly not a forecast of a population where disturbances will occur, as then either the population structure or vital rates are perturbed. In this case, projections can be used to look at the interaction of different disturbances on a population, by using different PPMs or IPMs for different environmental conditions.

Projection uses the measure of population size, but it can also use the number of individuals in each size class or number of new individuals produced. Projection of the population also allows extinction times to be calculated, which is when the population decreases to a size below that of a given extinction threshold.

Given a matrix $\mathbf{A}$ and the population structure $\mathbf{x}(t)$ at time t the projection equation to calculate the population at time $t+1$ is:

$$\mathbf{x}(t+1) = \mathbf{A}\mathbf{x}(t). \tag{3.28}$$

Therefore given an initial population structure $\mathbf{x}(0)$, the population structures at times $t = 1, 2, \ldots T$ are:

$$\mathbf{x}(1) = \mathbf{A}\mathbf{x}(0). \tag{3.29}$$

$$\mathbf{x}(2) = \mathbf{A}\mathbf{x}(1) = \mathbf{A}(\mathbf{A}\mathbf{x}(0)) = \mathbf{A}^2\mathbf{x}(0), \tag{3.30}$$

$$\vdots \tag{3.31}$$

$$\mathbf{x}(T) = \mathbf{A}^T\mathbf{x}(0). \tag{3.32}$$

This method for PPMs can be used for IPMs, where the matrix $\mathbf{A}$ is the numerical approximation of the kernel, and $\mathbf{x}(t)$ is an approximation of the size structure at time t.

3.3.3   Population Growth Rate

The population growth rate λ_1 describes the long term, year on year, growth or decline of a population. It is computed as the dominant eigenvalue of the matrix or operator (see Section 3.3.6 for more information). Depending on the size of λ_1 the population will fall into three distinct groups (Caswell, 2001). They are:

1. $\lambda > 1$, the population is in exponential growth.

2. $\lambda = 1$, the population is in stasis, neither growing nor declining.

3. $\lambda < 1$, the population is in exponential decay.

3.3.4   Stable Size Distribution

The structure of a population in asymptotic time, $t >> 1$, is a multiple of the stable size distribution. This structure is calculated as the right eigenvector of $\mathbf{A}$ for the dominant eigenvalue. This is determined by the right eigenvalue/eigenvector equation:

$$\mathbf{A}\mathbf{w} = \lambda\mathbf{w} \tag{3.33}$$

The vector $\mathbf{w}$ is normalized so that $\sum_i w_i = 1$, this gives the proportion of individuals in each size class and is therefore independent of initial size. There are many other methods of normalizing this vector, but in this Thesis this method is preferred as the 1-norm is used as a measure of population size. Thus for all populations $|\mathbf{w}|_1 = 1$ in order to allow easy comparison. In the case of a PPM $\mathbf{w} \in \mathbb{R}^{n \times 1}$. In the case of an IPM the stable size distribution is a function $w(x)$, approximated by $\mathbf{w}$.

3.3.5   Reproductive Value

The reproductive value was first introduced by Fisher (1930) in answer to the question: 'To what extent do individuals at time t contribute to future generations?' Subsequently, this was shown to be equal to the left eigenvector $\mathbf{v}^T$, which satisfies

the left eigenvalue/eigenvector equation:

$$\mathbf{v}^T \mathbf{A} = \lambda \mathbf{v}^T. \tag{3.34}$$

The transpose form of this equation is required as opposed to the more traditional complex conjugate transpose form because population models are fitted with real parameters. As in the case of the stable size distribution, the reproductive value is normalized to sum to one, *i.e.* $\sum_i v_i = 1$. The vector (or function) $\mathbf{v}$ ($v(x)$) shows which sizes contribute the greatest amount to the production of new individuals.

Usually the reproductive value is applied in a context of population models which include reproduction - hence its title. In the models here, where reproduction is not included explicitly, this indicator can still be used. It measures how the different size classes contribute to the production of new individuals, particularly through the process of fragmentation. Therefore it might be better to refer to this *fragmentation value*, a measure of the proportional long-term fragmentation of each size class.

3.3.6   Perron-Frobenius Theorem

The Perron-Frobenius Theorem (Frobenius, 1912; Perron, 1907a,b) is fundamental in the study of eigenvalue properties of matrices and operators. Loosely speaking, it shows under certain conditions, that the dominant eigenvalue is unique, real and positive. This allows the calculation of the dominant eigenvalue alone to describe the dynamics rather than requiring the complete system of eigenvalues, or spectrum, to be calculated. This is particularly important for IPMs where calculating the full spectrum of the system is computationally expensive.

3.3.7   Perron-Frobenius For Population Projection Matrices

To describe the Perron-Frobenius Theorem, the notions of non-negative, primitive, irreducible and reducible matrices must be introduced.

Non-negativity

A matrix $\mathbf{A} \in \mathbb{R}^{n \times n}$ is non-negative if all entries in $\mathbf{A}$ are non-negative (Berman and Plemmons, 1994), that is if:

$$a_{ij} \geq 0 \quad \forall \; i, j. \tag{3.35}$$

Irreducibility

A non-negative matrix $\mathbf{A} \in \mathbb{R}^{n \times n}$ is reducible if for some permutation matrix $\mathbf{P}$, $\mathbf{P}^T \mathbf{A} \mathbf{P}$ is a block upper triangular matrix (Gantmacher, 1959; Berman and Plemmons, 1994). Contrastingly if a matrix is not reducible then it is irreducible. Irreducibility of a matrix $\mathbf{A}$ is equivalent to any of the following statements:

- The life cycle of the population is strongly connected, meaning that every node on the life cycle is connected (via a pathway) to every other node (Rosenblatt, 1957; Berman and Plemmons, 1994).

- For a matrix $\mathbf{A} = (a_{ij})$, for each i,j there exists a k such that the $(i,j)th$ entry of $\mathbf{A}^k$ is positive.

It is possible to calculate if a matrix is irreducible numerically for a given $n \times n$ matrix $\mathbf{A}$, it is irreducible if and only if $(\mathbf{I} + \mathbf{A})^{n-1} > 0$ (Horn and Johnson, 1985), where $\mathbf{I}$ is the $n \times n$ identity matrix.

Primitivity

A non-negative matrix $\mathbf{A} \in \mathbb{R}^{n \times n}$ is primitive if there exists k such that $\mathbf{A}^k \gg 0$. Primitivity of $\mathbf{A}$ is equivalent to the following statements:

- If the life cycle of the population is strongly connected and the greatest common divisor of the length of the loops is 1 (Rosenblatt, 1957; Berman and Plemmons, 1994).

- $\mathbf{A}^k > 0$ for some sufficiently large k.

- If $\mathbf{A}^{n^2 - 2n + 2} > 0$ (Horn and Johnson, 1985).

Three theoretical PPMs ($\mathbf{B}_1$, $\mathbf{B}_2$ and $\mathbf{B}_3$) show the differences in the structure of the life cycles for reducible, irreducible and primitive PPMs (Table 3.6). For a 3×3 matrix, irreducibility is equivalent to if $(\mathbf{I} + \mathbf{B}_i)^2 > 0$ and primitivity by $\mathbf{B}_i^5 > 0$.

The Perron-Frobenius Theorem

Let $\mathbf{A} \in \mathbb{R}^{n \times n}$ be a non-negative matrix with spectrum $\sigma(\mathbf{A}) = (\lambda_1, \lambda_2, ..., \lambda_n)$. The spectral radius, $r(\mathbf{A})$, is defined as $r(\mathbf{A}) = \max_i |\lambda_i|$, which is equivalent to the dominant eigenvalue, λ_1, of $\mathbf{A}$, if $\lambda_1 \in \mathbb{R}$ and positive. The corresponding left and right eigenvectors for λ_1 are $\mathbf{v}_1$ and $\mathbf{w}_1$ respectively. Then by the Perron-Frobenius Theorem:

- if matrix $\mathbf{A}$ is irreducible:

$$|\lambda_1| \geq |\lambda_i| \quad \forall \lambda \in \sigma(\mathbf{A}), \quad \lambda \neq \lambda_1, \quad 1 < i \leq 1, \tag{3.36}$$

and furthermore that λ_1 is positive and real with associated non-negative, real eigenvectors $(\mathbf{v}_1, \mathbf{w}_1 \geq 0)$.

- if the matrix $\mathbf{A}$ is primitive, then λ_1 is unique, *i.e.*:

$$|\lambda_1| > |\lambda_i| \quad \forall \lambda \in \sigma(\mathbf{A}), \quad \lambda \neq \lambda_1, \quad 1 < i \leq n, \tag{3.37}$$

and λ_1 has associated strictly positive real eigenvectors $(\mathbf{v}_1, \mathbf{w}_1 > 0)$ which are the only non-negative eigenvectors of the system.

PPM	Lifecycle	$(\mathbf{I}+\mathbf{B}_i)^2$	$\mathbf{B}_i^5$	Conclusion
$\mathbf{B}_1 = \begin{pmatrix} 0.5 & 0 & 0 \\ 0.1 & 0.5 & 0 \\ 0 & 0 & 0.5 \end{pmatrix}$		$\begin{pmatrix} 2.25 & 0 & 0 \\ 0.3 & 2.25 & 0 \\ 0 & 0 & 2.25 \end{pmatrix} \geq 0$		Reducible
$\mathbf{B}_2 = \begin{pmatrix} 0 & 0 & 0.1 \\ 0.1 & 0 & 0 \\ 0 & 0.1 & 0 \end{pmatrix}$		$\begin{pmatrix} 1 & 0.01 & 0.2 \\ 0.2 & 1 & 0.01 \\ 0.01 & 0.2 & 1 \end{pmatrix} > 0$	$\begin{pmatrix} 0 & 0.00001 & 0 \\ 0 & 0 & 0.00001 \\ 0.00001 & 0 & 0 \end{pmatrix} \geq 0$	Irreducible
$\mathbf{B}_3 = \begin{pmatrix} 0.5 & 0 & 0.1 \\ 0.1 & 0.5 & 0 \\ 0 & 0.1 & 0.5 \end{pmatrix}$		$\begin{pmatrix} 2.25 & 0.01 & 0.3 \\ 0.3 & 2.25 & 0.01 \\ 0.01 & 0.3 & 2.25 \end{pmatrix} > 0$	$\begin{pmatrix} 0.0338 & 0.0125 & 0.0315 \\ 0.0315 & 0.0338 & 0.0125 \\ 0.0125 & 0.0315 & 0.0338 \end{pmatrix} > 0$	Primitive

Table 3.6: Three theoretical PPMs demonstrating tests of primitivity and irreducibility.

3.3.8 For Integral Projection Models

The functions used to construct an IPM kernel (See Table 3.4) are assumed to be continuous and as such the kernel itself is continuous on $\mathbf{X} \times \mathbf{X}$, where $\mathbf{X}$ is the space of individual states. The right-hand side of the projection equation is defined to be:

$$\mathbf{T} = \int_{\mathbf{X}} \mathbf{k}(y, x) \mathbf{n}(x, t) dx. \tag{3.38}$$

Power Positivity

A kernel is power-positive (PP) if and only if:

$$\mathbf{k}^m(y, x) > 0 \quad \forall \, x, y \, \in \, \mathbf{X} \quad \text{and for some } m. \tag{3.39}$$

This equation states that for a large enough power m the kernel is positive in all entries. The property of power-positivity in IPMs is equivalent to the primitivity property in PPMs (Ellner and Rees, 2006). If the kernel is continuous and compact then uniform power positivity (UPP) is defined such that there exists some $C > 0$ and $m > 0$ where:

$$\mathbf{k}^m(y, x) \geq C. \tag{3.40}$$

This stronger assumption of UPP rather than PP is required for stable population growth, as PP can be found from an unbounded kernel (Ellner and Rees (2006) Appendix B).

In order to calculate $\mathbf{k}^m$ for a probability density kernel the Chapman Kolmogorov formula is used. Which states that:

$$\mathbf{k}^{t+1} = \int_X \mathbf{k}(y, x) \mathbf{k}^t(z, x) dz. \tag{3.41}$$

This is the IPM equivalent of the PPM projection equation $\mathbf{A}^{t+1} = \mathbf{A}\mathbf{A}^t$.

u-boundedness

With a continuous initial population size structure $\mathbf{n}(x,0) = \mathbf{n}_0(x)$ and a probability function $u(x) \in \mathbf{X}$, the m-step kernel is u-bounded if:

$$\alpha(n_0)u(x) \leq \mathbf{n}(m,t) \leq \beta(n_0)u(x), \tag{3.42}$$

where $\alpha, \beta > 0$ are constants dependent on the initial condition $\mathbf{n}_0$ (Ellner and Rees (2006) Appendix B). This property ensures that given an initial population structure, the population at some time in the future is bounded. This condition is satisfied if there is mixing at birth, which means that the range of offspring sizes is the same for all parents (Ellner and Rees, 2006).

The Perron Frobenius Theorem

There is stable population growth for an IPM, if the two conditions of power-positivity and u-boundedness are satisfied (Ellner and Rees, 2006). If the kernel satisfies these properties then (Ellner and Rees (2006) Appendix C):

1. The operator $\mathbf{T}^m$ will have an eigenvalue equal to the spectral radius λ^m with corresponding eigenvectors $\mathbf{w}$, $\mathbf{v}$.

2. The dominant eigenvalue λ^m is simple and $\mathbf{w}$ is unique.

3. All other eigenvalues of $\mathbf{T}^m$, ρ, other than λ^m satisfy $|\rho| \leq q\lambda^m$ for some $q < 1$.

Stable population growth means that only the dominant eigenvalue and eigenvectors of the system need to be calculated in order to define the population growth rates.

3.3.9 Ergodicity

Parameterized PPMs often suffer from missing transitions, where some transitions are not parameterized because of uncaptured data from data collection or because

of poorly selected size class boundaries. This results in about 25% of PPMs in the database[1]being reducible. For example PPM $\mathbf{B}_1$ is reducible (Table 3.6), this can clearly be seen in the life cycle as the third state-class is isolated from the other two state classes. This is obviously not biologically realistic, but if transition $G_{3,2}$ was non-zero the PPM would be irreducible

Reducibility can severely affect the dynamics of the population, with the population growth rate potentially being initial condition dependent. To overcome this possibility, it is necessary to check that reducible PPMs are ergodic. Ergodicity states that regardless of the initial conditions the population will follow the same growth rate, that given by λ_1. It is often the case though that if a PPM is reducible it is non-ergodic with 63.2% of reducible PPMs in the date base being non-ergodic (Stott et al., 2010b). When the PPM is non-ergodic it is important to take into account the structure of the initial conditions in order to understand what growth rate is followed.

Ergodicity can be tested from the left eigenvector, if $\mathbf{v}_1$ is positive then the PPM is ergodic (Dietzenbacher, 1991). If $\mathbf{v}_1 \geq 0$ then the PPM is non-ergodic and a population may follow multiple growth rates. To determine the different growth rates, the PPM must be permuted into a block matrix where all sub-diagonal blocks are zero for example:

$$\mathbf{A} = \left(\begin{array}{c|c|c|c|c} A_1 & A_{1,2} & \cdots & A_{1,n-1} & A_{1,n} \\ \hline 0 & A_2 & \cdots & A_{2,n-1} & A_{2,n} \\ \hline \vdots & \vdots & \ddots & \vdots & \vdots \\ \hline 0 & 0 & \cdots & A_{n-1} & A_{n-1,n} \\ \hline 0 & 0 & \cdots & 0 & A_n \end{array} \right). \tag{3.43}$$

Then the dominant eigenvalues of each irreducible diagonal matrix are determined.

The PPMs created in Section 3.1.3 were tested for ergodicity: The matrix $\mathbf{A}_1$ (3.4) is primitive and so only one population growth rate will be followed; The

---

[1]The database of PPMs has been gathered by Iain Stott, David Carslake and Miguel Franco. It currently contains 652 PPMs for 171 species. These PPMs have been found from published studies and is continuously being added to. Further information and analysis of the database has been carried out by Stott et al. (2010b)

PPM	Block Permutations									
$\mathbf{A}_2$	0.933	0.375	0.409	0	0	0	0	0	4	0
	0	0.708	0.136	0	0	0	0	0	0	0
	0	0	0.727	0.167	0	0	0	0	0	0
	0	0	0	0.833	1	0	0	0	0	0
	0	0	0	0	0	0	0	0	0	0
	0	0	0	0	0	1	0	0	0	0
	0	0	0	0	0	0	1	0	0	0
	0	0	0	0	0	0	0	0	0	0
	0	0	0	0	0	0	0	0	0	0
	0	0	0	0	0	0	0	0	0	1
$\mathbf{A}_3$	0.630	0.091	0	0	0.037	0	0	0.08	0	0
	0	0.681	0.095	0.067	0.148	0	0.042	0	0.038	0.083
	0	0.045	0.810	0.267	0.037	0.042	0	0.04	0	0
	0	0	0.048	0.7	0.074	0.125	0	0.04	0	0.042
	0	0	0	0	0.630	0.083	0	0.083	0	0.083
	0	0	0	0	0.074	0.708	0.25	0.08	0.038	0.208
	0	0	0	0	0	0.042	0.625	0.2	0.115	0.042
	0	0	0	0	0	0	0.042	0.56	0.077	0.042
	0	0	0	0	0	0	0	0	0.808	0.125
	0	0	0	0	0	0	0	0	0	0.75

Table 3.7: The block permutations of two non-ergodic PPMs.

matrix $\mathbf{A}_4$ (3.17) is reducible but ergodic as $\mathbf{v} > 0$. In comparison $\mathbf{A}_2$ (3.5) is non-ergodic, as is $\mathbf{A}_3$ (3.6). This results in block permutations as given in Table 3.7. For $\mathbf{A}_2$ there are 6 possible growth rates that could be followed by the population depending on the initial conditions (Table 3.8). PPM $\mathbf{A}_3$ could follow 5 different growth rates depending on the initial conditions (Table 3.8). This shows the importance in determining ergodicity for PPMs, so that the correct asymptotic dynamics can be predicted.

3.3.10 Perturbation Analysis

In deterministic models, fitted parameters describe the dynamics of a population in a snap-shot of time. There are often errors associated with these parameters and perturbation analysis informs how sensitive λ_1 is to a change in a parameter. Perturbation analysis can be used to inform management strategies, answering the

PPM	Base vector	Growth rate
$\mathbf{A}_2$	$\mathbf{e}_1$	0.933
	$\mathbf{e}_2$	0.708
	$\mathbf{e}_3$	0.727
	$\mathbf{e}_4$	0.833
	$\mathbf{e}_5, \mathbf{e}_8, \mathbf{e}_9$	0
	$\mathbf{e}_6, \mathbf{e}_7, \mathbf{e}_{10}$	1
$\mathbf{A}_3$	$\mathbf{e}_1$	0.630
	$\mathbf{e}_2, \mathbf{e}_3, \mathbf{e}_4$	0.898
	$\mathbf{e}_5, \mathbf{e}_6, \mathbf{e}_7, \mathbf{e}_8$	0.814
	$\mathbf{e}_9$	0.808
	$\mathbf{e}_{10}$	0.75

Table 3.8: The differing initial condition base vectors, $\mathbf{e}_i$, and the growth rate which would be followed under these initial conditions.

questions: 'Which vital rates are most important?'; 'Which should be targeted in order to conserve the population?' or 'Which rates need to be reduced in order to minimize the invasive potential of a species?' The answers to these questions can inform managers of populations the best strategies to adopt. In this next section the methods that have historically been used for PPMs will be described, as well as a discussion on how these can be applied to IPMs.

Sensitivity Analysis for PPMs

Sensitivity Analysis calculates the impact of each transition probability on the population growth rate λ_1. In the case of a PPM, the sensitivity of λ_1 to each matrix entry a_{ij} is given by:

$$S(a_{ij}) = \frac{\partial \lambda_1}{\partial a_{ij}} = \frac{v_i w_j}{\mathbf{v}^T \mathbf{w}}, \tag{3.44}$$

where $\mathbf{v}$ and $\mathbf{w}$ are the left and right eigenvectors of the dominant eigenvalue. Often management strategies require a certain growth rate λ_d and through linear extrapolation the required perturbation for each entry to achieve λ_d can be calculated as follows:

$$PS(a_{ij}) = \frac{\lambda_d - \lambda_1}{S(a_{ij})}. \tag{3.45}$$

Some entries of the PPM are biologically zero, which can be seen in the life cycle graph of a population and perturbation analysis for these entries is not required as these can never be perturbed to be non-zero.

It is important to highlight perturbations which are impossible in combination with other vital rates. Some required perturbations result in a probability estimate greater than one, or could cause the column sum of non-fecundity values to be greater than one. These perturbations are impossible to achieve and need to be rejected.

Transfer Function Analysis for PPMs

Transfer Function Analysis (TFA) is promoted as an alternative to Sensitivity Analysis (Hodgson and Townley, 2004; Hodgson et al., 2006). The Transfer Function is better equipped to deal with both structured perturbations to a population, as well as non-linear extrapolations of required values, giving more accurate results. In order to apply TFA to a PPM $\mathbf{A}$ a perturbation matrix $\mathbf{P}$ is defined such that the perturbed matrix is $\mathbf{A} + \mathbf{P}$. In the case of a single perturbation this can be re-written as: $\mathbf{A} + \mathbf{P} = \mathbf{A} + p\mathbf{D}\mathbf{E}$, where $\mathbf{D} = \mathbf{e}_j$, the jth basis vector defines the column of the perturbation, and $\mathbf{E} = \mathbf{e}_i^T$ defines the row of the perturbation, whilst p defines the magnitude of the perturbation. The Transfer Function of the perturbed matrix is defined as:

$$G(z) = \mathbf{E}(z\mathbf{I} - \mathbf{A})^{-1}\mathbf{D}, \tag{3.46}$$

and given the desired population growth rate λ_d the magnitude of the perturbation required is:

$$p = \frac{1}{\mathbf{E}(\lambda_d\mathbf{I} - \mathbf{A})^{-1}\mathbf{D}}. \tag{3.47}$$

From these equations (3.46) and (3.47), the direct relationship between the perturbation and the population growth rate can be calculated, which allows the comparison of different management strategies.

Sensitivity Analysis for IPMs

The simplest form of Sensitivity Analysis for IPMs is to directly transfer the framework from PPMs to numerically estimated 'giant' matrix as suggested by Easterling et al. (2000). In IPMs this will suggest the area of the approximated kernel that is sensitive to perturbations. This method is unable to suggest management strategies or relate these sensitive areas back to parameter estimates, because each entry of the approximated kernel is formed from multiple biological functions. Given the fragmentation value $v(x)$ and the stable size distribution $w(x)$ sensitivity can be calculated as:

$$s(x,y) = \frac{\partial \lambda_1}{\partial k(x,y)} = \frac{v(x)w(y)}{\langle w, v \rangle}, \tag{3.48}$$

where $\langle w, v \rangle = \int_\Omega w(x)v(x)dx$. This is a continuous representation of equation (3.44). However, there is no value in translating equation (3.45) to the IPM as stating the size of a perturbation on a numerical approximation cannot be translated into a management strategy for IPMs.

Sensitivity of Parameters in the IPM to Perturbations

Numerical integration itself has numerical errors, therefore to apply sensitivity analysis to this numerical approximation will introduce errors to the sensitivity analysis. As explained above, traditional sensitivity analysis also does not allow conclusions about the best management strategies to be drawn. In order to calculate the parameters most sensitive to perturbations it is more realistic to calculate the effect of perturbing each parameter on the population growth rate. It is often the case that one or more parameters are connected to each other and as one increases another may increase or decrease, so it is often useful to look at the effect of perturbations on these parameter values together. In order to calculate this each parameter (or group of parameters) is perturbed and the new population growth rate is calculated. It is then possible to produce a contour plot of possible parameter values against population growth rate so that conclusions can be drawn about what perturbations are required for groups of parameters. This can be viewed as a form of simulated Transfer Function Analysis.

3.4 Transient Analysis

Asymptotic dynamics assume that environmental conditions will remain the same for $t >> 1$, but this is often not the case. Populations experience disturbances which either perturb the population structure or the parameters of the model. Transient analysis aims to understand the short term dynamics exhibited following a disturbance which perturbs the population structure away from $\mathbf{w}$. A number of indices exist which can be applied to populations to measure the effect of the initial conditions which are described below. All transient analysis can be are measured relative to the long-term growth rate (λ_1), in order to place an upper-bound on the trajectories in the case where $\lambda_1 > 1$. This will give how large or small the population could become in comparison to if the population began in its stable size distribution $\mathbf{w}$. This is achieved by measuring the transient indicators of a normalised matrix $\widehat{\mathbf{A}}$, where $\widehat{\mathbf{A}} = \frac{\mathbf{A}}{\lambda_1}$.

The aim of transient analysis is to calculate the upper and lower bounds of possible behaviour. This is called the transient envelope and consists of an upper bound ρ_t called amplification and a lower bound a_t called attenuation.

3.4.1 For Population Projection Matrices

Possible Trajectories

The simplest method of analysis biases the initial conditions in order to observe what would happen under biased initial conditions. In a PPM with five size classes, five initial conditions are tested by placing all individuals into each size class independently. The population density is set to 1, i.e. $|\mathbf{x}(0)| = 1$. For each initial condition, $\mathbf{e}_i, i = 1...5$, the population was projected through 10 time steps and the population size measured.

Reactivity

Reactivity is the largest possible population density which could be achieved after one time step, with *Attenuation* being the smallest possible population density

which can be achieved after one time step. Reactivity is calculated as:

$$Reactivity = \left\|\widehat{\mathbf{A}}\right\|_1. \tag{3.49}$$

As the 1-norm of a matrix is calculated as the maximum column sum of the matrix this is easily calculated and is also easily transferable to the attenuation parameter such that:

$$Attenuation = \min(CS(\widehat{\mathbf{A}})), \tag{3.50}$$

where CS stands for the column sum of a matrix. These measures are relatively simple to calculate and can be particularly useful in a system which is experiencing constant disturbances, for example a system experiencing many hurricanes, which could only have 1 or 2 times steps between disturbances.

Kreiss Bounds

The upper Kreiss bounds $\overline{K}$ give a theoretical lower bound for maximum amplification ρ_t whilst the lower Kreiss bound $\underline{K}$ calculates an upper bound of attenuation a_t (Kreiss, 1962). These are calculated as:

$$\overline{K}_\lambda^\star = max_{r>1}(r-1)\left\|(r\mathbf{I} - \widehat{\mathbf{A}})^{-1}\right\|_1. \tag{3.51}$$

and the lower bound is:

$$\underline{K}_\lambda^\star = min_{r>1}(r-1)minCS(r\mathbf{I} - \widehat{\mathbf{A}})^{-1}. \tag{3.52}$$

Maximum Amplification and Minimum Attenuation

This measure gives the maximum (or minimum) possible population density that can be achieved in the transient analysis. These are the outer bounds of the transient envelope. These can be calculated as:

$$\rho_{max} = max_{t\geq 0}\left(\left\|\widehat{\mathbf{A}}^t\right\|_1\right) \tag{3.53}$$

and

$$a_{min} = min_{t \geq 0} \left(minCS \left(\widehat{\mathbf{A}}^t \right) \right) \tag{3.54}$$

This measure is numerically calculated for each time step, in this case for $t = 1, ..., 10$ and the maximum and minimum densities are calculated. It is also useful to record the times at which this minimum or maximum is reached.

3.4.2 For Integral Projection Models

Transient Analysis for IPMs is less well studied, the analysis are more descriptive rather than following any particular formulas. The most basic form of Transient Analysis is to project the population under differing initial conditions. An IPM, which has been numerically integrated, will have a much larger number of 'size classes' than a PPM and so a greater number of initial conditions must be tested. If there are n size classes in the numerical approximation, n initial conditions must be tested namely $\mathbf{e}_i, i = 1...n$. This calculates a range of behaviour which could occur. To compare transient dynamics with those of the PPM a number of indicators are then calculated from these projections. The maximum and minimum population densities can be calculated at each time step to form a transient envelope of behaviour. Using these bounds, an equivalent to *Reactivity* is calculated by finding the maximum value of these bounds at the first time step and *Attenuation* the minimum. Also of interest is the maximum (ρ_{max}) and minimum (a_{min}) density reached during the first ten time steps. As with PPM analysis this is calculated numerically.

The Transient Analysis in this Thesis is carried out relative to λ_1. An alternative suggestion by Eager et al. (In Press) was to calculate transients at each time step relative to the population size at the previous time step and is calculated by the Transient Function $T(t, \rho)$. This method is not adopted in this Thesis to allow a direct comparison of IPM Transient Analysis to PPM Transient Analysis in Chapter 5.

Method	λ_1	% change from Data
I	0.9036	+1
II	1.0154	+14
III	0.9578	+7
IV	0.7378	-17
V	0.7670	-14
Data	0.894	

Table 3.9: Population growth rates for the five different models for *M. annularis*. The numerical approximation used 100 mesh points to calculate the dominant eigenvalue.

3.5 Selection of an IPM Functional Form for $M.$ $annularis$

Recall from Section 3.2.3 that five different functional forms for an IPM were suggested for *M. annularis*. They were:

   I. $s(x)\mathbf{g}(y,x) + p_f(x)n_f(x)\mathbf{f}_d(y,x)$

  II. $s(x)\mathbf{g}(y,x) + f_s(x)p_f(x)n_f(x)\mathbf{f}_d(y,x)$

 III. $(1 - p_f(x))s(x)\mathbf{g}(y,x) + s(x)f_s(x)p_f(x)n_f(x)\mathbf{f}_d(y,x)$

 IV. $(1 - p_f(x))s(x)\mathbf{g}(y,x) + s(x)f_s(x)p_f(x)n_f(x)\mathbf{f}_d(y,\frac{x}{n})$

  V. $(1 - p_f(x))s(x)\mathbf{g}(y,x) + s(x)f_s(x)p_f(x)n_f(x)\mathbf{f}_d(y,x,n)$

Each of the functions described above were parameterized for A_{No}, the non-hurricane time steps (Table 3.5). These have been combined and numerically integrated to give a graphical representation of the 'kernel'. These can be compared, along with the population growth rates, stable size structures and fragmentation values of these five models. This is to select the best functional form, which will be used in this Thesis. The population growth rate from data was calculated as the total change in population density between t and $t + 1$. This gives an approximate measure of the behaviour that the population growth rates from the models can be compared to.

Firstly, although method I produced the best estimate of λ_1 in comparison to the data (Table 3.9), it was not based on the life cycle for *M. annularis* (Figure 3.2), but rather was a suggestion from literature, therefore method I is rejected as a possibility. Secondly method II provided an estimate of λ_1, which is greater than 1, depicting a growing population. The estimate of λ_1 directly from data is a declining population, i.e. with $\lambda_1 < 1$. Method II therefore provides a poor estimate for the population growth rate and as such is rejected.

Methods III, IV and V provide estimates for λ_1, which are acceptable with all in decline, and within 17% of the growth rate from data (Table 3.9). The estimate of λ_1 from data only takes into account the change of total area on the population and not the effect of fragmentation producing additional patches as the model does, so it is likely that the growth rate from data is an over-estimate of the actual growth rate. Therefore the estimate produced by Method III must be questioned. This method fails to take into account the effect that the number of fragments produced by a 'parent' patch on the size of those fragments. The fragmentation value for this method shows a dependence on smaller patches fragmenting than methods IV and V, this is not biologically realistic as the majority of fragmentation occurs on large patches as shown by the fitted $p_f(x)$. For these reasons method III is also rejected.

The population growth rate estimates and the kernels are similar for methods IV and V (Table 3.9 and Figure 3.11). The stable size distributions are also very similar being dominated by small patches in asymptotic time (Figure 3.12 (a)). The fragmentation values are similar, but method IV stated that there is a greater contribution from patches between 100 and $300cm^2$ (Figure 3.12 (b)). As the asymptotic results are similar for both methods IV and V, the biological realism of these methods are considered. The difference lies in the distribution of fragment sizes and the inclusion of the number of fragments as a factor. It seems more realistic to take the 'parent' size and divide by the number of fragments produced as this affects the average size of the patches produced, then to include the number of fragments in an additive fashion. For this reason method IV is selected ahead

of method V for use in parameterising IPMs in this Thesis. That is all kernels of *M. annularis* in this Thesis will be estimated by the functions:

$$k(y, x) = (1 - p_f(x))s(x)g(y, x) + s(x)f_s(x)p_f(x)n_f(x)f_d(y, \frac{x}{n}). \qquad (3.55)$$

(a) Method IV

(b) Method IV
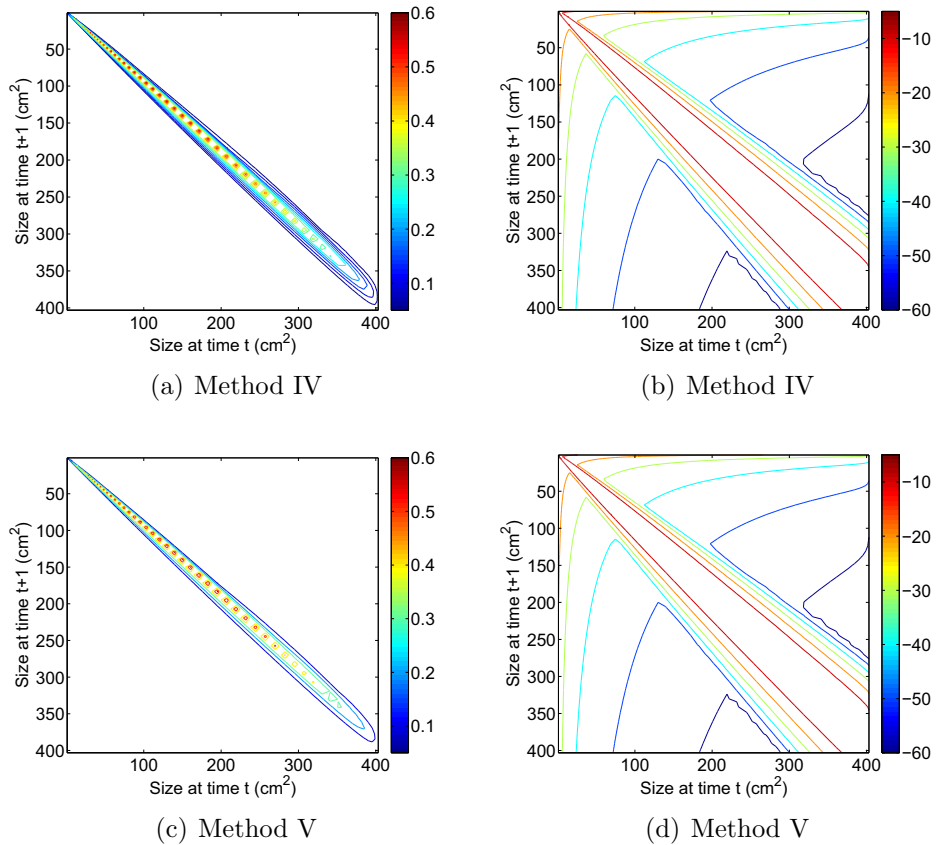
(c) Method V

(d) Method V

Figure 3.11: A comparison of kernels for method IV and method V as methods to parameterize the IPM of *M. annularis*.

3.6 Summary

In this Chapter the Population Projection Matrix and Integral Projection Model methods have been introduced. The methods for parameterizing *M. annularis* have been selected, as well as a description of the tools that will be used to analyse them. These will be used in Chapters 4, 5 and 7 to describe the dynamics exhibited on Glovers Reef.

(a) Stable Size Distribution

(b) Fragmentation Value
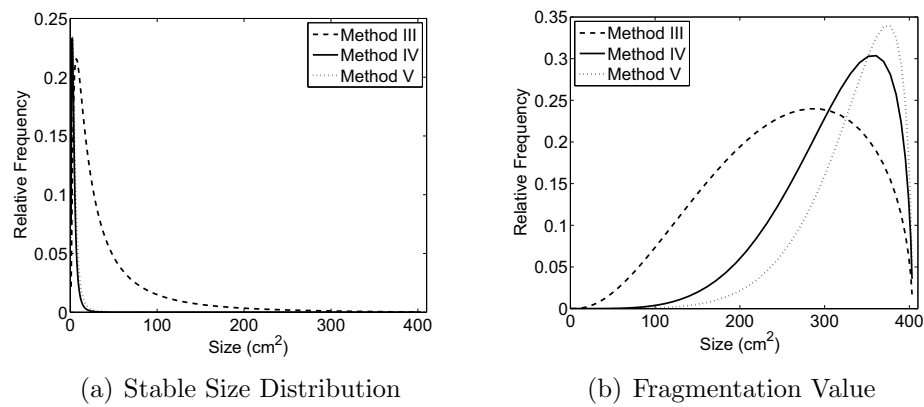
Figure 3.12: The stable size distribution and fragmentation values for methods *III*, *IV* and *V*.

This Chapter has focussed on answering the research questions RQ1, RQ2 and RQ3 given in Figure 1.4, concerning the objective of understanding current projection modelling techniques and how they can be adapted to *M. annularis*. It has also aimed at answering RQ5 in describing the current analysis techniques applied to projection modelling.

Part II

Should Population Projection Matrices or Integral Projection Models be used to model *Montastraea annularis*?

Chapter 4

The Population Projection Matrix

4.1 Introduction

Population Projection Matrices have been adapted for use with populations determined by size (Hughes, 1984) and, in particular, for coral colony populations (Hughes, 1984; Hughes and Tanner, 2000; Lasker, 1991). The necessity to model populations at patch, rather than colony scale, has been discussed in Chapter 2. In this Chapter, a PPM for coral patches of *Montastraea annularis* will be parameterized in order to investigate RQ6: Does initial trauma following a hurricane effect the dynamics of a coral patch population? The methods used to build and analyse these PPMs are given in Chapter 3.

4.1.1 Hypothesis

In order to test RQ6, the patch dynamics of *M. annularis* are quantified in order to test the hypothesis:

The initial impact of a hurricane influences the patch dynamics of Montastraea annularis.
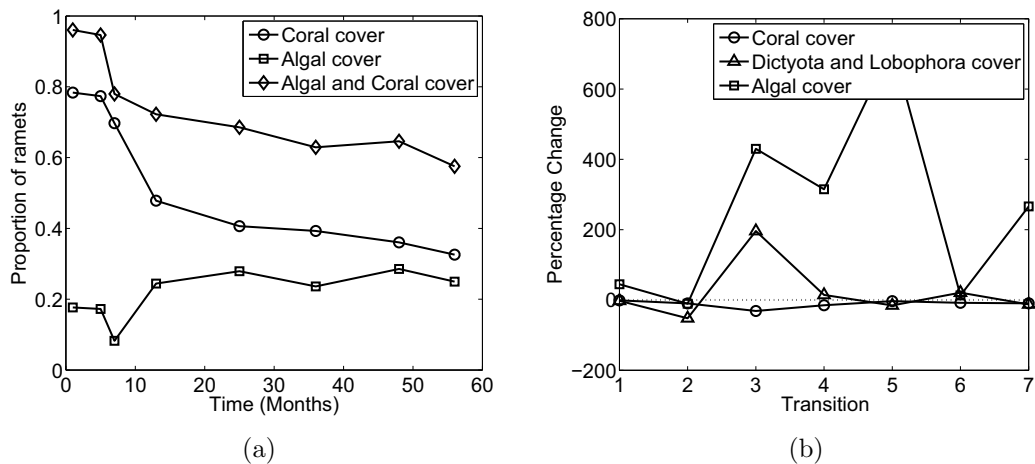
Figure 4.1: (a) The proportion of the total area of ramets (over the entire sampled population) covered by coral and algal patches. Algal patches comprise of *Dictyota*, *Halimeda*, *Lobophora variegata* and other macroalgal species. (b) Rate of change of coral and algal cover during the sampling period.

4.2 Methods

To test the hypothesis, the total area of coral patches on an individual ramet, not the patches themselves, were grouped according to the trauma experienced due to Hurricane Mitch. Although Hurricane Mitch occurred in October 1998, it is the decline in coral patch area between December 1998 and June 1999 that defines the trauma a patch undergoes as a result of Hurricane Mitch. A time lag was observed between the passing of the hurricane and the resulting decline in coral cover (Figure 4.1 (a)). This time lag may result from the delayed effects of hurricanes, such as scouring and increased sedimentation, rather than primary effects like ramet breakage.

The trauma a patch underwent is measured by the decline in coral cover. This initial trauma is different from the initial conditions. All coral patches on each ramet were summed together and it was assumed that all patches on the same ramet would experience similar trauma. An indicator, X, was defined to be the relative change in area between December 1998 and June 1999 such that:

$$X = \frac{\text{total area in June 1999}}{\text{total area in December 1998}}.$$
$$(4.1)$$

The range of observed values of X is between 0 and 1, where 0 indicates extinction of coral patches on a ramet and 1 indicates the area of coral remaining the same. It is possible for a value of X to be greater than 1, if growth was observed, but this is unlikely to occur when a coral patch is under stress.

Three trauma groups were defined using the indicator X, these were I_{Severe}, I_{Mild} and I_{Weak}. Group I_{Severe} contains ramets that experienced the most severe trauma and lost the greatest amount of relative area ($X \leq 0.47$). Group I_{Mild} contains those ramets with X in the range $0.47 < X \leq 0.78$ and group I_{Weak}, those that underwent the least trauma ($X > 0.78$). The aim was to create groups of approximately equal size, however, this was not possible as ramets which had the same X value were placed in the same group. Instead, following Hughes (1984) each group was required to have 80 ramets. This resulted in groups of size 88 (I_{Severe}), 88 (I_{Mild}) and 86 (I_{Weak}).

A PPM was parameterised for each group, using the individual patch sizes, rather than the grouped coral area on a ramet. Data was taken from the five sampling dates following Hurricane Mitch (June 1999 to January 2003). It was assumed that patch size and behaviour of each coral patch at the beginning of each transition is independent of the behaviour exhibited in the previous transition. All four transitions following Hurricane Mitch were grouped together to create one PPM for each category, rather than four for each category (one per transition). This should give an accurate description of post-hurricane behaviour and smooth out any yearly variations. It also reduces sampling errors resulting from a small data set. The data were collected at eight non-uniform time steps over a 4.5 year period. The time step of the PPMs was taken to be the average length of time between the data sampling points: 10.75 months. In addition, data collected on two sampling dates prior to Hurricane Mitch (June 1998 and October 1998) were used to capture the behaviour of the coral population prior to a disturbance event, this is known as the Pre-hurricane matrix (P) with a time step of 4 months. Percentage change and coral cover will also be calculated for the entire sampling period, this provides information about the behaviour observed, whilst PPMs will

project future behaviour.

The four PPMs (I_{Severe}, I_{Mild}, I_{Weak} and P) were parameterized using the methods described in Section 3.1.2. They use size classes chosen in Section 3.1.3 by the van der Meer and Moloney algorithm for the entire data set. In addition Section 3.1.3 gives details on the parameterization of a PPM for *M. annularis*, and these methods are adopted here. Once constructed the PPMs are analysed to understand both the asymptotic and transient dynamics (described in Sections 3.3 and 3.4) and the results are used to test the hypothesis.

4.3 Results

4.3.1 Coral Cover Results

Prior to Hurricane Mitch there was very little free space on the ramets in the study ($\approx 4\%$) and coral cover was approximately 80% (Figure 4.1 (a)). This was a healthy coral-dominated reef with four times as much coral as algae. The immediate response to Hurricane Mitch was a decrease in coral and algal cover, followed by a speedier recovery of algae than coral (Figure 4.1 (b)). The Algal cover recovers to a higher percentage coverage than pre-hurricane Mitch (25% compared to 18%), whilst the coral cover continued to decline, albeit at a slower rate than the initial decline, with only 33% coverage in January 2003 (Figure 4.1 (a)). There appears to have been very little colonisation of free space with the increase in free space mirroring the decline in coral cover (Figure 4.1 (a)).

Initially, the greatest number of patches was in ramet group I_{Severe}, but immediately following Hurricane Mitch, there was a 50% drop in number as a result of the extinction of 63 patches (Figure 4.2 (a)). Following the initial extinctions there was a continual slower decline in the number of patches for the remaining 43 months. The group with initially the most patches ended with the least (I_{Severe}). In contrast, for the two years following Hurricane Mitch coral patches on ramets in group I_{Mild} gradually increased in number as a result of fragmentation events. This initial growth in the number of patches was followed by decline, as a result

of further hurricanes hitting the reef. Nonetheless, in I_{Mild} at the end of the study there are more patches than at the beginning (Figure 4.2 (a)). Coral patches in I_{Weak} fluctuated in number throughout the study, but with an overall reduction of 8% by January 2003 (Figure 4.2 (a)). The greatest survival of individual patches over the study was measured as the percentage of patches identified in June 1998, which were still present in January 2003. By this measure, the greatest survival was observed in I_{Weak} (89%) compared to I_{Mild} (70%) and I_{Severe} (15%), the additional patches in Figure 4.2 (a) were new fragments produced by coral patches.
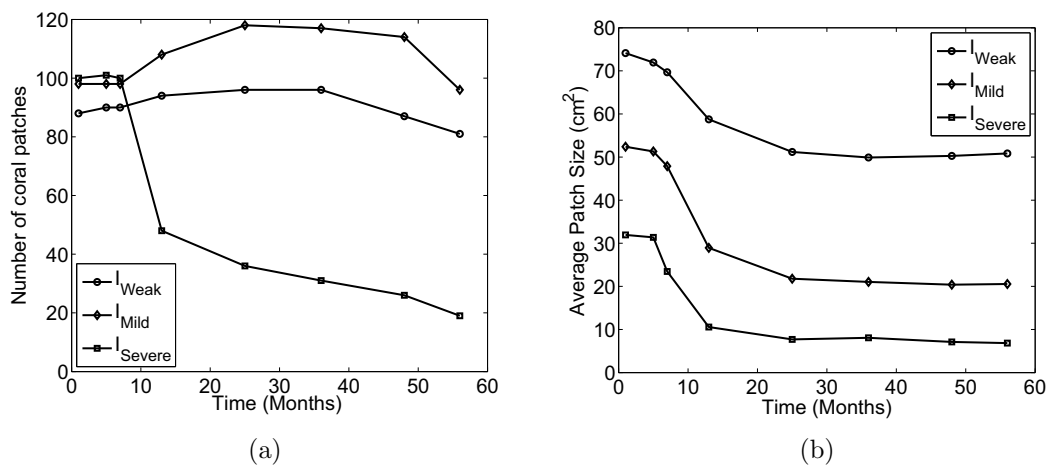
Figure 4.2: (a) The number of and (b) the average size of coral patches, in each initial hurricane impact group between June 1998 and January 2003.

Over the entire study, there was a decrease in average patch size, which strongly resembles the decrease in coral cover (Figures 4.1 (a) and 4.2 (b)). On average, coral patches in ramet group I_{Weak} were the largest, while ramets in I_{Severe} possessed the smallest patches of coral (Figure 4.2 (b)). The ramet groups were determined by relative change in area due to Hurricane Mitch and not absolute change, therefore the result is surprising. This shows that, on average, larger patches lost the lowest proportion of their size (found in I_{Weak}) and smaller patches lost the most (found in I_{Severe}). This gives an indication that ramets containing large patches are in the best position to lose the least relative area as a direct result of a hurricane.

Absolute growth (in cm^2) of a coral patch between sampling dates occurred mainly on ramets in categories I_{Mild} and I_{Weak}, with 33 and 23 growth events re-

spectively. In comparison, patches in group I_{Severe} experienced a total of only five growth events between June 1999 and January 2003. No absolute growth of coral patches was observed between October 1998 and June 1999 (the time period where the effects of Hurricane Mitch are assumed to have occurred). Stasis events, in which a coral patch remained the same size, were the most common throughout the sampling period (reflecting the slow growth of the species). The exception was the time period immediately following Hurricane Mitch when shrinkage events were the most prevalent. Coral patches in both I_{Severe} and I_{Weak} experienced half the number of fragmentation events than in group I_{Mild}. This shows that it was neither those patches that were affected the most nor the least that produced the most new patches through fragmentation.

Key Coral Patch Cover Results

1. There was very little colonization of free space.

2. Fragmentation mainly occurred in group I_{Mild}.

3. The largest number of growth events occurred in group I_{Mild}.

4. The best patch survival was in group I_{Weak}, and the worst in group I_{Severe}.

5. Ramets containing the largest patches lost the least relative area as a result of Hurricane Mitch.

4.3.2 The Population Projection Matrices

The PPMs for each trauma category and for the Pre-Hurricane state are given in Table 4.1. These were parameterized using methods described in Section 3.1.3 and size class boundaries given in Table 3.2. All four PPMs were dominated by stasis, shrinkage and fragmentation of patches, rather than growth, shown by the abundance of non-zero entries on the upper triangle of the PPMs. Those ramets, which experienced severe trauma from Hurricane Mitch (I_{Severe}), exhibit an abundance of zero entries in the largest 2 size classes. The only non-zero entry in columns 4 and

5 is the entry $R_{4,1}$, i.e. the shrinkage of all size class IV patches to size class I (from $49 - 153cm^2$ to $1 - 3cm^2$).

As the level of trauma decreased the stasis entries in the PPMs increased (Table 4.1). This showed a greater survival rate for those patches least traumatized by Hurricane Mitch, this is a similar pattern to that of survival of patches through the study where I_{Weak} had 89% of patches survived throughout the study. Patches in I_{Mild} had the most non-zero entries in the lower-triangle of the matrix, therefore growth was more common in I_{Mild} than the other trauma categories. This reflects that I_{Mild} had the most absolute growth events in the study.

Hurricane Trauma	PPM				
P	1.000	0.013	0.010	0.015	0
	0	0.974	0.030	0	0
	0	0.013	0.960	0	0.042
	0	0	0	0.985	0
	0	0	0	0	0.958
I_{Severe}	0.638	0.158	0.035	1	0
	0.017	0.684	0.276	0	0
	0	0	0.552	0	0
	0	0	0	0	0
	0	0	0	0	0
I_{Mild}	0.641	0.062	0.040	0.030	0
	0.016	0.872	0.152	0.075	0
	0	0.010	0.801	0.179	0
	0	0	0.007	0.702	0.167
	0	0	0	0	0.833
I_{Weak}	0.762	0.043	0	0.009	0
	0	0.819	0.070	0.026	0
	0	0	0.898	0.035	0.174
	0	0	0	0.922	0
	0	0	0	0.009	0.826

Table 4.1: The Population Projection Matrices for each initial trauma group as well as for pre-hurricane state.

Prior to Hurricane Mitch, a small amount of growth is observed between size classes II and III (from 4-12cm^2 to 13-48cm^2). The stasis probabilities are greater than for any post-hurricane PPM, showing greater survival of patches pre-

disturbance than post-disturbance. Five of the eleven non-zero entries in P describe stasis, which showed very little change in coral patch sizes prior to Hurricane Mitch.

4.3.3 Asymptotic Dynamics

As the initial trauma increased the population growth rate, λ_1, decreased (Table 4.2). The populations in all three trauma categories are in long-term decline ($\lambda_1 < 1$). This compares to the pre-hurricane population, which is in stasis ($\lambda_1 = 1$).

Initial Hurricane Impact	Population Growth Rate
P	1.00
I_{Severe}	0.718
I_{Mild}	0.894
I_{Weak}	0.922

Table 4.2: The Population Growth Rate for each initial hurricane trauma group.

The data were re-sampled 1000 times with replacement for each trauma category and PPMs were created for each of these re-samples. The population growth rate for I_{Severe} showed the greatest variability under re-sampling where extreme values for λ_1 ranged from approximately 0.58 to 0.9. (Figure 4.3). However, the middle 50% of λ values were smaller than the lowest extremes of I_{Mild} and I_{Weak}. The central 50% of values for I_{Weak} lie within the central 50% range from I_{Mild}, showing that it is possible for I_{Weak} to exhibit a larger growth rate than I_{Mild}. The median growth rate is higher for I_{Weak} than for I_{Mild} showed, on average, this is not the case. All estimates are less than 1 and so with re-sampling all populations are in decline.

Group I_{Severe} is projected to become extinct within 15 time steps (13 years), whereas group I_{Weak} is projected to contain over 75 coral patches after 50 time steps (45 years) (Figure 4.4). Here extinction is measured as at the time when the population number tends towards zero. Group I_{Mild} began with the largest number of patches, but showed a steeper initial decline and after 150 months there were
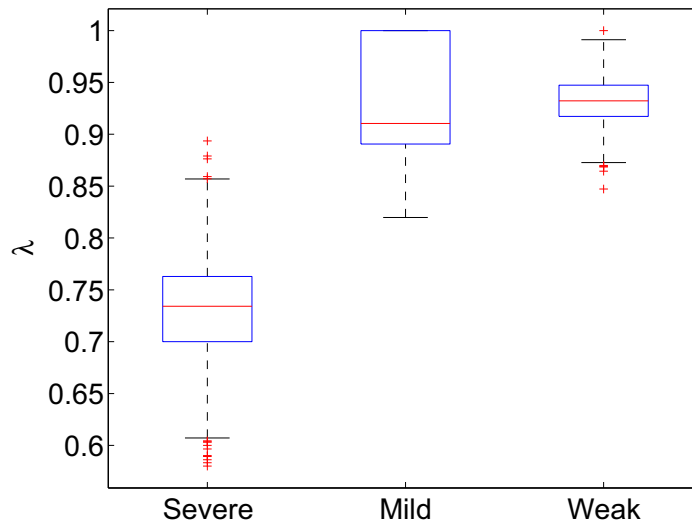
Figure 4.3: Confidence intervals for the growth rate λ_1, for 1000 resampled PPMs

projected to be fewer patches in I_{Mild} than in I_{Weak}. After 500 months (42 years) the best case scenario is the loss of 75% of patches (I_{Weak}) and the worst case scenario is that the population will be extinct (I_{Severe}) (Figure 4.4 (a)).
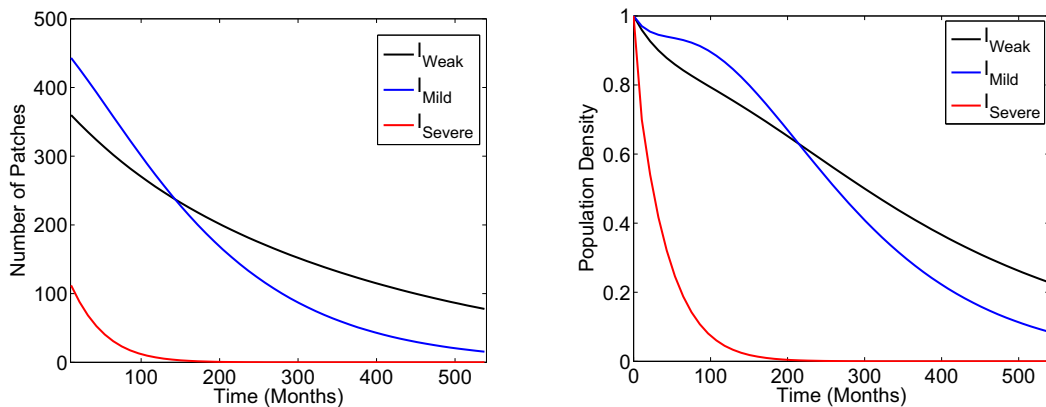
Figure 4.4: Population projections for each initial hurricane stress group over 50 time steps. Each time step represents 10.75 months. (a) The number of patches with initial conditions from data (b) Population density with uniform initial conditions across each sizes class.

With a uniform initial distribution of patches in each size class, the projection of the PPMs can be compared under the same initial conditions (Figure 4.4 (b)).

In this case, I_{Mild} showed a slower decline for the first 250 months, than either I_{Weak} or I_{Severe}, at which point I_{Weak} then contained a greater population density. Group I_{Severe} showed severe decline and after 200 months, became extinct. After 500 months 26% of patches remained in I_{Weak} compared to 11% in I_{Mild}.

Primitivity and ergodicity is vital in determining population growth rates (as discussed in Section 3.3.9). All four PPMs parameterized in this chapter are reducible. The PPMs P and I_{Mild} are ergodic as $\mathbf{v} > 0$ (Table 4.3) and in these ramet groups all initial conditions follow one growth rate - that given by the dominant eigenvalue. Ramet group I_{Severe} is also ergodic in spite of $\mathbf{v} \geq 0$, but as $\mathbf{v}$ is positive in those size-classes where the PPM in non-zero, it is classified as ergodic, confirmed by the block matrix permutation in Table 4.3. The only non-ergodic PPM is I_{Weak}, where the initial conditions will determine the population growth rate. Block permutation of I_{Weak} (Table 4.3) give four different growth rates for differing base vectors $\mathbf{e}_i$. These growth rates (Table 4.4) show that the larger the patch sizes in the initial condition the larger the growth rate. In fact λ_1 is only achieved if patches are initially in size classes IV or V. The largest growth rate is 21% larger than the smallest growth rate, showing the necessity in understanding the initial conditions in this trauma category.

The fragmentation values ($\mathbf{v}$ in Table 4.3) showed that new patches were predominantly formed by large patches in group I_{Mild}. In this trauma category over 55% of new patches were formed by size class V ($\geq 154\text{cm}^2$). In the other two trauma categories (I_{Severe} and I_{Weak}) larger patches also dominate the fragmentation value with at least 60% of new patches produced by patches in size class III to V ($\geq 13\text{cm}^2$). This post-disturbance dominance of larger patches in the fragmentation values is not seen pre-disturbance where all sizes equally contribute to fragmentation.

The stable size distributions of coral patches in all three categories were dominated by small patches under 50 cm^2 in area, which are size classes I to III, (Table

	PPM	$\mathbf{v}$	Ergodic?
P	$\begin{pmatrix} 1.000 & 0.013 & 0.010 & 0.015 & 0 \\ 0 & 0.974 & 0.030 & 0 & 0 \\ 0 & 0.013 & 0.960 & 0 & 0.042 \\ 0 & 0 & 0 & 0.985 & 0 \\ 0 & 0 & 0 & 0 & 0.958 \end{pmatrix}$	$\begin{pmatrix} 0.200 \\ 0.200 \\ 0.200 \\ 0.200 \\ 0.200 \end{pmatrix}$	Y
I_{Severe}	$\begin{pmatrix} 0.638 & 0.158 & 0.035 & 1 & 0 \\ 0.017 & 0.684 & 0.276 & 0 & 0 \\ 0 & 0 & 0.552 & 0 & 0 \\ 0 & 0 & 0 & 0 & 0 \\ 0 & 0 & 0 & 0 & 0 \end{pmatrix}$	$\begin{pmatrix} 0.067 \\ 0.310 \\ 0.560 \\ 0.093 \\ 0 \end{pmatrix}$	Y
I_{Mild}	$\begin{pmatrix} 0.641 & 0.062 & 0.040 & 0.030 & 0 \\ 0.016 & 0.872 & 0.152 & 0.075 & 0 \\ 0 & 0.010 & 0.801 & 0.179 & 0 \\ 0 & 0 & 0.007 & 0.702 & 0.167 \\ 0 & 0 & 0 & 0 & 0.833 \end{pmatrix}$	$\begin{pmatrix} 0.006 \\ 0.094 \\ 0.170 \\ 0.195 \\ 0.565 \end{pmatrix}$	Y
I_{Weak}	$\begin{pmatrix} 0.762 & 0.043 & 0 & 0.009 & 0 \\ 0 & 0.819 & 0.070 & 0.026 & 0 \\ 0 & 0 & 0.898 & 0.035 & 0.174 \\ 0 & 0 & 0 & 0.922 & 0 \\ 0 & 0 & 0 & 0.009 & 0.826 \end{pmatrix}$	$\begin{pmatrix} 0 \\ 0 \\ 0 \\ 1 \\ 0 \end{pmatrix}$	N

Table 4.3: The block permutation matrices for testing ergodicity. The table also shows the fragmentation values and whether the PPM is ergodic.

Base vector ($\mathbf{e}_i$)	λ
$\mathbf{e}_1$	0.762
$\mathbf{e}_2$	0.819
$\mathbf{e}_3$	0.898
$\mathbf{e}_4$, $\mathbf{e}_5$	0.922

Table 4.4: The differing growth rates taken by different base vectors for I_{Weak}

4.5). Group I_{Severe} will be dominated by coral patches only in the smallest two size classes (1-12cm^2) and 90% of coral patches in group I_{Mild} would also be in these size classes. Only the stable size distribution for ramet group I_{Weak} contained a full range of coral patches with over 90% ranging between 4 and 124 cm^2. Larger patches in I_{Weak} are rarer than smaller patches (2% in comparison to 9%), but their existence in the long term place this trauma category in a better position to survive future disturbances, as it has already been shown that ramets containing

larger patches are less likely to lose the greatest proportion of area in a hurricane.

Data	P	I_{Severe}	I_{Mild}	I_{Weak}
0.0804	1	0.6632	0.1889	0.0930
0.2692	0	0.3368	0.7225	0.3126
0.3462	0	0	0.0857	0.3904
0.2238	0	0	0.0029	0.1873
0.0804	0	0	0	0.0167

Table 4.5: The Stable size structures for each initial hurricane group and the initial distribution from data of coral patches in June 1998.

The surprising result is that, prior to Hurricane Mitch, the observed population was not in the stable size structure (Table 4.5). In fact, the stable size structure stated all individuals would range from 1 to 3cm^2. Even allowing for some error in these results, the stable size structure of the population prior to Hurricane Mitch would be largely dominated by small patches. This was not observed in June 1998, where the population of coral patches had a full range of sizes. If the population remained undisturbed then the population would more likely be dominated by smaller patches than would result following any level of trauma from Hurricane Mitch. This allows the conclusion that hurricanes are necessary in order to achieve a wider range in patch sizes in the long term.

Key Asymptotic Results

1. All PPMs parameterized are reducible and I_{Weak} is non-ergodic.

2. For all trauma categories the populations are in decline.

3. As the trauma level increased the population growth rate decreased.

4. Under projection, I_{Mild} faired better for the first 200 months, and then I_{Weak} faired best. After 500 months it still contained 26% of the initial population size.

5. There is projected to be a greater variety of patch sizes in I_{Weak} than other trauma categories.

6. There will be a greater range of patch sizes after a disturbance than if no disturbance occurred.

7. As trauma increased the stasis entries in the PPM decreased.

4.3.4   Perturbation Analysis

If a PPM is imprimitive, then by the Perron-Frobenius theorem **v** and **w** can contain zero entries. This hampers sensitivity analysis as there are some entries in the sensitivity matrix which are forced to be zero, and therefore some sensitivity values cannot be calculated. The sensitivity results and perturbations required to achieve $\lambda = 1$ are given in Table 4.6.

The most sensitive entries of the PPMs are the growth entries in the lower-triangle of the matrix (Table 4.6). The estimates for these entries in the PPMs are mainly zero (Table 4.1) and showed that, if growth is introduced to the population, the overall population growth rate would increase. The perturbation matrix showed that some growth entries required perturbations of less than 0.1, for example $G_{3,2}$ in I_{Mild} or $G_{4,3}$ in I_{Weak}. Although growth transitions required the smallest perturbations in I_{Severe}, the smallest attainable perturbation is 0.24 in $G_{2,1}$.

The upper triangular entries are least sensitive in I_{Mild}, the perturbations required to achieve $\lambda_1 = 1$ showed that there were no attainable increase in shrinkage or fragmentation. This is similar to the situation for stasis entries on the diagonal of all the PPMs where the perturbations required for $\lambda_1 = 1$ are biologically impossible.

	I_{Severe}	I_{Mild}	I_{Weak}
PPM	$\begin{matrix} 0.64 & 0.16 & 0.04 & 1 & 0 \\ 0.02 & 0.68 & 0.28 & 0 & 0 \\ 0 & 0 & 0.55 & 0 & 0 \\ 0 & 0 & 0 & 0 & 0 \\ 0 & 0 & 0 & 0 & 0 \end{matrix}$	$\begin{matrix} 0.64 & 0.06 & 0.04 & 0.03 & 0 \\ 0.02 & 0.87 & 0.15 & 0.08 & 0 \\ 0 & 0.01 & 0.80 & 0.18 & 0 \\ 0 & 0 & 0.01 & 0.70 & 0.17 \\ 0 & 0 & 0 & 0 & 0.83 \end{matrix}$	$\begin{matrix} 0.76 & 0.04 & 0 & 0.01 & 0 \\ 0 & 0.82 & 0.07 & 0.03 & 0 \\ 0 & 0 & 0.90 & 0.04 & 0.17 \\ 0 & 0 & 0 & 0.92 & 0 \\ 0 & 0 & 0 & 0.01 & 0.83 \end{matrix}$
Sensitivity	$\begin{matrix} 0.30 & 0.15 & 0 & 0 & 0 \\ 1.39 & 0.70 & 0 & 0 & 0 \\ 2.36 & 1.20 & 0 & 0 & 0 \\ 0.41 & 0.21 & 0 & 0 & 0 \\ 0 & 0 & 0 & 0 & 0 \end{matrix}$	$\begin{matrix} 0.01 & 0.05 & 0.01 & 0.00 & 0 \\ 0.21 & 0.81 & 0.10 & 0.003 & 0 \\ 0.38 & 1.46 & 0.17 & 0.01 & 0 \\ 0.44 & 1.68 & 0.20 & 0.01 & 0 \\ 1.20 & 4.59 & 0.55 & 0.02 & 0 \end{matrix}$	$\begin{matrix} 0 & 0 & 0 & 0 & 0 \\ 0 & 0 & 0 & 0 & 0 \\ 0 & 0 & 0 & 0 & 0 \\ 0.50 & 1.67 & 2.09 & 1.00 & 0.09 \\ 0 & 0 & 0 & 0 & 0 \end{matrix}$
Perturbation	$\begin{matrix} 0.95 & 1.89 & X & X & X \\ 0.20 & 0.40 & X & X & X \\ 0.12 & 0.24 & X & X & X \\ 0.68 & 1.34 & X & X & X \\ X & X & X & X & X \end{matrix}$	$\begin{matrix} 8.15 & 2.13 & 17.96 & 524.67 & X \\ 0.50 & 0.13 & 1.11 & 32.26 & X \\ 0.28 & 0.07 & 0.61 & 17.80 & X \\ 0.24 & 0.06 & 0.53 & 15.51 & X \\ 0.09 & 0.02 & 0.19 & 5.67 & X \end{matrix}$	$\begin{matrix} X & X & X & X & X \\ X & X & X & X & X \\ X & X & X & X & X \\ 0.16 & 0.05 & 0.04 & 0.08 & 0.87 \\ X & X & X & X & X \end{matrix}$
TFA	$\begin{matrix} 0.35 & 6.49 & * & * & * \\ 0.71 & 0.31 & * & * & * \\ 0.92 & 0.50 & 0.45 & * & * \\ 0.35 & 6.49 & * & 1.00 & * \\ * & * & * & * & 1.00 \end{matrix}$	$\begin{matrix} 0.4 & 2.7 & 51.1 & 2310.7 & * \\ 0.7 & 0.1 & 2.2 & 100.3 & * \\ 0.6 & 0.1 & 0.2 & 8.2 & * \\ 0.6 & 0.2 & 0.3 & 0.3 & * \\ 0.6 & 0.2 & 0.3 & 0.3 & 0.2 \end{matrix}$	$\begin{matrix} 0.24 & * & * & * & * \\ 1.01 & 0.18 & * & * & * \\ 1.46 & 0.26 & 0.10 & * & * \\ 0.85 & 0.25 & 0.18 & 0.08 & 1.57 \\ 1.46 & 0.26 & 0.10 & * & 0.17 \end{matrix}$
Perturbation	$\begin{matrix} 0.80 & 0.04 & X & X & X \\ 0.40 & 0.91 & X & X & X \\ 0.31 & 0.57 & 0.63 & X & X \\ 0.80 & 0.04 & X & 0.28 & X \\ X & X & X & X & 0.28 \end{matrix}$	$\begin{matrix} 0.30 & 0.04 & 0.002 & 0.00 & X \\ 0.16 & 0.90 & 0.05 & 0.001 & X \\ 0.19 & 0.72 & 0.58 & 0.01 & X \\ 0.18 & 0.66 & 0.36 & 0.36 & X \\ 0.18 & 0.66 & 0.36 & 0.36 & 0.63 \end{matrix}$	$\begin{matrix} 0.33 & X & X & X & X \\ 0.08 & 0.43 & X & X & X \\ 0.05 & 0.30 & 0.76 & X & X \\ 0.09 & 0.31 & 0.42 & 1.00 & 0.05 \\ 0.05 & 0.30 & 0.76 & X & 0.45 \end{matrix}$

Table 4.6: Sensitivity Analysis and Transfer Function Analysis for each hurricane trauma category. Entries marked X fail to have a perturbation attached to them either due to a zero value in the TFA, as a result of reducibility, or due to the structure of **v** and **w** in the sensitivity analysis. Entries in red are biologically impossible as it forces the column sums to be much greater than one.

Transfer Function Analysis (TFA), unlike sensitivity analysis, is not affected by imprimitivity. However, it is affected by reducibility. This results in some entries of the transfer function to be zero, and thus perturbing these entries will not change λ_1.

Transfer Function Analysis showed that in general a growth rate of $\lambda_1 = 1$ is hard to achieve, shown by the dominance of red entries in the perturbation matrix (Table 4.6). The majority of entries on the lower triangle are biologically impossible to achieve as the perturbations required are too large. Both methods of analysis showed that I_{Mild} was the PPM with the smallest perturbations required to achieve population stasis ($\lambda_1 = 1$). Not just because there are a greater number of possible strategies that managers could take, but also the perturbations required are generally smaller than the other PPMs. However, the possible strategies from TFA for I_{Mild} are in the upper triangle, suggesting that shrinkage and fragmentation must be increased in order to achieve overall population stasis (Table 4.6). This is because more patches are caused to form increasing population number, which is counter-intuitive as populations require larger patches if they are to withstand further disturbances.

The size of the perturbation required varies between the two analysis approaches. For example, $G_{4,1}$ in I_{Weak}, sensitivity stated a perturbation of 0.16 is required, whilst TFA stated that this perturbation needs to be only 0.09. However, the current estimate of $G_{4,1}$ was 0, so this entry is unlikely to be achievable biologically.

The top three management strategies are given in Table 4.7. For trauma category I_{Severe}, the top three strategies for sensitivity analysis are all growth entries, but for TFA, there is a full range of possible strategies from growth to stasis, fragmentation to shrinkage. The size of the perturbations required by TFA are much smaller than those from sensitivity. For I_{Mild}, sensitivity analysis suggests that growth should be targeted and TFA that shrinkage and fragmentation are best to target. For I_{Weak} TFA stated that growth of very small patches into medium or

large patches is required. Alternatively, the shrinkage or fragmentation from the largest to the second largest size class is also suggested by TFA. In comparison, sensitivity again states that growth is required in this case into size class IV.

	Sensitivity	TFA
I_{Severe}	$G_{3,1}$ (0.120)	$G_{4,2}$ (0.04)
	$G_{2,1}$ (0.204)	$R_{1,2}+D_{1,2}$ (0.04)
	$G_{3,2}$ (0.236)	$S_{5,5}$ (0.28)
I_{Mild}	$G_{4,2}$ (0.063)	$R_{2,4} + D_{2,4}$ (0.001)
	$G_{3,2}$ (0.072)	$R_{1,3} + D_{1,3}$ (0.002)
	$G_{5,3}$ (0.194)	$R_{3,4} + D_{3,4}$ (0.01)
I_{Weak}	$G_{4,3}$ (0.037)	$G_{3,1}$ (0.05)
	$G_{4,2}$ (0.047)	$R_{4,5} + D_{4,5}$ (0.05)
	$G_{4,1}$ (0.156)	$G_{5,1}$ (0.05)

Table 4.7: Top 3 management strategies suggested by both Sensitivity Analysis and TFA for each trauma category, taken from Table 4.6. The targeted entry is given, with the perturbation required to give $\lambda_1 = 1$ given in brackets.

Key Perturbation Analysis Results

1. Managers must focus on growth entries to achieve population stasis, if using sensitivity analysis, but must increase shrinkage and fragmentation, if using TFA.

2. TFA showed that the perturbations to growth entries must be much larger than calculated by sensitivity analysis, if population stasis is to be achieved and often these perturbations are biologically impossible.

3. I_{Mild} required the smallest perturbations to achieve population stasis.

4.3.5 Transient Analysis

(a) I_{Severe}

(b) I_{Mild}

(c) I_{Weak}

(d) P
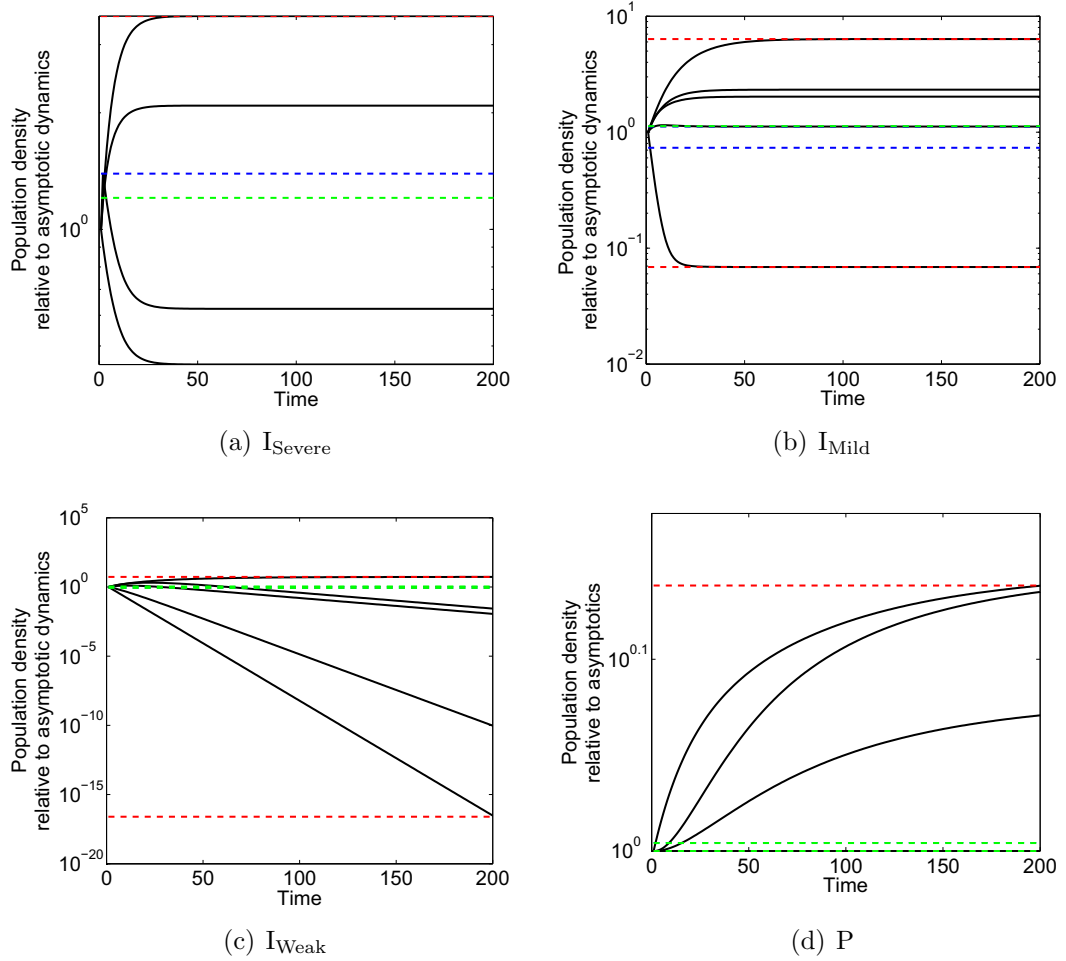
Figure 4.5: The transient dynamics for (a) I_{Severe} (b) I_{Mild} (c)I_{Weak} (d) P. The black lines are the possible dynamics with differing base vectors as initial conditions. The blue dotted line show Reactivity and Attenuation, the green dotted lines are the upper and lower Kreiss bounds and the red dotted lines are ρ_{max} and a_{min}.

In the first time step, I_{Severe} showed the greatest range of population densities (0-1.393) (Figure 4.5 and Table 4.8). In comparison, I_{Weak} had the smallest range (0.826-1.084). As initial trauma decreased the width of the first time step transient envelope decreased. Therefore, as initial trauma decreased, initial extremes decreased. In each trauma category the maximum possible population densities relative to asymptotics are greater than those in the first time step i.e. $\rho_{max} > Reactivity$, showing possible amplification over a number of time steps.

Indicator	P	I$_{\text{Severe}}$	I$_{\text{Mild}}$	I$_{\text{Weak}}$
Reactivity	1.01 (III)	1.3926 (IV)	1.1183 (V)	1.0841 (IV,V)
Attenuation	1 (I,II,III,IV)	0 (V)	0.7338 (I)	0.8260 (I)
ρ_{max}	1.3755 (II)	3.5545 (III)	6.3547 (V)	5.3144 (IV)
a_{min}	1 (I,III)	0 (V)	0.0687 (I)	<0.0001 (I)
$\bar{k}_\lambda$	1.0096	1.2064	1.1278	1.0837
$\underline{k}_\lambda$	1	0	0	0.8518

Table 4.8: Values of the transient bounds for each PPM, shown in brackets is the size class where this is achieved.

The speeds at which the populations reach these maximum amplifications vary for each trauma category. For example I$_{\text{Severe}}$ achieved ρ_{max} at $t = 38$ (≈ 34 years) with initial condition $\mathbf{e}_2$. Other trauma categories take longer than 100 time steps (about 90 years) with I$_{\text{Mild}}$ taking 103 time steps with initial condition $\mathbf{e}_5$, and I$_{\text{Weak}}$ slowest to reach ρ_{max} in 190 time steps with initial condition $\mathbf{e}_4$. As trauma increased the time at which ρ_{max} was achieved shortened.

Reactivity and maximum amplification results showed that under biased initial conditions the population density could be amplified above the expected asymptotic growth rate. In I$_{\text{Severe}}$, the maximum amplification occurred if the patches were biased to sizes $13 - 48cm^2$. In comparison, Reactivity results showed that the population was amplified the most when the initial population was between sizes $49 - 153cm^2$. This showed that long term amplification required smaller coral patch sizes than the largest immediate amplification. As trauma decreased the coral patch sizes, which result in the greatest amplification increase. In I$_{\text{Weak}}$, maximum amplification occurred for patches between 49 and $153cm^2$, whilst Reactivity occurred for all patches larger than $49cm^2$. The largest size classes required for amplification was for I$_{\text{Mild}}$, where both Reactivity and ρ_{max} were achieved for patches larger than $154cm^2$. For PPM P, smaller sizes achieved the greatest amplification than the PPMs post Hurricane Mitch. Reactivity was achieved with patches between 13 and $48cm^2$, but ρ_{max} was achieved with smaller patches of between sizes 4 and

$12cm^2$.

The minimum attenuation (a_{min}) is achieved in the first time step for I_{Severe}, showing instantaneous die off with initial condition $\mathbf{e}_1$ (Table 4.8). Minimum attenuation for I_{Mild} and I_{Weak} did not occur in the first time step, but was reached earlier than maximum amplification. The a_{min} value for I_{Weak} was found at the end of the monitored time and would decrease if a longer period of time was studied, but an a_{min} value of 0.00 is achieved after 29 time steps with initial condition $\mathbf{e}_1$, this is effectively extinction. Finally I_{Mild} achieved a_{min} in 23 time steps, with initial condition $\mathbf{e}_1$. All minimum attenuations were achieved with the initial condition $\mathbf{e}_1$, which consists of all coral patches between 1 and 3 cm^2. In comparison ρ_{max} is achieved with a range of initial conditions.

Key Transient Results

1. As initial trauma decreased so did initial extremes.

2. As trauma increased the time at which maximum amplification was reached shortened.

3. Minimum attenuation occurred earlier than maximum amplification for all trauma categories.

4. Minimum attenuations and maximum amplification were achieved faster in I_{Severe} than other trauma groups.

5. Attenuation is achieved regardless of initial trauma when all individuals began in the smallest size classes $(1 - 3cm^2)$.

6. In general, for amplification to occur all individuals must start in larger size classes.

4.4 Conclusions

4.4.1 Does Initial Trauma Determine the Dynamics of an Individual?

In this chapter it was shown that the initial trauma determines the dynamics of a coral patch. In particular, there is a distinct difference in the behaviour exhibited between ramets that experienced a greater than 50% loss in coral cover, compared to the ramets where there was a less than 50% loss in coral cover. The results are summarised in Table 4.9. This chapter has also highlighted the complexities in understanding the effect of hurricanes on a single species. In the case of *Montastraea annularis* hurricanes are benifical at a colonial scale, increasing asexual recruitment (Foster et al., 2007). However, at a patch scale fragmentation is detremental to future survival and growth (Table 4.9).

4.4.2 Issues Surrounding the Use of PPMs

Many of the modelling issues associated with PPMs could have affected the outcome of these results. Some transitions were not captured in this study, this could be due to the relatively short study period and due to the lack of recovery discussed above; this can affect the population growth rate. Methods such as the Integral Projection Model (Discussed in Chapter 5) can smooth over missing transitions through parameterization by curve fitting. Also the position of the size class boundaries can affect the model, for example growth of a patch by 1 cm^2 was observed, but if both pre and post transition sizes fall within the same size class then it is marked as a stasis transition. As growth occurs only at a small scale in this data set this can often lead to missing information in the model. In comparison shrinkage of patches is normally at a larger scale and is thus normally captured between size classes. This can paint an overly pessimistic outcome for

the population. This again can be solved through the application of an Integral Projection Model to the data set, which will capture the small scale growth that was observed to balance out the larger shrinkage.

Finally, the issue of ergodicity and primitivity means that there can be false conclusions about predicted growth rates of a population, this is particularly the case in this study where I_{Weak} was shown to follow four possible growth rates depending on initial conditions. All 4 PPMs created were reducible, which is the same for 24.7% of matrices in literature (Stott et al., 2010b). Using Integral Projection Modelling negates this issue, as all numerical estimates of IPMs in this data set are primitive and ergodic.

4.4.3   Conclusions

In this chapter, PPM modelling was adopted to test if the initial decline experienced by a coral patch affects its future dynamics. It was found that this was the case, with those the most severely traumatized showing worse dynamics than those the least traumatized. A greater discussion of these results and their affect on coral populations is given in Chapter 6.

There are issues with the framework of the PPM, especially in its application to size-determined populations. These include reducibility of the model, handling missing transitions and selection of size class boundaries. All of these issues can be solved through the use of Integral Projection Modelling. Three IPMs are parameterized in Chapter 5, to directly compare the results from the PPM and IPM methods. This will show if modelling issues affect the conclusions of this chapter.

Result	Key Facts	Implications	References
Severe trauma exhibits the worst dynamics	→ Over 50% of area lost in a Hurricane → Sharpest asymptotic decline → All patches will end up $< 12cm^2$ → Greatest transient extremes → Requires the greatest perturbations to achieve $\lambda_1 = 1$	If over 50% of area is lost then the patches are in the worst shape	Table 4.2 Table 4.5 Table 4.6 Table 4.8 Figure 4.5
Weak and Mild trauma exhibit similar dynamics	→ Similar growth rates → I_{Mild} is projected to contain a greater number of patches in the short term → I_{Weak} has a greater proportion of patches in the long term	Ramets experiencing a loss less than 50% of coral after a hurricane, the dynamics are better than I_{Severe}, but similar between I_{Weak} and I_{Mild}	Table 4.2 Table 4.5 Figure 4.4
Fragmentation is detrimental at a patch scale	→ Primarily in ramets in I_{Mild} → 63 events from 381 patches → Only 1 fragmentation event before Hurricane Mitch → Only 2 fragments went on to exhibit growth → 43% of fragments died before the end of the study	Fragmentation is not beneficial at a patch scale, in contrast to algae at a patch scale (Renken et al., 2010) or coral at a colonial scale (Foster et al., 2007)	Section 4.3.1
No growth observed prior to Hurricane Mitch	→ Population numbers will remain constant → Size structure will change → All patches under $3cm^2$ in the long term	Could be due to coral bleaching of Caribbean reefs in 1998 (Hoegh-Guldberg, 1999). Patches could be responding to this stress could show that hurricanes are needed for coral patches to exhibit full range of sizes.	Table 4.2 Table 4.5 Section 4.3.1

Table 4.9: A summary of the results from this chapter; highlights the implications of these results; and where the results can be found in this chapter.

Chapter 5

Comparison of Projection Models

5.1 Introduction

In Chapter 4, Population Projection Matrices (PPMs) were constructed and then used to test the hypothesis:

The initial impact of a hurricane influences the patch dynamics of Montastraea annularis.

However, in developing PPM models for coral patch dynamics a number of issues arose. The continuous nature of IPMs means discretization is not required in the selection of size classes, which means that fewer errors were introduced into the model. Also, the statistical modelling technique used to parameterize IPMs require less data and, since data for certain transitions is difficult to obtain, is well suited for modelling coral patches. In this chapter, IPMs are constructed for the three hurricane trauma categories defined in Chapter 4, in order to compare the results of the two modelling methods. Specifically in this chapter, the similarities and differences between the models will be highlighted and reasons for these differences will be discussed. This chapter focuses on answering the research question: 'How well do the results of different projection models compare?'

Category	I$_{\text{Severe}}$	I$_{\text{Mild}}$	I$_{\text{Weak}}$
X range	$0 \leq X \leq 0.47$	$0.47 < X \leq 0.78$	$X > 0.78$

Table 5.1: Range of impacts for each initial hurricane impact category.

5.2 Methods

Hurricane Mitch struck Glovers Reef in October 1998. This was followed by a sharp decrease in coral cover until June 1999 when the rate of decline decreased. To measure the trauma suffered by a coral patch, the area of all coral patches on each individual ramet were combined and a measure of initial trauma 'X' was defined as:

$$X = \frac{\text{Total coral area on ramet in June 1999}}{\text{Total coral area on ramet in December 1998}}. \tag{5.1}$$

Using this measure, the data was divided into three categories: I$_{\text{Severe}}$, I$_{\text{Mild}}$ and I$_{\text{Weak}}$ (Table 5.1). According to the ramet group they were placed in, the fate of coral patches from 5 sampling dates were combined to test the hypothesis:

The initial impact of a hurricane influences the patch dynamics of Montastraea annularis.

In Chapter 3, five size classes were selected to model a coral patch population of *M. annularis*. They were determined by the van der Meer and Moloney algorithm (van der Meer, 1978; Moloney, 1986), which resulted in the size classes: (I) 1-3 cm^2, (II) 4-12 cm^2, (III) 13-48 cm^2, (IV) 49-153 cm^2 and (V) 154+ cm^2.

These size classes were used to form a 5×5 generic PPM:

$$\mathbf{A} = \begin{pmatrix} S_{1,1} + D_{1,1} & D_{1,2} + R_{1,2} & D_{1,3} + R_{1,3} & D_{1,4} + R_{1,4} & D_{1,5} + R_{1,5} \\ G_{2,1} & S_{2,2} + D_{2,2} & D_{2,3} + R_{2,3} & D_{2,4} + R_{2,4} & D_{2,5} + R_{2,5} \\ G_{3,1} & G_{3,2} & S_{3,3} + D_{3,3} & D_{3,4} + R_{3,4} & D_{3,5} + R_{3,5} \\ G_{4,1} & G_{4,2} & G_{4,3} & S_{4,4} + D_{4,4} & D_{4,5} + R_{4,5} \\ G_{5,1} & G_{5,2} & G_{5,3} & G_{5,4} & S_{5,5} + D_{5,5} \end{pmatrix}, \tag{5.2}$$

where:

- $S_{i,i}$ represents the probability that a coral patch will remain in the same size class, i, between time t and $t+1$.

- $G_{j,i}$ represents the probability that a coral patch in size class i at time t grows to size class j at time $t+1$, where $j > i$.

- $R_{j,i}$ represents the probability that a coral patch in size class i at time t shrinks to size class j at time $t+1$, where $j < i$.

- $D_{j,i}$ represents the probability that a patch in size class i at time t fragments and produces a patch of size j at time $t+1$.

With a current population structure $\mathbf{x}(t)$ a PPM can be used to project the future population $\mathbf{x}(t+1)$ via the equation:

$$\mathbf{x}(t+1) = \mathbf{A}\mathbf{x}(t). \tag{5.3}$$

The Integral Projection Model (IPM) equivalently uses a kernel $\mathbf{k}(y, x)$ to project the population density function, $\mathbf{n}(x, t)$, via the equation:

$$\mathbf{n}(y, t+1) = \int_{\Omega} \mathbf{k}(y, x)\mathbf{n}(x, t)dx. \tag{5.4}$$

The PPM and the IPM kernel describe transitions in size, but where the PPM is discrete and requires the selection of size class boundaries, the IPM is continuous in size and does not require this discretization.

In Chapter 3, the IPM kernel for *M. annularis* was selected as:

$$\mathbf{k}(y, x) = (1 - p_f(x))s(x)\mathbf{g}(y, x) + s(x)f_s(x)p_f(x)n_f(x)\mathbf{f}_d(y, \frac{x}{n}), \tag{5.5}$$

where x is the log of the patch size. The biological processes captured in the IPM are:

- $s(x)$: the probability that a coral patch of size x at time t survives to time $t + 1$.

- $\mathbf{g}(y, x)$: gives the size y at time $t + 1$ which a coral patch of size x at time t will become, given that the patch has survived.

- $p_f(x)$: is the probability that a patch of size x at time t will fragment at time $t + 1$.

- $f_s(x)$: is the proportion of a patch of size x at time t which will remain after fragmenting at time $t + 1$.

- $n_f(x)$: is the number of fragments produced by a patch of size x at time t given that the patch fragments.

- $\mathbf{f}_d(y, \frac{x}{n})$: gives the size of a patch of size x at time t which produces n fragments, where the new fragment size is y at time $t + 1$.

The functions in the IPM and the entries of the PPM capture similar biological processes: The PPM entries $S_{i,i}$, $G_{j,i}$ and $R_{j,i}$ are combined in the functions $(1 - p_f(x))s(x)\mathbf{g}(y, x)$, whilst $D_{j,i}$ in the PPM is equivalent to the function $s(x)f_s(x)p_f(x)n_f(x)\mathbf{f}_d(y, \frac{x}{n})$. In numerically integrating the kernel the same areas of the kernel are equivalent to the PPM, but are created from modelling individual biological processes rather than being aggregated into combined transitions. In the results section below, the two modelling approaches are compared.

5.3 Results

The PPMs and IPMs were parameterized according to methods described in Sections 3.1.2 and 3.2.2. The PPMs were analyzed in Chapter 4, with the results
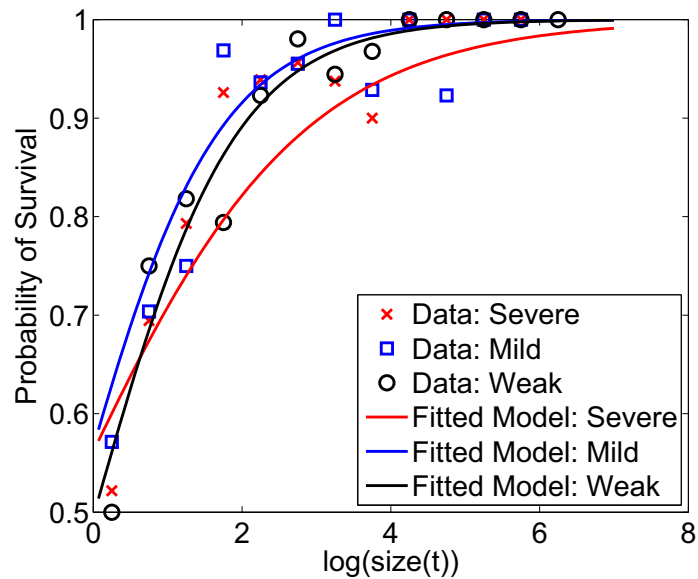
Figure 5.1: The numerical fit of the probability of survival function $s(x)$ used to parameterize the IPMs. For each function the data points are shown alongside the fitted models of log-size. Details of the functions plotted are given in Table 5.2.

given below as a reminder in order to make a comparison with the IPMs which are parameterized and analyzed in this chapter.

5.3.1 Parameterization of the IPMs

Probability of Survival. The fitted function is linear for all three trauma categories (Figure 5.1 and Table 5.2), with higher order non-linearities rejected in all cases ($I_{\text{Severe}} : P = 0.17$, $I_{\text{Mild}} : P = 0.18$, $I_{\text{Weak}} : P = 0.33$). As patch size increased the probability of survival increased. Survival is lower for smaller patches in I_{Weak}, but as size increased I_{Severe} had the lowest survival rate. At a patch size of approximately $55cm^2$, the survival probability for I_{Weak} and I_{Mild} was close to 1, whilst for I_{Severe}, the largest patches in this study have a survival probability of less than 1.

Mean Growth. The estimate is similar for I_{Weak} and I_{Mild}, and lies below the $x = y$ line. This showed, in general, that all patches are decreasing in size (Figure 5.3, Table 5.2). The relationship between sizes for all three trauma groups are linear
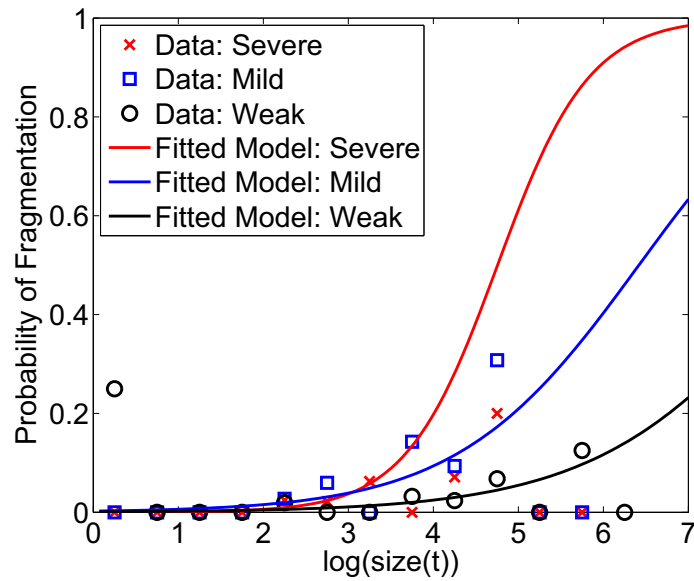
Figure 5.2: The numerical fit of the probability of fragmentation function $p_f(x)$ used to parameterize the IPMs. For each function the data points are shown alongside the fitted models of log-size. Details of the functions plotted are given in Table 5.2.
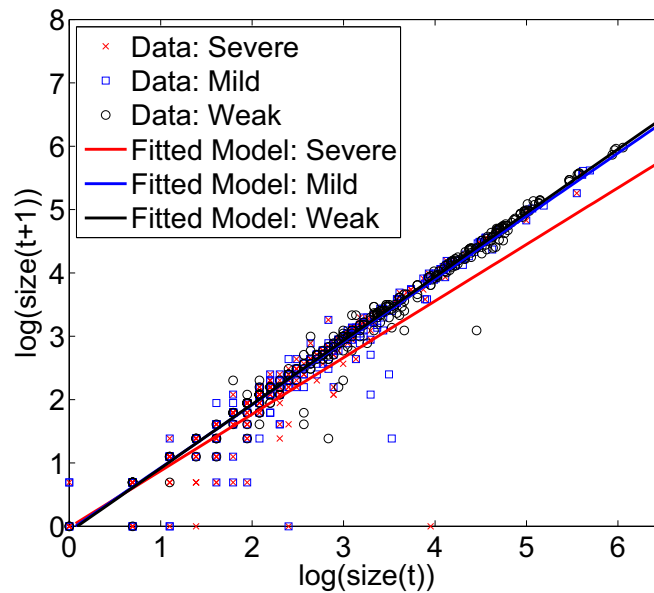
Figure 5.3: The numerical fit of the mean growth function $\overline{\mathbf{g}(y, x)}$ used to param-eterize the IPMs. For each function the data points are shown alongside the fitted models of log-size. Details of the functions plotted are given in Table 5.2.
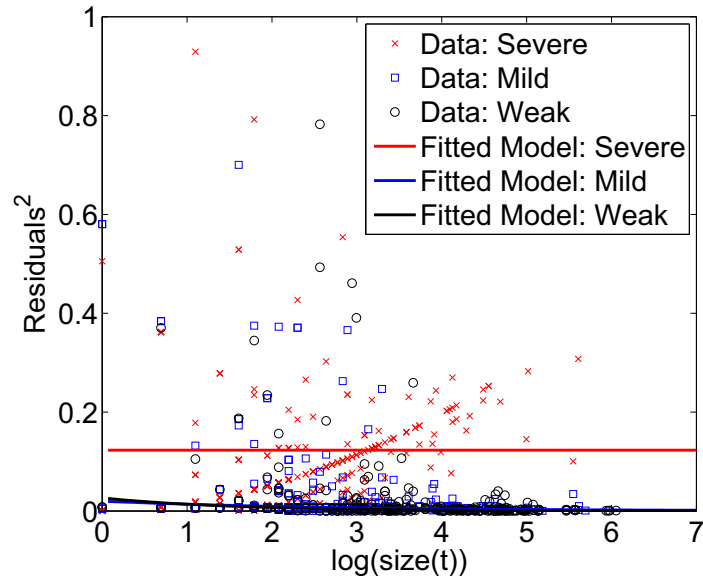
Figure 5.4: The numerical fit of the variance of growth function $\sigma^2(\mathbf{g}(y, x))$ used to parameterize the IPMs. For each function the data points are shown alongside the fitted models of log-size. Details of the functions plotted are given in Table 5.2.
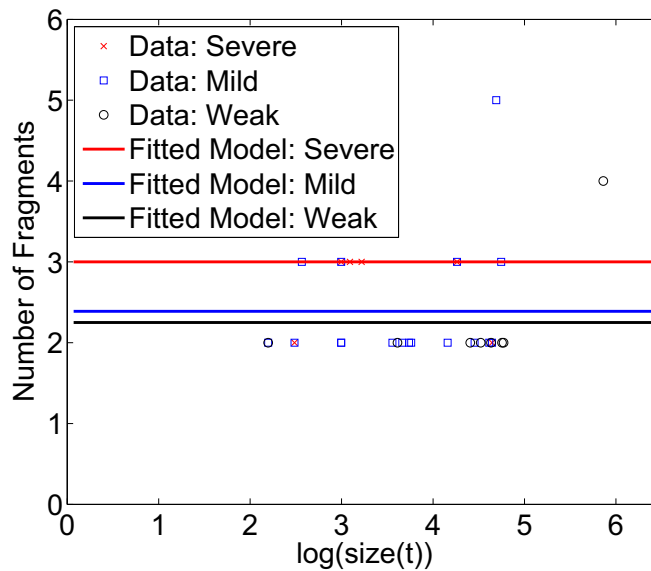
Figure 5.5: The numerical fit of the number of fragments function $2 + n_f(x)$ used to parameterize the IPMs. For each function the data points are shown alongside the fitted models of log-size. Details of the functions plotted are given in Table 5.2.
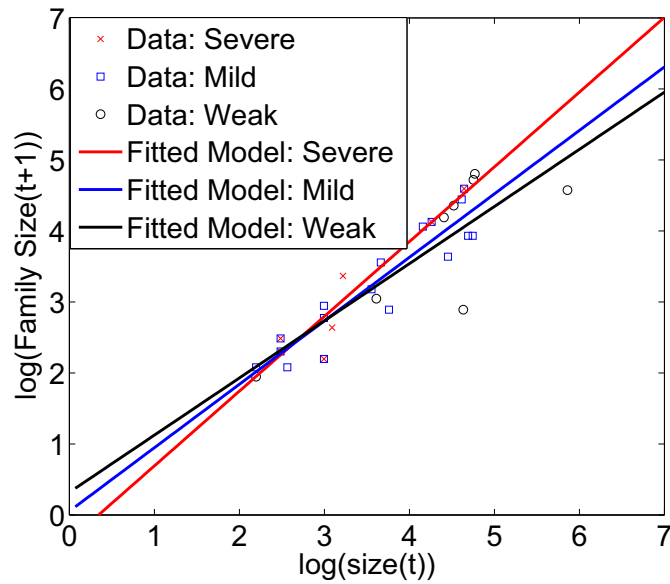
Figure 5.6: The numerical fit of the family sizes function $f_s(x)$ used to parameterize the IPMs. For each function the data points are shown alongside the fitted models of log-size. Details of the functions plotted are given in Table 5.2.
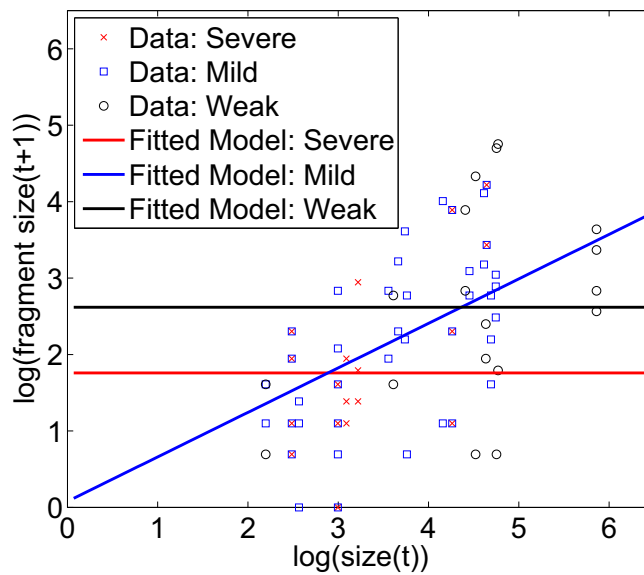
Figure 5.7: The numerical fit of the sizes of fragments function $\mathbf{f}_d(y, \frac{x}{n})$ used to parameterize the IPMs. For each function the data points are shown alongside the fitted models of log-size. Details of the functions plotted are given in Table 5.2.

Function	I_{Severe}
$\overline{s(x)}$	0.2468 (0.3662)+0.6399 (0.2305)x
$\overline{\mathbf{g}(y,x)}$	-0.0177 (0.0941)+0.8935(0.0475)x
$\sigma^2(\mathbf{g}(y,x))$	0.123 (0.049)
$p_f(x)$	-8.822(3.337)+1.855(1.045)x
$n_f(x)-2$	0
$f_s(x)$	-0.3625(0.51)+1.0527(0.15)x
$\mathbf{f}_d(y,x/n)$	1.759 (0.268)
σ^2	0.431
	I_{Mild}
$\overline{s(x)}$	0.2644(0.3464)+1.0601(0.1866)x
$\overline{\mathbf{g}(y,x)}$	-0.0687(0.0343)+0.9933(0.0125)x
$\sigma^2(\mathbf{g}(y,x))$	0.0199(0.2411)+0.6892(0.0880)x
$p_f(x)$	-6.0251(0.8349)+0.9387(0.2266)x
$n_f(x)-2$	-0.9445(0.3780)
$f_s(x)$	0.0524(0.3417)+0.8937(0.0921)x
$\mathbf{f}_d(y,x/n)$	0.0780(0.4471)+1.3910(0.2823)$\frac{x}{n}$
σ^2	1.1796
	I_{Weak}
$\overline{s(x)}$	-0.0191 (0.4913)+1.0612 (0.2136)
$\overline{\mathbf{g}(y,x)}$	-0.0892 (0.0274)+ 1.0071 (0.0077)x
$\sigma^2(\mathbf{g}(y,x))$	0.0265(0.3598)+0.5207(0.1014)x
$p_f(x)$	-6.9962(1.5813)+0.8286(0.3566)x
$n_f(x)-2$	-1.3863 (0.7071)
$f_s(x)$	0.3183(1.0463)+0.8050(0.2348)x
$\mathbf{f}_d(y,x/n)$	2.6177 (0.3105)
σ^2	1.7357

Table 5.2: The fits for the three models with standard errors given in brackets for each estimate.

(with non-linearities rejected: $I_{Severe} : P = 0.19$, $I_{Mild} : P = 0.08$, $I_{Weak} : P = 0.26$), and as size increased at time t so did the size of the patch at time $t + 1$. For small patches in I_{Severe}, the size of patches at time $t+1$ is similar to other trauma groups, but the gradient of the line is lower and for large patches there is a greater decrease in area than the other trauma categories.

Variance of Growth. The variance of growth was linear for I_{Mild} and I_{Weak} with quadratic terms rejected ($I_{Mild} : P = 0.527$, $I_{Weak} : P = 0.989$). This meant that as size increased the variability of sizes decreased (Table 5.2 and Figure 5.4). The variance for I_{Severe} was constant with linear terms rejected (P=0.29). This showed that variance did not vary with patch size.

Probability of Fragmentation. The probability for I_{Severe} showed that for patches larger than $55cm^2$ there is a greater than 50% chance of fragmentation (Figure 5.2). This seems unlikely and could be skewed by the low number of patches that fragmented in this category. The smallest chance of fragmentation is in I_{Weak}, where $p_f(x)$ is about half the value as I_{Mild}. There was no fragmentation predicted for patches of size $8cm^2$ or less for all categories. The fitted probability is linear (Table 5.2), as patch size increased so did the probability of fragmentation (non-linearities are rejected: $I_{Severe} : P = 0.08$, $I_{Mild} : P = 0.06$, $I_{Weak} : P = 0.94$).

Number of Fragments. For all three trauma categories, the number of fragments produced was not dependent on initial patch size (Figure 5.5 and Table 5.2), linear terms were rejected in I_{Mild} ($P = 0.12$). However, in the case of I_{Severe} and I_{Weak}, the mean number of fragments were calculated, due to the low number of fragmentation events in these categories. The greatest mean number of patches produced was in I_{Severe}, 3, and the fewest in I_{Weak}, 2.25.

Family Size. For all categories, as patch size increased so did family size (non-linearities rejected: $I_{Mild} : P = 0.82$, $I_{Weak} : P = 0.51$, Figure 5.6 and Table 5.2). I_{Mild} had a larger family size than I_{Weak}. This showed that larger patches kept a greater proportion of their area following fragmentation, compared to smaller

patches.

Fragment Size. When a patch fragmented in I_{Mild} the larger the original patch, the larger the patches produced. This relationship was linear with quadratic terms rejected ($P = 0.62$). In both I_{Weak} and I_{Severe}, the size of fragments did not depend on their initial size, with the mean fragment size giving the best fit of data (linear terms rejected, I_{Weak}: $P = 0.37$ and I_{Severe}: $P = 0.29$). The fragments produced in I_{Weak} were 33% larger than in I_{Severe}.

There were issues in fitting the number of fragments and family size functions in I_{Severe}. This was because of a lack of fragmentation data captured (only two patches fragmented) and this skewed the fitted models, or resulted in terms in the model being insignificant. In these cases the functions were fitted with the mean, either of the number of fragments or family size.

5.3.2 Comparison of IPM Kernels and PPMs

Similarities Between IPM Kernels and PPMs.

The IPM kernels and PPMs (Table 5.3) are similar in the following ways:

- In I_{Severe} the peak probability values, on the diagonal, in the IPM kernel are lower than in I_{Mild} and I_{Weak}. This showed that the survival in this trauma group is low. The PPM also showed low probability estimates in the stasis values.

- In the PPM of I_{Severe}, there are only zero transition rates for sizes above size class IV, reflected in an IPM that is zero in these areas. In the PPM there is growth from size class I to size class II, also shown in the IPM where non-zero contours are shown in these size classes.
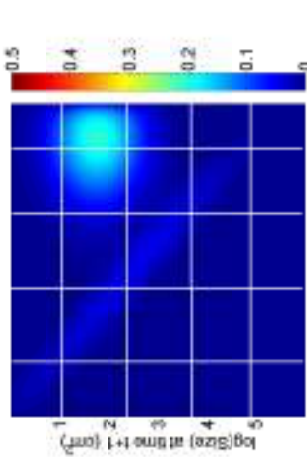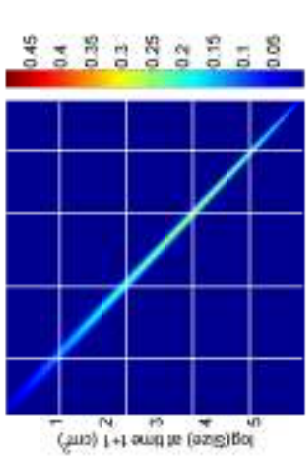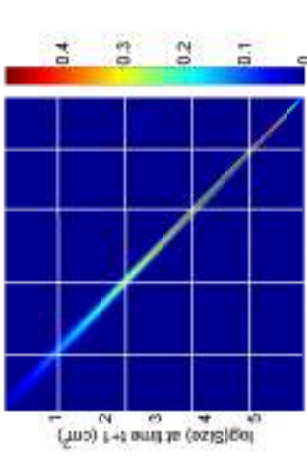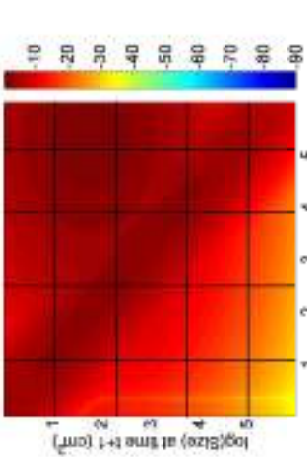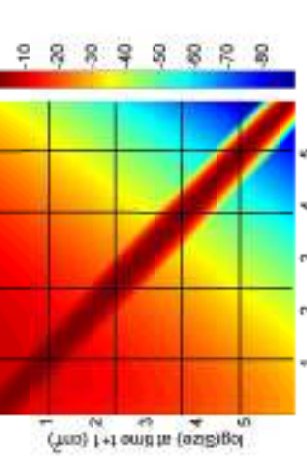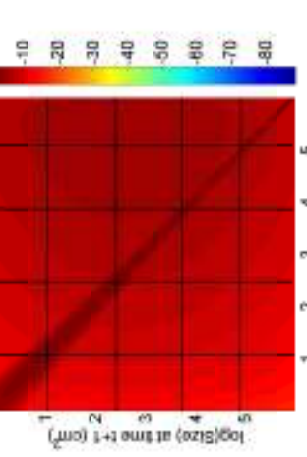
	I_{Severe}	I_{Mild}	I_{Weak}
PPM	$\begin{pmatrix} 0.64 & 0.16 & 0.03 & 1 & 0 \\ 0.02 & 0.68 & 0.28 & 0 & 0 \\ 0 & 0 & 0.55 & 0 & 0 \\ 0 & 0 & 0 & 0 & 0 \\ 0 & 0 & 0 & 0 & 0 \end{pmatrix}$	$\begin{pmatrix} 0.64 & 0.06 & 0.04 & 0.03 & 0 \\ 0.02 & 0.87 & 0.15 & 0.07 & 0 \\ 0 & 0.01 & 0.80 & 0.18 & 0 \\ 0 & 0 & 0.01 & 0.70 & 0.17 \\ 0 & 0 & 0 & 0 & 0.83 \end{pmatrix}$	$\begin{pmatrix} 0.76 & 0.04 & 0 & 0.01 & 0 \\ 0 & 0.82 & 0.07 & 0.03 & 0 \\ 0 & 0 & 0.90 & 0.03 & 0.17 \\ 0 & 0 & 0 & 0.92 & 0 \\ 0 & 0 & 0 & 0.0 & 0.83 \end{pmatrix}$
IPM Kernel			
IPM log-Kernel			

Table 5.3: The PPMs and IPM kernels (both kernels and log-kernels) for the three hurricane trauma categories. The size class boundaries from the PPMs are added to the IPM kernels.

- In I_{Mild} the IPM kernel is concentrated around the $x = y$ line, i.e. around the survival-growth line. There is a slight decrease in all sizes as the survival-growth line lies below the $x = y$ line. The probabilities are higher than in I_{Severe} and is greatest in size class III. The PPM also reflects this with the highest stasis values in size classes II, III and IV.

- Some growth is observed in the PPM of I_{Mild}, but the amount of growth and shrinkage decreased as size increased. There is no growth into size class V and there is no shrinkage from size class V into size classes I, II or III. This is reflected in the IPM where the log kernel shows a decrease in behaviour as size increased and in particular there was little growth into size class IV and shrinkage from size class V.

- The IPM for I_{Weak} showed the majority of behaviour will occur on the $x = y$ line. The width of this line was narrower than other kernels, and this behaviour lies within the diagonal size classes. This is reflected in the PPM where most non-zero entries were located in the stasis entries on the diagonal.

- In the PPM of I_{Weak}, there was a greater amount of behaviour in the upper right triangle than on the lower left triangle, and this is reflected in the IPM log-kernel where there is a darker region in the upper right triangle compared to the lower left triangle.

- In the PPM of I_{Weak}, growth is non-zero from size class IV to V and this is reflected in the IPM log-kernel where non-zero contours are located. As size increased stasis values increased in the PPM, this is the same in the IPM kernel where the largest contours were located in size class V.

Major differences between the IPM kernels and PPMs.

- The contribution from fragmentation is on a smaller scale in the IPM kernels than in the PPMs. The contribution to the IPM is only observed on a log-scale.

- In I_{Severe}, the IPM kernel showed a small amount of growth into size class V, although this is only observed on a log-scale. This transition is zero in the PPM.

- The kernel for I_{Mild} is symmetrical around the $x = y$ axis, which is particularly evident on the log-scale. This is not fully observed in the PPM where there are more zero entries on the lower-diagonal than on the upper diagonal.

- The behaviour in I_{Weak} is strictly confined to the diagonal entries in the IPM kernel, with no shrinkage or fragmentation contribution. This differs from the PPM where there are 6 upper-triangular non-zero transitions.

5.3.3 Comparison of Asymptotic Dynamics

The population growth rates (Table 5.4), stable size structures and fragmentation values (Table 5.5 and Figures 5.8 and 5.9) show similarities and differences between the two modelling approaches.

Category	PPM	IPM
I_{Severe}	0.718	0.680
I_{Mild}	0.894	0.691
I_{Weak}	0.922	0.981

Table 5.4: Population growth rates for all three trauma categories for both PPM and IPM modelling methods. Calculated as the dominant eigenvalue of either the PPM or of the numerical estimate of the kernel.
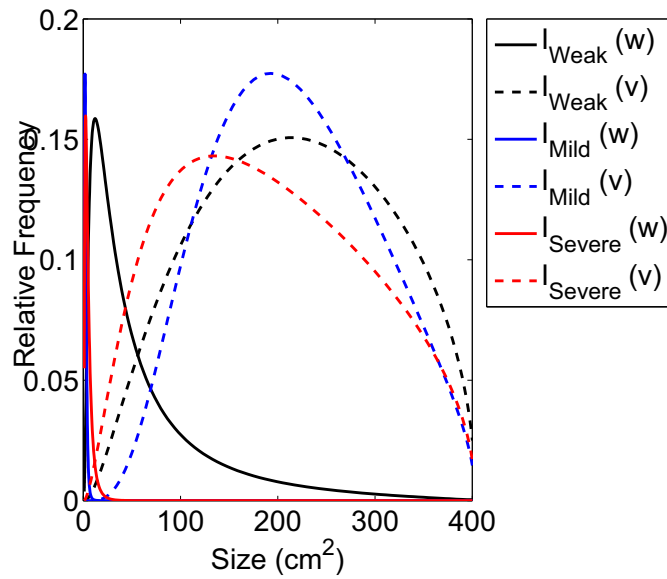
Figure 5.8: The stable size distributions and fragmentation values for each trauma category, calculated as the left and right eigenvectors of the dominant eigenvalue of the numerical estimation of the IPMs.
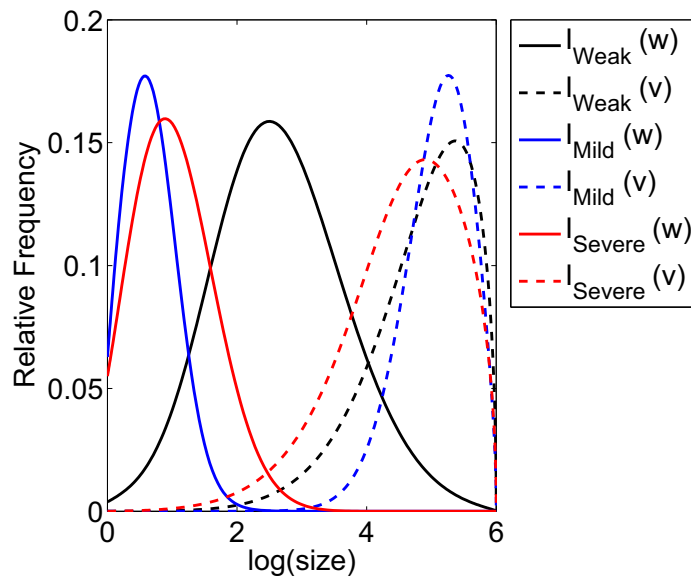
Figure 5.9: The stable size distributions and fragmentation values for each trauma category on a log-size scale, calculated as the left and right eigenvectors of the dominant eigenvalue of the numerical estimation of the IPMs.

	I_{Severe}	I_{Mild}	I_{Weak}
w	$\begin{pmatrix} 0.6632 \\ 0.3368 \\ 0 \\ 0 \\ 0 \end{pmatrix}$	$\begin{pmatrix} 0.1889 \\ 0.7225 \\ 0.0857 \\ 0.0029 \\ 0 \end{pmatrix}$	$\begin{pmatrix} 0.0930 \\ 0.3126 \\ 0.3904 \\ 0.1873 \\ 0.0167 \end{pmatrix}$
v	$\begin{pmatrix} 0.067 \\ 0.310 \\ 0.560 \\ 0.093 \\ 0 \end{pmatrix}$	$\begin{pmatrix} 0.006 \\ 0.094 \\ 0.170 \\ 0.195 \\ 0.565 \end{pmatrix}$	$\begin{pmatrix} 0 \\ 0 \\ 0 \\ 1 \\ 0 \end{pmatrix}$

Table 5.5: The stable size-structures for each trauma category **w** calculated as the right-hand eigenvectors for the dominant eigenvalue of the PPM. Also given is the fragmentation value **v** calculated as the left-hand eigenvector for the dominant eigenvalue of the PPM.

Similarities Between the Predicted Asymptotic Dynamics

Similarities between the two approaches:

- For all three trauma categories and both modelling methods, the population growth rates are below 1 (Table 5.4). This showed that all populations are in asymptotic decline.

- For both methods, I_{Severe} had the lowest growth rate, and I_{Weak} the largest. As trauma increased, the growth rate estimate decreased (Table 5.5).

- In I_{Mild}, the stable size structure for the IPM was dominated by patches under $12cm^2$ (Figures 5.8 and 5.9), whilst the distribution for the PPM projects only 91% of patches are under $12cm^2$ (Table 5.5).

- For I_{Weak} the stable size structure for both the IPM and PPM had a larger range of coral patch sizes than either of the other 2 trauma categories (Figures 5.8 and 5.9 and Table 5.5).

- The largest contribution in the stable size structure for I_{Weak} was under $50cm^2$ in the IPM (*i.e.* in size classes *I*, *II* and *III*). The PPM estimated the same

with under 20% of patches located in size classes IV and V.

- The IPM and PPM stable size structures for I_{Severe} and I_{Mild} are similar, with most patches predicted to lie in the first 2 size classes.

- In the case of I_{Weak}, the estimates of the stable size distributions are very similar, in both the distribution of sizes and the peak contribution of patch sizes.

- The estimates of the stable size distribution also showed the same increase in spread of sizes as trauma decreased for both the IPM and the PPM.

- The fragmentation value for I_{Severe} (Figures 5.8 and 5.9 and Table 5.5) showed a greater contribution from smaller coral patch sizes than either of the other trauma categories.

- The peak contribution to the fragmentation value occurred at approximately $100cm^2$ in the IPM of I_{Severe}, which is in size class IV, with the peak in the PPM occurring in size class III.

- In I_{Mild}, the IPM fragmentation value showed there is the greatest contribution from the largest patches than any other category. The PPM also showed this as the only non-zero value was in size class V.

- The greatest contribution in $\mathbf{v}$ for I_{Mild} came from patches larger than $100cm^2$ in the IPM (Size classes IV and V), and the PPM estimated over 75% of the fragmentation contribution came from size classes IV and V (greater than $49cm^2$).

Differences Between the Predicted Asymptotic Dynamics

The differences between the two approaches are:

- The level of the asymptotic decline varied between modelling methods (Table 5.5).

- For I_{Severe} and I_{Mild}, the growth rate estimated by the PPM was larger than the estimate by the IPM, by 5% and 23% respectively.

- For I_{Weak}, the PPM estimate was 6% lower than the IPM estimate.

- The PPM estimated growth rate for I_{Mild} was closer to the estimate for I_{Weak}, but for the IPM estimate it was nearer I_{Severe}. The differences in estimates are large enough to effect extinction times.

- The IPMs are all primitive and hence ergodic, therefore all initial conditions follow the same growth rate. This is not the case for the PPMs where the PPM for I_{Weak} in non-ergodic and therefore trajectories of population projections can follow very different growth rates depending on the initial conditions.

- In I_{Severe}, the IPM predicted the stable size structures would contain only small patches, with over 95% of patches lying within size class I and the remaining 5% in size class II. The PPM estimated that there will be a greater proportion of larger patches, with only 66% of patches lying in size class I, with the remainder in size class II.

- The maximum size in the stable size structure of I_{Weak} for the IPM was approximately $400cm^2$, the PPM showed that there was a complete range of patch sizes with no upper limits in area (Figures 5.8 and 5.9 and Table 5.5).

- The PPM for both I_{Severe} and I_{Mild} predicted larger patch sizes in the stable size structure than the IPM.

- In I_{Weak} the fragmentation values are different for the PPM and IPM. In the PPM, the contribution to the production of new patches came from size class

Category	Reactivity		Attenuation		ρ_{max}		a_{min}	
	PPM	IPM	PPM	IPM	PPM	IPM	PPM	IPM
I_{Severe}	1.39	12.71	0	0.02	2.74	56.08	0	0
I_{Mild}	1.12	1.35	0.74	0.02	2.50	19.6	0.12	0
I_{Weak}	1.09	1.46	0.83	0.01	1.82	4.10	0.15	0

Table 5.6: The transient dynamics for all three trauma categories for both the PPM and IPM methods.

IV, which is from sizes $49 - 153cm^2$. In the IPM the contribution came from all sizes, with the maximum contribution at about $200cm^2$.

5.3.4 Comparison of Transient Analysis

The transient analysis of the PPM and IPM methods (Figures 5.10, 5.11 and 5.12), show the upper and lower bounds of possible behaviour of the standardised matrices $\widehat{A} = \frac{A}{\lambda_1}$. This shows the relative upper and lower bounds of behaviour that could occur from biased initial conditions compared to if the popualtion was in an asymptotic state. The upper and lower bounds were calculated from projecting biased initial conditions $\mathbf{e}_i$ for all $i \in n$, where n is either the number of size classes in the PPM, or the number of mesh points in the IPM

Similarities in the Transient Dynamics

- The lower bounds for population density are the same in I_{Severe} for the PPM and IPM, with an Attenuation value of 0 (Figure 5.10 and Table 5.6).

- The PPM and IPM predict the highest relative maximum population density occurred in I_{Severe} compared to I_{Weak} and I_{Mild} (Figures 5.10, 5.11 and 5.12). This means that ρ_{max} was higher in I_{Severe} for both modelling methods (Table 5.6).

- I_{Severe} had the greatest range of possible behaviour in both the PPM and IPM, both after one time step and ten time steps (Figure 5.12 and Table
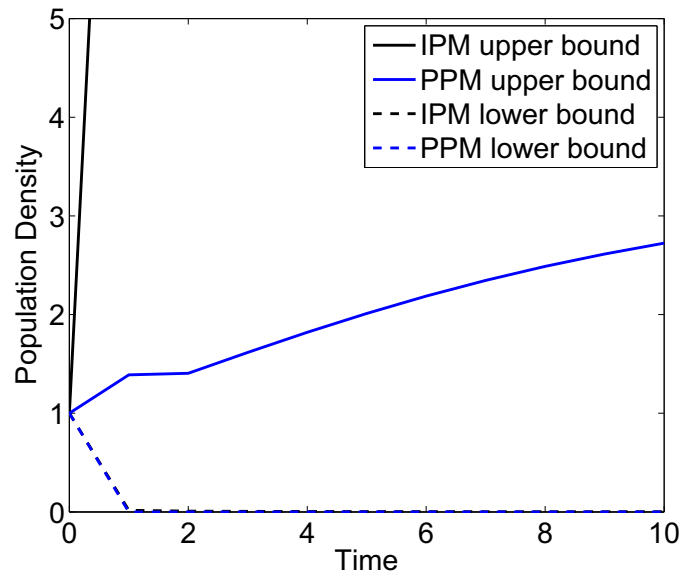
Figure 5.10: The upper and lower bounds of transient behaviour of the IPM and PPM models of I_{Severe} over ten time steps.
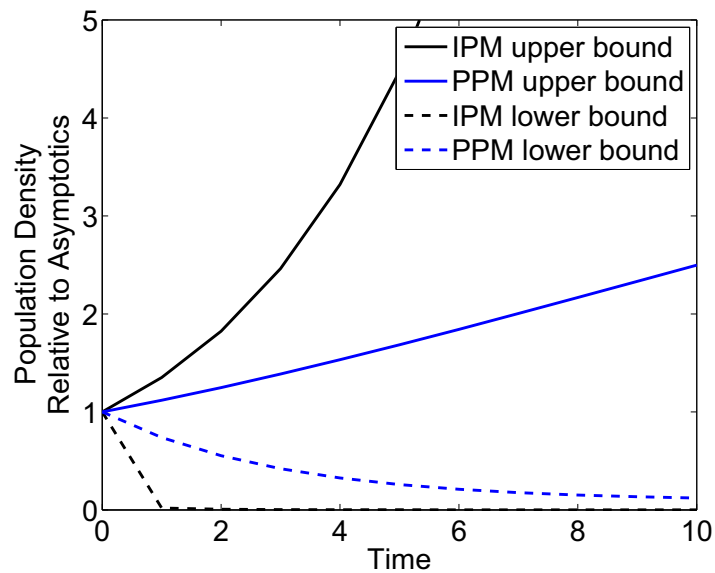
Figure 5.11: The upper and lower bounds of transient behaviour of the IPM and PPM models of I_{Mild} over ten time steps.
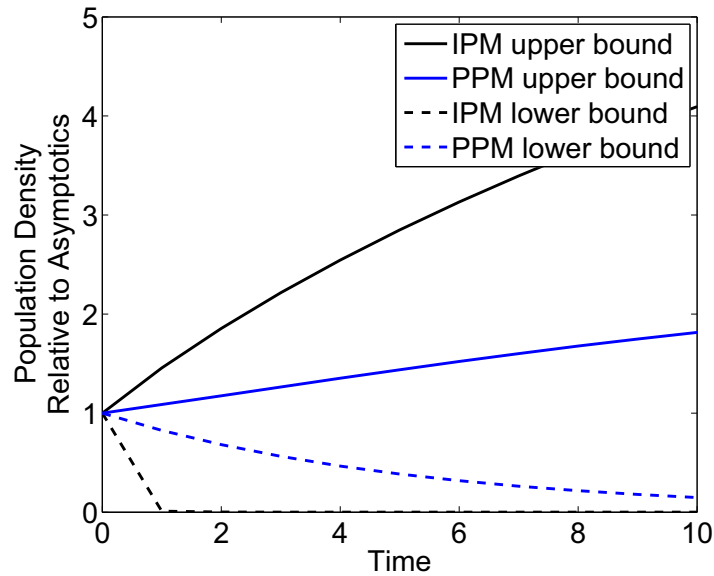
Figure 5.12: The upper and lower bounds of transient behaviour of the IPM and PPM models of I$_{\text{Weak}}$ over ten time steps.

5.6).

- The upper bounds for the IPM were always above that of the PPM, whilst the lower bounds for the IPM were always below that of the PPM (Figures 5.10, 5.11 and 5.12).

- I$_{\text{Weak}}$ had the lowest maximum densities for both the IPM and the PPM, showed by the lowest ρ_{max} values (Figure 5.12 and Table 5.6).

Differences in Transient Analysis

- The maximum population density ρ_{max} for I$_{\text{Severe}}$ for the PPM was achieved by the IPM in 2 time steps (Figure 5.10).

- The lower bound of behaviour in I$_{\text{Mild}}$ predicted extinction after one time step in the IPM, $Attention = 0$, but a population density of 0.74 in the PPM (Figure 5.11 and Table 5.6). In fact the PPM does not predict extinction after 10 time steps ($a_{min} > 0$).

- In I_{Weak}, the IPM states extinction after 1 time step, $Attenuation = 0$, but the PPM states the minimum possible relative density was 0.83 (Figure 5.12 and Table 5.6).

- In I_{Severe} and I_{Mild}, the PPM predicted a similar maximum amplification, ρ_{max}, however the IPM estimates are different with I_{Severe} much larger than I_{Mild} (Table 5.6).

- For the PPM lower bound of I_{Mild} and I_{Weak} the population density of 0 is not reached in the ten time steps ($a_{min} > 0$), whilst the IPM lower bound is 0 after 1 time step with $Attenuation = 0$ (Table 5.6).

5.3.5   Comparison of Sensitivity Analysis

The IPM estimates of sensitivity (Table 5.7) are highest in the lower triangular area, where growth of patches occurs. I_{Severe} had the highest sensitivity and I_{Weak} the lowest. In I_{Severe}, the kernel is most sensitive in growth from size classes I to size classes III or IV. The remaining kernel is not sensitive. This is similar to the sensitivity for the PPM, where the most sensitive entries are growth from size class I to size classes II and III, or growth from size class II to III. There is a greater number of non-zero sensitivity entries in the PPM, compared to the IPM.

In I_{Mild}, highly sensitive growth entries are seen in both the IPM and PPM. In particular the IPM highlights the importance of growth from size class I to size class V, whereas the PPM highlights the importance of growth from size class II to size classes III and IV or size class I to size class V. There are some areas which overlap, but the PPM gives a wider range of sensitive values.
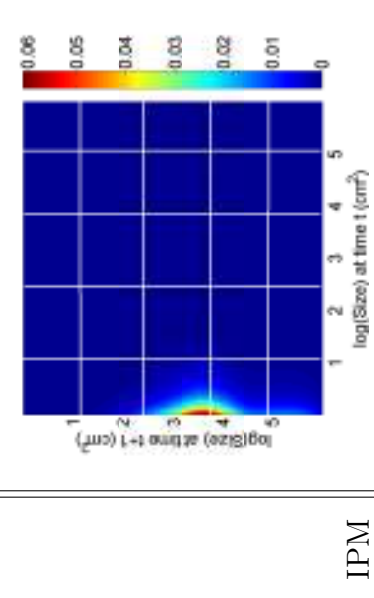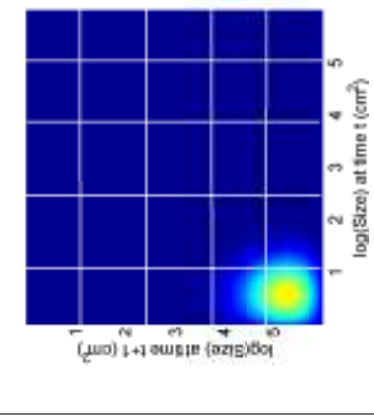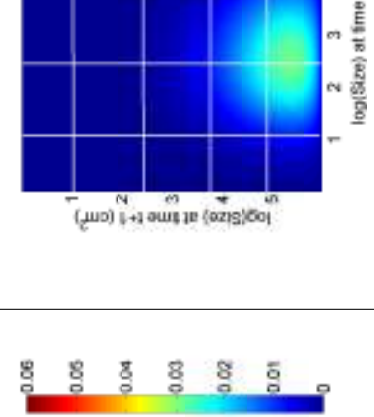
	I_{Severe}	I_{Mild}	I_{Weak}
PPM	$\begin{pmatrix} 0.297 & 0.151 & 0 & 0 & 0 & 0 \\ 1.385 & 0.703 & 0 & 0 & 0 & 0 \\ 2.358 & 1.197 & 0 & 0 & 0 & 0 \\ 0.414 & 0.210 & 0 & 0 & 0 & 0 \\ 0 & 0 & 0 & 0 & 0 & 0 \end{pmatrix}$	$\begin{pmatrix} 0.013 & 0.050 & 0.006 & 0.000 & 0 \\ 0.211 & 0.807 & 0.096 & 0.003 & 0 \\ 0.382 & 1.462 & 0.174 & 0.006 & 0 \\ 0.439 & 1.679 & 0.199 & 0.007 & 0 \\ 1.201 & 4.591 & 0.545 & 0.019 & 0 \end{pmatrix}$	$\begin{pmatrix} 0 & 0 & 0 & 0 & 0 \\ 0 & 0 & 0 & 0 & 0 \\ 0 & 0 & 0 & 0 & 0.089 \\ 0.497 & 1.669 & 2.085 & 1.000 & 0 \\ 0 & 0 & 0 & 0 & 0 \end{pmatrix}$
IPM			

Table 5.7: Sensitivity analysis for the IPM and PPM estimates for all three trauma categories. The size class boundaries are shown on a log-scale for the IPM. The sensitivity estimates of the PPM are affected by the imprimitivity if the PPMs and zero entries are forced in some cases.

In I_{Weak}, sensitivity is higher in all growth areas than either I_{Severe} or I_{Mild} in the IPM. It is most sensitive from size classes II and III to size classes IV and V and the PPM it is most sensitive in growth from size classes II and III to IV. The picture is similar for both methods.

5.4   Conclusions

In conclusion, the two projection methods paint a similar picture of the dynamics of the reef. There are some key differences in the results, namely in the size of the population growth rates; the distribution of proportions of patch sizes in the future; and short term dynamics of the populations. However, in general the picture shown is the same. Compared to the PPM, the IPM is easier to fit and is also more accurate at estimating the vital rates. There is also greater detail produced in the IPM kernel than in the PPM and this is, in turn, reflected in the greater detail of the corresponding stable size structure and fragmentation value. Moreover, using the IPM, solves the problem of discretization into size classes. It is for these reasons, that the IPM should be used ahead of the PPM.

The results of this chapter showed that the population dynamics of the two models - PPM and IPM - are similar. In particular, the population growth rates decreased as trauma increased regardless of the method used to model the population. It depended on the trauma category as to whether the PPM method over-estimated or under-estimated the population growth rate. Ramula et al. (2009) stated that for small data sets the growth rates for IPMs are less biased. Therefore, the population growth rates for IPMs are more reliable and closer to their actual values. There are 118 coral patches in I_{Weak}, 144 in I_{Mild} and 105 in I_{Severe}. Ramula et al. (2009) suggest that for smaller data sets of plants, the IPM is a better alternative to the PPM. It is only when there is greater than 600 pieces of data when the PPM and IPM population growth rates are the same (Easterling et al., 2000).

Easterling et al. (2000) state that the estimates of growth rates for IPMs and PPMs should be closely related. The fact this does not occur in this case could suggest that the PPM method does not accurately model fragmentation and this in turn affects the growth rate estimate. It is the trauma category with the most fragmentation where the discrepancy is most observed. In I_{Weak}, the estimate for the PPM is lower than the IPM, possibly because the fragmentation was over-estimated in this case. In I_{Severe}, the probability of fragmentation in the IPM could be under-estimated due to a lack of data and this could skew the results. In I_{Severe} and I_{Mild}, the size distribution of fragments is constant, as opposed to for I_{Weak} where it is linear. This shows greater realism, with larger patches creating larger fragments, especially as the number is independent of patch size. This could account for why the estimate of the growth rate of I_{Severe} and I_{Mild} is lower in the IPM than the PPM and, in the case of I_{Weak}, where there is a linear relationship, it is higher.

The IPM kernels showed a similar picture to the PPMs. The most common behaviour was stasis and this was the same for all trauma categories. The contribution from fragmentation to the kernel was much less in the IPM than the PPM and could account for the differences in growth rates and fragmentation value. The estimate of survival-growth in the PPM and IPM was similar and showed it is accurately modelled by both methods; however, the IPM should be better at capturing fragmentation. This is because the IPM accounts for different biological aspects that contribute to fragmentation where, as in the PPM case, the estimates attempt to calculate the fragmentation contribution in one hit.

Growth of an individual coral patch was only observed in small numbers throughout the study with the exception of the time step at which Hurricane Mitch occurred, where there was no growth observed. However, in the PPMs, even those few growth events are rarely captured. There are many reasons why growth was uncaptured. Some of these are inherent in the PPM structure, for example, the

discretization of size classes. It is also known that the population growth rate is sensitive to the width and number of sizes classes selected (Ramula and Lehtila, 2005). The uncaptured growth could also be because $M.\ annularis$ is a slow growing coral, therefore growth is only on a small scale compared to shrinkage. Finally it could be as a result of missing data, where the coral patches randomly selected did not exhibit growth, but other coral patches did.

The issues in capturing growth could account for the variation of growth rates between the different modelling methods. The growth rate for I_{Weak} could be under-estimated by the PPM, as growth transitions are not captured. The two remaining population growth rates are over-estimated by the PPM model; this could be because of a bias caused by missing transitions. There could also have been some shrinkage events that were classified as stasis in the PPM, hence over-estimation of behaviour. The IPM is not affected by discretization or sensitivity to selection of the number of size classes and hence is assumed to give more accurate results.

The 'giant' matrix estimates of the IPMs are primitive and hence ergodic. This gives confidence to the values of the population growth rate. Especially in the case of I_{Weak}, the PPM is non-ergodic and the initial conditions determine the growth rate, in the case of the IPM all initial conditions will follow the same growth rate. This also aids sensitivity analysis where in the PPM imprimitivity affects its calculation by introducing forced zero entries.

The PPM and IPM showed a similar pattern in the behaviour of the stable size structure $\mathbf{w}$ for I_{Weak}. In estimating the stable size structure for I_{Severe} and I_{Mild}, the PPM stated that there will be larger patches than the IPM. This could be linked to the smaller growth rates estimated by the IPM, as larger patches have better survival rates and a greater chance of fragmentation. The IPM gives greater detail in the distribution and also showed the distribution of the patches within the size class boundary.

The fragmentation value of the PPM and IPMs for I_{Severe} and I_{Mild} are very similar with peak contributions in the same range of sizes. However the fragmentation value for I_{Wild} showed different results. In particular, the IPM showed that not only is **v** non-zero for the complete range of sizes, but also the peaks of the **v** are not in the same place as the PPM. This could be as a result of slight differences in the kernel as a result of modelling fragmentation in a more biologically realistic method.

There are fewer parameters used to describe the IPM as opposed to the PPMs. In particular there are approximately 14 parameters for an IPM rather than 25 for the PPM. The continuous nature of the IPM means that, where transitions are not observed in the data set, they are still found in the IPM. The PPM is unable to capture transitions, which should be observed but are not. Fewer parameters also mean that there is a greater amount of data to calculate each parameter in the IPM, which reduces the sampling errors in the model.

The transient analysis showed very different pictures between the PPM and IPM models. The lower bounds for the IPM fall to zero instantly, inspite of the numerical estimates being primitive. This is due to some initial conditions falling within categories that have a zero transition rate and this is an issue with transient analysis of IPMs. The upper bounds of the IPM population densities relative to the asymtotics is always greater than the PPM, whilst the lower bounds of the IPM are always lower than the PPM. It is unclear if this is as a result of the transient analysis techniques or as a result of this particular model.

Transient techniques are better developed for PPMs than IPMs, and PPMs should always be analyzed in this manner (Townley et al., 2007). However, for the IPM these techniques are less well developed. Due to the increased number of 'size classes' in the numerical approximation of the IPM, the lower bound will always fall to zero and there will always be some zero entries. Therefore, the transient analysis will always be more descriptive when it comes to the upper bounds. The

transient growth in the IPMs suggested that the missing growth transitions from the PPM are now captured.

Sensitivity analysis showed that for all 3 categories it is perturbations to growth where λ_1 is most sensitive. Sensitivity analysis of IPMs allows a visual demonstration of which part of the kernel the growth rate is most sensitive. In comparison sensitivity analysis of the PPMs give only which entry is most sensitive. Where this lies on the upper triangle, this could be through the shrinkage of patches or through fragmentation. See Chapter 8 for a deeper discussion on sensitivity methods and management strategies for Integral Projection Modelling.

5.4.1   Modelling Issues of IPMs

Integral Projection Models solve many of the problems that arose in modelling *M. annularis* by a Population Projection Matrix. Namely, there is no false definition of size class boundaries that skew results by not capturing the small scale transitions. The IPM is also able to smooth over missing transitions from data. Therefore, the use of IPMs for a coral population is better than the use of PPMs. However, there are some issues arising from modelling these populations.

The main issue in modelling a coral patch population using Integral Projection Models comes from the parameterization of fragmentation. This has not previously been modelled in IPMs and the functional form of the kernel that was felt to best reflect the dynamics was selected. However, there are many other possible forms this model could take and further research should aim to understand the biological process. In fact, fragmentation at the patch scale of algal patches is seen as beneficial to a population (Renken et al., 2010), but the opposite seems to be true here, more patches fragment when there is a stronger hurricane and the growth rate then declines.

Further issues surround the numerical integration of the kernel. This is nec-

essary in order to analyze the results, but it does introduce errors to the results. The selection of the integration boundary and the number of mesh points required are inter-linked and should ideally be selected for each IPM created. The selection of the integration boundary and the number of mesh points was not dealt with in this chapter, instead Section 7.3.1 will select these for this Thesis, and the results are used in this chapter. This is because the IPMs parameterized in Chapter 7 will be used in Chapter 9 to project possible hurricane scenarios.

5.4.2 Conclusions

In conclusion the acceptance of the hypothesis in Chapter 4 was the same as when modelled using the IPM. This chapter has shown that although there are some differences in behaviour, the conclusions remain the same. This chapter has shown that the IPM fixes many of the issues of the PPMs. There are some issues that arise from using the IPMs, but the benefits out way the costs. As a result the Integral Projection Model will be used in Part III of this Thesis instead of the Population Projection Matrix.

Chapter 6

Discussion of Results

6.1   Introduction

In Part I and Part II of this Thesis, the projection models for *M. annularis* have been parameterized (Chapters 4 and 5). The results are discussed here. This discussion is divided into five sections. Section 6.2 gives a brief summary of the results so far, in particular focussing on answering the first six research questions shown in Chapter 1. Section 6.3 highlights the main problems of the models and methods used in this study, but will also explain why the results are valid in light of these shortcomings. Section 6.4 will look at how the results are consistent with other research in this area, whilst Section 6.5 looks at why the results are important. Finally Section 6.6 will suggest areas for further research.

6.2   Summary of Main Findings

In Chapter 3, the techniques on how to fit a projection model to *M. annularis* were explained. In particular, different methods for how to fit the kernel of an Integral Projection Model were shown, as well as methods for how to select the most appropriate method. It was shown that a combination of biological information and

reasonable analytical results can give the best fit for how to fit a fragmentation area of a kernel.

The Population Projection Matrix is a popular method for modelling populations (Caswell, 2001). However, there are many issues surrounding their suitability for populations where size determines the dynamics of the population. The main challenges of modelling a population by a PPM in this Thesis was the issue of missing transitions (Chapter 4). This lead to not only reducible matrices being produced that are biologically unrealistic (Stott et al., 2010b), but also non-ergodic matrices (for example I_{Weak}). This meant that the asymptotic dynamics were not independent of the initial conditions and makes it very difficult to project the population with confidence. In the case of $M.\ annularis$, it is growth transitions that are missing. As growth was recorded on a scale of $1 - 2cm^2$, it meant growth was often missed and recorded as stasis within a size class instead. It was for this reason that the Integral Projection Model was applied to the same data set in Chapter 5.

Integral Projection Models solve the solution of missing transitions, due to the way that they are parameterized. Statistical techniques used to fit the models mean that there is a smoother fit. By numerically integrating the kernel, there are a greater number of 'size classes'; this is possible as each size class does not require its own set of data in order to parameterize it, meaning that a greater number of size classes can be modelled. This issue is dealt with further in Chapter 7. There are still issues surrounding the method of modelling fragmentation. This makes up a small part of the kernel, with fragmentation being a rare event with only 63 events observed in the data set. This means that there is only a small amount of data to fit these functions. Future studies should focus on retrieving more information on fragmentation in order to more accurately model this part of the kernel.

The results for the IPM and PPMs do not compare as well as other studies suggest they should. In their study, Easterling et al. (2000) found that the population growth rates for the IPM and PPM were the same to 2 decimal places and for

theoretical studies found little difference or bias. However, the population growth rate estimates used for this study were very different. This initially raises issues on the validity of the models, but could be due to the modelling of fragmentation within the models. In the PPM, this is achieved in a very crude method, which may over-estimate the contribution of fragmentation to the population. In addition, the growth rate is sensitive to the width of the size classes and emphasizes again that, for coral populations, it is the IPM that should be used. Inspite of this, the different growth rates did not affect the conclusions of RQ6.

Most studies focus on the asymptotic dynamics of a population and these methods of analysis are well developed (See Caswell (2000) for a summary for PPMs). All studies so far that use IPMs only focus on the asymptotic dynamics (Easterling et al., 2000; Childs et al., 2003, 2004; Ellner and Rees, 2006; Hesse et al., 2008; Kuss et al., 2008; Rees and Ellner, 2009), with the exception of Eager et al. (In Press). However, the transient dynamics of a population are just as important in understanding the response of a population to disturbances (Townley et al., 2007; Townley and Hodgson, 2008). In the case of modelling a population following a hurricane, transient dynamics are important. In this Thesis, transient dynamics of both the PPM and IPM have been carried out (See Chapters 4 and 5). The transient techniques for IPMs are not well developed, but it would be assumed that the transient bounds from PPM analysis should be transferable to the IPM framework. In particular the effect of biased initial conditions has been measured to compare with those in a PPM. Often the results are similar, with the PPM upper and lower bounds being enclosed in the IPM bounds.

In Chapter 4 the research question: 'Does initial trauma following a hurricane affect the dynamics of a population?' was investigated. It was found that the stronger the initial trauma, the stronger the asymptotic decline. In transient time, the more severe impact had greater extremes of behaviour than those with weaker initial trauma. It was shown that the dynamics on a ramet with a greater than

50% coral cover loss was markedly different from those with a less than 50% loss. It also showed that transient growth was possible for all patches.

6.3 Short-comings of Methods

The PPM method is particularly useful for populations determined by age or stage where biological indicators determine the boundaries of state class. With a population determined by size, as in the case of *M. annularis*, these class boundaries are artificially chosen (Ramula and Lehtila, 2005). As discussed in Chapter 3, the errors surrounding these boundaries can be reduced in order to reduce the modelling errors. This method is popular with coral populations (Hughes, 1984), but this does not mean that this is the best method that could be used by Ecologists. The PPMs built in Chapter 4 were reducible, due to missing transitions (Stott et al., 2010b). These missing transitions, particularly when it comes to growth transitions, could result in an under-estimation of the population growth rates for all PPMs. This is due to the growth observed in this study being on a scale of 1 or $2cm^2$, whereas shrinkage of patches was on a larger scale. Therefore, the Van der Meer and Moloney algorithms selected that shrinkage transitions need to be captured more than the small scale growth (Moloney, 1986; van der Meer, 1978).

The IPMs created and used in Chapter 5 solved many of these problems. They are particularly useful when there is only a small data set (Zuidema et al., 2010). In Chapter 5, it was shown that the PPM actually over-estimated the population growth rates in some cases, this is due to it being less able to capture small scale transitions.

The issue with using the IPM for coral populations is the lack of comparable models in literature. The methods adopted to parameterize these models are an initial attempt to describe the dynamics. Much is known about the biological processes of colonies of *M. annularis* (Foster et al., 2007) and about their reproduction

and fragmentation, but little is known about the patch dynamics of this species. Therefore, assumptions have had to be made about the decision processes involved in fragmentation. It is known that fragmentation is a rare event for patches (only 63 fragment events were observed in our data set) and, therefore, will only contribute a small amount to the population dynamics. It is vital that this is captured accurately, as this is the only method that is used in this model to create new patches.

Reproduction does not occur at a patch scale (Szmant, 1991), which resulted in a closed system being modelled with no contribution from other populations of *M. annularis*. It is known that there is asexual and sexual reproduction at the colonial scale of *M. annularis* (Foster et al., 2007). This model only captured the asexual reproduction at a patch scale through fragmentation, but the sexual reproduction is not captured, as it was not included in the data set. As this was not captured in the data, the reproductive value only captured the contribution of patch sizes to fragmentation. This meant that the reproductive value was instead labelled as the fragmentation value. Future studies would need to focus on the contribution of recruitment to the population, in fact it is thought that the ability of a coral population to withstand hurricanes is as a result of their recruitment levels (Hughes, 1994; Hughes and Tanner, 2000; Coles and Brown, 2007). The results of this Thesis are still valid, as there is some thought that hurricane stress actually reduces the ability of coral to sexually reproduce as energy is instead required to repair damage (Crabbe et al., 2008). This is in part due to the competition of space between algae and coral and, as algae are quicker at colonization, it often means that coral populations miss out (Connell, 1997; Connell et al., 1997).

The low number of patches that fragment can indeed skew the results. For example in I_{Severe} there were only 2 patches which fragmented. The IPM method cannot accurately model the process, as such low numbers of data skew the statistical fits. There is little that can be done about this. The confidence in the fitted

models comes from the fact that there is a similar shape in the results of other categories.

6.4 Are the Results Consistent with Previous Research?

Coral reefs are in long term decline, with no pristine reefs remaining (Jackson et al., 2001; Pandolfi et al., 2003); one fifth already destroyed; one fifth under immediate threat and another quarter under long term threat (VanOppen and Gates, 2006). This shows the extent of the threat hanging over coral reefs. There is currently a rapid shift to alternate states (Bellwood et al., 2004), with a dominance of branching corals or even algae rather than the dominance of reef-building corals seen in the past (Lugo et al., 2000). This research agrees with this long-term threat to coral reefs. It showed that in the long-term, even under weak trauma, there is asymptotic decline in coral cover. As coral patch cover declines, so the healthiness of the reef will decline, as the reef-building coral will then have no method of growing and recovering after disturbances. In the Caribbean basin, there are no examples of recovery of reefs following a hurricane disturbance (Connell, 1997) and this study only adds to the growing collection of these studies.

Gardner et al. (2005) found that, on average, a population will decrease by 17% following a hurricane. This study has shown that there was a decrease in coral cover of 31% following Hurricane Mitch, but only 3% and 8% following hurricanes Keith and Iris, which on average was 14% for all three hurricanes.

No recovery has been observed on a coral reef for at least 8 years after a hurricane (Gardner et al., 2005). In fact, it has been suggested that most reefs follow a synergy trajectory after a hurricane, where the decline experienced prior to a hurricane is only increased by the hurricane (Gardner et al., 2005). This study

confirmed this with no recovery observed in the data. This could be because the data was not collected for a long period following the hurricanes. The population showed a synergy of effects, where the decline was increased, following the hurricanes with all hurricane trauma categories at a greater rate of decline than that prior to the hurricane. The reason for this increase in decline is because the reefs are now at a reduced capacity to deal with hurricanes (Rogers and Laffoley, 2011). This is because other stresses like overgrazing reduce the capacity of the reef to recover from a hurricane. This is causing there to be a shift from coral dominated reefs to algal dominated reefs. Once this shift has occurred, the reefs will have a diminished capacity to recover (McClanahan et al., 2001).

6.5 Why are these Results Important and Novel?

The results discussed in this chapter are important in that they add to the body of knowledge of how coral reefs respond to hurricanes. It was shown that the long-term and short-term dynamics of a coral patch is determined by the initial trauma experienced following a hurricane.

In Chapter 2, it was highlighted that the Integral Projection Model lends itself perfectly to modelling a coral population, but that this has not been done by any other study. This Thesis is a first step towards a better understanding of how to model coral patches by IPMs. It suggests possible methods of parameterization, which give an insight into the issues surrounding fragmentation.

Comparisons of the PPM and IPM methods have shown that Coral Reef Ecologists should turn to the IPM to model their populations. It provides a more accurate model and allows the capture of small scale behaviour, which had been previously missed by PPMs. It also allows better fit for small data sets (Zuidema et al., 2010), and does not require the false definition of size class boundaries that have no biological motivation.

Most understanding of the effect of hurricanes on coral populations is at the colonial level (Edmunds and Elahi, 2007; Hughes, 1984). Although, as was discussed in Chapter 2, it is vital that the dynamics on a patch scale are understood. This Thesis has modelled the population at this smaller scale, as it is at this scale at which live coral is found. Even though colonies may survive longer than the coral patches, if there is no live coral on a colony effectively the colony is dead. Without the live coral, there is no way that the colony can grow and recover, thus understanding these dynamics is vital.

6.6   Further Study

The results from Parts I and II of this Thesis have investigated the effect of hurricanes on a coral patch population. It has raised further questions which need to be answered. Some of these questions will be answered in Part III of this Thesis. Namely, how a coral patch population be better managed into growth, using the IPM method as an indicator (see Chapter 8). A further question is how looking at climate change affects these results. In order to answer these questions the data set must be divided in a different manner to Chapter 4, so that the population can be projected under different scenarios to calculate the range of possible behaviour that could occur. This will be done in Chapters 7 and 9.

There are other questions which have arisen that have not been investigated in this Thesis. The data failed to capture recovery following hurricanes. Although it is now thought that many coral populations experience a sharper decline after a hurricane (Gardner et al., 2005), it is also thought that recovery is unlikely to be seen in the first 8 years after a hurricane (Gardner et al., 2005). Therefore, any further research should aim to study a coral population for a longer period of time in order to capture the natural recovery on a reef rather than the continued decline following a hurricane.

As has been discussed above, further research should also aim to understand the level of recruitment required in order to boost the population size sufficiently between hurricanes and the level of recruitment that is required for the population to survive.

6.7   Conclusions

In the first two parts of this Thesis, different projection models have been fitted to the data set in order to understand the dynamics on the reef. It has shown that the IPM is a better alternative to the PPM at modelling coral patch dynamics. However, it has also shown that further research is required to accurately capture the process of fragmentation. In Parts I and II the first six research questions from Figure 1.4 have been investigated. In Part III the remaining four questions will be answered.

Part III

On the Applications of Integral Projection Models to Management and Climate Change.

Chapter 7

The Integral Projection Model

7.1   Introduction

In Part II, it was concluded that the Integral Projection Model (IPM) was a better alternative to the Population Projection Matrix (PPM) at modelling a patch population of *Montastraea annularis*. The IPM solved many of the issues that arose from PPM modelling, for example, the problem of missing transitions and the selection of size classes. By being continuous in state, size class selection is not necessary and distribution errors are not introduced into the model. An IPM is parameterized through statistical curve fitting and is, therefore, able to smooth out missing transitions. This makes the IPM an ideal model for size-determined populations like *M. annularis*.

In this chapter, IPMs are parameterized to answer the research question: 'Do the dynamics exhibited during a hurricane vary with hurricane strength?' In Chapter 4, it was concluded that the initial trauma experienced by a coral patch following a Category 5 hurricane determined the long-term behaviour of a coral patch. This chapter differs by investigating the total dynamics of the reef ignoring relative initial decline and uses a different subdivision of the data (see Figure 1.5). The methods for parameterization and analysis of an IPM were discussed in Chapter 3

and are applied here to answer the research question.

By parameterizing three different IPMs (A_{Strong}, A_{Weak} and A_{No}) it allows the projection of possible future dynamics under different scenarios of hurricane frequency and intensity. These scenarios are motivated by the expected effect of climate change on hurricane activity. The IPMs parameterized in this chapter are used in Chapter 9 to investigate a range of possible population densities with different hurricane patterns and in Chapter 8 to suggest possible management strategies.

7.2   Methods

The Glovers Reef data set, see Chapter 1, was divided into three groups according to the hurricane activity that occurred at each time step (Table 7.1). The three IPMs, A_{Strong}, A_{Weak} and A_{No}, are parameterized using the log-size of a coral patch, due to the distribution of coral patch sizes in June 1998 being approximately lognormally distributed.

Three individual IPMs were parameterized, as opposed to one with a hurricane factor included, to allow controlled projection into the future (see Chapter 9). Climate change is thought to be increasing the intensity of hurricanes (IPCC, 2007). Three models allow differing scenarios to be projected in a controlled manner to compare possible future dynamics on a reef.

IPM	Transitions	Number of data	Hurricanes
A_{Strong}	2 (October 1998 to December 1998) 3 (December 1998 to June 1999)	577	Mitch
A_{Weak}	5 (June 2000 to May 2001) 6 (May 2001 to May 2002)	494	Keith Iris
A_{No}	1 (June 1998 to October 1998) 4 (June 1999 to June 2000) 7 (May 2002 to January 2003)	762	

Table 7.1: Division of data used to create three IPMs, A_{Strong}, A_{Weak} and A_{No} and the number of data available to parameterize them.

Chapter 3 discussed the differing methods that could be adopted in selecting the functional form of the kernel for $M.\ annularis$. Application to A_{No} data caused the selection of the kernel form to be:

$$\mathbf{k}(y,x) = (1 - p_f(x))s(x)\mathbf{g}(y,x) + s(x)f_s(x)p_f(x)n_f(x)\mathbf{f}_d(y, \frac{x}{n}), \qquad (7.1)$$

with corresponding IPM equation:

$$\mathbf{n}\,(y, t+1) = \int_{\Omega} \mathbf{k}\,(y,x)\,\mathbf{n}\,(x,t)\,dx. \qquad (7.2)$$

In this projection equation, Ω is the range of possible patch sizes and $\mathbf{n}(x,t)$ is the distribution of patch sizes at time t. The kernel $\mathbf{k}(y,x)$ incorporates the following functions:

- $s(x)$: The probability a patch of size x at time t survives to time $t+1$, fitted using logistic regression.

- $\mathbf{g}(y,x)$: Given that a patch of size x at time t survives to time $t+1$, this function approximates its size y at time $t+1$. This function models both the growth and shrinkage of coral patches. It is fitted by a Gaussian distribution, with fitted mean and variance.

- $p_f(x)$: The probability that a patch of size x at time t will fragment at time $t+1$. This is fitted using a logistic regression.

- $f_s(x)$: Given that a patch of size x at time t fragments, $f_s(x)$ is the proportion of the original patch x which will survive in fragment form. This is fitted through linear regression with a Gaussian error structure.

- $n_f(x)$: Given a patch x fragmented at time t, $n_f(x)$ approximates the number of patches which are produced. This is fitted through a transformed variable $X = x - 2$ and a Poisson error function.

- $\mathbf{f}_d(y, \frac{x}{n})$: This gives the size of a fragment y at time $t + 1$ given a patch size x at time t fragments and the number of fragments produced n. Fitted to a Gaussian distribution with fitted mean and variance taken as the variance of fragment sizes y at time $t + 1$.

7.3   Fitted Models

The parameterized IPMs and their fits are given in Table 7.2 and Figures 7.1 to 7.7, with the complete functional form of the IPMs given in equations (7.3), (7.4), (7.5).

Probability of Survival: For all three groups, quadratic terms were rejected (A_{No}: $P = 0.70$, A_{Weak}: $P = 0.67$, A_{Strong}: $P = 0.51$). As patch size increased so did survival rates (Table 7.2 and Figure 7.1). For patches over $140 cm^2$, the probability of survival is close to one, irrespective of whether or not a hurricane occurred and of the hurricane strength. For smaller patches, there was a greater variety in the probability of survival. Where patches of $1 cm^2$ in A_{Strong} had a 29% chance of survival, this doubled for A_{Weak} to 62%, whilst A_{No} had 58% survival. As patch size increased, there was a steeper increase in survival in A_{Strong} than A_{Weak} or A_{No}. There was a slightly greater probability of survival for all patch sizes in A_{Weak} than in A_{Strong}.

Growth: For all fitted mean growths and variances, quadratic terms were rejected (A_{No}: $P = 0.34$ and $P = 0.88$, A_{Weak}: $P = 0.07$ and $P = 0.41$, A_{Strong}: $P = 0.2$ and $P = 0.60$). This showed a linear relationship between size at time t and size at time $t + 1$ (Table 7.2 and Figure 7.3). The proximity of the fitted mean growth lines to the $x = y$ line showed only small scale growth and shrinkage of patches. The estimates for mean growth are similar for all three groups, but there were slight differences for small patch sizes. Small patches in A_{Strong} had a greater decrease in size than in A_{Weak} and A_{No}.

Function	A_{No}	A_{Strong}	A_{Weak}
$s(x)$	0.2392(0.2844)+1.0669(0.1474)x	-0.9980(0.3123)+1.2216(0.1446)x	0.4165(0.3224)+1.0013(0.1722)x
$\mathbf{g}(y,x)$	-0.1198(0.0242)+1.0129(0.0076)x	-0.3753(0.0503)+1.0351(0.0147)x	-0.0747(0.0256)+1.0046(0.0086)x
$log(\sigma^2(\mathbf{g}(y,x)))$	-3.3197(0.1543)-0.6000(0.0482)x	-2.8768(0.2955)-0.2800(0.0864)x	-3.9492(0.2131)-0.5482(0.0715)x
$p_f(x)$	-5.9059(0.7673)+0.6730(0.1867)x	-6.1804(0.7761)+0.8759(0.1759)x	-5.5855(0.9244)+0.5850(0.2475)x
$n_f(x)-2$	-0.9163(0.3536)	-1.421(0.378)	-1.2993(0.5773)
$f_s(x)$	0.2102(0.3682)+0.8592(0.0905)x	-0.1209(0.5148)+0.8799(0.1157)x	-0.0427(0.6090)+0.9087(0.1655)x
$\mathbf{f}_d(y,\frac{x}{n})$	0.5721(0.4612)+1.1439(0.2665)$(\frac{x}{n})$	0.3508(0.4888)+1.1275(0.2409)$(\frac{x}{n})$	0.0927(0.6725)+1.2039(0.4067)$(\frac{x}{n})$
$\sigma^2(\mathbf{f}_d(y,\frac{x}{n}))$	1.2683	1.6887	1.5998

Table 7.2: The fitted parameters for each function in the IPM kernels. The standard errors for each fitted parameter are shown in brackets.

Mean growth for large patches was similar for all categories. There was a greater variability in patch size for A_{Strong} than A_{Weak} or A_{No} (Figure 7.4 and Table 7.2), as evidenced by a greater number of data located away from the mean line.

Probability of Fragmentation: The greatest chance of a patch fragmenting was in A_{Strong}, whilst A_{Weak} showed the least (Figure 7.2 and Table 7.2). This was confirmed by data in A_{Strong}, where 5% of patches fragmented compared to 2.6% in A_{No} and 2.2% in A_{Weak}. The fitted functions showed a much higher probability of fragmentation for larger patches than smaller patches. For patches under $8cm^2$, fragmentation did not occur in all groups. The largest probability of fragmentation occurred in A_{Strong} for patches over $400cm^2$, where there was a 29% chance of fragmentation. The relationship between size and fragmentation was linear with quadratic terms rejected (A_{No}: $P = 0.054$, A_{Weak}: $P = 0.18$ and A_{Strong}: $P = 0.08$).

Number of Fragments: For all categories linear terms were rejected (A_{No}: $P = 0.07$, A_{Weak}: $P = 0.85$, A_{Strong}: $P = 0.61$) and the number of fragments were independent of initial patch size. The most common number of fragments produced was two in all categories, *i.e.*, it is most common for one patch to divide in half. The fitted mean is similar for both A_{Strong} and A_{Weak}, but lower than for A_{No} (Table 7.2 and Figure 7.5). It showed that more patches are produced if fragmentation occurred naturally than if forced by a hurricane event, even though the chances of fragmentation increased with a hurricane event.

Family Size: The relationship between the size of the 'parent' patch x and the total area of the fragments produced is linear for all categories with quadratic terms rejected (A_{No}: $P = 0.20$, A_{Weak}: $P = 0.74$, A_{Strong}: $P = 0.28$). This showed that as the patch size increased so the total area remaining after fragmentation increased (Table 7.2 and Figure 7.6). In A_{No}, a greater area of coral remained than both A_{Weak} and A_{Strong} with the lowest amount in A_{Strong}.

Fragment Size: For all three categories, a linear relationship is observed, as the original patch size increased, so did the fragment patch sizes (Table 7.2 and

Figure 7.7). Quadratic terms were rejected in all categories (A_{No}: $P = 0.72$, A_{Weak}: $P = 0.39$, A_{Strong}: $P = 0.04$). In A_{Strong}, although $P < 0.05$, the quadratic terms were rejected because the inclusion caused all factors to be not significant and so a linear relationship was assumed. There is greater variability between estimates for small patches, with large patches having similar estimates for all three categories.

Key Function Results

1. Larger patches have better survival rates than smaller patches, regardless of hurricane strength (Figure 7.1) .

2. Smaller patches survive better in A_{Weak} and A_{No} than in A_{Strong} (Figure 7.1).

3. Patches in A_{Strong} have a higher chance of fragmenting (Figure 7.2).

4. Patches under $8cm^2$ do not fragment regardless of hurricane occurrence or strength (Figure 7.2).

5. More patches are created by fragmentation in A_{No} than in A_{Weak} and A_{Strong} (Figure 7.5).

6. When large patches fragment, a greater area will remain than with small patches (Figure 7.6).
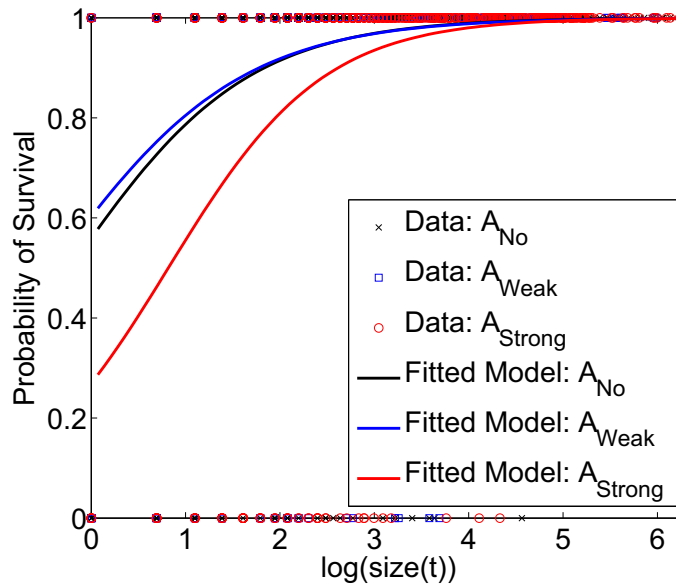
Figure 7.1: The fitted probability of survival function $s(x)$ for the IPMs A_{Strong}, A_{Weak} and A_{No}, shown on the log-size scale. The fitted models are shown in comparison to the data.
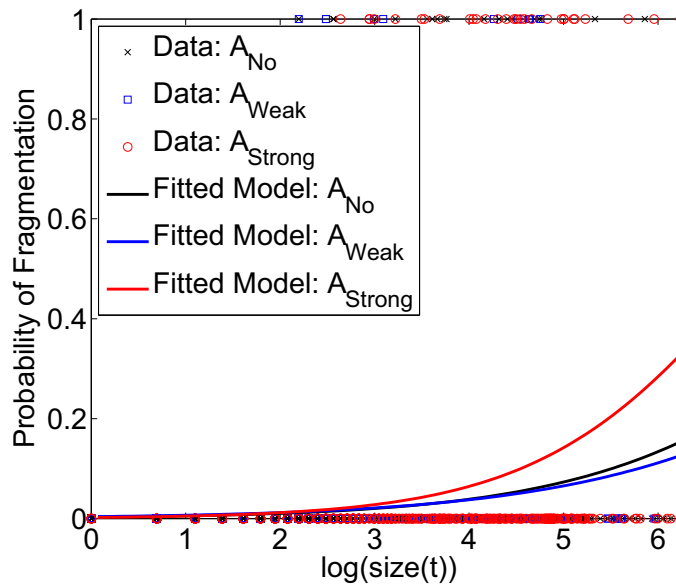
Figure 7.2: The fitted probability of fragmentation function $p_f(x)$ for the IPMs A_{Strong}, A_{Weak} and A_{No}, shown on the log-size scale. The fitted models are shown in comparison to the data.
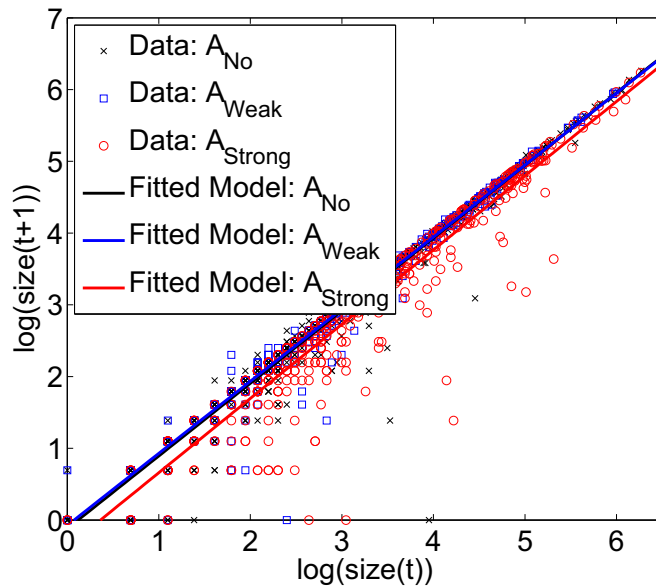
Figure 7.3: The fitted mean growth function $\overline{g(y,x)}$ for the IPMs A_{Strong}, A_{Weak} and A_{No}, shown on the log-size scale. The fitted models are shown in comparison to the data.
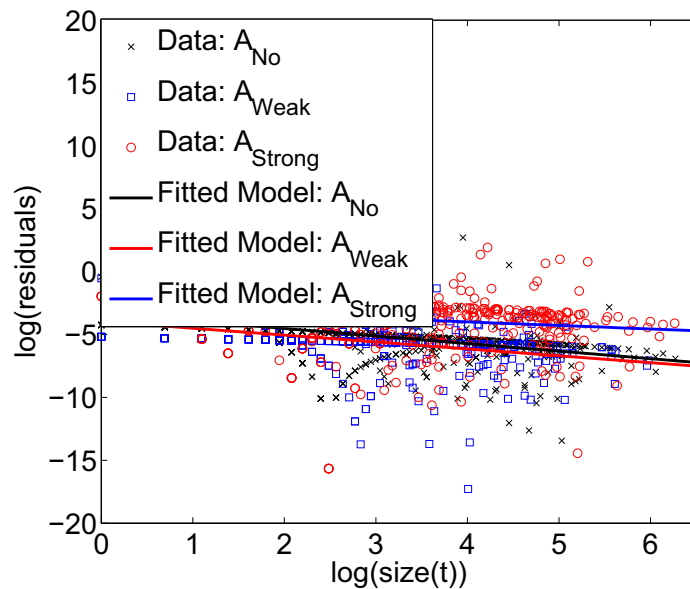
Figure 7.4: The fitted variance of growth function $\log(\sigma^2(\mathbf{g}(y,x))$ for the IPMs A_{Strong}, A_{Weak} and A_{No}, shown on the log-size scale. The fitted models are shown in comparison to the data.
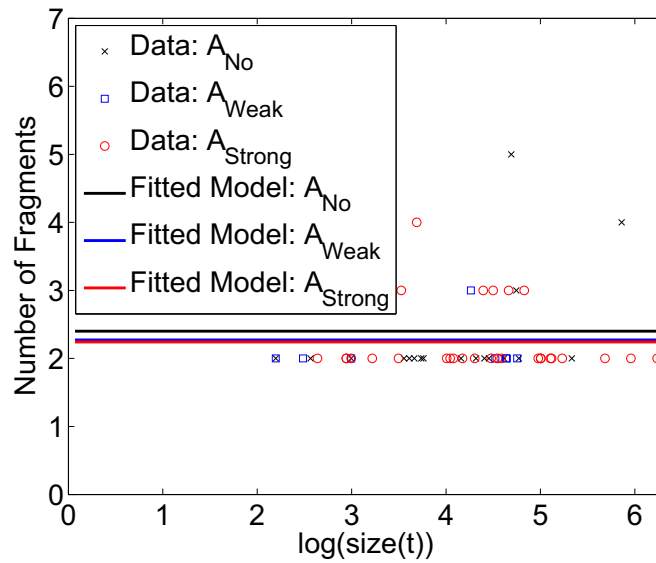
Figure 7.5: The fitted number of fragments function $n_f(x)$ for the IPMs A_{Strong}, A_{Weak} and A_{No}, shown on the log-size scale. The fitted models are shown in comparison to the data.
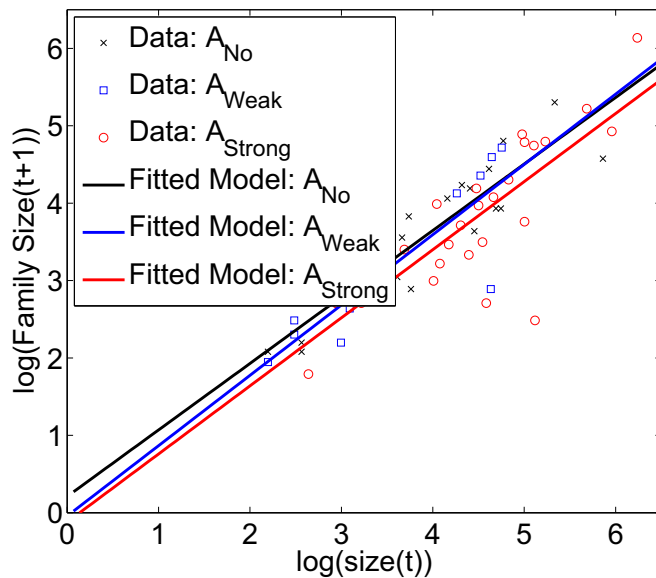
Figure 7.6: The fitted family size function $f_s(x)$ for the IPMs A_{Strong}, A_{Weak} and A_{No}, shown on the log-size scale. The fitted models are shown in comparison to the data.
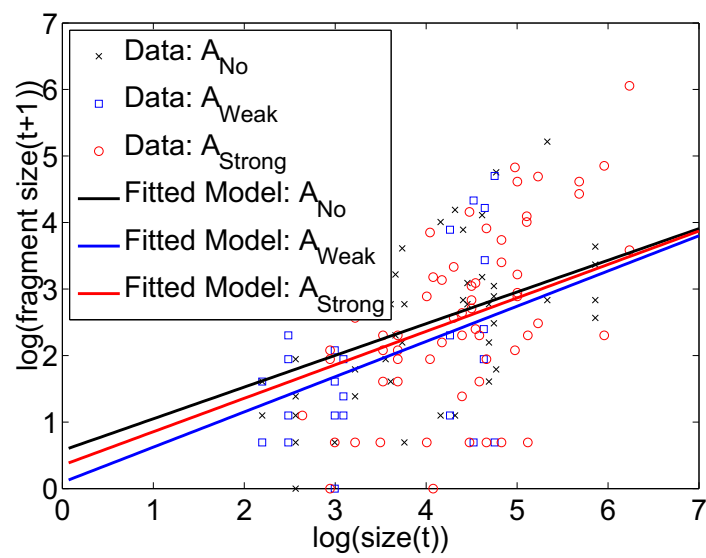
Figure 7.7: The fitted fragment size function, $\mathbf{f}_d(y, \frac{x}{n})$, for the IPMs A_{Strong}, A_{Weak} and A_{No}, shown on the log-size scale. The fitted models are shown in comparison to the data.

A_{No}

$$\mathbf{k}(y,x) = \left(1 - \frac{exp\left(-5.91+0.67x\right)}{1+exp\left(-5.91+0.67x\right)}\right)\frac{exp\left(0.24+1.07x\right)}{1+exp\left(0.24+1.07x\right)}\frac{1}{\sqrt{2\pi exp\left(-3.3-0.60x\right)}}exp\left(\frac{-(y+0.12-1.01x)^2}{2exp\left(-3.32-0.60x\right)}\right) + \cdots$$

$$\frac{exp\left(0.24+1.07x\right)}{1+exp\left(0.24+1.07x\right)}\frac{exp\left(-5.91+0.67x\right)}{1+exp\left(-5.91+0.67x\right)}\frac{1}{\left(2+exp\left(-0.92\right)\right)\left(0.21+0.86x\right)}\frac{1}{\sqrt{2.54\pi}}exp\left(\frac{-\left(y-0.57-1.14\frac{x}{2+exp(-0.92)}\right)^2}{2.54}\right).$$

(7.3)

A_{Weak}

$$\mathbf{k}(y,x) = \left(1 - \frac{exp\left(-5.59+0.59x\right)}{1+exp\left(-5.59+0.59x\right)}\right)\frac{exp\left(0.42+1.00x\right)}{1+exp\left(0.42+1.00x\right)}\frac{1}{\sqrt{2\pi exp\left(-3.95-0.55x\right)}}exp\left(\frac{-(y+0.07-1.00x)^2}{2exp\left(-3.84-0.55x\right)}\right) + \cdots$$

$$\frac{exp\left(0.42+1.00x\right)}{1+exp\left(0.42+1.00x\right)}\frac{exp\left(-5.59+0.59x\right)}{1+exp\left(-5.59+0.59x\right)}\frac{1}{\left(2+exp\left(-1.30\right)\right)\left(-0.04+0.91x\right)}\frac{1}{\sqrt{3.20\pi}}exp\left(\frac{-\left(y-0.09-1.20\frac{x}{n_f(x)}\right)^2}{3.20}\right).$$

(7.4)

A_{Strong}

$$\mathbf{k}(y,x) = \left(1 - \frac{exp\left(-6.18+0.88x\right)}{1+exp\left(-6.18+0.88x\right)}\right)\frac{exp\left(-1.00+1.22x\right)}{1+exp\left(-1.00+1.22x\right)}\frac{1}{\sqrt{2\pi exp\left(-2.88-0.28x\right)}}exp\left(\frac{-(y+0.38-1.04x)^2}{2exp\left(-2.88-0.28x\right)}\right) + \cdots$$

$$\frac{exp\left(-1.00+1.22x\right)}{1+exp\left(-1.00+1.22x\right)}\frac{exp\left(-6.18+0.88x\right)}{1+exp\left(-6.18+0.88x\right)}\frac{1}{\left(2+exp\left(-1.42\right)\right)\left(-0.12+0.88x\right)}\frac{1}{\sqrt{3.38\pi}}exp\left(\frac{-\left(y-0.35-1.13\frac{x}{n_f(x)}\right)^2}{3.38}\right).$$

(7.5)

7.3.1 Mesh Size and Integration Boundary

The IPMs for A_{Strong}, A_{Weak} and A_{No} were fitted in the previous section, but in order to analyze these functions, numerical integration methods must be adopted. Recall from Section 3.2.2 that two different methods to select the integration boundaries were defined. The integration boundary defines Ω as the minimum and maximum sizes that the kernel is integrated over and requires the inclusion of all possible sizes that the coral patches could achieve. The mesh size defines the number of points that are used during integration. To calculate the integration boundary, certain parameters from the data are calculated, namely:

- l the minimum observed size

- u the maximum observed size

- σ^2 the variance of observed patches sizes

Given these parameters the two possible methods of choosing the integration boundary $\Omega = [L\ U]$ are:

(I) $[L\ U] = [0.9l\ \ 1.1u]$

(II) $[L\ U] = [l - 3\sigma^2\ \ u + 3\sigma^2]$

The integration boundaries are calculated for all three IPMs and for each boundary ((I) and (II)) the population growth rate λ was used to calculate the number of mesh points required. The population growth rate is used ahead of other metrics as the dominant eigenvalue converges to the overall population growth rate, λ_1, as the number of mesh points increases (Easterling et al., 2000).

The mesh size was selected as the minimum size required for λ_1 to converge to 4 decimal places (Table 7.3). As the integration boundary widened, the number of mesh points required increased. It is impossible to separate the selection of boundary values and mesh points, as one directly affects the other. It is important to take

into account both of these measures as the benefits of using a wider integration boundary are often out-weighed by the increased computational cost of increasing the number of mesh points. When a very small number of mesh points are selected there is a large numerical error in the calculation of λ_1. It can result in values of λ_1 which are not realistic. For example, in Figure 7.8 when the number of mesh points is under 10 for A_{No}, $\lambda_1 > 5$. As the number of mesh points increased, the population growth rate was calculated as 0.74. This demonstrates the importance of the correct calculation of the number of mesh points required to accurately describe the dynamics of the population.

In general, using method (II) is computationally more expensive than method (I) (Table 7.3). The number of mesh points for method (II) was over three times higher than method (I), despite the integration area being only 2.5 times larger for method (II) than method (I).

The λ_1 estimate for A_{Weak} and A_{Strong} were the same to 2 decimal places, for both integration boundary methods. However, the growth rates for method (I) was slightly larger than method (II). For A_{No}, the growth rate is larger for method (II) than method (I) and are only the same to one decimal place. There was no systematic bias in the growth rate by shrinking the integration boundary. A compromise of $\Omega = [L\ U] = [0\ 7]$ is used for all three IPMs, in order to unify the choice of integration boundary. The required mesh sizes for this boundary are given in Figure 7.8. This showed that a mesh size of 145 is required for A_{No}, 60 for A_{Strong} and 200 for A_{Weak}. As a result of this, a mesh size of 200 will be used for all IPMs, to ensure that there is convergence to 4 d.p for the population growth rate in all three categories.

The number of mesh points and integration boundaries are unified for all three IPMs to allow direct comparison for all sizes. It will also allow the projection of different hurricane scenarios in Chapter 9. If they were not unified then this analysis could not be carried out.

IPM	Boundary Method	Boundary	λ_1	Mesh Size
A_{No}	I	[0 6.898]	0.7387	115
	II	[−5.286 11.557]	0.7450	445
A_{Weak}	I	[0 6.5768]	0.7836	135
	II	[−4.852 10.83]	0.7834	425
A_{Strong}	I	[0 6.890]	0.4345	55
	II	[−5.465 11.728]	0.4279	145

Table 7.3: The population growth rates for the two different integration boundaries. The mesh size given is the minimum size required for λ_1 to converge to 4 decimal places.
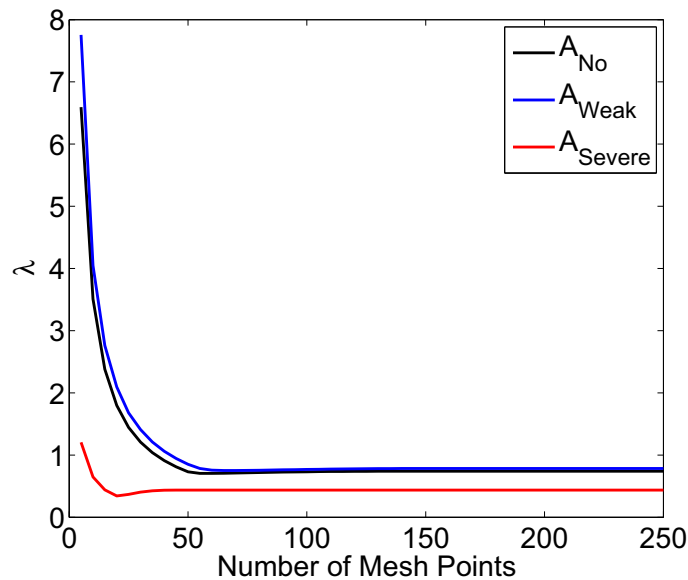
Figure 7.8: The population growth rate calculated on the range $\Omega = [0, 7]$ for a varying number of mesh points.

7.4   Results

The parameterized IPMs are analyzed using methods described in Chapter 3 to determine their basic dynamical properties. In terms of the overall patch dynamics of the systems, it requires an assumption that the environmental conditions remain unchanged each year. In the case of A_{Strong}, this means that a strong hurricane occurs every year; for A_{Weak} that a weak hurricane occurs every year; and for A_{No} that there is never a hurricane. These situations are highly improbable with

hurricane frequency and intensity varying annually, but this assumption allows the comparison of behaviour under different situations. To allow for annual variation, the IPMs can be interweaved to project possible behaviour. This analysis will be carried out in Chapter 9.

Analyses of the asymptotic dynamics give an indication of the behaviour that is being exhibited by the three IPMs (See Section 7.4.2). In particular, it allows comparison of metrics like the population growth rate. It is often the case that the population will not reach the asymptotic dynamics and so it is necessary to also carry out transient analysis (see Section 7.4.3). The combination of the information from asymptotic and transient analysis gives a better overall picture of the behaviour, which is seen under these varying hurricane conditions.

7.4.1 Kernel Results

The majority of coral patch behaviour was concentrated around the $x = y$ line. This showed a greater contribution from survival and growth than from fragmentation (Figure 7.9). Kernel values are higher in A_{Weak} than either A_{Strong} or A_{No} (Figure 7.9 (a) (c) and (e)), which showed greater survival rates, in particular between sizes $200 - 600cm^2$. The lowest survival is in A_{Strong} (Figure 7.9 (e)).

The log-kernels (Figure 7.9 (b), (d), (f)) are given to accentuate the contribution of fragmentation. The greater intensity of colour showed greater contribution from fragmentation in A_{Strong}, than either of the other categories. The smallest amount of fragmentation occurred in A_{No}. The log-kernels also showed that the survival-growth region is wider for A_{Strong} than either A_{Weak} or A_{No}. This showed that under stronger hurricanes there was greater variability in resulting patch size. The proximity of the survival-growth contribution to the $x = y$ line for A_{No} and A_{Weak} showed only small-scale change in size. Whereas for A_{Strong}, the survival-growth contribution lies below the $x = y$ line, which showed a systematic decrease in area.

(a) A_{No} kernel

(b) A_{No} log-kernel

(c) A_{Weak} kernel

(d) A_{Weak} log-kernel

(e) A_{Strong} kernel

(f) A_{Strong} log-kernel
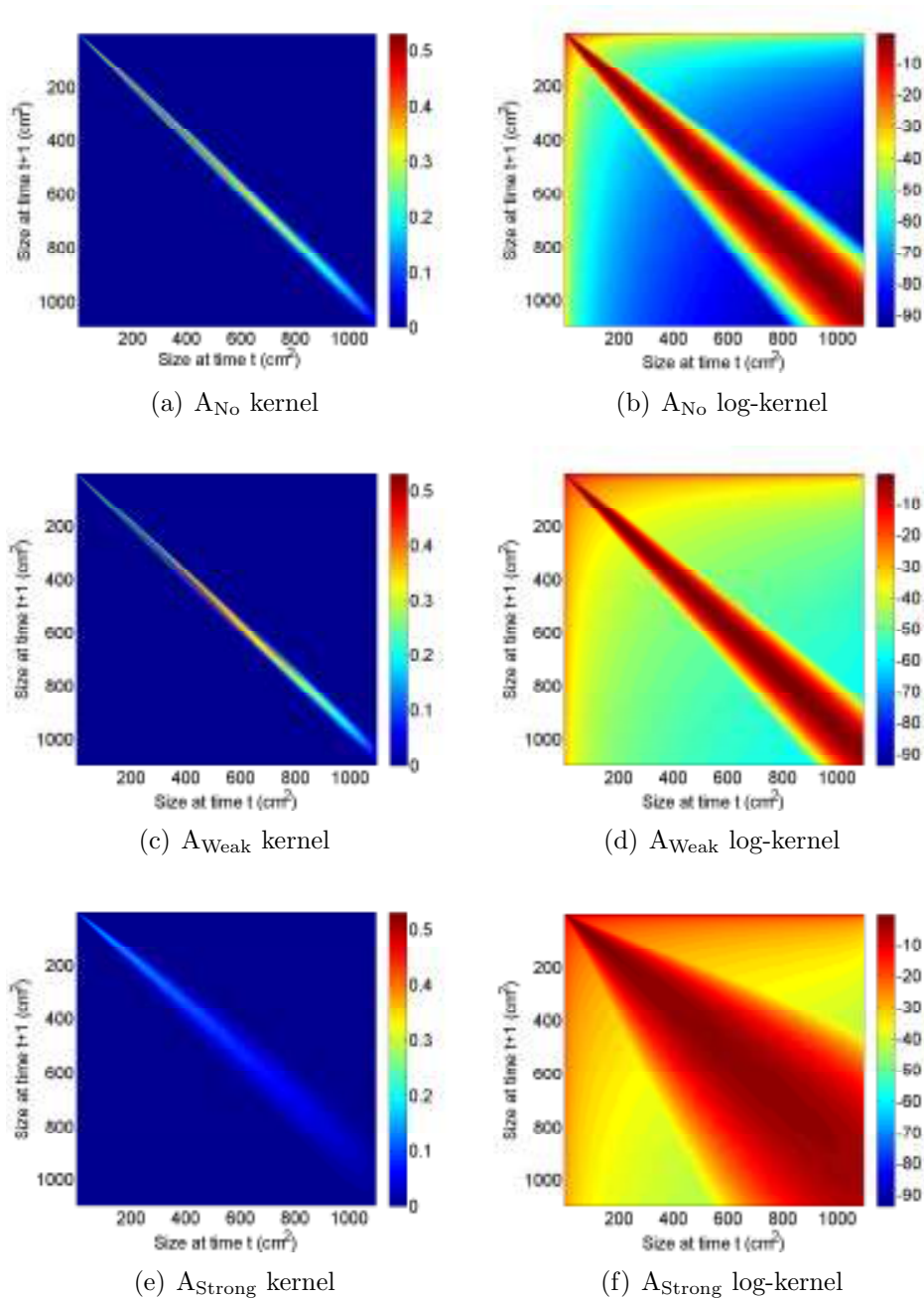
Figure 7.9: The kernels and log-kernels for the fitted IPMs A_{No}, A_{Weak} and A_{Strong}.

7.4.2   Asymptotic Dynamics

All three IPMs had a population growth rate of less than 1, indicating long term decline. The smallest growth rate was observed in A_{Strong} ($\lambda_1 = 0.43$), which was 41% lower than A_{Weak} ($\lambda_1 = 0.78$) and 42% lower than A_{No} ($\lambda_1 = 0.74$). An

unexpected result was that the growth rate of A_{Weak} was higher than A_{No}; this is counter-intuitive, as it would be expected that a hurricane would lower the growth rate. This showed that a weak hurricane benefits a reef, having said that, it could also indicate that A_{No} does not exclusively model non-hurricane behaviour, but instead that there is some residual effects captured in this IPM.

The stable size structure for all categories showed all individuals will ultimately be smaller than $20cm^2$ (Figure 7.10 (a)). On the log-size scale, small differences in distribution can be seen (Figure 7.11 (a)), where A_{Weak} showed slightly larger patches than A_{No} and A_{Strong}. There is also a lower proportion of smaller patches in A_{Weak}. The worst case scenario is in A_{Strong}, where the greatest proportion of smaller patches will dominate. This result paints a bleak picture for the population regardless of hurricane strength, still it must be remembered that very few populations will ever reach asymptotic time. This is because hurricanes do not occur every year and so there will be some interaction between these IPMs. This interaction may perturb the population in a way that increases the proportion of larger patches on the reef. This interaction is investigated in Chapter 9.

The models that have been produced do not include reproduction and recruitment, therefore, as was explained in Section 3.3.5, the reproductive value instead models the contribution that different size coral patches make to fragmentation. The fragmentation values (Figures 7.10(b) and 7.11(b)) showed it was large patches that contribute to fragmentation. However, A_{Weak} had a higher contribution from slightly smaller patches than A_{No}. The sizes contribution to fragmentation for A_{Strong} lies within the sizes for A_{Weak} and A_{No}. For all categories, there is little contribution to fragmentation from sizes below $200cm^2$.

Initial conditions from data calculated the number of patches of each size, which existed at time t, as opposed to $t + 1$. This effectively created a 200×1 vector where the 'size class' boundaries are those defined under numerical integration (Figure 7.12). These initial conditions were calculated independently for each of
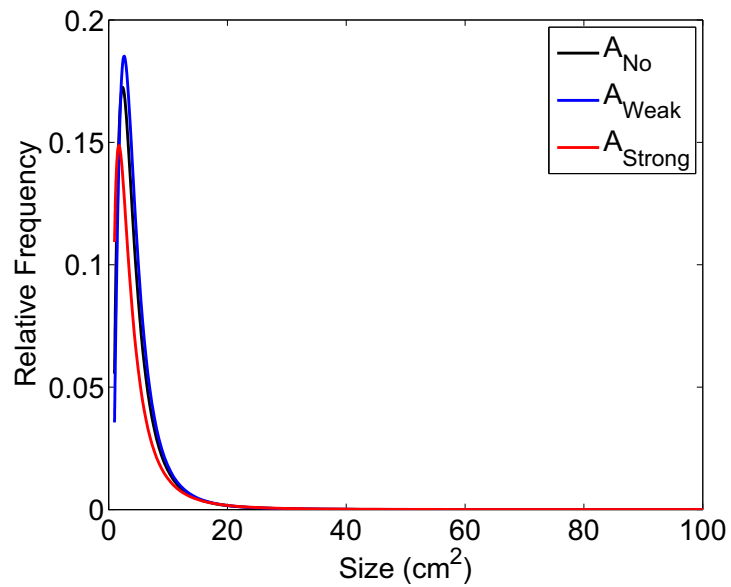
(a) Stable size structure, **w**
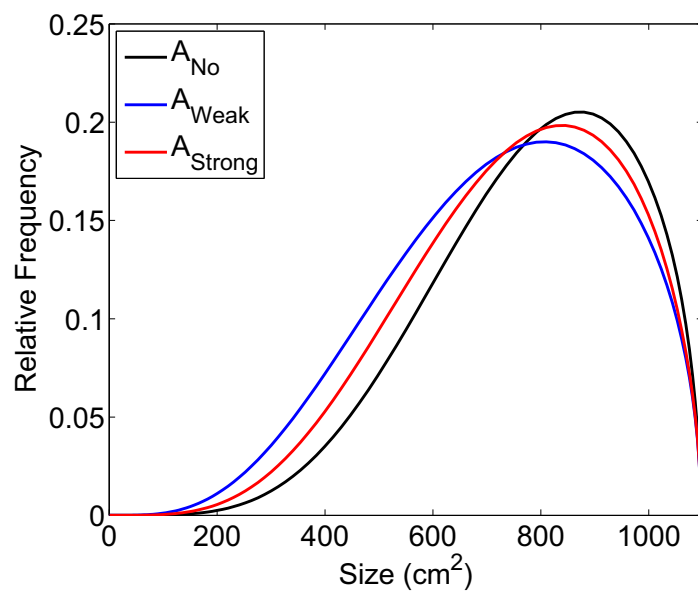
(b) Fragmentation value, **v**

Figure 7.10: The stable size structure, **w**, and fragmentation values, **v** for all three IPMs on a size scale.
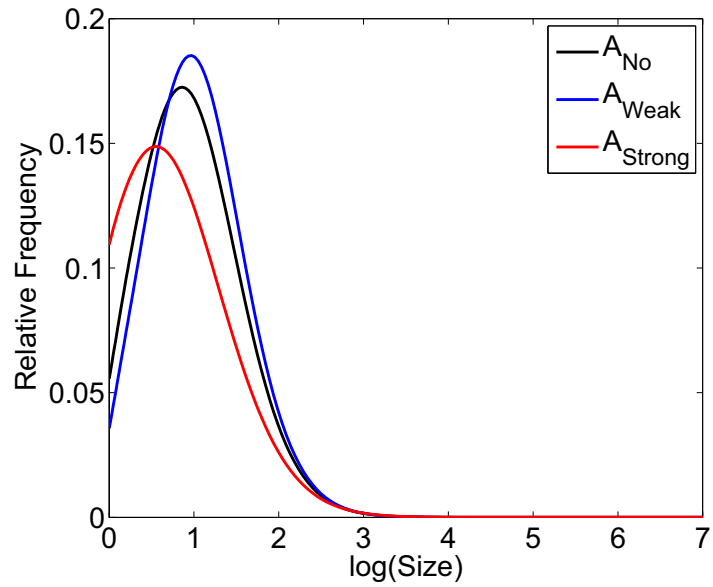
(a) Stable size structure
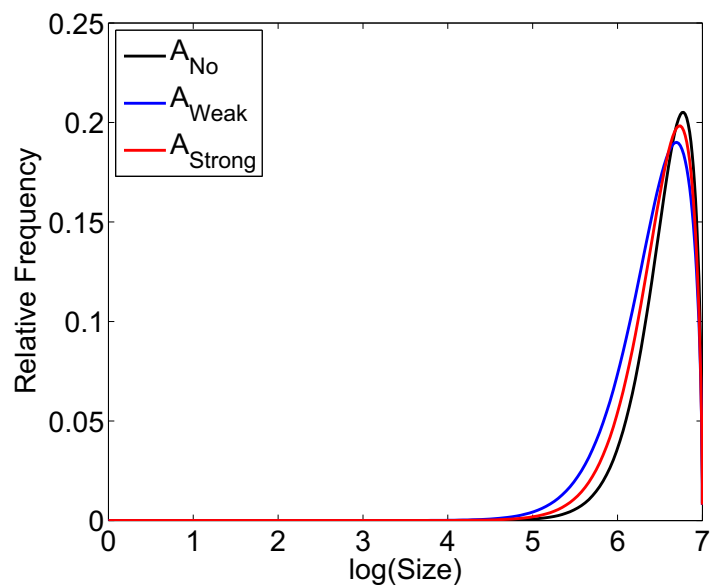
(b) Fragmentation value

Figure 7.11: The stable size structure $w(x)$ and fragmentation values, $v(x)$ for all three IPMs, both on a log-size scale.

the IPMs, using the patch behaviour observed in each category. Each IPM was then projected through time using their initial conditions, in order to project when population numbers decline to zero.

Using initial conditions from data, there were initially a greater number of patches in A_{No}, with the fewest in A_{Weak} (Figure 7.13 (a)). After 10 months, there were a greater number in A_{Weak} than in A_{Strong}, with the population becoming extinct in approximately 60 months. After 100 months, there are approximately the same number of patches in A_{No} and A_{Weak} and both populations then follow a similar decline with extinction after approximately 150 months. Extinction is measured as the time when no patches remain in the population. Patches in A_{Strong} become extinct two and a half times quicker than A_{Weak} and A_{Strong}.

Each of the initial conditions for the above projections were different. This allowed comparison of number of patches on the reef, according to observed patch numbers. However, it is also informative to compare the models using one set of initial conditions. This will allow the intrinsic dynamics of the models to be compared. It highlights the differences in the models, rather than the difference in initial conditions. This required the construction of a theoretical initial condition, which followed a log-normal distribution. A log-normal distribution was selected, as it was earlier assumed that the coral patches followed a log-normal distribution, when fitting the growth and fragmentation distribution functions. This was achieved through randomly generating a large number of patch sizes on a log-scale, where the random generation was taken to be normally distributed. This randomly generated data were then divided amongst the 'size-class' boundaries from the numerical integration. These boundaries were the same for all three IPMs as the same integration boundary and numbers of mesh points were used. In this case population density is used ahead of number of patches, as the number of patches are artificially selected and the density gives a better idea of the proportion of patches in each size class at each time step.
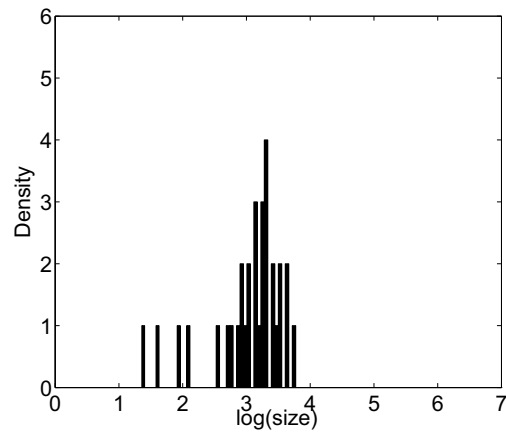
(a) A_{No}
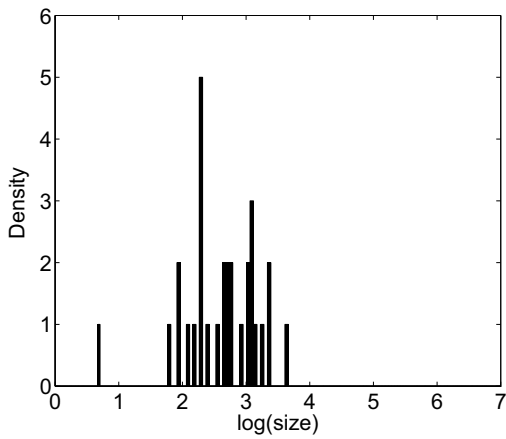
(b) A_{Weak}
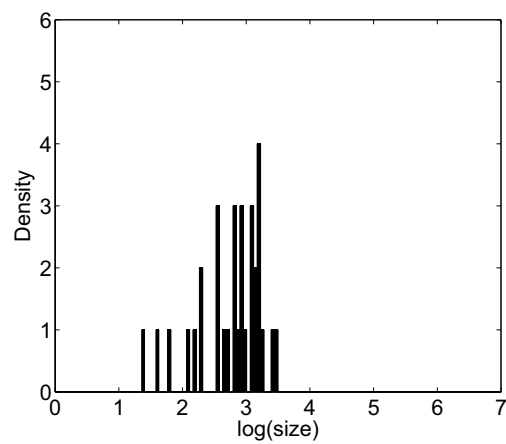
(c) A_{Strong}

Figure 7.12: Initial conditions for A_{No}, A_{Weak} and A_{Strong}. These are shown on a log scale, using the mesh boundaries selected during numerical integration.
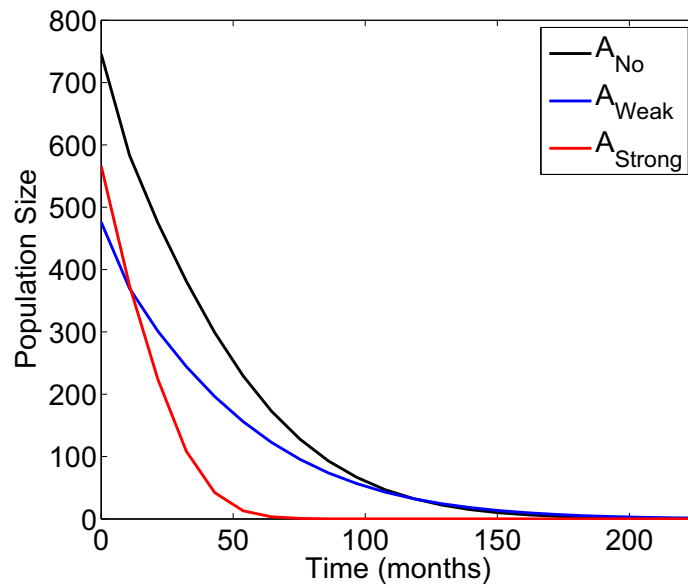
(a) Data
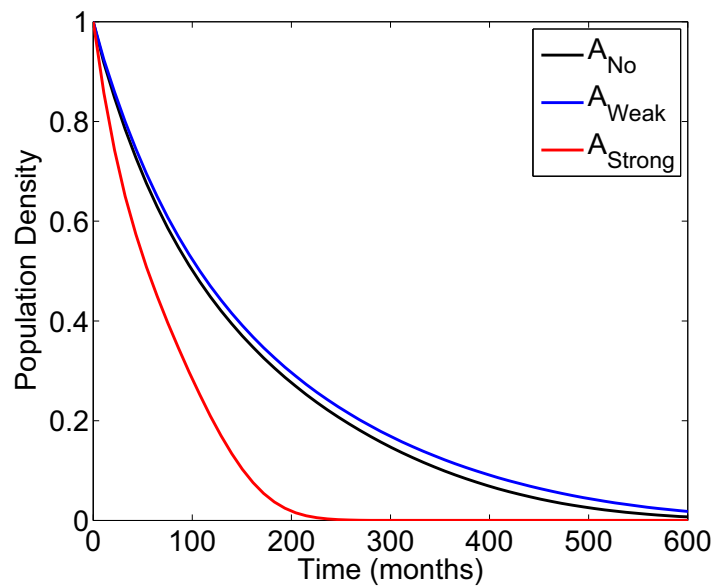
(b) log-normal

Figure 7.13: (a)Projection of population sizes under initial conditions from data.
(b) Projection of population density under log-normal initial conditions.

When the populations are projected using randomly generated log-normal ini-
tial conditions (Figure 7.13 (b)), the population under A_{Strong} will become extinct
after approximately 200 months, three times quicker than A_{Weak} or A_{No}. The popu-
lation in A_{Weak} faired slightly better than A_{No}, due to the slightly higher population

growth rate, but after 600 months it will also be extinct.

Key Asymptotic and Kernel Results

1. In A_{Strong}, the kernel showed a systematic decrease in patch size.

2. Survival-growth dominates all the kernels and influences dynamics more than fragmentation.

3. A_{Strong} had the steepest asymptotic decline.

4. The asymptotic growth rate of A_{Weak} is higher than A_{No}.

5. The stable size distribution of patches are all dominated by patches less than $20cm^2$ in area, but there are patches of a slightly larger size in A_{Weak} in comparison to A_{Strong} or A_{No}.

6. Large patches contributed the most to fragmentation for all three categories.

7. With a log-normally distributed initial patch structure, coral patches in A_{Strong} will die off three times quicker than those in A_{Weak} or A_{No}.

7.4.3 Transient Analysis

It is unlikely that these IPMs will ever reach their asymptotic dynamics due to varying hurricane occurrences each year. It is important to describe the dynamics immediately following a disturbance. Transient analysis gives the relative amplification or attenuation of behaviour, compared to what would be exhibited if the population was in its stable size structure (as shown in Figure 7.10). To calculate the maximum amplification, as well as the minimum attenuation, each IPM was projected over 10 time steps. The initial conditions were biased, so all members were in one 'size class' (from numerical integration), and the maximum (and minimum) amplification calculated for each time step.

There is a greater range of possbile behaviour after 1 time step for A_{Strong}. Re-activitiy shows an amplification of 2.1825, whilst attenuation is 0.003. This gives a range of 2.18, which is much larger than either A_{Weak} or A_{No}, with ranges 1.20 and 1.28 respectively (Table 7.4). This showed that the stronger the hurricane the greater range of amplfication and attenuation that could be achieved by biased initial conditions. It also showed a greater range in behaviour by a population experiencing a weak hurricane, than a population experiencing no hurricane. Reactivity showed a similar picture to the range of Reactivity and Attenuation (Figure 7.14).

Attenuation was achieved by the smallest possible patch sizes of between 1.000 and $1.001 cm^2$ for all three IPM categories (Table 7.4). In comparison, the sizes for which Reactivity was achieved vary slightly. The smallest sizes were in A_{Weak} and A_{No} of between 25.88 and $27.33 cm^2$, whilst for A_{Strong} it was achieved by slightly larger patches of between 27.33 and $28.87 cm^2$ (Table 7.4).

For all biased initial conditions, the maximum amplification (ρ_{max}) and minimum attenuation (a_{min}) are achieved after ten time steps (Figure 7.14). Minimum attenuation for all three IPMs is 0.00 (Table 7.4). Maximum amplification showed that for certain biased initial conditions the population could be amplified massively in comparison to amsyptotic dynamics. There is a marked difference between A_{Strong} and A_{Weak}, where a maximum amplification for A_{Weak} was 7.11, but for A_{Strong} was 1451.9. The maximum amplification for A_{No} was larger than for A_{Weak}.

The sizes, for which maximum amplification occurred, was much larger for A_{Strong}, than either A_{Weak} or A_{No} (Table 7.4). In A_{Strong}, maximum amplification occurred with patches of between 94.90 and $99.98 cm^2$, this was over double the size of patches in A_{Weak} and A_{No}. However, A_{No} achieved maximum amplification with patches slightly larger than A_{Weak}. In comparison minimum attenuation occurred in all categories with patches under $2 cm^2$. These patches were slightly larger for

Indicator	A_{Strong}	A_{Weak}	A_{No}
Reactivity	2.18 (27.33 to 28.87)	1.22 (25.88 to 27.33)	1.29 (25.88 to 27.33)
Attenuation	0.003 (1.000 to 1.001)	0.02 (1.000 to 1.001)	0.01 (1.000 to 1.001)
ρ_{max}	1451.9 (94.90 to 99.98)	7.11 (37.98 to 40.12)	12.73 (40.12 to 42.38)
a_{min}	0.00 (1.14 to 1.16)	0.00 (1.000 to 1.001)	0.00 (1.000 to 1.001)

Table 7.4: The transient dynamic indicators for the three IPMs; A_{Strong}, A_{Weak} and A_{No}. In brackets are the range of sizes which achieve these values.

A_{Strong} at 1.14 to $1.16cm^2$, compared to 1.000 to 1.001 in both A_{No} and A_{Weak}.

Under log-normal initial conditions, the population density after 10 time steps was very different for the three IPMs. However, for all three IPMs the log-normal initial conditions fair better than the asymptotic stable size structure (Figure 7.14). Under log-normal initial conditions, A_{No} achieved a lower relative population density to A_{Weak} and A_{Strong}. On the other hand the relative population density was much larger in A_{Strong} than those that would be achieved under log-normal initial conditions.

Key Transient Results

1. There is a greater range of amplification and attenuation for A_{Strong} than A_{Weak}, both after 1 time step and after 10.

2. Under certain biased initial conditions, A_{Strong} can exhibit large amplification.

3. Amplification and attenuation under A_{Weak} is lower than A_{No}.

4. Attenuation after 1 or 10 time steps was achieved by very small patches.

5. Reactivity is achieved in all three categories by patches between 25 and $30cm^2$.

6. ρ_{max} was achieved by patches larger than those which achieved Reactivity.
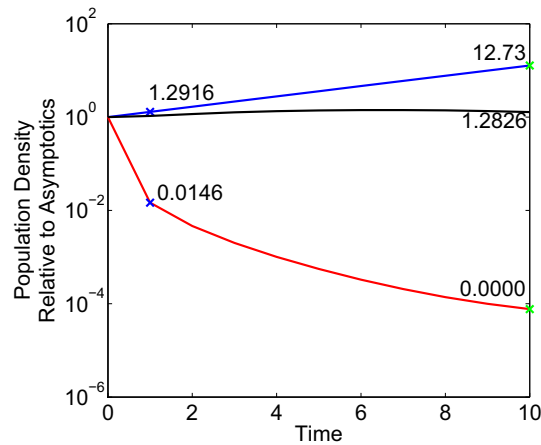
(a) A_{No}
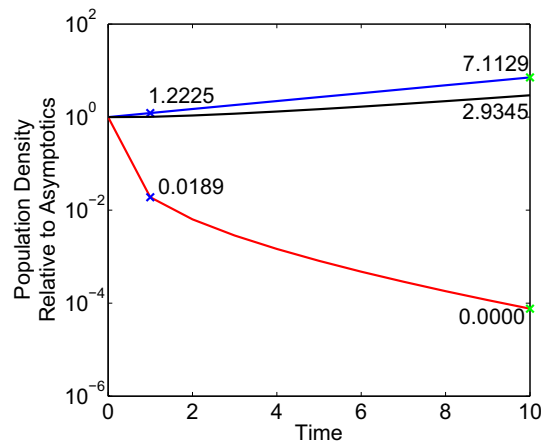
(b) A_{Weak}
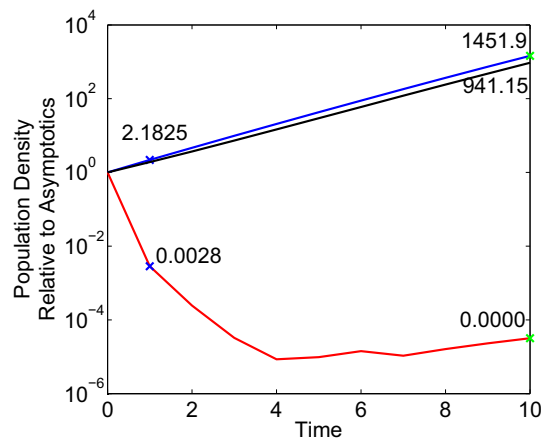
(c) A_{Strong}

Figure 7.14: Transient dynamics of (a) A_{No}, (b) A_{Weak} and (c) A_{Strong}. The range of possible dynamics relative to those exhibited if the population was in stable size distribution. The behaviour under log-normal initial conditions (black line) and the maximum and minimum possible behaviour for each time step (blue and red lines) are shown, with the values of Reactivity, Attenuation, ρ_{max} and a_{min} given.

7.4.4 Perturbation Analysis

Parameters selected in Section 7.3 were the best fit to the data, but each estimate has an associated standard error ($s.e.$). With this standard error, it is possible to perturb related parameters within a given region, in order to estimate a range of possible growth rates. This gives the confidence in each estimate and also shows which parameters are most sensitive. To calculate a 95% confidence interval, parameters were perturbed within a range of values:

$$\overline{x} \pm 1.96 s.e.$$

In Table 7.5, the associated range of values for the population growth rate under these perturbations are given when both the intercept and slope parameters for each function were perturbed at the same time. Figures 7.15, 7.16 and 7.17 give a visual display of the effect of these perturbations on the population growth rate. The closer the mean estimate lay to a λ-contour, the more sensitive λ_1 was to the parameter estimate.

7.4.5 Confidence Intervals for λ

Function	A_{Strong}	A_{Weak}	A_{No}
s(x)	[0.3718,0.4735]	[0.6923,0.8268]	[0.6760,0.7768]
$\overline{\mathbf{g}(y,x)}$	[0.2527,0.8529]	[0.6052,0.9409]	[0.5796,0.9352]
$log(\sigma^2(\mathbf{g}(y,x)))$	[0.4080,0.5836]	[0.7793,0.8034]	[0.7317,0.7579]
$p_f(x)$	[0.3638,0.4644]	[0.6871,0.8049]	[0.6728,0.7707]
$n_f(x)$	[0.4019,0.4555]	[0.7315,0.7899]	[0.7193,0.7529]
$f_s(x)$	[0.3968,0.4632]	[0.7624,0.7988]	[0.7163,0.7497]
$\mathbf{f}_d(y,\frac{x}{n})$	[0.3508,2.5841]	[0.7320,0.8707]	[0.7005,0.7981]

Table 7.5: The 95% confidence intervals for λ_1, formed through the perturbation of the intercept and slope parameters simultaneously. The boundaries of perturbations are given by $\overline{x} \pm 1.96 s.e.$

In A_{Strong}, the mean estimate for λ_1 is 0.43, but could range from 0.253 to

2.58, depending on which parameters were perturbed (Table 7.5). It is surprising that the upper confidence interval for λ_1 is above 1 for $\mathbf{f}_d(y, \frac{x}{n})$. The growth rate increased dramatically when the intercept parameter dropped below -0.25 (Figure 7.15). With the exception of $\mathbf{f}_d(y, \frac{x}{n})$, all other upper estimates for λ_1 lie below 1 and confidence that the population is in decline is high. The lowest growth rate is 0.25 is found when the mean growth estimates are perturbed. The number of fragments parameter has the smallest range of λ values, showing this parameter is least sensitive to perturbations.

In A_{Weak}, all estimates for λ lie below 1 (Table 7.5), which means that there is high confidence that the population is in decline. The lowest estimate for λ is 0.6052 and the highest 0.9409, both found in the 95% confidence interval for mean growth. The highest lower estimate is 0.7793 and the lowest upper estimate is 0.8034, in the 95% confidence intervals for the variance of the growth.

For A_{No}, all estimates are lower than the critical value of $\lambda = 1$ (Table 7.5), meaning that the population is in decline for the 95% confidence interval. The lowest growth rate is 0.5796 and the highest is 0.9352, both found from the mean growth estimate. The highest lower bound is 0.7317 from the variance of growth and the lowest upper bound is 0.7497 from the family size estimate.

For A_{Weak} and A_{No} the mean growth estimates are most sensitive to perturbations, whilst for A_{Strong} it is the fragment disctribution.

7.4.6 Comparison of Parameters

- **Survival**: Similar for all three categories, requires an increase in both intercept and slope to see population growth rate increase (Figures 7.15 (a), 7.16 (a) and 7.17 (a)). Within the 95% confidence interval, A_{Weak} can achieve the highest growth rate. The highest growth rate achieved in A_{Strong} is lower than the lowest growth rate in A_{Weak} and A_{No}.

- **Probability of Fragmentation**: Requires a decrease in both intercept and slope parameter values for all three categories (Figures 7.15 (b), 7.16 (b) and 7.17 (b)). This will decrease the probability of fragmentation for all patches, but will in particular decrease the probability for larger patches. In the 95% confidence interval, A_{Strong} is smaller than A_{Weak} and A_{No} for all possible values. Again, A_{Weak} can achieve a higher growth rate than A_{No}.

- **Mean Growth**: For both A_{Weak} and A_{No}, the fitted parameters lie closer to an increasing contour than a decreasing. The largest possible growth rate occurs in A_{Weak} and A_{No} of 0.9, whilst A_{Strong} can achieve a growth rate of 0.8 (Figures 7.15 (c), 7.16 (c) and 7.17 (c)).

- **Variance of Growth**: These parameters are the least sensitive to perturbations for all three categories. All are more likely to be higher than the nominal value in the 95% confidence interval than lower (Figures 7.15 (d), 7.16 (d) and 7.17 (d)).

- **Family Size**: For all three categories, a small decrease in slope will cause a larger population growth rate decrease than if the decrease in slope was larger (Figures 7.15 (e), 7.16 (e) and 7.17 (e)). There is very little effect due to changing the intercept parameter and it is more important to increase the slope parameter. This means it is more important to increase the proportion of a large patch remaining than it is for small patches.

- **Fragment Size**: These show two different stories. For A_{Strong}, there was little sensitivity to small perturbations in the intercept, followed by a rapid increase for larger perturbations (Figure 7.15 (f)). This showed that increasing all fragment sizes in A_{Strong} could cause a quick increase in population growth and is the most sensitive within the 95% confidence interval. In comparison, A_{Weak} and A_{No} showed a similar picture of proportional responses to perturbations

(Figures 7.16 (f) and 7.17 (f)). In all cases, the intercept needs to decrease to cause an increase in growth rate. This means all fragment sizes need to decrease in size. It also required for the slope to increase, which is equivalent to increasing the size of fragments produced by large patches. The horizontal nature of the λ-contours in A_{Weak} and A_{No} showed that perturbations to the slope are more sensitive.

- **Number of Fragments**: All three categories are very similar and population growth rate increased as the number of fragments decreased (Figures 7.15 (g), 7.16 (g) and 7.17 (g)).

7.5   Conclusions

7.5.1   Does Hurricane Strength Affect Patch Dynamics?

The results in this chapter showed that the strength of a hurricane affects the dynamics of a population. If a strong hurricane strikes a population, the long-term growth rate was much lower than if there was no hurricane or even a weak hurricane. The surprising result was that, under a weak hurricane, there was a slightly larger growth rate than if there was no hurricane. Historically, hurricanes were thought to benefit a coral reef by creating free space, however this result showed they can also boost the long term growth rate at a patch scale. It is not just in the long term that the differences can be seen, transient analysis has shown that a population experiencing a weak hurricane could have the lowest amplification after one time step, and a strong hurricane the highest.

Other results that support this conclusion are that individual patches are more likely to fragment under a strong hurricane, and that survival rates of patches are lower under strong hurricanes. It is also interesting that larger patches in all categories are more likely to survive and more likely to fragment than smaller

patches. Therefore, it is more beneficial for populations to be dominated by larger patches in order to survive future disturbances, but it also puts them at greater risk of fragmenting.

In spite of the differences, some results are the same regardless of hurricane strength. All populations are in decline and will be dominated by patches under $20cm^2$. This showed agreement with other studies on the Caribbean reef, which currently predict that all coral populations are experiencing coral cover decline (for example Gardner et al. (2003)).

7.5.2 Modelling Issues of IPMs

Further issues surround the numerical integration of the kernel. This is necessary in order to analyze the results, but it does introduce errors to the results. The selection of the integration boundary and the number of mesh points required, are inter-linked and should ideally be selected for each IPM created. However, to allow the projection of interacting IPMs in Chapter 9, these needed to be identical for all three IPMs in this Thesis. This meant that some compromises were reached to get the most accurate results for all 3 IPMs. The other issue of numerical integration was the selection of L in $\Omega = [L, U]$. Due to the log-size assumption L had a natural lower boundary of $L = 0$ or in terms of patch size $L = 1cm^2$. In the data set, the minimum recorded size was $1cm^2$, as all measurements were calculated to the nearest cm^2. This excludes patches smaller than $1cm^2$, but which were not extinct. This could also underestimate the number of patches in the population, but in terms of area would have little affect on the results.

The final issue surrounded the choice to create three IPMs, rather than one with an additional hurricane factor. This increased the sampling error in the model, as more parameters were required to be fitted with the same number of data. This lead to three survival functions (with two parameters for each) being parameterized

from 1833 pieces of data. In comparison, if a hurricane factor was included in one IPM, only three parameters would need to be fitted. However, by calculating the 95% confidence interval for λ_1 for all parameters, showed that all but one parameter still lead to population decline.

Modelling fragmentation was an issue, as fragmentation is a rare event. Even so, these models give the best approximation to the dynamics. There are always fewer pieces of data to parameterize the fragmentation part of the kernel than the survival-growth parameters. For example, all 1833 pieces of data can be used to parameterize survival, but only a fraction of those can be used to model number of fragments.

7.5.3   Conclusion

In this chapter, Integral Projection Models were parameterized in order to understand if the strength of a hurricane affected the dynamics of the population. This was achieved by the division of the data into three categories: to compare the dynamics under no hurricane; a weak hurricane effect and a strong hurricane effect. It has been concluded that this does affect the dynamics, but surprisingly a population under A_{Weak} has better long-term and short-term dynamics than A_{No}. This will be further discussed in Chapter 10. The IPMs created in this chapter will be used in Chapters 8 and 9, to assess what effect there is on a population when the IPMs interact and to suggest management strategies and to investigate the effect that climate change may have on the population.

(a) Survival

(b) Probability of Fragmentation

(c) Mean Growth

(d) Variance of Growth

(e) Family Size

(f) Fragment Size

(g) Number of Fragments
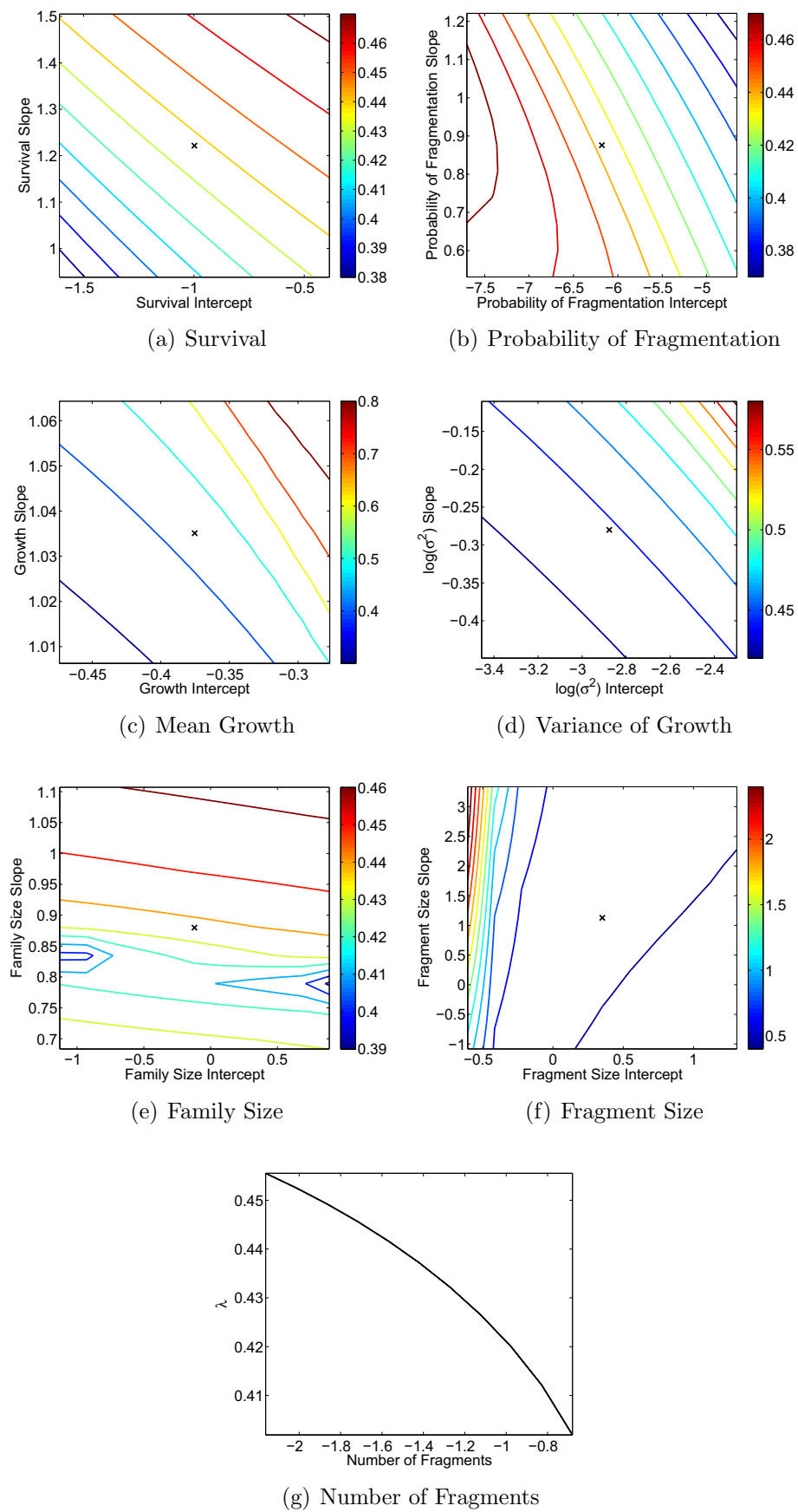
Figure 7.15: The population growth rates of A_{Strong} under perturbations of the parameters.

(a) Survival

(b) Probability of Fragmentation

(c) Mean Growth

(d) Variance of Growth

(e) Family Size

(f) Fragment Size

(g) Number of Fragments
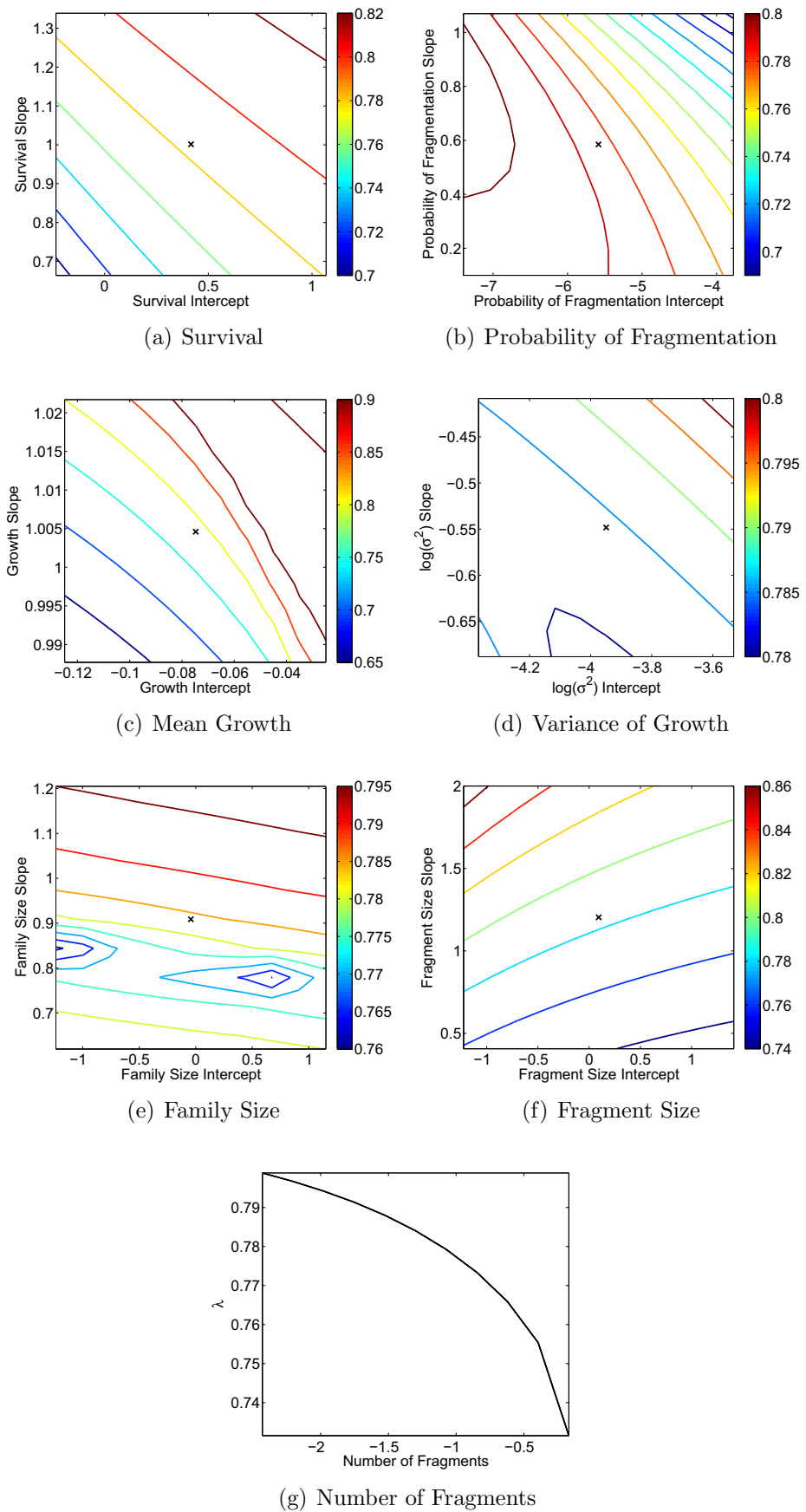
Figure 7.16: The population growth rates of A_{Weak} under perturbations of the parameters.

(a) Survival

(b) Probability of Fragmentation

(c) Mean Growth

(d) Variance of Growth

(e) Family Size

(f) Fragment Size

(g) Number of Fragments
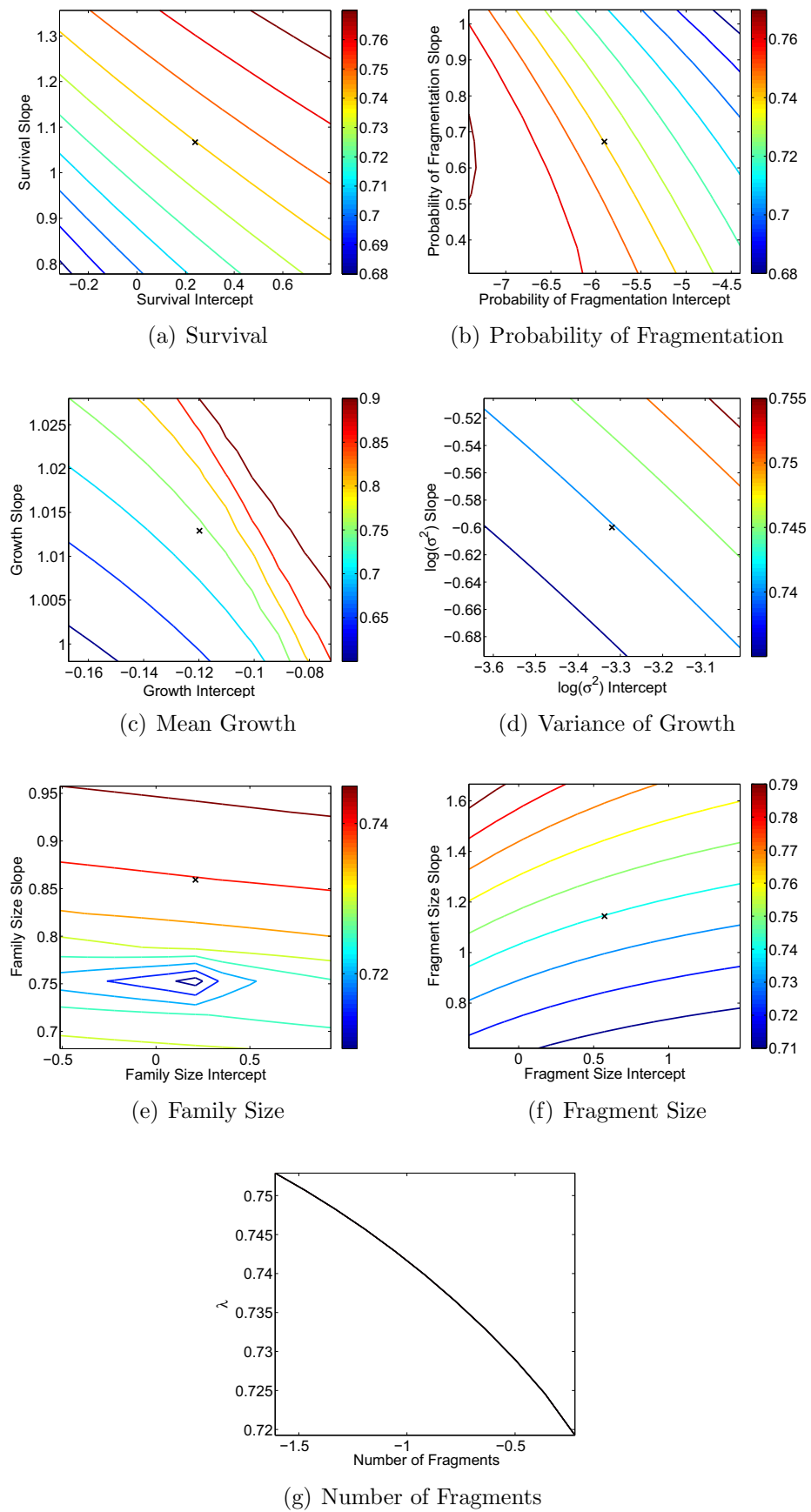
Figure 7.17: The population growth rates of A_{No} under perturbations of the parameters.

Chapter 8

Management Strategies for *Montastraea annularis.*

8.1   Introduction

When populations are in decline, a natural question to ask is 'how can the population be managed so that it grows?' In this chapter, methods for selecting plausible strategies are suggested. The Integral Projection Model for non-hurricane transitions (A_{No}), which was parameterized in Chapter 7, is used in order to demonstrate how mathematical models can aid managers in selecting how best to manage a population. The non-hurricane transitions are used as managers are able to control the population best in periods of senescence.

By using Integral Projection Modelling, it allows the perturbation of individual processes. In contrast, the PPM can only recommend areas of behaviour to be targeted, as one or more processes could be modelled by the same parameter, for example fragmentation and shrinkage.

The aim is to suggest strategies, which will aid recovery between hurricanes. As was discussed in Section 2.3, the definition of recovery is not clear from the literature. In this chapter, recovery is defined as 'an increase in population growth

rates alongside the existence of large patches in a population'. It was decided to include the requirement of larger patches as it was shown in In Chapters 4 and 7 that larger patches are better able to survive disturbances, therefore the increase in patch sizes should also be an aim of any management strategy. The ideal management strategy will increase the population growth rate above 1, *i.e.* $\lambda_1 \geq 1$, as well as exhibiting a stable size structure dominated by larger patches. This is not always achievable. In Chapter 7, it was shown that the 95% confidence interval for λ_1 were all less than 1 for A_{No}. This showed that the population is firmly in decline, and could mean that it is not possible that some functions, when managed, are able to achieve $\lambda_1 \geq 1$. In this chapter, when $\lambda_1 \geq 1$ is not achievable the best achievable strategy will be suggested.

This chapter firstly describes the methods, which can be used to calculate management strategies, before going on to suggest possible strategies that managers could use in the case of *M. annularis*. Two types of management strategies are suggested in this chapter: those that target only one biological function and those that target two interlinked functions.

8.2 Methods

The methods adopted to select management strategies are illustrated in this section through their application to one of the functions in the IPM kernel. Recall that the IPM kernels fitted in Chapter 7 are of the form:

$$\mathbf{k}(y,x) = (1 - p_f(x))s(x)\mathbf{g}(y,x) + p_f(x)n_f(x)f_s(x)\mathbf{f}_d(y, \frac{x}{n}), \qquad (8.1)$$

the function $\mathbf{g}(y,x)$ captures the growth and shrinkage of coral patches from one time step to the next. The growth function was an obvious function to target as, by increasing the mean size of a coral patch, it would be expected that the overall

population growth rate should increase. In particular, the mean size of patches $\overline{\mathbf{g}(y, x)}$ was managed. Unmanaged, the fitted mean growth function for A_{No} was:

$$\overline{g(y, x)} = -0.1198 + 1.0129x,$$

which resulted in a growth rate of $\lambda_1 = 0.74$. In Section 7.4.4, both the intercept (-0.1198) and slope (1.0129) parameters were perturbed concurrently to calculate the 95% confidence interval of the growth rate as $\lambda_1 = [0.5796 \quad 0.9352]$. The same method of numerical simulation was adopted here, with the exception that there is no upper or lower bounds for the parameters. Instead of finding the maximum possible λ within a defined range of parameter values, the aim is to find the maximum possible λ within a reasonable range of parameters. In this case, the growth parameters were perturbed for ranges: [-0.3144 1.6656] for the intercept and [0.499 2.489] for the slope parameter. This results in Figure 8.1 (a), a contour map of the population growth rate (λ_1) for each possible combination of intercept and slope parameters within this range. This range was selected through trial and error as the best range that gave the best λ_1. From Figure 8.1 (a), different management strategies can be selected by selecting the required λ_1 and reading off the intercept and slope parameter values. This case is an example of where $\lambda_1 = 1$ is unachievable.

The largest achievable growth rate was $\lambda_1 = 0.953$, a relative increase in λ_1 of 73%. It was achieved when the function was perturbed to $\overline{\mathbf{g}(y, x)} = 0.1156 + 1.0129x$ (Figure 8.1 (b)). This is achieved through the perturbation of the intercept parameter alone. Perturbing the intercept parameter alone is equivalent to managers needing to increase all sizes of coral patches proportionally, whilst if the slope parameter was perturbed, managers would need to increase larger patches by a larger proportion than smaller patches.

The perturbation resulted in an increase in patch sizes from below the 1 : 1 line

(a)

(b)

(c)

(d)
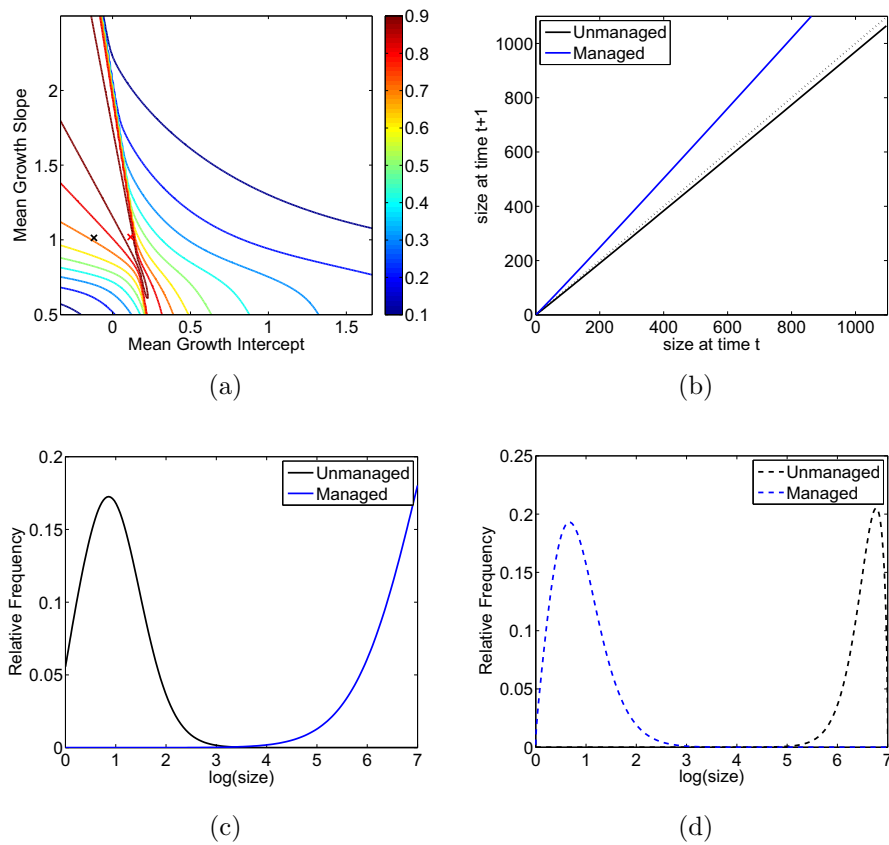
Figure 8.1: Management of mean growth: (a) The contour map of possible λ_1 values, the black cross shows the unmanaged parameter values and the red cross the managed parameter values. (b) The selected management strategy, given the size of a patch, x, at time t it gives its size at time $t+1$. The dotted line is the $1:1$ line where the size at time t is equal to the size at time $t+1$. (c) The stable size structure of the managed and unmanaged population shown on a log-size scale. (d) The fragmentation value of the managed and unmanaged population shown on a log-size scale.

to above the 1 : 1 line, where all patches remain the same size (Figure 8.1 (b)). On average, coral patches need to grow rather than shrink as is currently the case. Given that *M. annularis* is a slow growing coral, the feasibility of a mean increase in size must be questioned.

The perturbations do not exclusively affect the population growth rate, but also the stable size structures and the fragmentation values. Under the perturbation described above, the stable size structure and fragmentation value changed dramatically (Figure 8.1 (c) and (d)). Where left unmanaged, the population was dominated by small patches, whilst the managed population will be dominated by larger patches (Figure 8.1 (c)). This is logical, as the management strategy calls for an increase in the mean growth of patches, resulting in more patches growing to larger sizes. The fragmentation value changed, instead of larger patches contributing the most to fragmentation, it is instead smaller patches that contribute to fragmentation (Figure 8.1 (d)). This in turn causes fewer patches to fragment, as smaller patches have a lower probability of fragmentation.

It is possible to reject management strategies purely on these results, for example if the stable size structure was dominated by smaller patches when managed, then the effort and cost required to implement the strategy would not be worthwhile. From this, a definition of feasibility of a management strategy can be defined as follows.

A management strategy is classified as **feasible** if the following conditions are met:

1. The perturbations required are within a reasonable range.

2. The stable size structure is not dominated by smaller patches.

3. The new function seems reasonable for a *M. annularis* population.

Not all functions have feasible management strategies, but this information can be

just as useful for managers, as it shows which functions should not be targeted or would waste resources if they were targeted.

Under this definition of feasibility, is the above management strategy feasible? It satisfies the first criteria, with perturbations of 196% and 0.6% for the intercept and slope parameters. The second criteria is satisfied as under management the stable size structure is dominated by large patches. Finally, the third criteria can be tested. The strategy fails at this final hurdle, due to the large increase in patch sizes required at each time step by a slow growing coral. Therefore it is concluded that this strategy is infeasible.

8.3 Results

8.3.1 One Function Strategies

In this section, each biological function is targeted in turn and assumes that managing one function will not impact or alter any other function.

Probability of Survival

The best management strategy is to increase survival rates for all patches, regardless of size to greater than 90% (Figure 8.4). The strategy required the perturbation of both the intercept (by 1008%) and slope (by 2%) parameters (Table 8.1). A perturbation of 1008% is large, but is required, in order to increase the survival rates of smaller patches. These large perturbations only lead to an increase in λ_1 by 8%. The stable size structure (Figure 8.2) was little affected by this management strategy, in fact it slightly shrinks the peak sizes and is dominated by patches under $3cm^2$. It is concluded that this strategy is not feasible for two reasons: firstly the stable size structure is dominated by smaller patches and secondly the perturbations required to achieve a small increase in λ_1 are large.

Biological Process		Old Parameters	λ	% Change	New Parameters	Effect of **w** and **v**
Probability of Survival	Intercept	0.2392	0.8000	8	2.65 (+1008%)	**w** dominated by smaller patches
	Slope	1.0669			1.05 (+2%)	Smaller patches contribute to fragmentation
Mean Growth	Intercept	-0.1198	0.9020	22	0.0756 (-163%)	**w** now dominated by large patches
	Slope	1.0129			1.009 (-0.4%)	**v** dominated by smaller patches
Variance of Growth	Intercept	-3.3197	0.8803	19	-3.0771 (+7%)	**w** changes little.
	Slope	-0.6000			-0.447 (+26%)	**v** shows all patch sizes will fragment.
Probability of Fragmentation	Intercept	-5.9059	0.736	-0.5	-9 (-52%)	little change to **w**
	Slope	0.6730			0.85 (+26%)	**v** is dominated by large patches.
Number of fragments	Intercept	-0.9163	0.8997	22	0.3 (+133%)	**w** contains a full range of patches
Family Size	Intercept	0.2102	0.77	4	0.2885 (+37%)	No change in **v** or **w**
	Slope	0.8592			0.9552 (+11%)	
Fragment Sizes	Intercept	0.5721	0.76	3	0 (-100%)	
	Slope	1.1439			2 (+75%)	

Table 8.1: A summary of the best management strategies for each biological function in A_{No}. Those shaded red are infeasible and those in green are feasible.
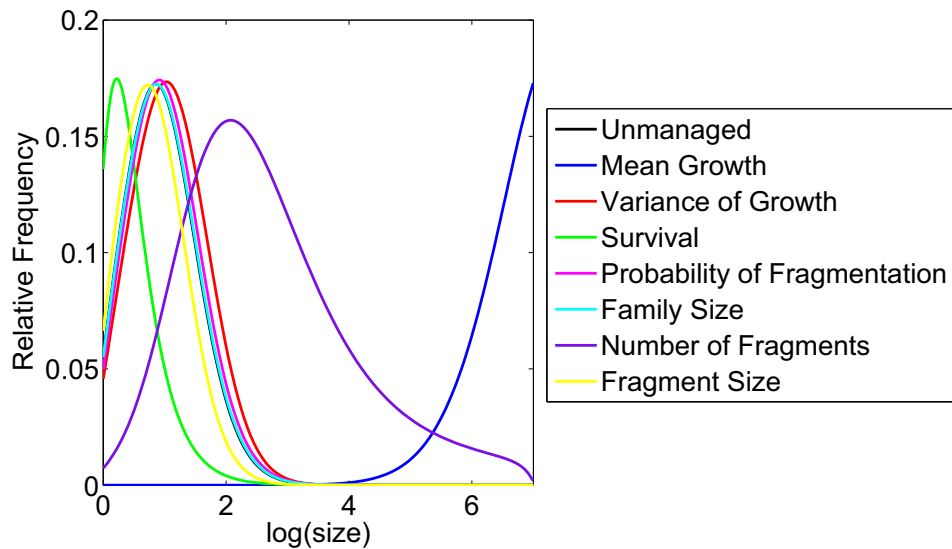
Figure 8.2: The stable size structure of the different management strategies suggested in Table 8.1

Mean Growth

Increasing the mean growth line such that all patches experience growth was the best management strategy. It achieves an increase in the population growth rate by 22%, but required an increase in the intercept parameter by 163% (Figure 8.5 and Table 8.1). Increasing the intercept parameter, and not the slope parameter, requires a manager to proportionally increase all patch sizes, rather than larger patches more than smaller patches. Alongside increasing the growth rate, the stable size structure also changes (Figure 8.2). The population will be dominated by larger patches when managed, rather than smaller patches when unmanaged, and will place the population in a better position to survive future disturbances. The question about this strategy is if coral patches are able to achieve the growth required for this strategy (Figure 8.5 (a)). The mean growth line falls just above the 1 : 1 line, showing only slight growth of patches and, therefore, should be achievable. This strategy fulfils the three criteria of feasibility.
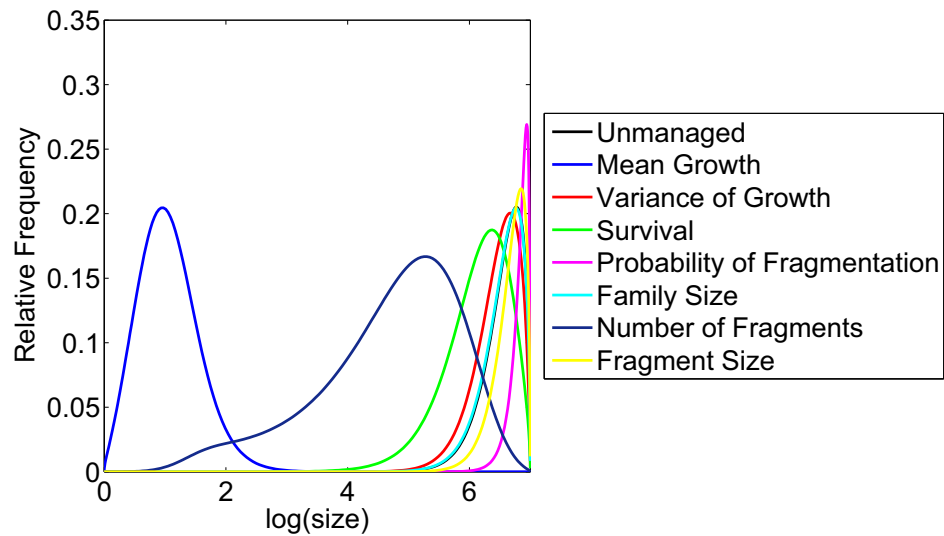
Figure 8.3: The fragmentation values of the different management strategies suggested in Table 8.1

Variance of Growth

Greater variability in patch sizes is required, in order to increase the population growth rate (Figure 8.6). It is unclear how this could be achieved by managers, but to get a 19% increase in the population growth rate it only requires increases in the parameters of 7% and 26% (Table 8.1). This management strategy did not alter the stable size structure by a significant amount, with only a slight increase in peak sizes observed (Figure 8.2). By the definition of feasibility, this management strategy is indeed feasible, but the biological achievability of this strategy must be questioned.

Probability of Fragmentation

Perturbations of parameters showed that the probability of fragmentation should decrease, in order to achieve a change in the population growth rate (Figure 8.7 (b)). In turn, this increases the survival and growth contribution to the kernel and decreases the fragmentation contribution. The probability of fragmentation can be
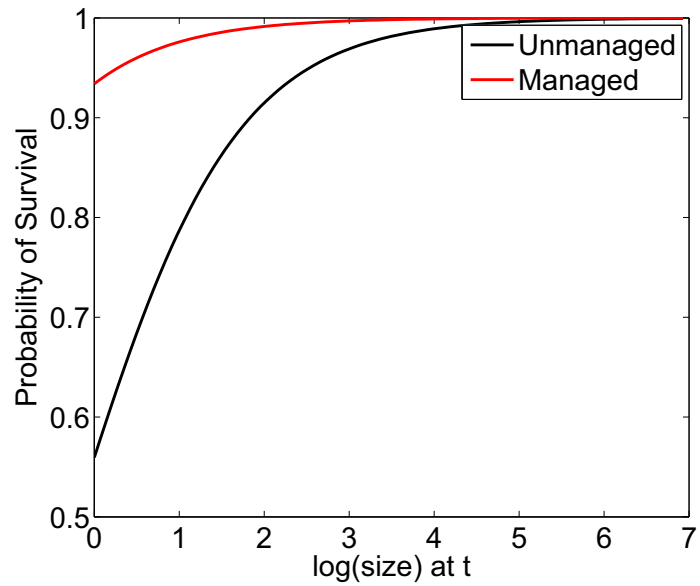
(a)
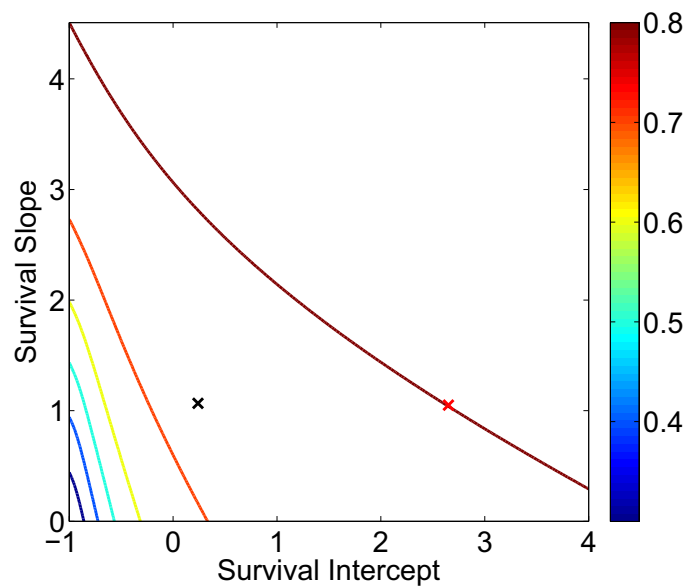
(b)

Figure 8.4: Survival management strategies. (a) The probability of survival for the unmanaged and managed population, shown on a log-size scale. (b) λ-contour plot, the black cross shows the unmanaged parameter values, and the red cross the managed population parameters.
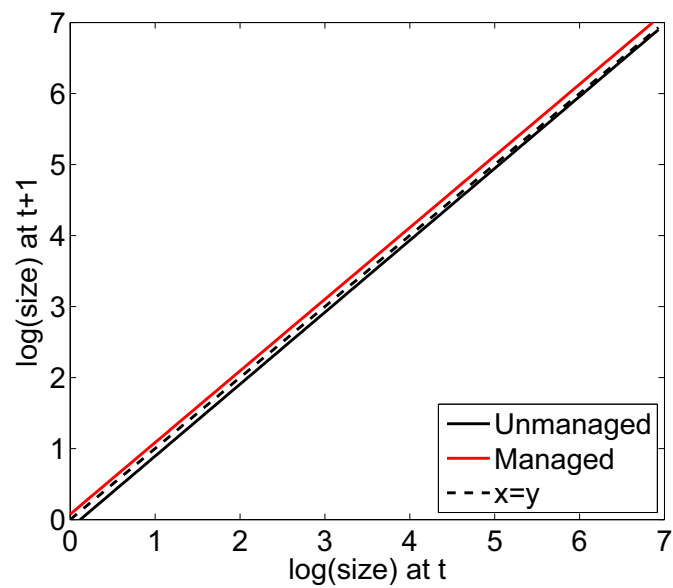
(a)
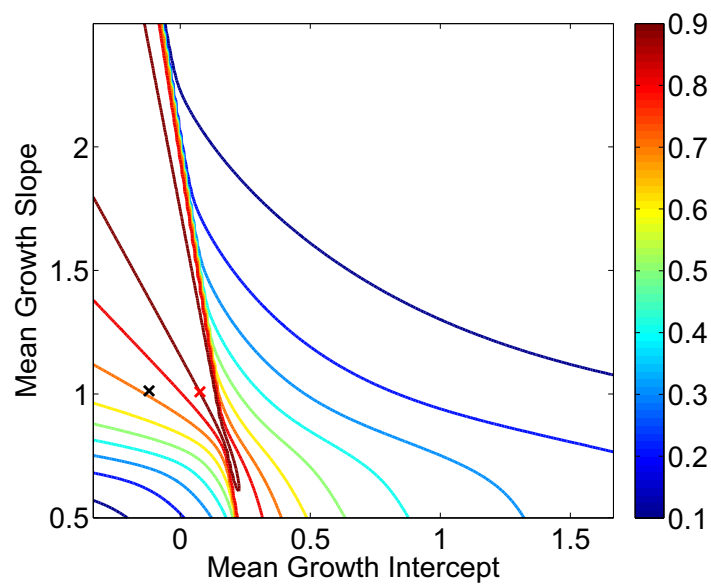
(b)

Figure 8.5: Mean growth management strategies. (a) The mean size of coral patches at time $t + 1$ given the size of a patch at time t for the unmanaged and managed population, shown on a log-size scale. (b) λ-contour plot, the black cross shows the unmanaged parameter values, and the red cross the managed population parameters.
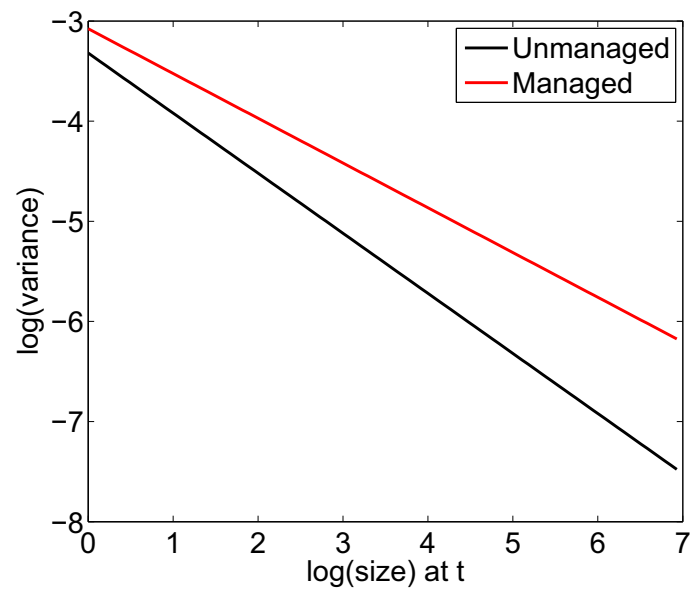
(a)
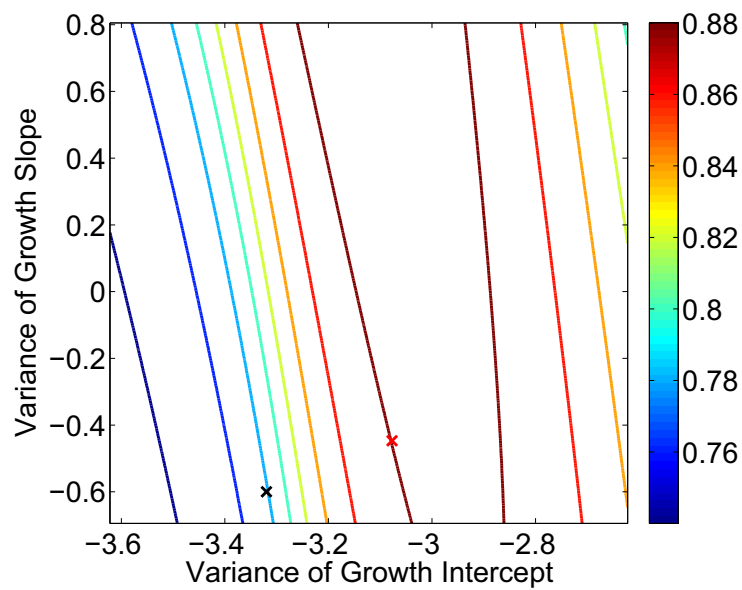
(b)

Figure 8.6: Variance of growth management strategies. (a) The log variance of mean growth for the unmanaged and managed population. (b) λ-contour plot, the black cross shows the unmanaged parameter values, and the red cross the managed population parameters.

decreased through the reduction of stress on coral patches, as fragmentation is a by-product of this stress. The best strategy decreased the probability of fragmentation for patches of size $1000cm^2$ from 0.2 to 0.05 (Figure 8.7 (a)). This is achieved by decreasing the intercept parameter by 52% and increasing the slope parameter by 26% (Table 8.1). Under this strategy, certain patch sizes will not fragment, in particular patches under $30cm^2$ (Figure 8.7 (a)). This strategy has minimal effect on the stable size structure (Figure 8.2). Therefore, this strategy is not feasible as the perturbations will not give an increase in the stable size structure or, in fact, an increase in the growth rate.

Number of Fragments

This strategy could perturb the population to a growth rate of 1, but this strategy was infeasible, as it required the number of fragments to increase from 2.4 to 4.01. An alternative strategy is to increase the number of fragments produced from 2.4 to 3.35, which increased the population growth rate to 0.9 (Table 8.1 and Figure 8.8). It is counter-intuitive to increase the number of fragments, as it would in turn decrease the size of these fragments. It may result in a decrease in the total area on the reef temporarily, but the existence of a greater number of patches, under positive conditions for growth, may in the long-term increase the overall structure and size of the population. It is unclear how this can be achieved by managers, but it is feasible, as it increases the maximum sizes in the stable size structure significantly (Figure 8.2). It does this without significantly decreasing the size of patches contributing to fragmentation (Figure 8.3).

Family Size

The total area of the fragments constricts the area remaining post fragmentation. Under perturbations, the intercept parameter does not affect the population growth rate (Table 8.1 and Figure 8.9 (b)). This result is important as it informs managers
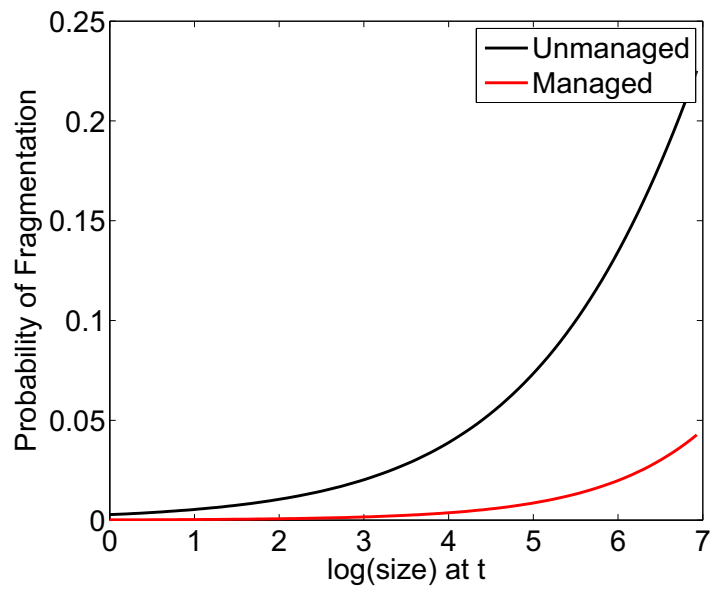
(a)
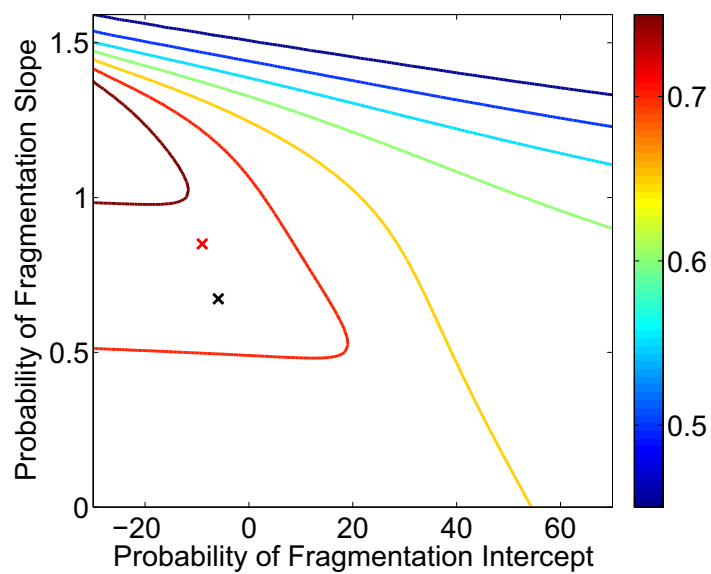
(b)

Figure 8.7: Probability of Fragmentation management strategies. (a) The probability of fragmentation for the unmanaged and managed population, shown on a log-size scale. (b) λ-contour plot, the black cross shows the unmanaged parameter values, and the red cross the managed population parameters.
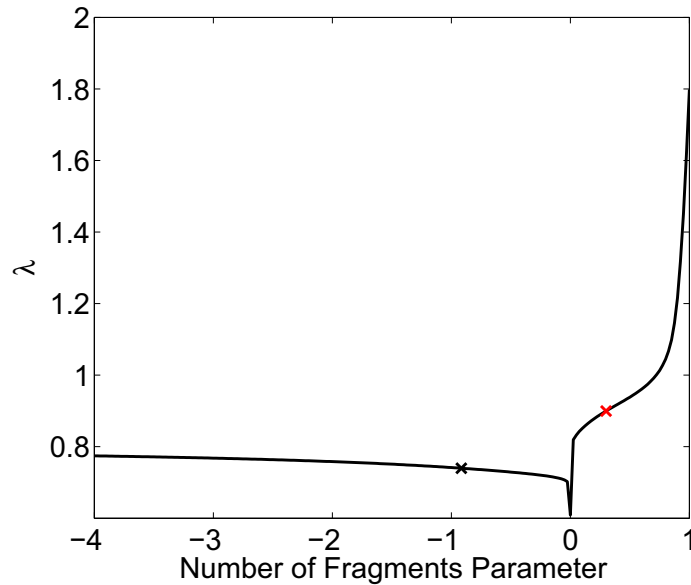
Figure 8.8: The management strategy for the number of fragments function. A plot of the population growth rate given a perturbation in the number of fragments parameter, the black cross shows the unmanaged parameter values, and the red cross the managed population parameters.

that increasing family size of all patches equally will not benefit the population. Instead, managers should focus on increasing the family size for larger patches. The suggested management strategy required at least a 100% of a coral patch area to remain post fragmentation (Figure 8.9 (a)). This is infeasible as fragmentation is known to occur under stress and so it is highly likely that some coral patch area would be lost.

Fragment Distribution

In order to increase the population growth rate, the size of fragments needs to increase (Figure 8.10 (a)). However, to increase the population growth rate by only 3% required large perturbations of the parameters by 100% and 75% respectively (Table 8.1 and Figure 8.10 (b)). In doing so, the stable size structure of the population would slightly decrease in patch size (Figure 8.2). Therefore, this strategy is infeasible as the effort required for such a small increase in the population growth
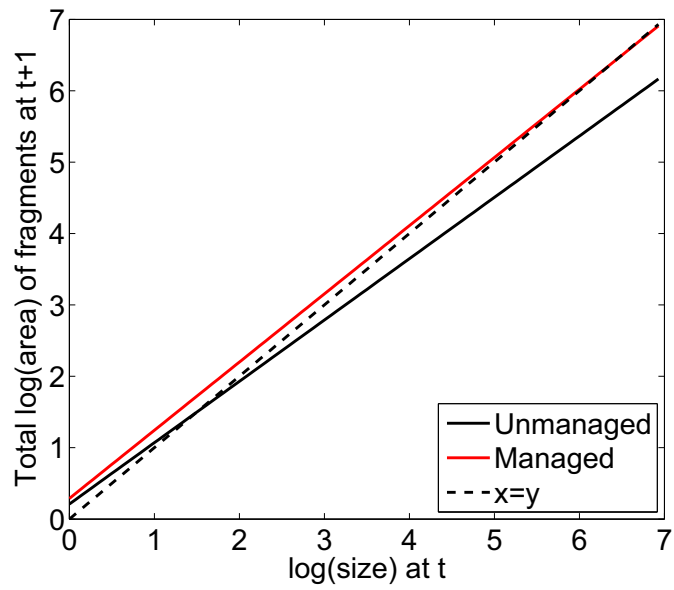
(a)
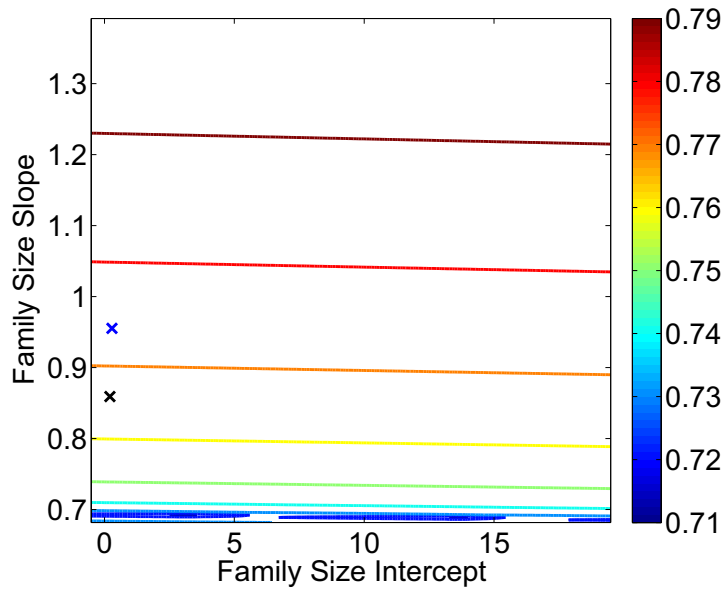
(b)

Figure 8.9: Family size management strategies. (a) The total area of coral remaining given the size of the parent patch. Shown on a log-size scale. (b) λ-contour plot, the black cross shows the unmanaged parameter values, and the red cross the managed population parameters.

rate is high and would result in a population consisting of smaller patch sizes.

Conclusions

In conclusion, under single-function perturbations only three strategies were feasible:

1. Increasing mean growth of patches

2. Increasing variability in patch sizes

3. Increasing the number of fragments produced

These three strategies would increase the growth rate to 0.9, 0.88 and 0.9 respectively.

8.3.2   Management Strategies Targeting Two Biological Functions

Strategies that targeted one function did not increase the population growth rate into population growth. Of the three strategies considered feasible, it would be interesting to investigate what would happen if another function was targeted simultaneously in two of the strategies. In particular, what would occur if fragmentation probabilities decreased as mean growth increased. It would also be interesting to investigate what would happen if the size of fragments altered as the number of fragments increased. The first strategy was selected, because in reducing stress on a reef, both the mean growth will increase and the fragmentation probability would decrease. The second strategy was selected, because the fragment size function depended not only on the size of the 'parent' patch, but also on the number of fragments produced. As these functions are linked in the functional form, it makes sense to investigate the effect of management on both of the functions.
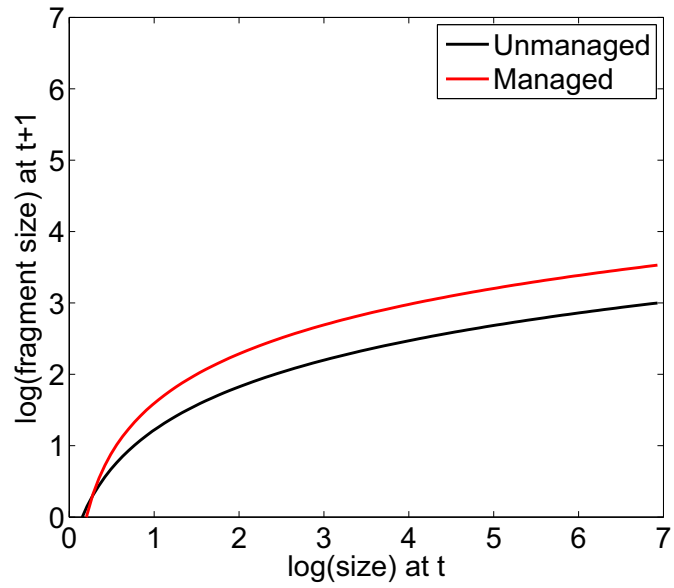
(a)
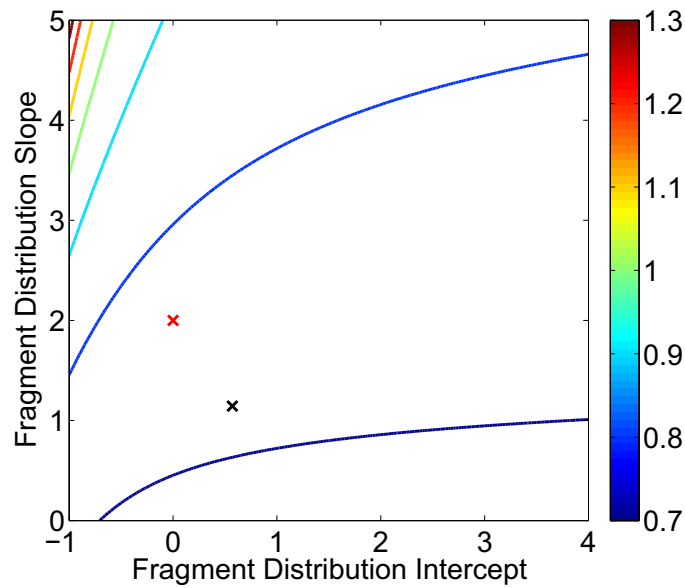
(b)

Figure 8.10: Fragment sizes management strategies. (a) The fragment size given the size of the parent patch for the unmanaged and managed population, shown on a log-size scale. (b) λ-contour plot, the black cross shows the unmanaged parameter values, and the red cross the managed population parameters.

The two functions were managed by selecting the probability of fragmentation and number of fragment strategies in Table 8.1. Then by perturbing the parameters of mean growth and fragment distribution, the best management strategy can be calculated.

Probability of Fragmentation and Mean Growth

In decreasing the probability of fragmentation alone the growth rate altered little. However, when the mean growth function is increased alongside this, the population growth rate can be increased to $\lambda_1 = 0.9108$ (Table 8.2). The effect on the stable size structure was the increased dominance of larger patches, above and beyond that of when mean growth alone was targeted (Figure 8.11 (a)). In fact, the minimum patch size, which is found in the stable size structure is $150cm^2$, compared to the unmanaged population, where the maximum patch size in the stable size structure was $20cm^2$. The fragmentation value in the combined management strategy showed slightly larger patch sizes than mean growth alone. However, patches contributing to fragmentation were still much smaller than the unmanaged population. This shows few patches fragment as the fragmentation value consists of patches smaller than $20cm^2$, but the population will consist only of patches over $150cm^2$ and the strategy shows patches under $20cm^2$ have a probability of zero of fragmenting. This is consistent with a reduction in stress on the reef and increased growth. This is similar to behaviour that should be seen in periods of senescence.

Number of Fragments and Fragment Distribution

The function of fragment size $(\mathbf{f}_d(y, \frac{x}{n}))$ is determined by the size of the 'parent' patch, as well as the number of fragments. When both are managed, the population growth rate can increase to $\lambda_1 = 0.975$ (Table 8.2), in comparison to 0.8997 $(n_f(x))$ and 0.76 $(\mathbf{f}_d(y, \frac{x}{n}))$ if managed individually (Table 8.1).

Biological Processes		λ (% change)	Old Parameters	New Parameters	Effect of **w** and **v**
Probability of Fragmentation	Intercept	0.9108 (+23%)	-5.9	-9 (−52%)	**w** dominated by large patches
	Slope		0.673	0.85 (+26%)	**v** dominated by small patches
Mean Growth	Intercept		-0.1198	0.0756 (+163%)	
	Slope		1.0129	1.009 (−0.4%)	
Number of Fragments	Intercept	0.975 (+32%)	-0.9	0.3 (+133%)	In **w**, patches over $20cm^2$
Fragment Distribution	Slope		0.5721	-0.95 (−266%)	are equally likely. Whilst **v** was
			1.1439	0.6320 (−45%)	dominated by medium sized patches

Table 8.2: Management strategies for perturbing two biological functions concurrently. The percentage change of λ is compared to if no management is adopted. The new parameters required to achieve these management strategies are given, with percentage change in brackets.

The effect on the stable size structure was to increase the dominance of larger patches than either of the two single-function management strategies. There would be a full range of patch sizes in a population, with patches over $20cm^2$ equally likely to be in the population. This result appears counter-intuitive, as the strategy is decreasing the size of patches post fragmentation, but by increasing the number of fragments produced there is a greater chance that some of these patches will survive and grow in the future. Patch sizes in the fragmentation value will decrease in size, to be almost symmetrical in the patch size range (Figure 8.11 (b)). The combination of the two strategies causes smaller patches to contribute to fragmentation.

8.4 Conclusions

In conclusion, better growth rates can be achieved if two functions are managed concurrently. In particular, this chapter highlights two strategies that managers could target, namely a **Growth** strategy, where the probability of fragmentation and mean growth are targeted and a **Fragment** strategy, where the number of fragments is increased and the size of these fragments decreased. Both of these strategies increased the dominance of larger patches in the stable size structure placing the population in a better position to survive future disturbances, as well as increasing the population growth rate by at least 23%. How these strategies can be achieved is discussed in Chapter 10.

This chapter has shown one possible method by which management strategies could be selected for a population of coral patches in years of senescence. These strategies can be used when investigating the interaction of hurricane frequency and intensity on a population, in order to understand the effect of climate change on the reef (see Chapter 9).
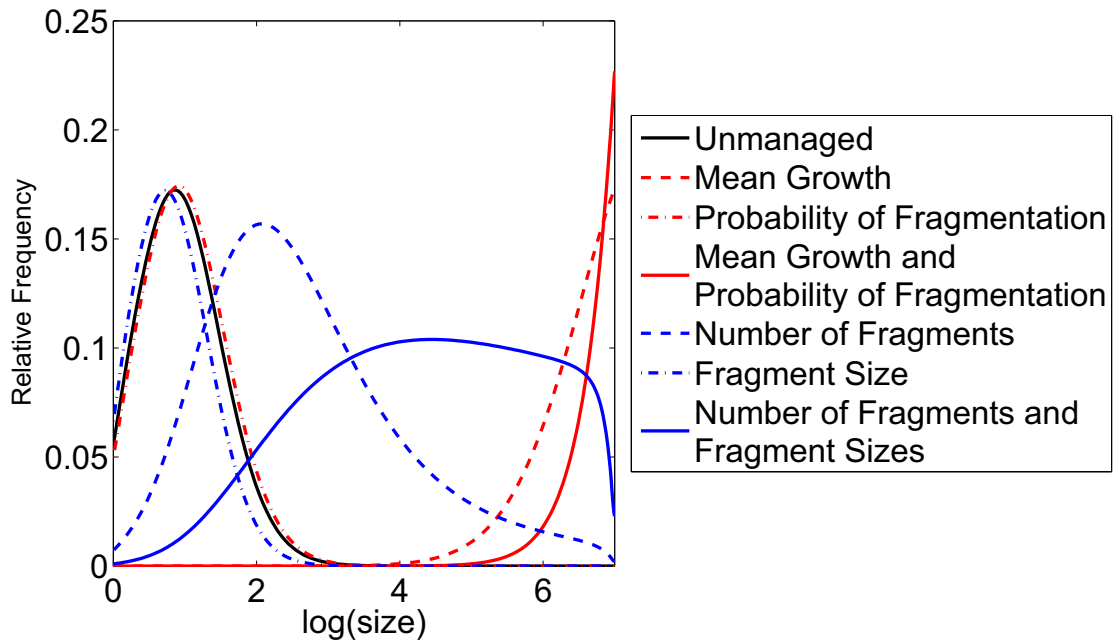
(a)
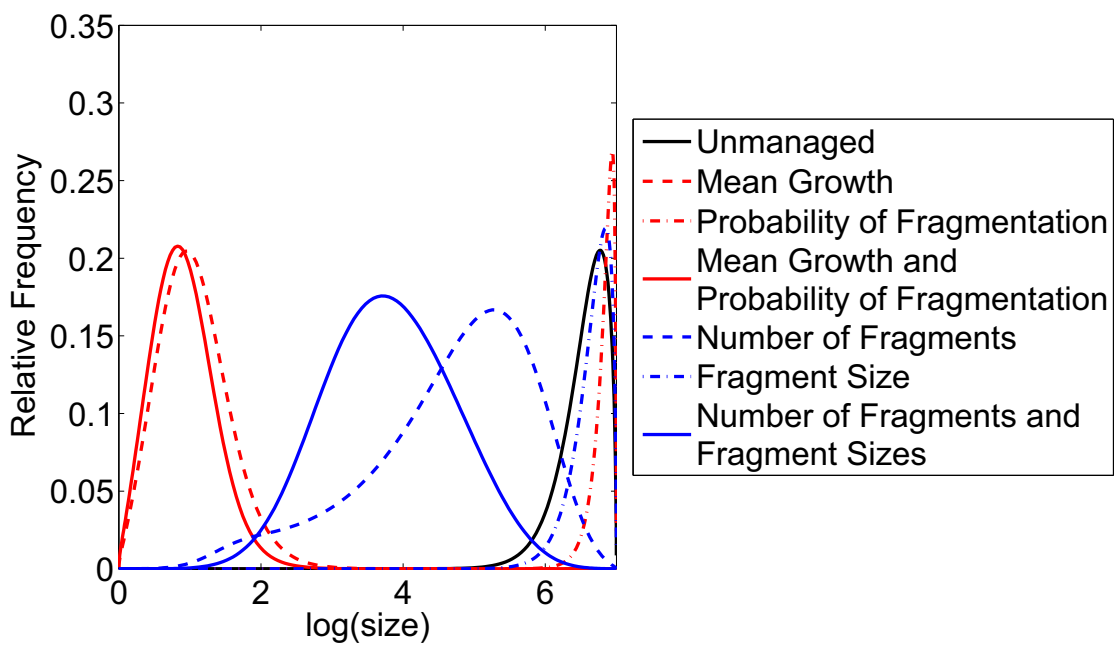
(b)

Figure 8.11: (a)The stable size structure, and (b) the fragmentation values, given on a log-size scale. Given for the single-function and two-function management strategies.

Chapter 9

Extinction times for *Montastraea annularis* Under Differing Hurricane Scenarios

9.1 Introduction

It is forecast that, with climate change, the intensity and duration of hurricanes will increase (IPCC, 2007; Knutson et al., 2010). This chapter investigates the population dynamics projected to occur on the coral patch population under differing hurricane scenarios associated with climate change. To do this, the IPMs parameterized in Chapter 7 are used and the frequency and intensity of hurricanes are varied to investigate the extinction times on the reef. At the end of this chapter, the two main management strategies from Chapter 8 are included in the model to investigate if management could increase the extinction time of the *M. annularis* population.

9.2 Methods

An Integral Projection Model (IPM) can be used to project the future behaviour of a population (See Section 3.3.2). Projection uses the numerical approximation of the kernel $\mathbf{K}$ and the initial conditions approximation $\mathbf{X}(0)$. By repeated pre-multiplication of $\mathbf{K}$, the population at time $t = l$ is:

$$\mathbf{X}(l) = \mathbf{K}^l \mathbf{X}(0). \tag{9.1}$$

The numerical approximation of A_{No} is $\mathbf{N}$; of A_{Weak} is $\mathbf{W}$ and of A_{Strong} is $\mathbf{S}$. At each time step in the projection, one of the approximations ($\mathbf{N}$, $\mathbf{W}$ or $\mathbf{S}$) are selected in place of $\mathbf{K}$. For example, over a 10 year projection, with a strong hurricane in the third year and a weak hurricane in the 7th year, the population at time $t = 10$ would be:

$$\mathbf{X}(10) = \mathbf{N}^3 \mathbf{W} \mathbf{N}^3 \mathbf{S} \mathbf{N}^2 \mathbf{X}(0). \tag{9.2}$$

This can be adapted to include differing frequencies of $\mathbf{S}$ and $\mathbf{W}$, with $\mathbf{N}$ selected in the interim years. In Chapter 4, the time step of the IPM is calculated at 10.75 months, therefore for a projection of 45 years, 50 time steps need to be used and for 52 years there will be 58 time steps. These are the lengths of projections used in this chapter.

Hurricanes occur in the Caribbean between June and November each year. In the model, there is a time step of 10.75 months, which is a large enough time step that it is always possible for a hurricane to occur within the time step.

The initial conditions used in the projections $\mathbf{X}(0)$ are constructed by randomly generating a large data set ($n = 3000$) from a normal distribution on the log-size to give the distribution $\mathbf{n}(x, 0)$. Log-normality was assumed due to the assumption that the data was log-normal in the parameterization of the IPMs. The initial
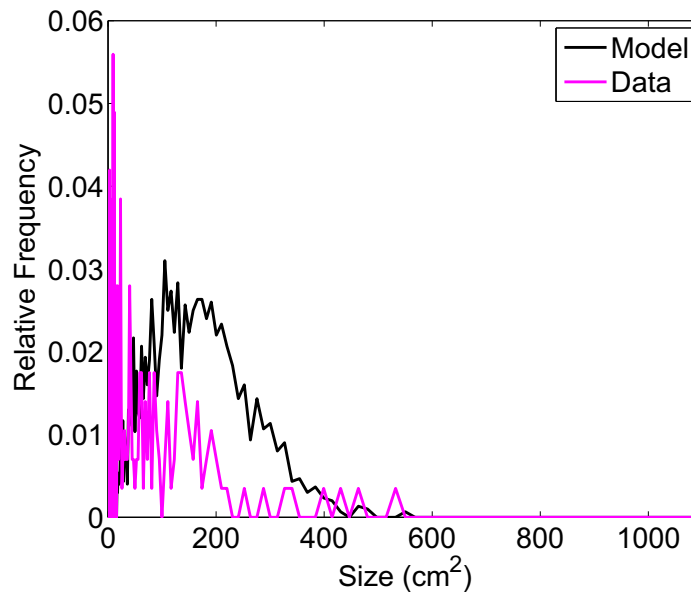
Figure 9.1: The initial conditions as used in the projections compared to the structure of the data in June 1998.

conditions $\mathbf{n}(x, 0)$ is discretized using the 'size class' boundaries defined through the numerical integration to form $\mathbf{X}(0)$. The same initial conditions are used in every projection in this chapter.

The theoretical initial conditions (Figure 9.1) under-estimated the proportion of smaller individuals ($< 100cm^2$) in comparison to the data, and over-estimated the proportion of individuals between 100 and $400cm^2$. All individuals in the theoretical initial conditions were forced to be under $600cm^2$ to match the initial conditions observed in data. The initial condition $\mathbf{X}(0)$ is standardized so that $|\mathbf{X}(0)|_1 = 1$, in order to use population density as a relative comparison of sizes, as the number of patches was artificially chosen, with $n = 3000$. This allowed the comparison in population densities of different scenarios at each time step.

The **critical density** is defined to be a population density of 0.05 (5% of the initial size). This is when a population is assumed to be in a critical state from which it is unlikely to recover. Many of the scenarios tested in this chapter reach population densities below the critical density prior to the end of the projection

Name	Date	Strength
Dean	21/08/07	5
Iris	09/10/01	4
Keith	01/10/00	3
Mitch	27/10/98	5
Greta	19/07/78	2
Fifi	19/09/74	2
Carmen	02/09/74	3
Francelia	03/09/69	2
Hattie	31/10/61	4
Anna	24/07/60	1
Abby	15/07/60	1
Janet	28/09/55	5

Table 9.1: The hurricane activity for Glovers Reef between 1955 and 2011 (Belize National Meteorological Service, 2010).

period; in these cases the **Extinction Time** is measured as the first time at which the population density falls below the critical density. If the population is above the critical density at the end of the projection period, then it is the population densities that are compared.

Population projections measure the population density at each time step, but the size structures of the population can also be calculated for every time step by measuring the structure $\mathbf{X}(t)$ at all t. The population structures are normalized so that the proportions of patches of each size can be compared. They are normalized by:

$$\widehat{\mathbf{X}}(t) = \frac{\mathbf{X}(t)}{|\mathbf{X}(t)|_1}. \tag{9.3}$$

Since Hurricane Janet struck Glovers Reef in 1955, eleven further hurricanes have hit the reef (Table 9.1). There are three measures of hurricane activity used in this chapter:

1. **Return Time** (RT): the average length of time between hurricanes of a given category. Calculated as $RT = E(Y)$, where Y is the length of time between hurricanes of a given strength.

	A_{Weak}	A_{Strong}
Return Time	5.12	26
Rate of Occurrence	5.8	17.3
Frequency	0.17	0.06

Table 9.2: The measures of hurricane occurrences on Glovers Reef between 1955 and 2011. All Category 5 hurricanes were assigned to A_{Strong} and all others to A_{Weak}, tropical storms were not included.

2. **Rate of Occurrence** (RO): is how often a hurricane of a given strength occurs. It is calculated as $RO = \frac{52}{\text{number of hurricanes}}$, where 52 is the number of years observed in Table 9.1.

3. **Frequency** (ω): the average number of hurricanes of a given strength striking Glovers Reef each year. Calculated as $\omega = \frac{\text{number of hurricanes}}{52}$, or as $\omega = \frac{1}{RO}$.

To calculate these measures on Glovers Reef, all Category 5 hurricanes were assumed to be A_{Strong} and all remaining hurricanes as A_{Weak}, this leads to the results in Table 9.2. These showed the frequency of A_{Strong} was about one third of A_{Weak}. The return time for A_{Weak} was slightly smaller than the rate of occurrence with both between 5 and 6 years. In comparison for A_{Strong}, the return time was much larger than the rate of occurrence, with both measures being larger than A_{Weak}. On average, A_{Weak} are almost three times more likely to occur in a given year than A_{Strong}.

Climate change is predicted to increase intensity and duration of hurricanes. In order to test the impacts that hurricanes could have on Glovers Reef, a number of scenarios will be projected. Namely:

(I) **Observed Hurricane History**: The hurricane history of Glovers Reef since Hurricane Janet in 1955 will be reproduced to capture the dynamics of the system if this situation were to be replicated and to test the model. This assumes that all Category 5 hurricanes in Table 9.1 can be modelled by A_{Strong} and all others by A_{Weak}. Where two hurricanes occurred in the same

year, it was assumed that the effect was equal to the strongest hurricane observed.

(II) **Periodic vs. Clustered**: Hurricanes rarely occur at periodic intervals, but instead are often clustered together in groups. In this scenario, the difference in behaviour from these two scenarios are tested. Theoretically a clustering of hurricanes will cause a steeper initial decline but give a longer recovery time between clusterings. Also the decline from clustered hurricanes, although sharp, should decrease with every hurricane (Gardner et al., 2005). Periodic occurrences will have a shorter recovery time but should have smaller initial tissue loss. This scenario tests this theory.

(III) **Increased Intensity**: The 2007 IPCC report claimed that the total global number of hurricanes will remain the same, but that the intensity of these hurricanes will increase (IPCC, 2007). This would result in an increase in number of strong hurricanes, alongside a decrease in weaker hurricanes. This scenario tests what would occur if the same number of hurricanes, 12, hit the reef in a 52 year period (as were observed to strike Glovers Reef between 1955 and 2007), but that the ratio of A_{Strong} to A_{Weak} increased (Table 9.3).

(IV) **Decreased Return Time of $A_{\textbf{Strong}}$**: It is projected that with climate change the intensity of hurricanes will increase. This will result in a greater number of strong hurricanes, which could potentially cause an increased amount of damage to the reef. This is modelled by decreasing the return time of A_{Strong}.

Scenario I was tested in two parts. Firstly, the observed population densities from June 1998 to January 2003 were compared to the model. After eight time steps, the population density was:

$$\mathbf{X}(8) = \mathbf{NWNWN^2SNX}(0). \tag{9.4}$$

Secondly, it was assumed that in September 1955 the population density was equal to 1, and the size structure $\mathbf{X}(0)$ was projected over the 52 year history on Glovers Reef (Table 9.1).

To test scenario II, both A_{Weak} and A_{Strong} are investigated separately. The average return time for A_{Weak} is 5.12 years, whilst for A_{Strong} it is 26 years, over a 45 year period, therefore 8 A_{Weak} hurricanes should occur, but for A_{Strong} only 2 would occur. To test the idea of clustering for A_{Weak}, two sets of 4 hurricanes were assumed to occur at the beginning and in the middle of the projection, with the periodic hurricanes occurring every 6 time steps. Whilst for A_{Strong}, the clustered scenario was tested with two hurricanes assumed to occur in subsequent time steps at the beginning of the study and for the periodic 29 time steps apart. The same numbers of hurricanes were selected, for both clustered and periodic, so that the only differing factor was clustering or periodic nature of the hurricanes, not the number that occurred.

Scenario III is modelled by taking the time period between Hurricanes Janet and Dean (52 years) and the number of hurricanes observed in this time (12). The initial population structure $\mathbf{X}(t)$ in then projected through the next 52 years with 12 hurricanes occurring in this time. Ten scenarios are tested with the ratio of A_{Strong} to A_{Weak} reducing for each scenario (Table 9.3). The proportion of A_{Weak} to A_{Strong} was calculated as the number of A_{Weak} for every A_{Strong}. A proportion of three A_{Weak} for every A_{Strong} - the current ratio, to no A_{Weak} for every A_{Strong} are tested. This will give a range of population densities, which could occur with increased intensity, but with no increase in the number of hurricanes. This projection assumed periodic occurrences of A_{Weak} and A_{Strong} independently through the projection period calculated for each scenario and for each category of hurricane independently.

In order to test scenario IV, it was assumed that hurricanes would occur at periodic intervals through a 45 year time period, according to their average return

Scenario	Number of A_{Strong}	RO A_{Strong}	Number of A_{Weak}	RO A_{Weak}	Proportion
A	3	17.3	9	5.8	3
B	4	13	8	6.5	2
C	5	10.4	7	7.4	1.4
D	6	8.7	6	8.7	1
E	7	7.4	5	10.4	0.71
F	8	6.5	4	13	0.5
G	9	5.8	3	17.3	0.33
H	10	5.2	2	26	0.2
J	11	4.7	1	52	0.09
K	12	4.3	0	-	0

Table 9.3: The 10 different scenarios used in testing Scenario III. The number of each classification is given, alongside their rate of occurrence. Finally, the number of A_{Weak} hurricanes for every A_{Strong} hurricane is given.

time (Table 9.2). The return time for A_{Strong} began at 26 years and was decreased to 13 years and also to 6 years. This scenario did not assume that the number of hurricanes remained the same, but did assume that no weak hurricanes occurred in this time frame. The population density after 45 years or the time at which the population reached a density of 0.05 was recorded.

9.3 Results

9.3.1 How Does the Model Compare to Observed Data?

The model consistently under-estimated the population density from data (Figure 9.2). At the end of the study, January 2003, the population density from the data is 0.67, compared to 0.56 from the model, an under-estimation of 16%. This could be because A_{No} may not purely capture non-hurricane dynamics, but also include some residual hurricane effects. This could account for the difference shown after one time step. In the data, the reef had been undisturbed for many years and slight growth in density at the beginning of the study was observed, but the model
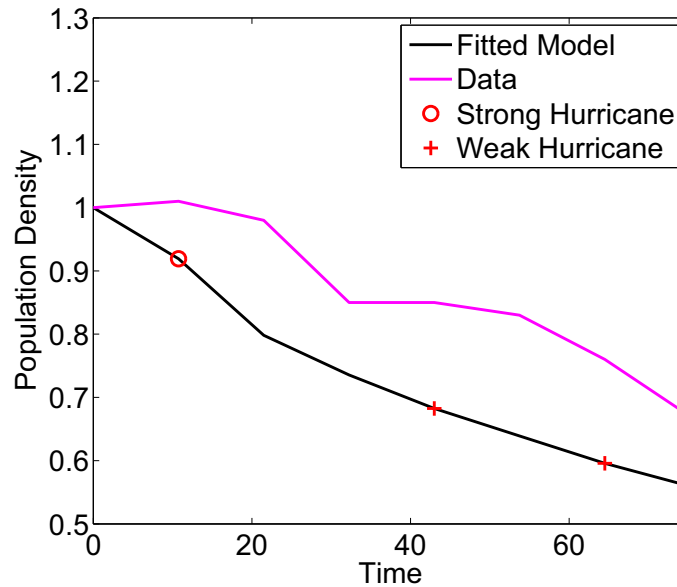
Figure 9.2: Projection of the observed hurricane history between June 1998 and January 2003 compared to the population densities recorded.

experienced decline. In spite of this difference, both the model and the data showed the same pattern of decline.

9.3.2   Scenario I: Observed Hurricane History.

Table 9.1 gave the hurricane activity at Glovers Reef since 1955. The combination of A_{Weak} and A_{Strong} hurricanes were applied to the initial conditions $\mathbf{X}(0)$ in order to assess what could have occurred to the population density on the reef in the past. Figure 9.3 showed that the population density fell below the critical density prior to June 1998. It suggests two things, firstly that the reefs were already depleted at the beginning of the study relative to their historical size, with the population being over 95% higher 47 years prior to the start of the study in 1998 (Figure 9.3). Secondly, that the model does not accurately capture the recovery of a reef in a period of calm. In particular, between Hurricanes Greta and Mitch there was a period of 30 years without a hurricane disturbance. The model continues to decline in this time, but some recovery should have been observed.
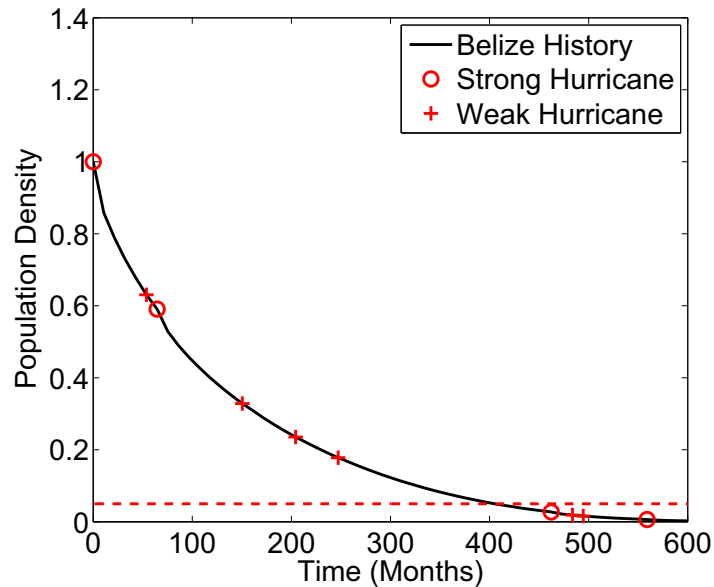
Figure 9.3: The projection of the model using the hurricane history on Glovers Reef. The red dashed line shows the critical density.

9.3.3 Scenario II: Periodic vs. Clustered

A$_{\text{Weak}}$ Hurricanes

Over a 50 year period, 8 hurricanes occurred in each scenario, either in two groups of four or periodically. In the case of the periodic model, these occurred every 5.12 years (the average return time on Glovers reef). This is compared to the clustered scenario where 4 hurricanes occurred in subsequent time steps in two groups. It was found that, in spite of the increased recovery time between the clustering of hurricanes, the periodic group had a slightly later extinction time than the clustered scenario (Figure 9.4). The periodic scenario had an extinction time of $t = 365.5$ months (30 years) compared to $t = 322.5$ months (28 years) for the clustered scenario. This highlights the question of recovery, it would be expected that a longer period of calm (as in the case of clustered) should allow recovery on the reef, which was not observed. For a periodic occurrence of hurricanes, there are shorter periods of calm and you would expect further decline as a result. This
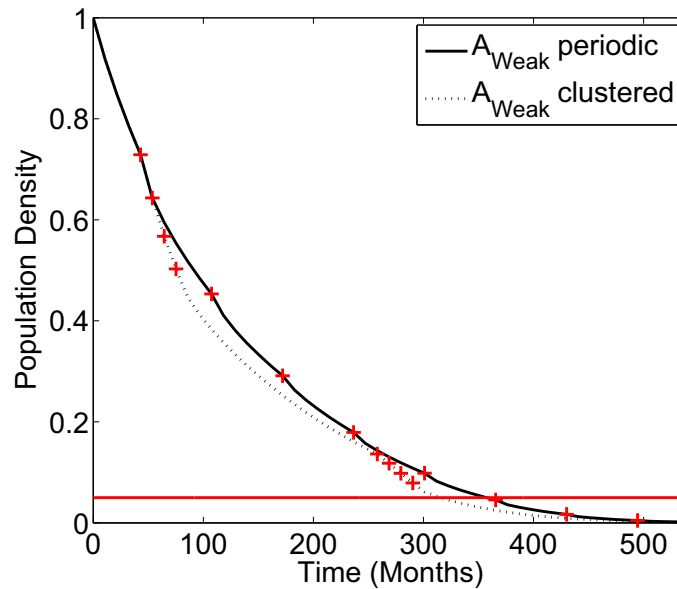
Figure 9.4: Projection over 45 years with A_{Weak}. This gives the population density for either a clustering of hurricanes or periodic occurrences. 8 hurricanes occurred for both the clustering and periodic scenarios. The red line shows the critical density and the red '+' when a weak hurricane occurred.

scenario showed that the decline after the 2nd, 3rd and 4th clustered hurricanes was smaller than that after the 1st. This confirmed other observed studies that the loss experienced after a hurricane is in part determined by the length of time since the previous hurricane (Gardner et al., 2005).

The size structures of the population over the projection period showed similar behaviour for both the clustered and the periodic population (Figure 9.5). After one time step, there was a smoothing out of the initial conditions; this was followed by a decline in the sizes observed. After 10 years, the maximum size of a patch in either scenario is approximately $200cm^2$, after 20 years - $100cm^2$ and after 30 years under $50cm^2$. In the periodic case after 10 years, there was a very small proportion of patches over $200cm^2$ (Figure 9.5 (b)), unlike the clustered case, where all patches are below $200cm^2$ (Figure 9.5 (a)).
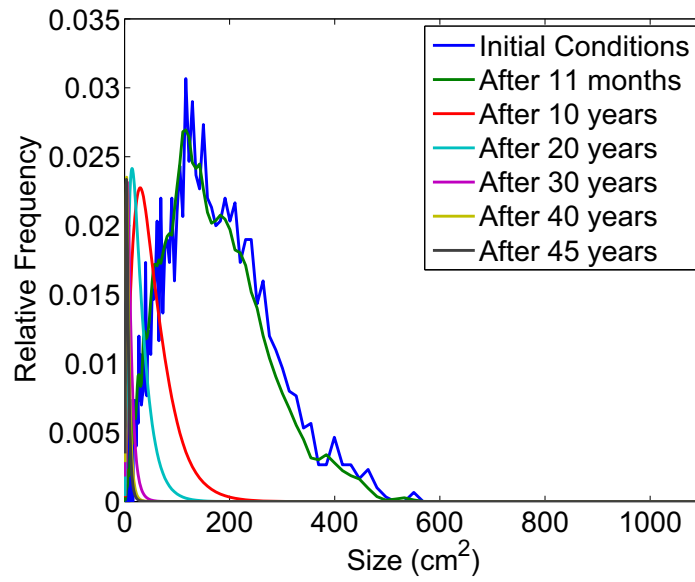
(a) Clustered
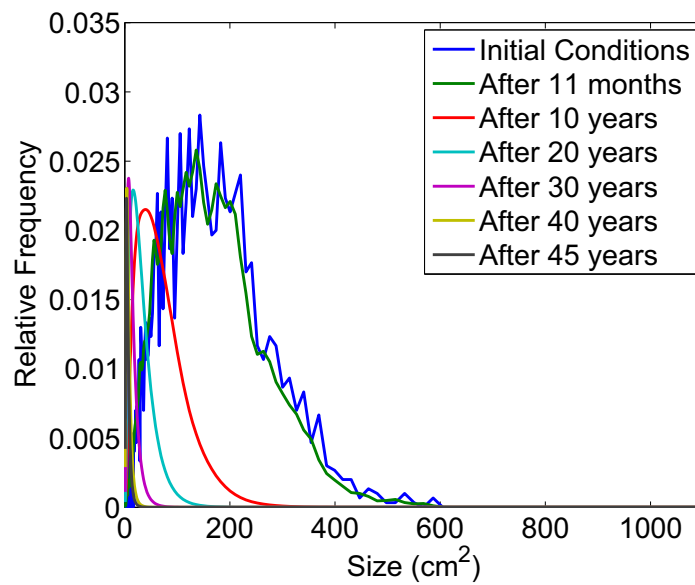
(b) Periodic

Figure 9.5: The size structures of the populations over time for both the clustered and periodic scenarios for A_{Weak}.
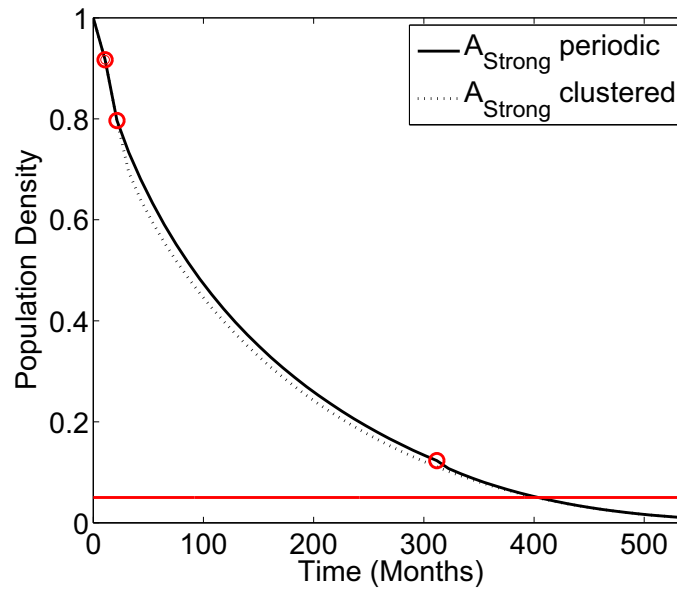
Figure 9.6: The population densities for A_{Strong} comparing the periodic and clustered scenarios, with 2 hurricanes occurring in a 45 years period. The red line shows the critical density and the red circles where a strong hurricane occurred.

A_{Strong} Hurricanes.

For A_{Strong}, the two hurricanes in the clustered scenario are in the first two time steps, whilst for the periodic scenario they are 26 years apart. Theoretically, it was expected that the clustered hurricanes should end with a greater density, as there is a longer period of calm. The current model showed that there is no recovery in the projection period and for A_{Strong} there is no difference in the behaviour, when it comes to assessing extinction time (Figure 9.6). In both cases, this occurred after approximately 34 years, later than the extinction time for A_{Weak} of between 28 and 30 years (Figure 9.6).

The population structures were similar for the periodic and clustered scenario (Figure 9.7). For the periodic case (Figure 9.7 (b)) there are slightly larger patches at each comparable time than the clustered case (Figure 9.7 (a)). Again, as with A_{Weak}, the population is dominated by a decrease in patch sizes. After 30 years, both populations consist only of patches smaller than $50cm^2$.
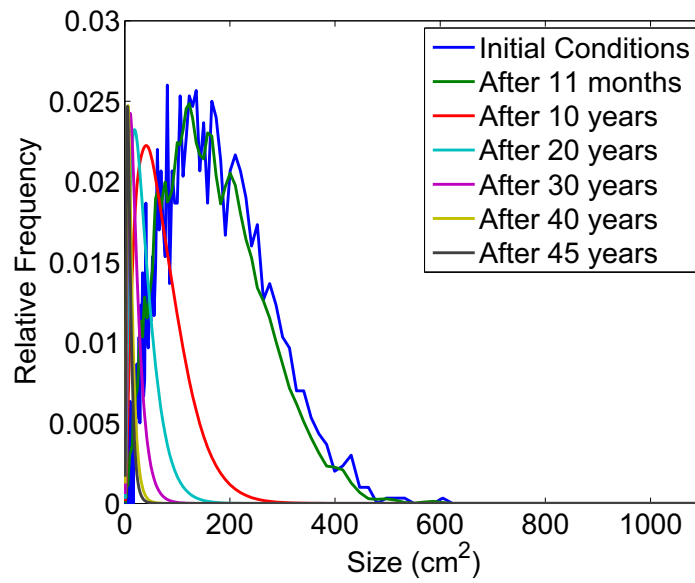
(a) Clustered
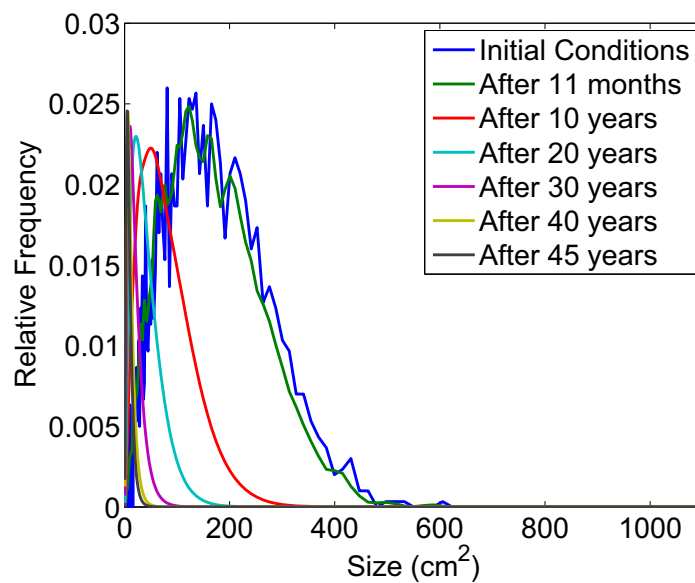
(b) Periodic

Figure 9.7: The size structures for A_{Strong} over time for (a) the clustered scenario (b) the periodic scenario.
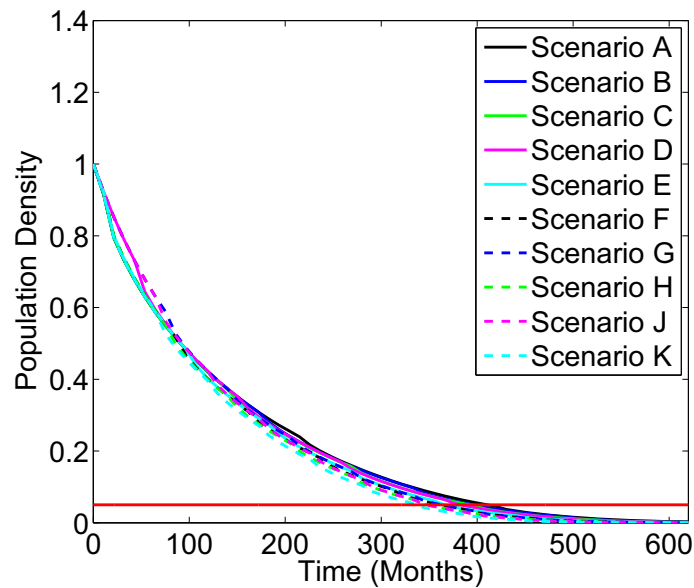
Figure 9.8: Scenario III: with 12 hurricanes over a 52 year period, the ratio of A_{Strong} to A_{Weak} increased from scenario A to scenario K as defined in Table 9.3

9.3.4 Scenario III: Increased Intensity

As the ratio of A_{Weak} to A_{Strong} decreased, so the extinction time decreased (Figure 9.8). With the current historical rate of hurricanes on Glovers Reef (Scenario A), the extinction time is $t = 419.3$ months. As the ratio increased to Scenario K, the extinction time is $t = 344$ months, a difference of 6.3 years. Scenario A, with the lowest number of A_{Strong}, has the latest extinction time, and scenario K, with the most A_{Strong}, had the shortest extinction time.

9.3.5 Scenario IV: Decreased Return Time of A_{Strong}.

As the return time decreased from 26 years to 6 years the extinction time shortened (Figure 9.9). At best, the extinction time is $t = 408.5$ months for a return time of 26 years to $t = 365.5$ months for 6 years. This is a difference of 4 years as the return time decreased.
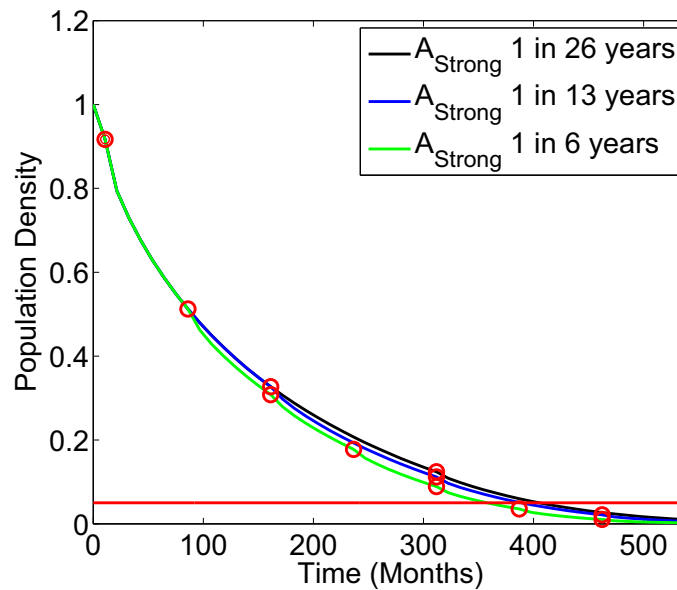
Figure 9.9: Scenario IV: measuring the effect of decreased return time of A_{Strong}. The critical density is shown by the red line and a strong hurricane by a red circle.

9.3.6 Conclusions

Under these four different scenarios the key results are:

1. The model under-estimated population density from data.

2. Recovery between hurricanes is not captured.

3. For A_{Weak}, clustered hurricanes have a lower population density than periodic hurricanes. For A_{Strong} there is no difference in the extinction time between periodic and clustered hurricanes.

4. For both clustered and periodic hurricanes, there is a decrease in the maximum patch size in the population.

5. Increasing the intensity of hurricanes varies the extinction time by up to 6.3 years.

6. Decreasing the return time of A_{Strong} varied the extinction time by up to 4 years.

9.4 Do Extinction Times Change with Management on the Reef?

In the previous section, it was found that no recovery was captured. In Chapter 8, some management strategies were recommended that could increase the population density. The two most effective strategies were:

- **Growth** (GS): Decreasing the probability of fragmentation, alongside increasing the size of patches that do not fragment.

- **Fragments** (FS): Increasing the number of fragments produced and decreasing the size of these fragments.

The numerical approximation of GS was $\mathbf{G}$ and FS was $\mathbf{F}$. These can be applied in the same way as equation (9.2), with the exception that $\mathbf{N}$ is replaced by either $\mathbf{G}$ or $\mathbf{F}$. Therefore, equation (9.2) becomes:

$$\mathbf{X}(10) = \mathbf{G}^3\mathbf{W}\mathbf{G}^3\mathbf{S}\mathbf{G}^2\mathbf{X}(0), \tag{9.5}$$

or

$$\mathbf{X}(10) = \mathbf{F}^3\mathbf{W}\mathbf{F}^3\mathbf{S}\mathbf{F}^2\mathbf{X}(0). \tag{9.6}$$

Each of the scenarios investigated above will be tested, assuming that management had occurred. This is to compare what is projected to occur on the reef, alongside what could occur, if these management strategies were adopted. Recall the scenarios were:

  (I) **Observed Hurricane History**

 (II) **Periodic vs. Clustered**

(III) **Increased Intensity**

(IV) **Decreased Return Time of A$_{\textbf{Strong}}$**

Until now, the metric of population density was used. This is the proportional number of patches remaining compared to the initial population size, at each time step. Alongside this calculation, the minimum total area of the population will be calculated. This analysis was carried out because the population density can be misleading. It does not take into account the structure of the population and because of this, a high population density could consist entirely of very small patches and, therefore have a low total area. The opposite can also occur; a small population density may consist of a few very large patches and, therefore, have a larger total area.

To calculate the minimum total area, a total population of $n = 1000$ was assumed to occur at the start of the projection period. This population was then projected through time under the differing hurricane scenarios, but with the total area calculated at each time step. This was done by taking the 'size class' boundaries calculated during numerical integration. These were then used to calculate the lowest possible total area by multiplying the number of individuals in each 'size class' by the lower bound of the size classes. These were then summed together in order to give the minimum total area on the reef at each time step. The reason this is a minimum is because the lower bound of each size class was used and individuals could lie anywhere within the size classes.

9.4.1 Do Management Models Give a Better Fit to Observed Data?

Both of the managed populations over-estimated the final population density (Figure 9.10), in comparison the unmanaged population under-estimated the population density by 16%. Strategy GS over-estimated the density by 3%, whilst FS over-estimated by 25%. In fact, GS closely mirrored the population density from
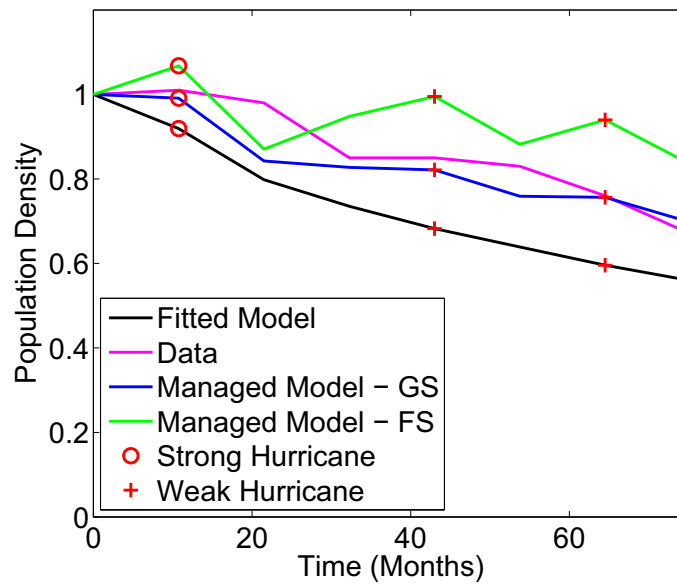
Figure 9.10: A comparison of the population density from the data to the model, assuming that either the fragment or growth management strategies have occurred.

data, which suggests that this is the best fit to the data. A large difference between the models was observed when Hurricane Mitch damaged the reef. This was because the data was affected for two time steps, but the model only one.

The coral patch structure in January 2003 was dominated by small patches, with patch sizes ranging up to $400cm^2$ (Figure 9.11). All models under-estimated the contribution of small patches (under $50cm^2$) to the population and over-estimated the contribution of patches larger than $100cm^2$. The unmanaged model had no patches over $300cm^2$, an under-estimation of maximum size. As larger patches are more likely to survive future disturbances, this could explain the difference in density at the end of the study. FS over-estimated the contribution of patches over $400cm^2$, with all patch sizes still in existence, but is a good fit for coral patches of between 50 and $200cm^2$, closely resembling the data. Finally GS largely over-estimated the proportion of patches between 100 and $600cm^2$, but limited patches to be under $600cm^2$. It is this slight over-estimation, which could account for the slight over-estimation of final population density. The size structure of the
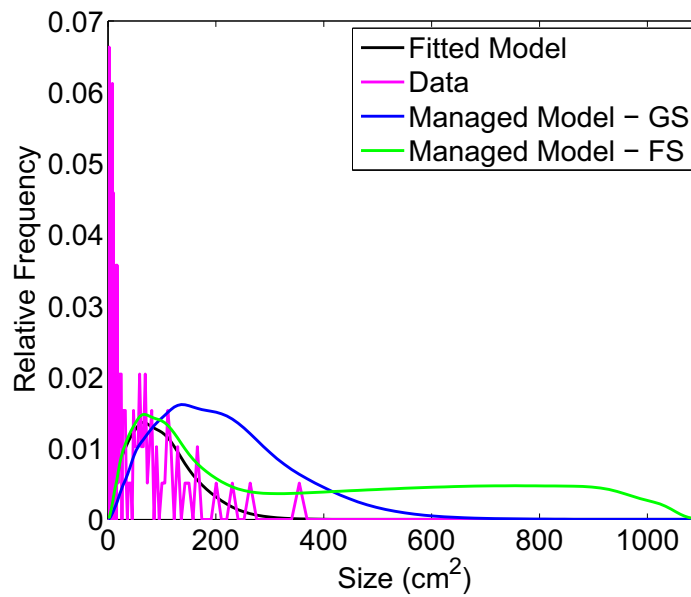
Figure 9.11: The size structures of the populations in January 2003, comparing the unmanaged model, the managed models GS and FS and the population structure observed in the data in January 2003.

unmanaged population showed a closer resemblance to the data than either of the managed populations.

9.4.2   Scenario I: Observed Hurricane History

The results for population density and total area present very different pictures. In terms of population density, strategy GS has a larger density than the unmanaged population for the first 300 months (Figure 9.12 (a)). Under GS, there was a decline after each hurricane, but GS performed better with short recovery periods. The extinction time under GS was 63 months after the unmanaged population. In comparison, FS exploits the transient dynamics better. This strategy results in a higher population density trajectory, ending with 23% of its initial size.

Whilst the population density showed FS always outperformed GS, this was not the case in terms of total area (Figure 9.12 (b)). In fact after 150 months, strategy GS had a larger total area, but a steeper decline between Hurricanes
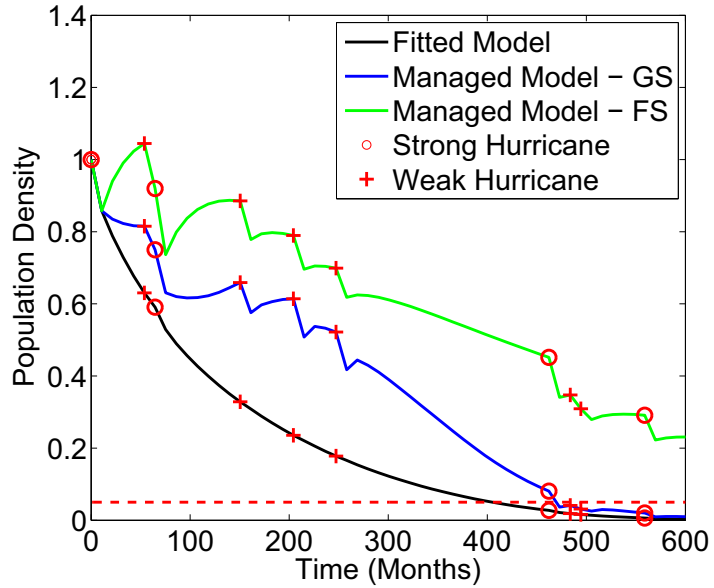
(a) Population Density
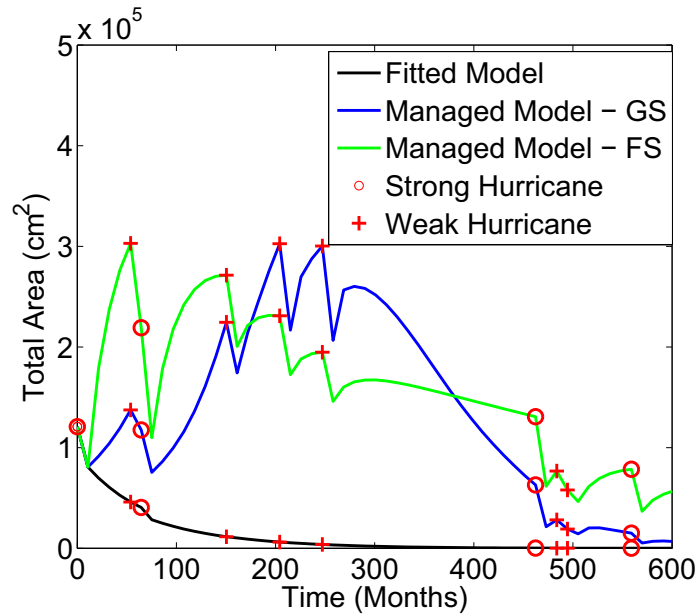
(b) Total Area

Figure 9.12: Observed hurricane history on Glovers Reef over the past 52 years with management strategies assumed to occur replacing A_{No} (a) The population density (b) The total area of the population.

Greta and Mitch resulted in FS finishing with the largest area. The decline for the unmanaged population was greater for total area than population density with a very small area remaining after 250 months. In comparison, FS saw large scale transient growth increasing to over three times its initial size in terms of total area. The same increase was seen in GS later in the projection period. At the end of the projection period, FS had 47% of its initial area remaining, in comparison to GS, which had only 6% and the unmanaged population 0.007%.

9.4.3   Scenario II: Periodic vs. Clustered

A$_{\text{Weak}}$ Hurricanes

In terms of population density and under management by GS, the population faired better at the end of the projection period with clustered hurricanes than periodic hurricanes. This is due to the time between the two groups of hurricanes allowing some recovery to occur (Figure 9.13 (b)). In comparison, in the periodic occurrence of hurricanes there is decline following every hurricane. There were small periods of recovery, but as more hurricanes occurred, there is not enough strength in the model to see the recovery for the entire period (Figure 9.13 (b)). After 5 hurricanes, there is only stasis following a hurricane, rather than the growth observed after the first hurricane.

After the first set of clustered hurricanes, it takes 100 months for the population to recover before growth is then observed (Figure 9.13 (b)), but the growth observed is not enough for the population to return to its initial population density. If a longer period of calm occurred then there may have been further growth. Following the first hurricane in a group of clustered hurricanes, there is a steeper decline than the other 3 hurricanes. This showed that the impact of subsequent hurricanes was smaller. The clustered scenario reached a population density of 0.07 after 45 years, whilst with periodic hurricanes there is an extinction time of $t = 505.3$ months

(42 years), supporting the fact that clustered hurricanes give a better population density for GS.

The managed population FS faired much better than either the unmanaged or GS populations, with the population surviving to 45 years. The periodic scenario resulted in a population density of 0.19 and for the clustered of 0.20 (Figure 9.13 (b)). This showed that neither of the scenarios gave a substantially better population density than the other. The clustered scenario was dominated by a sharp decline following the first hurricane in a group, but this decline continued at a slower rate for each subsequent hurricane. After 4 hurricanes had occurred for both scenarios, the clustered scenario faired slightly better. This was due to a growth in population density during periods of calm. The transient growth began to fall away before the second group of hurricanes struck the reef. This showed that, at the point when there were an equal number of hurricanes, the clustering scenario tended to fair slightly better.

In relation to total coral area, the management strategy GS was always smaller than strategy FS (Figure 9.13 (a)). For an initial population size of $n = 1000$, the total area after 100 months was larger for GS than FS in the periodic scenario. In fact the periodic scenarios for both GS and FS had a similar maximum area of 316780 and 318140 cm^2 respectively. These are achieved at different times with FS achieving this maximum area at $t = 53.75$ months and GS at $t = 182.75$ months. This showed that, although GS may have contained fewer patches, these patches were larger in area. After 300 months, strategy FS contained a larger area of coral tissue than GS because the population lost more area and patches at this point.

The clustered population for GS showed a sharp decline during both groups of hurricanes in both density and area (Figure 9.13 (a)). In the recovery period after the first clustering, the total area recovered to $259000 cm^2$ compared to the initial size of $123640 cm^2$. This was due to the growth of individual patches, rather than an increase in patch numbers. The clustering of hurricanes under FS showed
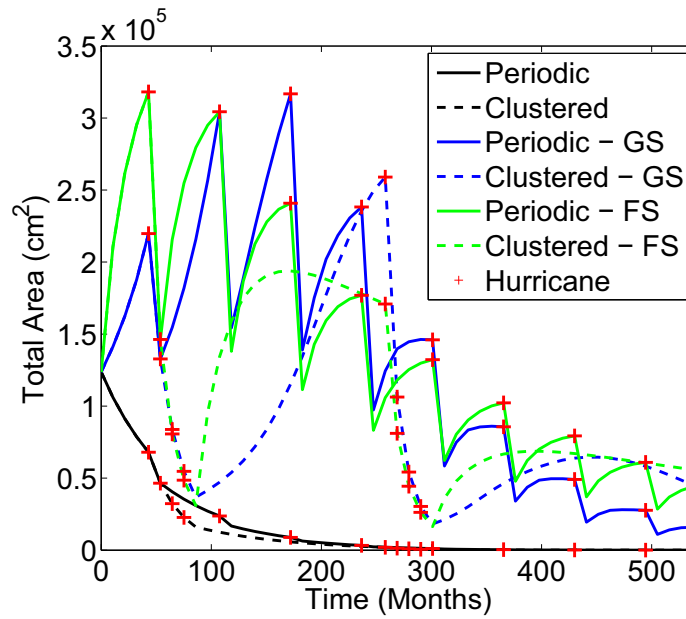
(a) Total Area
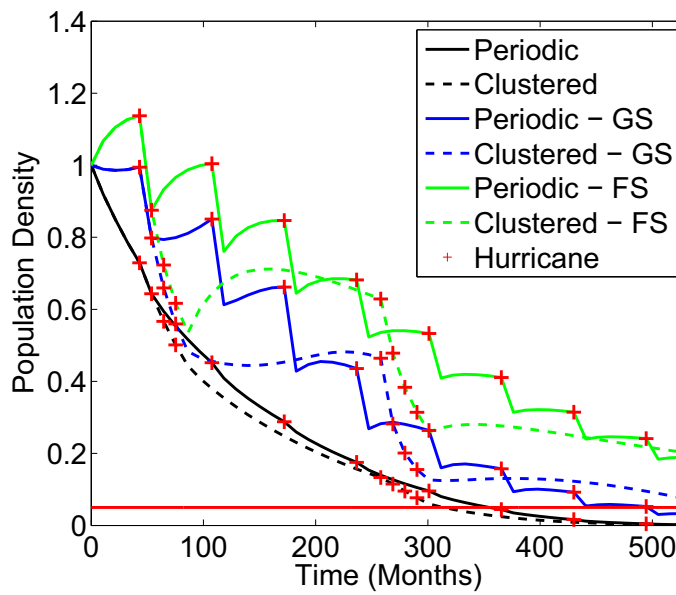
(b) Population Density

Figure 9.13: Scenario II: The population densities of clustered and periodic hurricane occurrences for A_{Weak} under management strategies GS and FS. The red line shows the critical population density and red crosses a strong hurricane.

similar recovery to GS, but the transient growth initially observed in the total area was curtailed before the second group of hurricanes, this is not the case for GS.

Using the population density measure, FS performed better than GS, but in terms of total area both clustering scenarios performed better than either periodic scenario. For GS, the final area in the clustering scenario was 36% of the initial area, but this was outperformed by the FS strategy by a further 9% remaining. The periodic scenario under FS performed much better than GS, with a final area of 36% its initial size, compared to 13%.

In terms of population density, the unmanaged population decreased steadily with an extinction time of between 28 and 30 years. However, the total area showed a much sharper decrease in the first 100 months, so that after 200 months there is very little area remaining. In fact, after 45 years for both scenarios under $10cm^2$ of area remained, which was under 0.004% of the original area.

A_{Strong} Hurricanes

The unmanaged population reached the critical population density at $t = 408.5$ months, with little difference observed between clustering and periodic scenarios. For strategy GS, the population density showed transient growth for both the clustered and periodic scenarios (Figure 9.14 (b)). The clustered strategy peaked later and at a lower population density than the periodic case due to the additional hurricane at the beginning of the study. The unmanaged population reached the critical density at $t = 451.5$ months for the clustered scenario and $t = 440.8$ months for the periodic scenario. The management strategy GS increased the extinction time by approximately 40-50 months. After 200 months, the clustered scenario had a larger density than the periodic scenario; this showed the population faired better with two strong hurricanes occurring in succession rather than spread out.

The population structure at the end of the study showed the population was dominated by larger patches under GS (Figure 9.15). This suggested only a few

large patches remained, rather than an abundance of smaller patches. Although it is better for future disturbances that large patches exist, it is also necessary for there to be a range of patch sizes.

Under strategy FS, the population ended at a population density of 0.43 for the periodic scenario and 0.46 for the clustered scenario (Figure 9.14 (b)). This showed a good level of patch survival under this management strategy. The population density for the periodic scenario is slightly higher than the clustered scenario in the period prior to the second hurricane, at which the population density dropped below the clustered scenario and remained there. The population structure (Figure 9.15) showed a full range of patch sizes, both large and small. This placed the population in a good position to survive future disturbances. The structure is the same for both the clustered and periodic scenarios.

If the population started with 1000 individuals, the total area at the beginning of the projection was $120950cm^2$ (Figure 9.14 (a)). This was the maximum area achieved by the unmanaged population for both scenarios. The decline was steep for the first 50 months and then levelled off when the area was already low. At the end of the projection period, the area for both clustered and periodic scenarios was $54cm^2$, this was 0.04% of the initial population area, although low this is higher than in the case of A_{Weak}.

Under the measure of population density, management strategy FS outperformed strategy GS for both scenarios for the entire projection period. However, with regard to the total area, strategy GS had a larger area between 100 and 300 months. This showed that, although there were fewer patches in GS (Figure 9.14 (b)), these patches were larger and summed to a larger total area (Figure 9.14 (a)). After 300 months, the higher patch numbers in FS summed to a larger area than GS. The sharp decline in patch numbers after 200 months in GS was mirrored in the decline of total area. The extinction time for GS was only slightly larger than the unmanaged population, but the final total area was between 108% and 116%
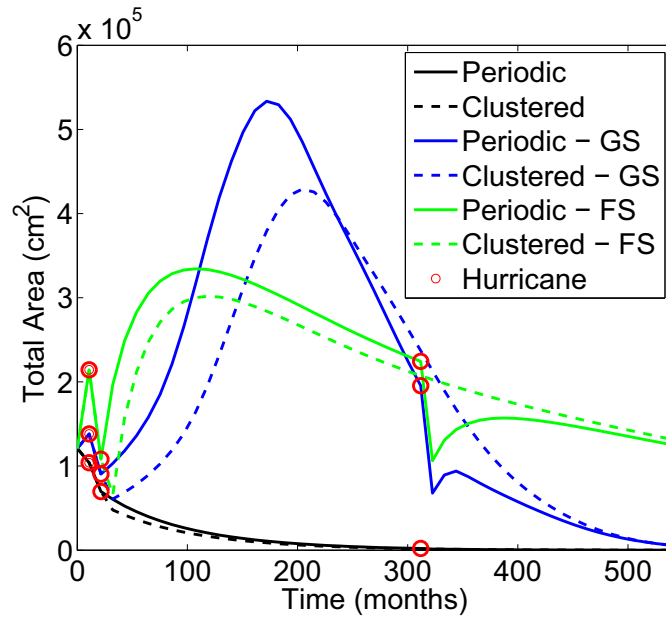
(a) Total Area
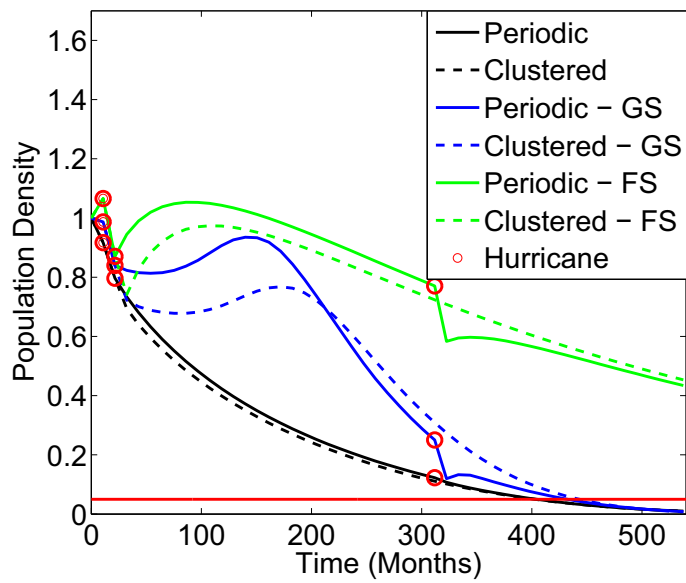
(b) Population Density

Figure 9.14: Scenario II: Periodic vs. clustering of A_{Strong}. (a) The minimum total area (b) The population density.
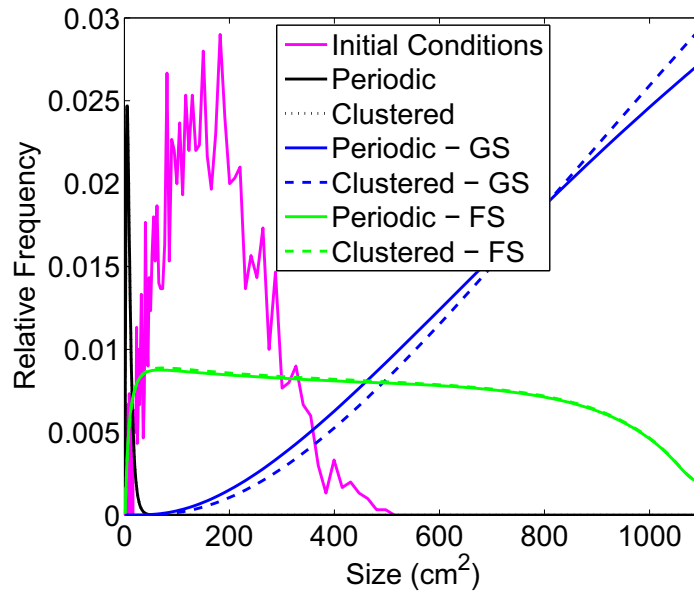
Figure 9.15: The size structures of the populations at the end of the period studied for the clustered and periodic scenarios under management of A_{Strong}, shown alongside the log-normal initial conditions.

higher. For strategy FS, 43% of the population density remained in the periodic scenario, but this lead to an increase in total area of 4%. This demonstrated that, although patch numbers were in decline, the total coral area was in growth. The total area increase was higher in the clustered scenario by 9% in area, but had a decline of 64% in population density (Figure 9.14 (b)). In fact, under FS neither scenario ever fell below the initial total area, due to the transient growth observed at the beginning of the projection period.

9.4.4   Scenario III: Increased Intensity

Ten different hurricane intensity scenarios were suggested, which increased the ratio of A_{Strong} to A_{Weak} (See Table 9.3). In an unmanaged population, the extinction time was longest with lowest intensity and shortened slightly as intensity increased, from 35 years to 28.7 years.

Under management strategy GS, all scenarios A to K reached the critical density

Scenario	Extinction Time Unmanaged	Extinction Time GS	Population Density FS	Area Remaining GS	Area Remaining FS
A	419.3	516	0.23	0.20	0.53
B	397.8	505.3	0.20	0.12	0.35
C	397.8	516	0.18	0.08	0.24
D	387	483.8	0.19	0.20	0.53
E	376.3	526.8	0.16	0.09	0.19
F	365.5	494.5	0.15	0.22	0.39
G	365.5	473	0.12	0.08	0.53
H	354.8	537.5	0.12	0.10	0.18
J	354.8	505.3	0.10	0.14	0.29
K	344	505.3	0.09	0.16	0.27

Table 9.4: Extinction times, population densities and proportion of area remaining for the ten different scenarios of increased hurricane intensity. The worst scenario is highlighted in red, and the best in green.

of 0.05 within the 45 year projection period. Unusually, the extinction times did not decrease in order of increasing intensity (Figure 9.16 (a) and Table 9.4). On average, GS increased the extinction time by 11.25 years, with the range of increases of extinction time between 8.05 and 13.4 years. The worst scenario of GS was strategy G - three A_{Strong} for every A_{Weak}, whilst the best was strategy H - five A_{Strong} for every A_{Weak} (Figure 9.16 (a) and Table 9.4). This was an unexpected result as intuitively fewer strong hurricanes should be better for a population. Strategies J and K had the same extinction time as strategy B, again unusual as B had two A_{Weak} for every A_{Strong} and K purely had A_{Strong}.

In terms of total area, the lowest remaining area was 8% for strategies C and G (Table 9.4). This confirmed the population density result, where G had the shortest extinction time. The low population density did not always tally with lowest total area. Strategies F and D had the greatest remaining area (22% and 20% respectively), but were the 2nd and 3rd shortest extinction times. Therefore, although there were fewer patches, these patches had a larger area. Strategies E and H had the two longest extinction times, but were amongst the lowest in total
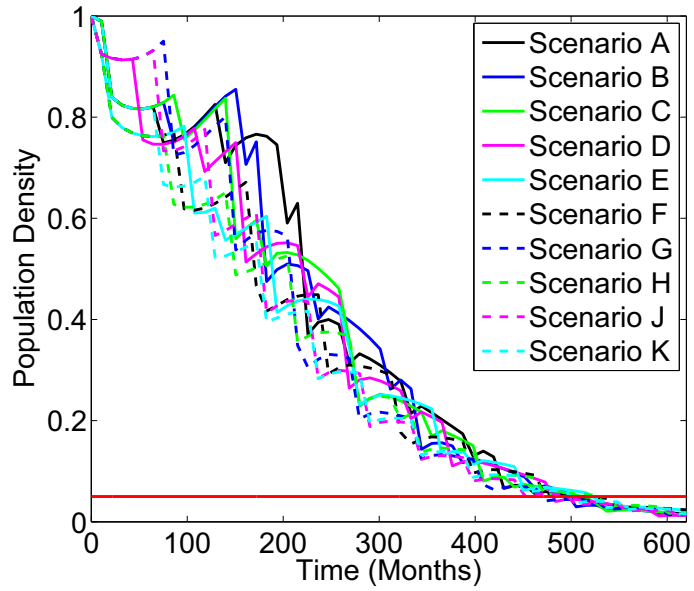
(a) Strategy GS
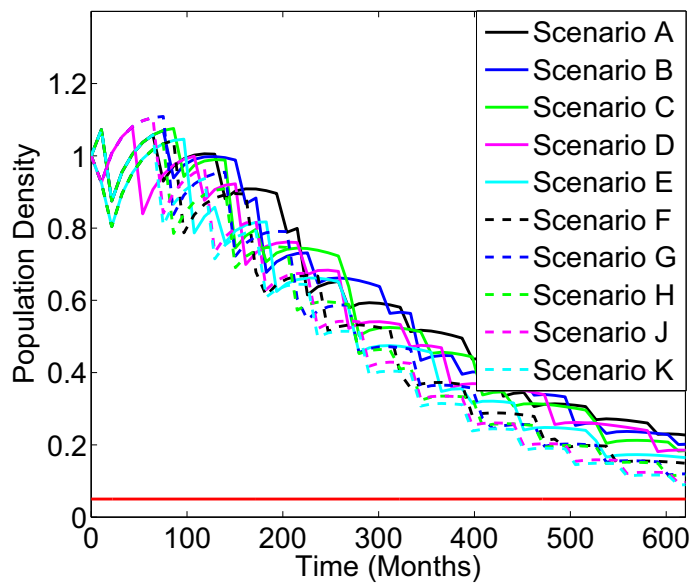
(b) Strategy FS

Figure 9.16: Scenario III: Increased intensity. The number of hurricanes are held at 12 in 52 years, the intensity of hurricanes increased as strategies go from A to K. (a) for strategy GS (b) for strategy FS

area remaining, indicating these strategies were dominated by small patches.

Under FS, the critical density of 0.05 is not reached in the 45 years of the projection period (Figure 9.16 (b)). The pattern of population density for the 10 strategies was the same as in the unmanaged population, where strategy A (lowest intensity) finished with the highest population density (0.23) and strategy K (highest intensity) ended with the smallest population density (0.09). This showed that under FS, the population density will decrease with growing intensity. There was an overall decrease in population density of 61% from strategy A to strategy K. Transient growth is shown by some strategies, and up to 200 months into the projection the population can be larger than the initial size, depending on which scenario is observed.

In terms of total area, the best strategies were A, D and G, which resulted in a remaining area of 53% (Table 9.4). The worst strategy was H, with a remaining area of 18%. Strategies A and D were also good strategies for GS and whilst H was bad. Where G was one of the worst strategies for GS, it is one of the best for FS.

In comparing the possible minimum and maximum trajectories of population density (Figure 9.17), patches under FS survived better than GS and the unmanaged population. The upper limit of GS, in terms of population density for the first 200 months, lay above the lower limit of FS, this showed it was possible for the population density in GS to be higher than FS under different intensities. What is clear is that any form of management (either FS or GS) resulted in higher population densities for the entire 45 year period, compared to the unmanaged population. In terms of total area, the upper limit for GS was higher than FS between 100 and 400 months. Although there are fewer patches, these patches were larger than in FS. For GS, there was a greater variety in possible total area than FS, showing a greater impact on the total area of the population with increased intensity. At best, a population could be four times the initial area in GS, whilst in FS it can be over three times its initial size. The unmanaged population became dominated
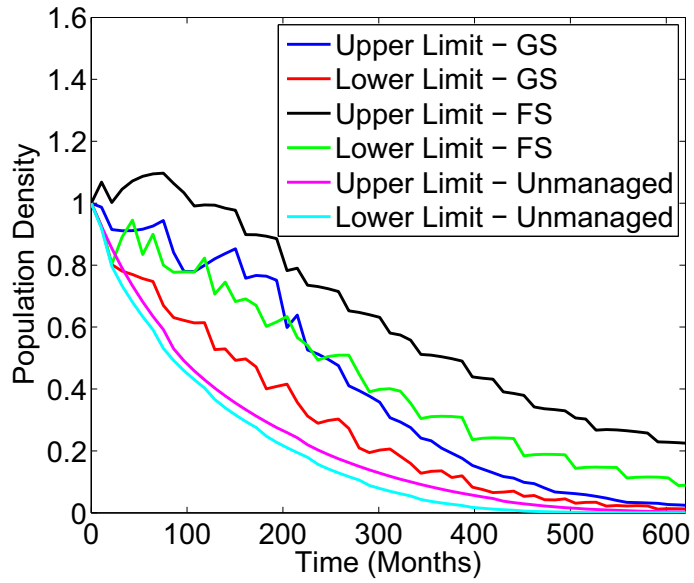
(a) Population Density
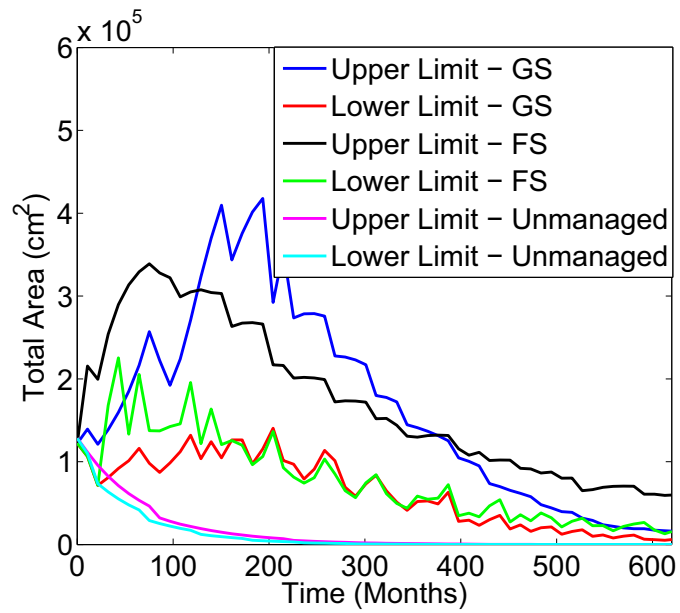
(b) Total Area

Figure 9.17: The upper and lower bounds of the population densities for strategy III for the unmanaged population and the managed populations FS and GS.

by smaller patches and, after 200 months, only a small area remained on the reef, in spite of patches remaining for a further 200 months.

9.4.5 Scenario IV: Decreasing Return Time of A$_{\text{Strong}}$

Management of Fragments

By managing fragments, the coral patch population will no longer reach the critical density in 45 years with a decreased return time of A$_{\text{Strong}}$ (Figure 9.18 (b)). Instead of becoming extinct at $t = 365.5$ months for a return time of 6 years, a population density remained of 0.23. With the current return time and under FS, a density of 0.43 remained, this showed a decrease in population density of 47% for the decreased return time in comparison to current rates. Even with the shortest return times, the population density will increase following each hurricane, but the size of this increase will decline after each subsequent hurricane.

The picture from total area is similar to that shown by population density (Figure 9.18). With $RT = 26$ years there was a higher total area than that of $RT = 6$. It differed in that, under FS, $RT = 26$ years saw an increase in area of 105% at the end of the projection period. Even with a decreased return time to $RT = 6$ years, over half of the total area still remained. The decline following a hurricane was clearer in total area, compared to that in population density. This was from the reduced population density, but also from partial mortality reducing the area of patches that were not killed by the hurricane. This partial mortality is not captured in the population density.

Management of Growth

Management of growth caused an unusual result; there was a longer extinction time for a $RT = 6$ years than there was for $RT = 26$ years. The extinction time was $t = 473$ months, compared to $t = 430$ months. However, for the first 300 months,
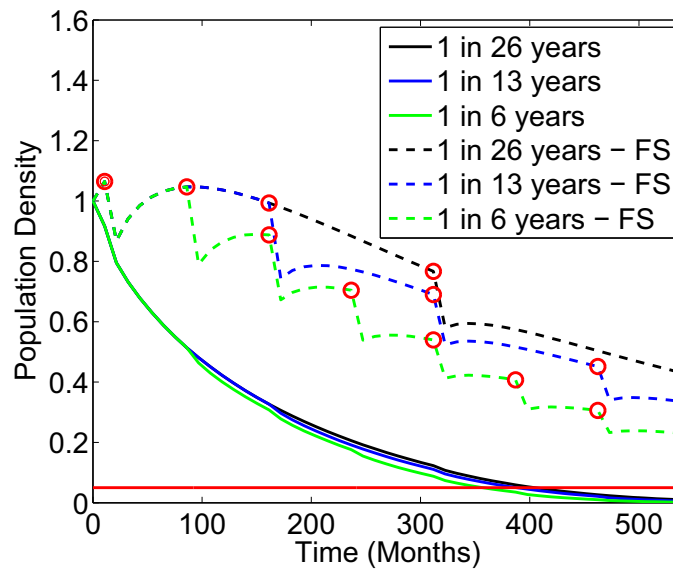
(a) Population Density
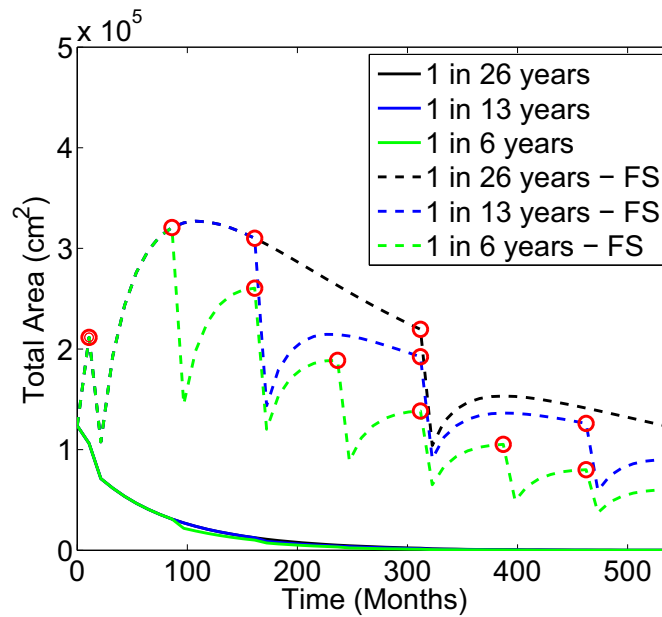
(b) Total Area

Figure 9.18: Scenario IV: The effect of decreasing the Return Time of A_{Strong} under strategy FS. (a) The population density compared to the unmanaged population. The solid red line is the critical population density, and the red circles where a strong hurricane occurred. (b) The total area compared to the unmanaged population.

$RT = 26$ years outperformed that of 6 years. The same pattern was observed in terms of total area, where $RT = 26$ years reached the highest total area at about 200 months before declining in size (Figure 9.19 (b)). At the end of the study for $RT = 6$, there was a remaining area of 16% compared to 5% for $RT = 26$ years. This showed that a management strategy of growth required a regular disturbance, in order to perturb the population away from being dominated by a few large patches. This strategy reduces the possibility of producing new patches, and this could explain the behaviour.

9.4.6   Conclusions

The use of management strategies, when calculating the extinction times, lead to the following conclusions:

1. Management of growth most closely resembles the observed data.

2. Strategy GS performed well when there were small return times, but FS performed better when return times were longer.

3. The total area measure painted a different picture to population density, highlighting when populations were dominated by a few large patches, or by a large number of small patches, as well as taking into account partial mortality of patches.

4. Strategy GS often performed better during the projection period in terms of total area, with FS performing better in terms of population density.

5. Clustered A_{Weak} hurricanes had a larger area remaining for all management strategies than a periodic scenario.

6. Periodic hurricanes of A_{Weak} have a later extinction time than clustered hurricanes.
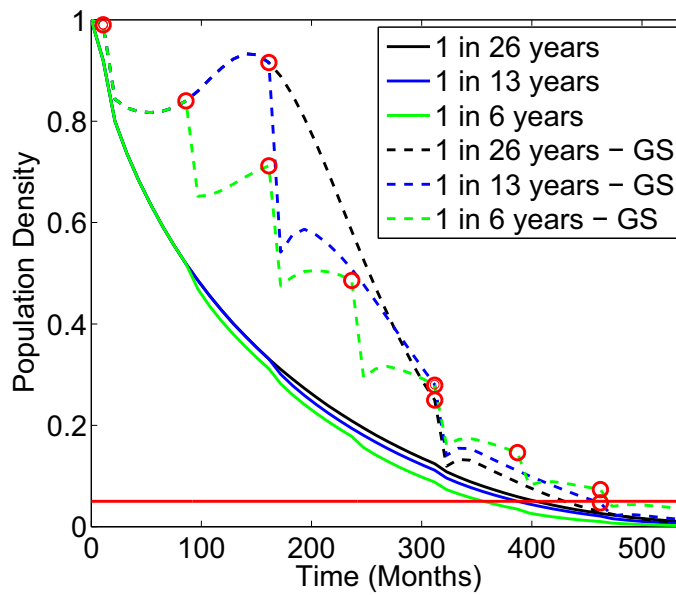
(a) Population Density
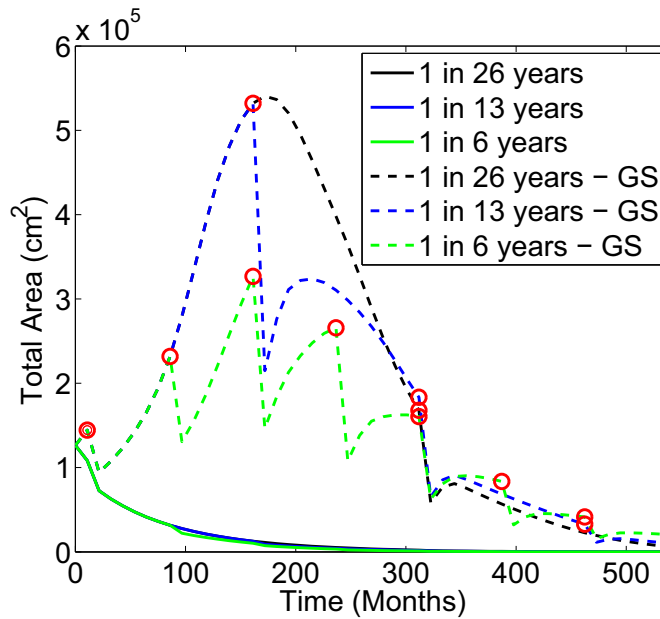
(b) Total Area

Figure 9.19: Scenario IV: The effect of decreasing the Return Time of A_{Strong} under strategy GS. (a) The population density compared to the unmanaged population. The solid red line is the critical population density, and the red circles where a strong hurricane occurred. (b) The total area compared to the unmanaged population.

7. For both periodic and clustered, strategy FS performed better than GS for A_{Weak}.

8. Strategy FS was a better management strategy for A_{Strong}, regardless of clustering or periodicity. It had a larger population density and greater total area at the end of the projection period.

9. With increased intensity under GS, the critical density will occur within 45 years.

10. With management strategy GS, the population density for three A_{Strong} hurricanes for every A_{Weak} hurricane had the shortest extinction time, but five A_{Strong} hurricanes for every A_{Weak} had the longest extinction time.

11. For management strategy GS, the total area measure showed two A_{Strong} hurricanes for every A_{Weak} had the largest remaining area, with either three or 0.7 A_{Strong} for every A_{Weak} giving the smallest remaining area.

12. With increased intensity under strategy FS, the final population density will decrease in order of increasing intensity from 23% of patches remaining at best to 9% at worst.

13. In terms of total area and under management strategy FS, it is best for either one A_{Strong} for every 3 A_{Weak}, an equal amount of A_{Weak} and A_{Strong} or three A_{Strong} for every A_{Weak} to give the largest remaining area of 53%. The worst case was when there was five A_{Strong} for every A_{Weak} with a remaining area of 18%.

14. Decreasing the return time of A_{Strong} under FS will reduce the population density and total area.

15. The decline following a hurricane was larger if the total area at the time of the hurricane was larger.

9.5 Conclusions

This chapter has investigated the resulting dynamics when the three IPMs parameterized in Chapter 7 are interweaved. It has shown that, under current forecasts of climate change, *M. annularis* populations will decrease in size and area. This chapter has also investigated the effect of management on these projections. In particular taking strategies from Chapter 8 and applying them. It was shown that under management of growth, a regular occurrence of strong hurricanes was required to help the growth of the population, whilst management of fragments required longer periods of recovery.

Finally, this chapter has shown that the regular measure of population density is not sufficient to fully predict behaviour on the reef as it does not take into account partial mortality after a hurricane, or the size of the patches in the population. It was shown that, in terms of minimum total area, the picture painted was often different to the picture painted by population density.

Chapter 10

Discussion of Results

10.1 Introduction

In Part III of this Thesis, Research Questions 7 to 10 were answered (Figure 1.4). In particular the aim of this part was to, firstly, understand the possible methods of management and, secondly, to investigate the effect of climate change on extinction times. This chapter will discuss the results of Chapters 7, 8 and 9 and is broken down into six sections. Section 10.2 answers the question of what is the best management strategies for *M. annularis* and discusses how these theoretical strategies could be achieved. Section 10.3 investigates OBJ 3: Climate Change (Figure 1.4). It will discuss the results from Chapter 9 and their consequences. This chapter will then discuss the modelling issues that arose in this part of the Thesis (Section 10.4), before going on to discuss how the results presented here are consistent with previous research (Section 10.5). It will then briefly discuss why these results are important (Section 10.6), before finally suggesting areas for further research (Section 10.7).

10.2 What is the Best Management Strategies for a *Montastraea annularis* Population?

In Chapter 8, it was shown that the best methods to manage a population of *M. annularis* patches was to target two biological functions at the same time. In particular, two strategies were suggested: a **Growth** strategy, by increasing the mean size of a patch and reducing the probability of fragmentation, and a **Fragments** strategy, which increased the number of fragments, whilst reducing the size of these fragments. A population growth rate of 1 was not possible, even when managing two functions concurrently. This indicates the presence of other stresses on the reef. These could be overfishing (Hawkins and Roberts, 2004; Hughes et al., 2003); coral bleaching (Brown, 1997; Muller and D'Elia, 1997); tourism (Nystrom et al., 2006) or increased run off from sedimentation (Koop et al., 2001) to name a few. In fact, understanding the impact of only one of these stresses on a population, like hurricanes, is not enough to understand the behaviour on a reef. It is now thought that the combined effect of these stressors is greater than the sum of the individual stresses, which many populations exhibiting synergy effects. This is where two stresses interact with each other amplifying the effect on the population (Rogers and Laffoley, 2011).

The **Growth** strategy could be achieved through the introduction of a marine reserve to an area. Marine reserves protect limited areas of reefs, in order to reduce human stresses (Bellwood et al., 2004). In particular, they focus on reducing the overfishing exploitation on the reef, in order to increase the density of grazers in the area (McClanahan et al., 2006; Mumby and Harbourne, 2010). In marine reserves, there have been up to double the density of grazers observed than outside the reserve (Mumby et al., 2006a) and this can keep algal levels under control, which reduces stress on coral patches and provides free space for colonization. Other studies have found that over-fishing and the *diadema* die-off have inhibited the

ability of a reef to recover following a hurricane (Hughes and Connell, 1987; Hughes, 1994; Lugo et al., 2000) and has shown that this must be a focus for managers, if coral populations are to bounce back. It has been found that *M. annularis* exhibited recovery inside a marine reserve, but net mortality outside (Mumby and Harbourne, 2010). If a reef experiences a disturbance in an already degraded state, then the reef can exhibit a phase change away from being coral dominated to being algal dominated (Mumby et al., 2006b).

It has been suggested that coral reefs can follow a hysteresis effect when the grazing on a reef is reduced (Mumby et al., 2007). Grazing levels need to be much higher than historical levels to recover to a pre-disturbance state, if there is already degradation on the reef (Mumby et al., 2006b). When the level of grazing on a reef is reduced, it places the population at greater risk of degradation following a disturbance. For example, in Figure 10.1, if a population undergoes a disturbance, the result is dependent on the level of grazing. If a reef has a high level of grazing, then it will bounce back from the coral cover loss to a stable equilibrium. However, if there is a reduction in grazers (for example the *Diadema* die-off of 1983) and a disturbance reduces the coral cover to below the dotted line, then the population will shrink to the other stable equilibrium. In this case, the proportion of the reef that is required to be grazed must then be higher than the original amount, in order for it to recover. This shows the importance of maintaining high grazing levels on a reef.

It is also now thought that the impact of climate change on a reef is primarily determined by the extent to which the reef is already in decline (Knowlton, 2001; Hughes et al., 2003). By introducing marine parks onto a reef, the coral patches should be in a healthier state to bounce back.

These marine parks must cover a large enough area, in order to fully benefit the reef. Historically, marine parks and no take zones are on a small scale and their benefits have not been fully felt. It has been suggested that it is important
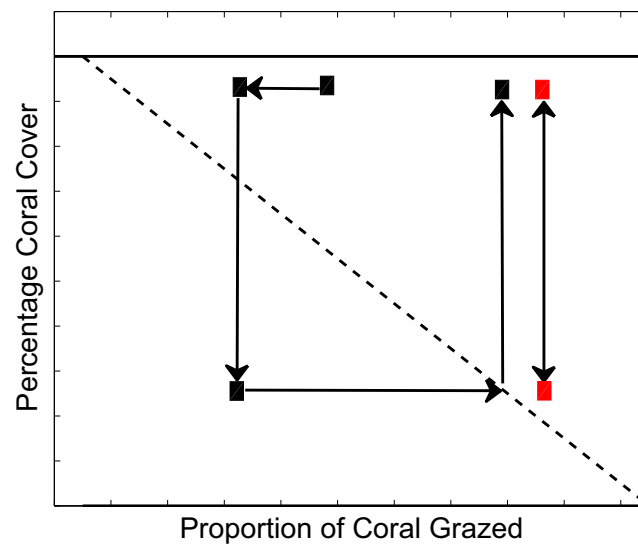
Figure 10.1: The hysteresis effect in relation to grazing and coral cover. The black squares show that if grazing decreased alongside a disturbance reducing coral cover, then a higher proportion of grazing is required for the reef to recover to the initial coral cover. Alternatively, the red square shows the situation where, if grazing levels are high enough, a disturbance reduces coral cover and it can recover without changing the grazing levels. The black solid lines are stable equilibrium and the dotted line an unstable equilibrium.

to begin protecting corals at an entire ecosystem level, if the management is to be effective at reducing the region wide coral cover decline in the Caribbean (Hughes et al., 2003; Pandolfi et al., 2005).

Success of a management strategy should be measured as the recovery of a diverse population structure on the reef (Bellwood et al., 2004). Marine Parks, when effectively managed, are a great way of achieving this. When this is achieved, coral patch populations will also be healthier, as the stress on the reefs will be less, and this will allow the coral patches to recover better following a disturbance.

For the **Fragment** management strategy, it is less obvious how this could be achieved by managers. In fact, the strategy seems counter-intuitive. It has been shown in Chapters 4 and 7 that larger patches survive hurricanes better, but this strategy calls for the creation of more, smaller fragments, when fragmentation does occur. The success of this strategy is seen best under the metric of population density and hence the population growth rate. It increases the number of patches on a reef, but the total area of this reef may shrink. Under this metric, the benefits to the reef are less obvious (see Chapter 9). This strategy provides an alternative method to traditional management of growth, but managers would be well advised to target growth, in order to form a population more robust to future disturbances.

10.3 Hurricanes, Climate Change and Recovery.

10.3.1 How Does a Change in Hurricane Activity Effect the Projections of Population Dynamics?

The effect of subsequent hurricanes is lower when the time of recovery between hurricanes is reduced. In previous research, the effect of Hurricane Gilbert on the USVI was less because Hurricane Allen had struck the reef eight years previously (Woodley, 1989). Instead, Hurricane Gilbert reset the recovery time on the reef.

The results in this Thesis has shown that the loss following a hurricane depended on the time since the last hurricane (Chapter 9). It meant that in a clustering of hurricanes, the loss following each subsequent hurricane was lower. This could be as a result of the first hurricane removing weaker, more vulnerable patches and so, when the next hurricane strikes, the weaker patches do not exist. Instead, the hurricane affects the stronger patches, therefore the loss is lower. However, this loss could be more devastating, as it is damaging the stronger patches. In fact, it is plausible that it is the shrinkage of larger patches that is more damaging than the removal of smaller patches, as it places the population at a greater risk of collapse if another hurricane strikes before recovery is achieved. This is seen in the clustering of hurricanes reducing population density more than periodic hurricanes, where some recovery is seen in the unmanaged population.

Recovery (a return to pre-disturbance density) did not occur in the study. Growth rates of *Montastraea annularis* coral patches are unknown, but colonial growth rates are relatively slow for *M. annularis*, with documented rates between 0.37 and 1.6 cm/year (Foster, 2007). Therefore, recovery time for slow growing coral is probably longer than the monitored period of 5 years. Coral reefs are thought to recover over a much longer period of 10-25 years (Glynn, 1973; Woodley, 1992; Sorokin, 1995; Gardner et al., 2005). Thus this study is painting a bleak picture for the population of coral patches and recovery could be observed outside of the time frame studied.

Severe, Category five hurricanes are rare, with only two such events being recorded in the vicinity of Glovers reef since 1889 (Hurricanes Janet and Mitch in 1955 and 1998 respectively). Coral populations may, therefore, have a number of years in which to recover between acute disturbance events. However, less severe disturbance events occur with greater frequency (current return time on Glovers Reef is 5.12 years (Table 9.2)) and a rise in sea temperatures resulting from global warming is predicted to increase the frequency and magnitude of both

coral bleaching and hurricane events (Elsner, 2006; Elsner et al., 2008; Emanuel, 2005; Goldenberg et al., 2001; Holland and Webster, 2007; Webster et al., 2005). The response of corals observed in this study paints a bleak picture for the future of coral reefs unless either corals are able to adapt to such changes in conditions or local management measures, such as the placement of marine reserves, are able to lessen the immediate and long-term impacts of disturbances.

The ability of a reef to recover from a disturbance will depend, to an extent, on the outcome of interactions between coral and algal patches. Empty space created on ramets, following coral mortality, can be colonized by algal species. They have a competitive advantage over corals, due to their faster growth rate (Mumby et al., 2005). In this study, we did not model coral-algal interactions, but algal patch dynamics on the same coral colonies have been studied in Mumby et al. (2005). Disturbances have been shown to push coral reefs over a 'tipping point' from coral-dominated reefs into algal dominated reefs (Mumby et al., 2007). Once the population passes through this tipping point then greater recovery is needed, for a reef to become coral dominated. This is of particular concern where there are interacting disturbances affecting the reefs, for example coral bleaching and disturbances. Therefore, it is vital to study how to help coral patches bounce back immediately following disturbances to ensure this tipping point is not reached.

Extinction times on the reef are predicted to lie within the next 45 years (Chapter 9). With an increased intensity, but not frequency, of hurricanes it has been shown that this time frame for extinction could reduce by 11 years. It has recently been said that coral reefs could become extinct within this generation (Rogers and Laffoley, 2011) and this study supports this. It is thought that coral reefs will adapt to climate change, rather than become extinct (Hughes et al., 2003). This adaptation could come from a changing structure of species on the reef, with previously abundant reef-building corals are likely to be replaced by branching coral species. This study appears to support this, if the coral patch population of M.

annularis dies off within 45 years as predicted, then the colonial scale die off will follow.

10.3.2 Does Management Alter Population Dynamics as a Result of Climate Change?

It has been shown that if marine parks are effective and a growth management strategy is adopted, then a population requires hurricanes at certain return times to achieve the greatest range of coral patches. It was found that without a disturbance the population is dominated by a few large patches, rather than a larger number of small patches. A weak hurricane in particular will disturb a population and create new patches, which are then in the position to grow between hurricanes. This strategy seems the most likely strategy to have existed in the past. With the growth of coral patches in between hurricanes, followed by a perturbation of size structure at regular intervals. With climate change, this will change how this structure works.

Increasing the intensity of hurricanes with climate change ultimately decreased the time to extinction, even when there was management on the reef. This showed that if recovery can be forced on a reef, through the use of marine parks, that hurricanes would still result in the extinction of patches of *M. annularis* on a reef.

10.4 Modelling Issues

The IPMs do not include the hurricane stress as a factor so that projections in Chapter 9 could be calculated. Therefore, the more traditional method of creating three projection models to compare was adopted (Hughes, 1984). The alternative method of including it as a factor (Dahlgren and Ehrlen, 2009; Childs et al., 2003, 2004) would not allow independent projection, but would instead include hurricane

occurrence as a random factor.

There is an additional issue of balancing the number of size classes with the computational cost of numerical integration. In order to do this, the metric of population growth rate was used. This selected both the integration boundaries and the number of mesh points. Even with a declining population, it is important to ensure that the integration boundary was large enough to include all possible behaviour. However, this is still only a numerical estimate of the behaviour.

There was a lack of recovery captured in the data and this effected the prediction of extinction time of the population. This is shown by the population growth rate of the no-hurricane transitions being lower than for a weak hurricane. This limitation was solved by introducing possible management strategies on the population. For example, by introducing increased growth on the population introduced the idea of what could occur on the population when the stress on a population was reduced.

The Glovers Reef data set from June 1998 to January 2003 captured the dynamics of coral patches under the presence of three hurricane disturbances. There were no other types of disturbances on the reef at this time. However, the mass coral bleaching event of 1998 was not captured explicitly in these models, but coral patches were under stress at the start of this data set. It is known that, at a colonial scale, many colonies experienced partial mortality following the mass bleaching event (Mumby et al., 2005), but the effect at a patch scale is unknown. This could account for the lack of recovery observed on the reef, which hindered the ability of the models to capture recovery between hurricane disturbances.

It was shown in Chapter 9, that coral patch populations will become extinct in the next 45 years, even if there is some management of growth on the reef. Therefore, the population is in a situation that, under the threat of hurricanes alone, the population will become extinct, particularly with climate change. This model does not account for the additional, more direct impacts of climate change on coral reefs. The increase in coral bleaching in the models of hurricane scenarios

and the impact that it could have on the coral population is not accounted for. It is also thought that there will be an increase in acidification on reefs, which could decrease the strength of coral to withstand disturbances (IPCC, 2007).

The measure of population density and population growth rate can often mislead the results of the population. This is because it does not take into account the structure of the population or for partial mortality of patches following a hurricane disturbance. This lead to a misleading benefit for the fragments strategy that was dominated by a large number of small patches, whilst the growth strategy was dominated by a few patches of large area. This meant that the measure of total area was introduced in Chapter 9, in order to fully understand the dynamics on the reef.

10.5 Are the Results Consistent with Previous Research?

It has been observed in other studies that subsequent hurricanes will have a smaller effect on a coral population than the initial hurricane (Gardner et al., 2005) and that this decline is larger when there has been a longer period of senescence preceding a hurricane, the results of this study support this. The decline following Hurricanes Keith and Iris was smaller than Hurricane Mitch, this was in part because Hurricane Mitch was a stronger Category 5 hurricane but the Hurricane Index for Hurricane Keith was on a similar level to that from Hurricane Mitch (Chapter 1). The presence of Hurricane Mitch reduced the cover loss after Hurricanes Keith and Iris than would otherwise have been expected. This could also give some reason as to why A_{Weak} had a higher growth rate than A_{No}.

In disagreement with the above theory, these results have shown that there is the possibility of short term growth following a hurricane. This depends on the

initial conditions on a reef and show that it is not only the strength of the hurricane which is important, but also the structure of the reef, which affects its ability to grow immediately following a hurricane.

Many studies have been carried out on single site populations and this study adds to this body of knowledge (for example Woodley et al. (1981; 1989) and Bythell et al. (1993)). It is important that these studies are added to, so that a wider understanding of the change in coral cover following a hurricane can be understood. Few studies go on to forecast future dynamics (See Hughes *et al.* (1984) as an exception), it is this that is the unique part of the study. It not only quantifies the decline following a hurricane, but also showed that this decline will continue in the longer term. These results also add to the body of knowledge of the effect of two or more hurricanes on a single site, for example (Woodley et al., 1981; Woodley, 1989) monitored the effect of hurricanes Allen and Gilbert on the USVI reefs. They found a similar picture, in that the second hurricane did not have the same level of decline, but instead reset the time at which recovery could begin.

There should be urgency in the study of coral reefs after hurricanes and other effects from climate change, as it has recently been stated that ecosystems like coral reefs could be lost within the next generation (Rogers and Laffoley, 2011). The projections of the populations in these studies does not contradict this, but instead increases confidence in these results, with all coral populations in this study projected to become extinct within 45 years.

10.6 Why are These Results Important and Novel?

The results from Part III of this Thesis are important as an Integral Projection Model is fitted to a coral patch population. The issues that surround the fitting of these models were discussed (Section 10.4). The method was adapted to allow for fragmentation, with different methods for modelling this biological process

discussed in Part I.

This Thesis is novel as it suggests how models can help in the understanding of the indirect impact of climate change on coral reefs. It investigates how the increasing intensity of hurricanes could effect the extinction time on the reef, not only in terms of population density, but also in terms of minimum total area. It has been shown that there can be a marked difference between the results from population density and the results from total area. This was particularly the case when management of coral patches was introduced into the model. This Thesis has, therefore, highlighted the importance of selecting the correct metric when comparing results.

10.7 Further Study

Further research is required to understand the synergistic effect of climate change on the reefs. This study has aimed to understand the impact of increased hurricane activity on the reef. It is important that future studies aim at understanding what would happen under a more realistic scenario of decreased strength of reefs to withstand disturbances; increased coral bleaching events and an increase in hurricane activity. Future study should also aim to understand the impact of climate change on coral reefs by a combination of these effects. It is also important that research takes into account the changing structure on the reef and the changing dominance from reef-building corals to branching corals.

10.8 Conclusions

In conclusion, Part III of this Thesis has investigated Research Questions 7 to 10 by parameterizing three IPMs. These IPMs were then used to investigate management and the impact of climate change on the population.

Part IV

Conclusions

Chapter 11

Conclusions

11.1 Introduction

The aim of this Thesis was to investigate the effect of hurricane activity on the dynamics of the reef-building coral *Montastraea annularis* (Chapter 1). To do this, a data set from Glovers Reef was used to understand the dynamics following Hurricanes Mitch, Keith and Iris between June 1998 and January 2003. To fully investigate this aim, the Thesis was divided into three main sections: to understand the modelling techniques required to use projection models; to understand and develop methods of analysis and then to understand what could occur under climate change. In this chapter, the main findings will be summarized by answering each of the ten research questions asked in Figure 1.4, whilst then summarizing the contribution this Thesis has made and suggest areas for future research.

11.2   Summary of Main Findings

11.2.1   Research Objective One: Modelling

RQ1: What are the current techniques used to apply projection models to coral populations?

The majority of previous studies into the response of coral populations to hurricanes used the coral percentage metric to describe the dynamics of the population through the study. The drawbacks of these models were discussed in Chapter 2, in particular they do not attempt to understand the underlying dynamics of the observed behaviour and are useless in projecting future dynamics on the reef. Some studies were found to use Population Projection Matrices for coral populations in order to understand the transitions on individual members of the population, and to use these PPMs to project the future dynamics on a population.

It was found that the selection of size classes in these models was arbitrary and can skew the results. It was decided to use the PPM to model the *M. annularis* population on Glovers Reef, but to ensure that the sizes classes are selected using the van der Meer and Moloney algorithms, in order to reduce modelling errors (See Chapters 3 and 4).

Finally the Integral Projection Model (IPM) was discussed as a possible method for modelling coral populations. Although no coral populations have previously been modelled by this method (see Chapter 2), they are ideally suited to modelling populations described by size. It was decided that these were an ideal fit for coral populations like *M. annularis* and were modelled in this manner in Chapters 5 and 7.

RQ2: How can *Montastraea annularis* be modelled by projection models?

Population Projection Matrices have been used to model *M. annularis* at a colonial scale (for example Hughes and Tanner (2000)), but never at a patch size scale. The methods for modelling the population were felt to be transferable, but with some differences in modelling biological processes. For example, no sexual reproduction or recruitment occur at the patch scale (Szmant, 1991), but instead fragmentation creates new patches in these models. Similar methods to Renken *et al.* (2010) were used to capture fragmentation and that an adapted Lefkovitch matrix was to be used (Lefkovitch, 1965). This was because modelling *M. annularis* required the inclusion of shrinkage and fragmentation entries in all upper triangular entries in the matrix, which are not found in the Lefkovitch matrix.

It was concluded that the IPM structure from plant populations were transferable to modelling *M. annularis*, but instead of the kernel consisting of the survival-growth and fecundity contributions to the population, the fecundity contribution is replaced by the contribution of fragmentation (Chapter 3). To model *M. annularis*, five different forms of the fragmentation functions were tested to find the best fit to the data (see Section 3.2.3). This was the first attempt to model fragmentation and further research is required to fully understand the biological processes at a patch scale, if further accuracy in the model is to be achieved.

RQ3: What modelling issues arise from applying projection models to *Montastraea annularis*?

Patches of *M. annularis* are best modelled by size, and the Population Projection Matrix method required the discretization of sizes to form size classes. The boundaries created were artificial and some within size class information was lost. It was shown in Chapter 4 that shrinkage of patches was captured, but growth of patches was often missed, due to the scale of these processes. These problems were solved

by the IPM (Chapters 5 and 7), where size was not discretized and growth was better captured.

Some PPMs produced in Chapter 4 were reducible and non-ergodic. This is a common problem in PPM modelling and is caused either by the inaccurate selection of size classes or by transitions not being captured in the data set. In this Thesis, the main issue is from missing transitions from the data set. The IPM solved this problem by not requiring discretization and by using statistical curve fitting so that missing transitions are smoothed out.

Modelling by the IPM solved many of the issues arising from the PPM, but had its own challenges. These issues were mainly surrounding the numerical integration of the kernel. However, as mesh points were chosen after the fitting of the model to data, the issues of discretization are not as severe. As long as a large enough number of mesh points are selected (so that λ_1 converges to 4 decimal places) the errors from this should be small. The greatest issue was in selecting the width of the integration boundary to include all possible patch sizes. In particular in selecting the lower boundary (See Chapter 6).

The issue of modelling fragmentation is the same in both the IPM and PPM methods. The process is poorly understood on a patch scale and modelling techniques are the best currently available. It has resulted in a possible over-estimation of the fragmentation contribution in the PPM compared to the IPM (Chapter 5).

RQ4: How well do the results of different projection models compare?

In direct comparison the IPMs and PPMs allowed similar conclusions to be drawn for a given hypothesis (See Chapter 5). Previous research stated that there should be a close resemblance of results between PPMs and IPMs (Easterling et al., 2000), but this was not found here. As discussed in Chapter 5, this could result from the modelling of fragmentation in the two models. The greater complexity of modelling techniques in the IPM should more accurately capture the dynamics than the PPM.

The size of the data set could also account for the difference, with IPMs better able to capture the dynamics for small data sets (Ramula et al., 2009).

The transient dynamics of IPMs and PPMs have not previously been compared. It was found that there was a greater difference in the results than observed in the asymptotic dynamics (Chapter 5). Some transient results of the IPMs are as a direct result of the modelling methods, but as IPMs are primitive, these results are more accurate than those from the PPM, which are affected by reducibility. Further research should aim to transfer the transient bounds from PPM analysis (Townley et al., 2007; Stott et al., 2010a) to IPM analysis.

11.2.2 Research Objective Two: Analysis

RQ5: What current methods of analysis exist?

Methods of analysis for the IPM and PPM are given in Chapter 3. It was shown that, post numerical integration, the IPM and PPM can be analyzed in a very similar fashion. The main difference was in the analysis of transient dynamics where techniques for IPMs were less well developed. Due to reducibility of PPMs, the analysis of IPMs should be more accurate and their greater complexity gives greater detail to the possible dynamics.

Projection modelling is particularly well suited to projecting populations into the future. This allows investigation into interactions of one or more models (for example Chapter 9). This has been carried out on PPMs in the past (Hughes, 1984), but is better suited to the IPM, where a greater number of size classes gives greater detail into possible behaviour.

RQ6: Does initial trauma following a hurricane effect the dynamics of a population?

It was shown in Chapters 4 and 5 that the initial trauma experienced by a coral patch affected the long term and short term dynamics of the population. The more severe the initial trauma, the greater the asymptotic decline. In the first 200 months it was those patches, neither the least not the most affected, which were projected to fair better. The weakest trauma leads to a greater range of coral patch sizes, with populations under the severest trauma being dominated by small patches. Finally, in transient time there are greater extremes of possible behaviour with increased trauma.

In Chapter 6, it was explained that patches are more likely to survive future disturbances, if it is dominated by larger patches. This meant that the long-term dynamics was determined by initial trauma, but also the ability of the population to withstand future disturbances was also determined by initial trauma, as populations experiencing the weakest trauma contained the largest patches.

The picture painted in this study is one of a worst case scenario. All populations, regardless of initial trauma, are in severe decline. This could be the result of other stresses on the reef inhibiting the ability of the reef to recover from a disturbance, for example over-fishing or coral bleaching. This, alongside the fact that reefs have been shown to require at least 8 years to recover from a hurricane (Gardner et al., 2005), meant that recovery was not captured in this Thesis. In spite of this, it does not alter the conclusion that initial trauma does affect the dynamics exhibited.

RQ7: Do the dynamics exhibited during a hurricane vary with hurricane strength?

It was shown in Chapter 7 that a strong hurricane severely damages a population. It was also shown that a population under a weak hurricane faired better than a

hurricane under no hurricane. This was counter-intuitive and could be explained by the lack of recovery captured in the model.

It was also found that strong hurricanes increased the rates of fragmentation and decreased rates of survival, but that regardless of hurricane strength, larger patches are more likely to survive or fragment than smaller patches.

As it is rare for two hurricanes to strike the reef in two consecutive years, transient dynamics are a better indicator of behaviour than asymptotic dynamics. It showed a similar picture with greater transient attenuation in A_{Strong}, but similar levels for both A_{Weak} and A_{No}.

It has been accepted that hurricanes can benefit coral populations on a reef scale by creating free space for coral to colonize and destroying more abundant species which in turn increases biodiversity. However, it has never previously been shown at a patch scale.

RQ8: What are the best management strategies for a $Montastraea\ annularis$ population?

Management strategies for $M.\ annularis$ are easier to capture using IPMs than with PPMs. This is because individual biological functions can be perturbed, as opposed to PPMs, where groups of biological functions are perturbed together. Through mathematical modelling, it is possible to suggest areas that should be targeted by managers. It was found that management of one function alone would not promote population growth, but two functions needed to be managed to reduce the asymptotic decline by a greater amount. The aim of management strategies was to not only increase the population growth rate, but also to increase the size of patches in the population. This was because larger patches are more likely to survive future disturbances.

It was found that the best strategies were to either target the mean growth, whilst reducing the probability of fragmentation, or to increase the number of

fragments at the same time as decreasing the size of these fragments. The first strategy could be achieved through the positioning of marine parks and no-take zones, which will increase the density of grazers, such as parrot fishes, in turn decreasing algae cover and providing free space for coral patches. It remains unclear how managers could achieve the second strategy.

It is important that there is an increase in coordination between managers, who are trying to manage the population from different threats. Managing against the threat of hurricanes alone will not save the population.

11.2.3   Research Objective Three: Climate Change

RQ9: How does a change in hurricane activity effect projection of population dynamics?

In 2007, the IPCC report stated that with an increase in global temperature, it is likely that hurricanes will increase in intensity and duration (IPCC, 2007). By projecting the coral population and increasing intensity from its current rate on Glovers Reef, the extinction time decreased on the reef by 6.3 years (Chapter 9).

Recovery was not captured in these models with the population in decline even in years between hurricanes. Caribbean reefs are in decline and, therefore, decline on the reefs between hurricanes is to be expected, but if the reefs are to survive past 45 years, recovery must be achieved on the reefs.

RQ10: Will management improve the projected population dynamics under climate change?

Two management strategies suggested in Chapter 8 were to either target mean growth and reduce fragmentation or to focus on managing fragments. It has been shown that, even with management, increasing intensity of hurricanes will still decrease the extinction time on the reef and that management will increase the ex-

tinction time of the population. On average, management increased the extinction time by 11 years if managing growth, but, if managing fragments, extinction will not be reached within 45 years (Chapter 9).

It is important that the right metric is used in measuring population size. Population density often gave a misleading picture. It failed to capture the size of patches or partial mortality of patches following a hurricane. Total area on a reef is a better metric and often showed transient growth in total area in periods of calm. This showed that there is some hope for a *M. annularis* population; if management on reefs can be successful then a significant area of *M. annularis* can remain after 45 years, even with increased hurricane intensity.

One interesting result was that to exploit total area transients, management targeting mean growth required a Category 5 hurricanes to occur at an increasing rate. Otherwise, the initial transient growth tails off and decline is recaptured on the reef (Chapter 9).

11.3 Research Contribution

The aim of this research was to not just explain what happened through the time period that the data was collected, but to also use this information to project possible future behaviour. In this, my research has contributed in three main ways:

- It advances modelling techniques by promoting the use of Integral Projection Models (IPMs) for coral populations. IPMs have never, to my knowledge, been used to model coral populations, but instead have been applied to plant or tree populations. As IPMs are a better alternative to Population Projection Matrices, when the behaviour of an individual is determined by its size, it seems natural to use IPMs on coral populations. This has involved developing the IPM framework to include the biological process of fragmentation.

It is hoped that this research will encourage coral reef ecologists to use IPMs, ahead of PPMs to model populations in the future.

- The research lies at the interface between climate change, hurricanes and coral reefs. This research takes into account the possible effects of climate change on hurricane activity in the Caribbean and simulates what the effect would be on coral patch cover. It is important to understand the range of possible behaviour that coral patches could exhibit, in order to inform future management strategies.

- It has investigated the impact of hurricanes on *Montastraea annularis* at a patch scale. It has shown that initial trauma determines the dynamics of a patch and also that the strength of the hurricane also affects the dynamics. It showed that, regardless of hurricane strength or initial trauma, that larger patches survive disturbances better, but are also more likely to fragment.

11.4 Recommendations for Future Research

There are two main areas where further research is needed to develop the results of this Thesis. Firstly, better understanding of the biological process of fragmentation at the patch scale is required, if there are to be improvements in the fitting of an Integral Projection Model to coral patch populations. It would also be useful if IPMs were applied to a greater variety of coral species to develop further techniques for analysis. It is also important that transient bounds are developed for the analysis of IPMs further. It has been shown in this Thesis that it is unlikely that a population will ever reach asymptotic dynamics and so the transient analysis is vital to understanding the future behaviour of a coral patch population.

Finally, future research should aim to look at the synergistic effects of climate change on reef-building corals. The impact of climate change on hurricanes is just

one area in which coral reefs will be affected. It is important that future research aims at combining the impact of hurricanes, alongside the decreasing resilience of coral reefs to disturbances and the increasing risk of coral bleaching and coral disease.

11.5 Conclusion

In this Thesis, Population Projection Matrices and Integral Projection Models have been used to analyze the data set from Glovers Reef. They have been used to investigate the behaviour exhibited by the population (Chapters 4, 5 and 7), as well as to project future possible behaviour under both climate change and management (Chapters 8 and 9). The results of this Thesis have been summarized above and show that projection models are required, if the underlying dynamics on a reef are to be fully understood.

Bibliography

W.H. Adey. Coral Reef Morphogenesis: A Multidimensional Model. *Science*, 202: 831–837, 1978.

G.W. Allison, S.D. Gaines, J. Lubchenco, and H.P. Possingham. Ensuring Persistence of Marine Reserves: Catastrophes Require Adopting an Insurance Factor. *Ecological Applications*, 13:S8–S24, 2003.

R.B. Aronson and W.F. Precht. Conservation, Precaution and Caribbean Reefs. *Coral Reefs*, 25:441–450, 2006.

R.G. Barry and R.J. Chorley. *Atmosphere, Weather and Climate*. Routledge, New York, 2003.

Belize National Meteorological Service. Historical storms, July 2010. URL `http://www.hydromet.gov.bz/Historical_Storms.html`.

D.R. Bellwood, T.P. Hughes, C. Folke, and M. Nystrom. Confronting the Coral Reef Crisis. *Nature*, 429:827–833, 2004.

A. Berman and R.J. Plemmons. *Nonnegative matrices in the Mathematical Sciences*. Society for Industrial and Applied Mathematics, Philadelphia, Pennsylvania, USA, 1994.

C. Birkeland. Introduction. *Life and Death of Coral Reefs*, pages 1–10, 1997.

B.E. Brown. Coral Bleaching: Causes and Consequences. *Coral Reefs*, 16:S129–S138, 1997.

H.R. Burgess. Matrix Projection Modelling of a Caribbean Reef-Building Coral Montastraea annularis. MMath Project, 2008. SECAM, University of Exeter.

J.C. Bythell, E.H. Gladfelter, and M. Bythell. Chronic and Catastrophic Natural Mortality of 3 Common Caribbean Reef Corals. *Coral Reefs*, 12:143–152, 1993.

R.C. Carpenter. Mass Mortality of a Caribbean Sea-Urchin - Immediate Effects on Community Metabolism and Other Herbivores. *Proceedings of the National Academy of Sciences of the United States of America*, 85:511–514, 1988.

H. Caswell. Prospective and Retrospective Perturbation Analyses: Their Roles in Conservation Biology. *Ecology*, 81:619–627, 2000.

H. Caswell. *Matrix Population Models: Construction, Analysis and Interpretation.* Sinauer Associates Inc. Publishers, Sunderland, Massachusetts, 2001.

H. Caswell and M.G. Neubert. Reactivity and Transient Dynamics of Discrete-Time Ecological Systems. *Journal of Difference Equations and Applications*, 11: 295–310, 2007.

D.Z. Childs, M. Rees, K.E. Rose, P.J. Grubb, and S.P. Ellner. Evolution of Complex Flowering Strategies: An Age- and Size-Structured Integral Projection Model. *Proceedings: Biological Sciences*, 270:1829–1838, 2003.

D.Z. Childs, M. Rees, K.E. Rose, P.J. Grubb, and S.P. Ellner. Evolution of Size-Dependent Flowering in a Variable Environment: Construction and Analysis of a Stochastic Integral Projection Model. *Proceedings: Biological Sciences*, 271: 425–434, 2004.

S.L. Coles and E.K. Brown. Twenty-five Years of Change in Coral Coverage on a Hurricane Impacted Reef in Hawai'i: The Importance of Recruitment. *Coral Reefs*, 26:705–717, 2007.

J.H. Connell. Diversity in Tropical Rain forests and Coral Reefs. *Science*, 199: 1302–1310, 1978.

J.H. Connell. Disturbance and Recovery of Coral Assemblages. *Coral Reefs*, 16: S101–S113, 1997.

J.H. Connell, T.P. Hughes, and C.C. Wallace. A 30-year Study of Coral Abundance, Recruitment, and Disturbance at Several Scales in Space and Time. *Ecological Monographs*, 67:461–488, 1997.

M.J.C. Crabbe, E. Martinez, C. Garcia, J. Chub, L. Castro, and J. Guy. Growth Modelling Indicates Huricane and Severe Storms are Linked to Low Coral Recruitment in the Caribbean. *Marine Environmental Research*, 65:364–368, 2008.

K.R. Crooks, M.A. Sanjayan, and D.F. Doak. New Insights on Cheetah Conservation through Demographic Modeling. *Conservation Biology*, 12:889–895, 1998.

W.P. Cropper Jr. and D. Di Resta. Simulation of a Biscayne Bay, Florida Commercial Sponge Population: Effects of Harvesting after Hurricane Andrew. *Ecological Modelling*, 118:1–15, 1999.

D.T. Crouse, L.B. Crowder, and H. Caswell. A Stage-Based Population-Model for Loggerhead Sea-Turtles and Implications for Conservation. *Ecology*, 68:1412–1423, 1987.

J.P. Dahlgren and J. Ehrlen. Linking Environmental Variation to Population Dynamics of a Forest Herb. *Journal of Ecology*, 97:666–674, 2009.

C. Darwin. *The Structure and Distribution of Coral Reefs*. The University Arizona Press, 1842.

E. Dietzenbacher. *Chapter 12: a limiting property for the powers of a reducible, nonnegative matrix. Perturbations and eigenvectors: essays.* PhD thesis, 1991.

D. Doak, P. Kareiva, and B. Klepetka. Modeling Population Viability for the Desert Tortoise in the Western Mojave Desert. *Ecological Applications*, 4:446–460, 1994.

D.F. Doak, K. Gross, and W.F. Morris. Understanding and Predicting the Effects of Sparse Data on Demographic Analyses. *Ecology*, 86:1154–1163, 2005.

S.J. Dollar. Wave Stress and Coral Community Structure in Hawaii. *Coral Reefs*, 1:71–81, 1982.

T.J. Done. Phase Shifts in Coral Reef Communities and their Ecological Significance. *Hydrobiologia*, 247:121–132, 1992.

J.P. Donnelly and J.D. Woodruff. Intense Hurricane Activity Over the Past 5000 Years Controlled by El Nino and the West African Monsoon. *Nature*, 447:465–468, 2007.

S.E. Dudas, J.F. Dower, and B.R. Anholt. Invasion Dynamics of the Varnish Clam (*Nuttallia obscurata*): A Matrix Demographic Modelling Approach. *Ecology*, 88:2084–2093, 2007.

E.A. Eager, R. Rebarber, and B. Tenhumberg. Choice of Density-Dependent Seedling Recruitment Function Affects Predicted Transient Dynamics: A Case Study With Platte Thistle. *Theoretical Ecology*, In Press.

M.R. Easterling, S.P. Ellner, and P.M. Dixon. Size-Specific Sensitivity: Applying a New Structured Population Model. *Ecology*, 81:694–708, 2000.

P.J. Edmunds. Evidence That Reef-Wide Patterns of Coral Bleaching may be the Result of the Distribution of Bleaching Susceptible Clones. *Marine Biology*, 121:137–142, 1994.

P.J. Edmunds and R. Elahi. The Demographics of a 15-year Decline in Cover of the Caribbean Reef Coral *Montastraea annularis*. *Ecological Monographs*, 77:3–18, 2007.

T.P. Eichler. Hurricanes. *Encyclopedia of Climate and Weather*, 1:407–411, 1996.

S.P. Ellner and M. Rees. Integral Projection Models for Species with Complex Demography. *The American Naturalist*, 167:410–428, 2006.

S.P. Ellner and M. Rees. Stochastic Stable Population Growth in Integral Projection Models: Theory and Application. *Journal of Mathematical Biology*, 54: 227–256, 2007.

S.P. Ellner, J. Fieburg, D. Ludwig, and C. Wilcox. Precision of Population Viability Analysis. *Conservation Biology*, 16:1–5, 2002.

J.B. Elsner. Evidence in Support of the Climate Change-Atlantic Hurricane Hypothesis. *Geophysical Research Letters*, 33:L16705, 2006.

J.B. Elsner, J.P. Kossin, and T.H. Jagger. The Increasing Intensity of the Strongest Tropical Cyclones. *Nature*, 455:92–95, 2008.

K. Emanuel. Increasing Destructiveness of Tropical Cyclones Over the Past 30 Years. *Nature*, 436:686–688, 2005.

L. Esparza-Olguin, T. Valverde, and E. Vilchis-Anaya. Demographic Analysis of a Rare Columnar Cactus (*Neobuxbaumia macrocephala*) in the Tehuacan Valley, Mexico. *Biological Conservation*, 103:349–359, 2002.

J. Fieburg and S.P. Ellner. Stochastic Matrix Models for Conservation and Management: A Comparative Review of Methods. *Ecology Letters*, 4:244–266, 2001.

R.A. Fisher. *The Genetical Theory of Natural Selection*. Clarendon Press, Oxford, UK, 1930.

D.A. Fisk and V.J. Harriott. Are Understory Coral Communities Recruitment-Limited? pages 517–520, 1993.

I.J. Fiske, E.M. Bruna, and B.M. Bolker. Effects of Sample Size on Estimates of Population Growth Rates Calculated with Matrix Models. *PLoS ONE*, 3:e3080, 2008.

N.L. Foster. Population Dynamics of the Dominant Caribbean Reef-Building Coral, Montastraea annularis. PhD Thesis, 2007. University of Exeter.

N.L. Foster, I.B. Baums, and P.J. Mumby. Sexual vs. Asexual Reproduction in an Ecosystem Engineer: the Massive Coral *Montastraea annularis*. *Journal of Animal Ecology*, 76:384–391, 2007.

G. Frobenius. Uber Matrizen aus Nicht-Neativen Elementen. *Sitzungsberichte der Berliner Akademie der Wissenschaften*, pages 456–477, 1912.

F.R. Gantmacher. *Matrix Theory*. Chelsea Publishing Company, New York, New York, USA, 1959.

T.A. Gardner, I.M. Cote, J.A. Gill, A. Grant, and A.R. Watkinson. Long-Term Region-Wide Declines in Caribbean Corals. *Science*, 301:958–960, 2003.

T.A. Gardner, I.M. Cote, J.A. Gill, A. Grant, and A.R. Watkinson. Hurricanes and Caribbean Coral Reefs: Impacts, Recovery Patterns, and Role in Long-Term Decline. *Ecology*, 86:174–184, 2005.

J.P. Gilmour. Size-structures of Populations of the Mushroom Coral *Fungia fungites*: the Role of Disturbance. *Coral Reefs*, 23:493–504, 2004.

P.W. Glynn. Ecology of a Caribbean Coral Reef, the *Porites* Reef Flat Biotope - Part 1: Meteorology and Hydrography. *Marine Biology*, 20:297–318, 1973.

P.W. Glynn. Coral-Reef Bleaching - Ecological Perspectives. *Coral Reefs*, 12:1–17, 1993.

P.W. Glynn and L. D'Croz. Experimental-Evidence For High-Temperature Stress As The Cause Of El-Nino-Coincident Coral Mortality. *Coral Reefs*, 8:181–191, 1990.

H.C.J. Godfray and M. Rees. Population Growth Rates: Issues and an Application. *Philisophical Transactions of the Royal Society of London B*, 357:1307–1319, 2002.

S.B. Goldenberg, C. Landsea, A.M. Mestas-Nunex, and W.M. Gray. The Recent Increase in Atlantic Hurricane Activity. *Science*, 293:474–479, 2001.

N.A.J. Graham, K.L. Nash, and J.T. Kool. Coral Reef Recovery Dynamics in a Changing World. *Coral Reefs*, 30:283–294, 2011.

R.R. Graus and I.G. Macintyre. *A Quantitative Evaluation of Growth Response to Light Distribution using Computer Simulation*, volume 12, chapter Variation in growth forms of the reef coral Montastrea annularis. Smithsonian Press, 1982.

R.R. Grauss, I.G. Macintyre, and B.E. Herchenroder. Computer Simulation of the Reef Zonation at Discovery Bay, Jamaica: Hurricane Disruption and Long-Term Physical Oceanographic Controls. *Coral Reefs*, 3:59–68, 1984.

K. Gross, W.F. Morris, M.S. Wolosin, and D.F. Doak. Modelling Vital Rates Improves Estimation of Population Projection Matrices. *Population Ecology*, 48: 79–89, 2006.

A. Halford, A.J. Cheal, D. Ryan, and D.M. Williams. Resilience to Large Scale Disturbance in Coral and Fish Assemblages on the Great Barrier Reef. *Ecology*, 85:1892–1905, 2004.

M.L. Harmelin-Vivien. The Effects of Storms and Cyclones on Coral Reefs: A Review. *Journal of Coastal Research*, 12:211–231, 1994.

A. Hastings, R.J. Hall, and C.M. Taylor. A Simple Approach to Optimal Control of Invasive Species. *Theoretical Population Species*, 70:431–435, 2006.

J.P. Hawkins and C.M. Roberts. Effects of Artisanal Fishing on Caribbean Coral Reefs. *Conservation Biology*, 18:215–226, 2004.

A. Henderson-Sellers, H. Zhang, G. Berz, K. Emanuel, W. Gray, C. Landsea, G. Holland, J. Lighthill, S-L. Shieh, P. Webster, and K. McGuffie. Tropical Cyclones and Global Climate Change: A Post-IPCC Assessment. *Bulletin of the American Meteorological Society*, 79:19–38, 1998.

E. Hesse, M. Rees, and H. Muller-Scharer. Life-History Variation in Contrasting Habitats: Flowering Decisions in a Clonal Perennial Herb (*Veratrum album*). *American Naturalist*, 172:E196–E213, 2008.

D. Hodgson, S. Townley, and D. McCarthy. Robustness: Predicting the Effects of Life History Perturbations on Stage-Structured Population Dynamics. *Theoretical Population Biology*, 70:214–224, 2006.

D.J. Hodgson and S. Townley. Linking Management Changes to Population Dynamic Responses: The Transfer Function of a Projection Matrix Perturbation. *Journal of Applied Ecology*, 41:1155–1161, 2004.

O. Hoegh-Guldberg. Climate Change, Coral Bleaching and the Future of the World's Coral Reefs. *Marine Freshwater Research*, 50:839–866, 1999.

O. Hoegh-Guldberg. Coral Reefs in a Century of Rapid Environmental Change. *Symbiosis*, 37:1–31, 2004.

G.J. Holland and P.J. Webster. Heightened Tropical Cyclone Activity in the North Atlantic: Natural Variability or Climate Trend? *Phil. Trans. Royal Soc. A*, 365: 2695–2716, 2007.

R.A. Horn and C.R. Johnson. *Matrix Analysis.* Cambridge University Press, Cambridge, UK, 1985.

D.K. Hubbard. Reefs as Dynamic Systems. *Life and Death of Coral Reefs*, pages 43–67, 1997.

D.K. Hubbard, K.M. Parsons, J.C. Bythell, and N.D. Walker. The Effects of Hurricane Hugo on the Reefs and Associated Environments of St. Croix, US Virgin Islands - A Preliminary Assessment. *Journal of Coastal Research*, 8: 33–48, 1991.

T.P. Hughes. Population Dynamics Based on Individual Size Rather than Age: A General Model with a Reef Coral Example. *The American Naturalist*, 123: 778–795, 1984.

T.P. Hughes. Community Structure and Diversity of Coral Reefs: The Role of History. *Ecology*, 70:275–279, 1989.

T.P. Hughes. Catastrophes, Phase Shifts and Large Scale Degradation of a Caribbean Coral Reef. *Science*, 265:1547–1551, 1994.

T.P. Hughes and J.H. Connell. Population Dynamics Based on Size or Age? A Reef-Coral Analysis. *The American Naturalist*, 129:818–829, 1987.

T.P. Hughes and J.H. Connell. Multiple Stressors on Coral Reefs: A Long-term Perspective. *Limnology and Oceanography*, 44:932–940, 1999.

T.P. Hughes and J.B.C. Jackson. Population Dynamics and Life Histories of Foliaceous Corals. *Ecological Monographs*, 55:141–166, 1985.

T.P. Hughes and J.P. Tanner. Recruitment Failure, Life Histories and Long-term Decline of Caribbean Corals. *Ecology*, 81:2250–2263, 2000.

T.P. Hughes, D.C. Reed, and M.J. Boyle. Herbivory on Coral Reefs: Community Structure Following Mass Mortalities of Sea Urchins. *Journal of Experimental Marine Biology and Ecology*, 113:39–59, 1987.

T.P. Hughes, A.H. Baird, D.R. Bellwood, M. Card, S.R. Connolly, C. Folke, R. Grosberg, O. Hoegh-Guldberg, J.B.C. Jackson, J. Kelypas, J.M. Lough, P. Marshall, M. Nystrom, S.R. Palumbi, J.M. Pandolfi, B. Rosen, and J. Roughgarden. Climate Change, Human Impacts, and the Resilience of Coral Reefs. *Science*, 301:929–933, 2003.

T.P. Hughes, M.J. Rodrigues, D.R. Bellwood, D. Ceccarelli, O. Hoegh-Guldberg, L. McCook, N. Moltschaniwskyj, M.S. Pratchett, R.S. Steneck, and B. Willis. Phase Shifts, Herbivory, and the Resilience of Coral Reefs to Climate Change. *Current Biology*, 17:360–365, 2007.

IPCC. *Climate Change 2007: The Physical Science Basis. Contribution of Working Group I to the Fourth Assessment Report of the Intergovernmental Panel on Climate Change.* 2007.

J.B.C. Jackson. Reefs Since Columbus. *Coral Reefs*, 16:S23, 1997.

J.B.C. Jackson. What was Natural in the Coastal Oceans? *Proceedings of the National Academy of Sciences of the United States of America*, 98:5411–5418, 2001.

J.B.C. Jackson, M.X. Kirby, W.H. Berger, K.A. Bjorndal, L.W. Botsford, B.J. Bourque, R.H. Bradbury, R. Cooke, J. Erlandson, J.A. Estes, T.P. Hughes, S. Kidwell, C.B. Lange, H.S. Lenihan, J.M. Pandolfi, C.H. Peterson, R.S. Ste-

neck, M.J. Tegner, and R.R. Warner. Historical Overfishing and the Recent Collapse of Coastal Ecosystems. *Science*, 293:629–638, 2001.

R.E. Johannes. Traditional Coral Reef Fisheries Management. *Life and Death of Coral Reefs*, pages 380–385, 1997.

E. Jongejans, K. Shea, O. Skarpaas, D. Kelly, and S.P. Ellner. Importance of Individual and Environmental Variation for Invasive Species Spread: A Spatial Integral Projection Model. *Ecology*, 92:86–97, 2011.

P. Kareiva, M. Marvier, and M. McClure. Recovery and Management Options for Spring/Summer Chinook Salmon in the Columbia River Basin. *Science*, 290: 977–979, 2000.

K.M. Klemow and D.J. Raynal. Demography of Two Facultative Biennial Plant Species in an Unproductive Habitat. *The Journal of Ecology*, 73:147–167, 1985.

N. Knowlton. Thresholds and Multiple Stable States in Coral Reef Community Dynamics. *American Zoology*, 32:674–682, 1992.

N. Knowlton. The Future of Coral Reefs. *Proceedings of the National Academy of Science, USA*, 98:5419–5425, 2001.

N. Knowlton, J.C. Lang, M.C. Rooney, and P. Clifford. Evidence for Delayed Mortality in Hurricane-Damaged Jamaican Staghorn Corals. *Nature*, 294:251–252, 1981.

N. Knowlton, J.C. Lang, and B.D. Kellar. Case Study of Natural Population Collapse: Post-Hurricane Predation on Jamaican Staghorn Corals. *Smithsonian Contribution to Marine Science*, 31:1–25, 1990.

T.R. Knutson, J.L. McBride, J. Chan, G. Holland, C. Landsea, I. Held, J.P. Kossin, A.K. Srivastava, and M. Sugi. Progress article: Tropical Cyclones and Climate Change. *Nature Geoscience*, 3:157–163, 2010.

K. Koop, D. Booth, A. Broadbent, J. Brodie, D. Bucher, D. Capone, J. Coll, W. Dennison, M. Erdmann, P. Harrison, O. Hoegh-Guldberg, P. Hutchings, G.B. Jones, A.W.D. Larkum, and J. O'Neil. ENCORE: The Effect of Nutrient Enrichment on Coral Reefs. Synthesis of Results and Conclusions. *Marine Pollution Bulletin*, 42:91–120, 2001.

M. Kot. Discrete-Time Travelling Waves: Ecological Examples. *Journal of Mathematical Biology*, 30:413–436, 1992.

M. Kot and W.M. Schaffer. Discrete-Time Growth-Dispersal Models. *Mathematical Biosciences*, 80:109–136, 1986.

M. Kot, M.A. Lewis, and P. van den Driessche. Dispersal Data and the Spread of Invading Organisms. *Ecology*, 77:2027–2042, 1996.

H.O. Kreiss. Uber die stabilitatsdefinition fur differenzengleichungen die partielle differentialgleichungen approximieren. *BIT*, 2:153–181, 1962.

P. Kuss, M. Rees, H. Hanna Egisdottir, S.P. Ellner, and J. Stocklin. Evolutionary Demography of Long-Lived Monocarpic Perennials: A Time-Lagged Integral Projection Model. *Journal of Ecology*, 96:821–832, 2008.

H.R. Lasker. Population Growth of a Gorgonian Coral: Equilibrium and Non-Equilibrium Sensitivity in Life History Variables. *Oecologia*, 86:503–509, 1991.

L.P. Lefkovitch. The Study of Population Growth in Organisms Grouped by Stages. *Biometrics*, 21:1–18, 1965.

P.H. Leslie. On the Use of Matrices in Certain Population Mathematics. *Biometrika*, 33:183–212, 1945.

M.P. Lesser. Oxidative Stress Causes Coral Bleaching During Exposure to Elevated Temperatures. *Coral Reefs*, 16:187–192, 1997.

H.A. Lessios. Mass Mortality of *Diadema antillarum* in the Caribbean: What have we Learned? *Annual Review of Ecology and Systematics*, 19:371–393, 1988.

H.A. Lessios, D.R. Robertson, and J.D. Cubit. Spread of *Diadema* Mass Mortality Through the Caribbean. *Science*, 226:335–337, 1984.

W.D. Liddell and S.L. Ohlhorst. Ten Years of Disturbance and Change on a Jamaican Fringing Reef. In *Proceedings of 7th International Coral Reef Symposium*, pages 144–150, 1993.

C. Linares, D.F. Doak, R. Coma, D. Diaz, and M. Zabala. Life History and Viability of a Long-Lived Marine Invertebrate: the octocoral *Paramauricea clavata*. *Ecology*, 88:918–928, 2007.

D. Ludwig. Is it Meaningful to Estimate a Probability of Extinction? *Ecology*, 8: 298–310, 1999.

A.E. Lugo, C.S. Rogers, and S.W. Nixon. Hurricanes, Coral Reefs and Rainforests: Resistence, Ruin and Recovery in the Caribbean. *Ambio*, 29:106–114, 2000.

A. Lugo-Fernandez and M. Gravois. Understanding Impacts of Tropical Storms and Hurricanes on Submerged Bank Reefs and Coral Communities in the Northwestern Gulf of Mexico. *Continental Shelf Research*, 30:1226–1240, 2010.

D.P. Manzanello, M. Brandt, T.B. Smith, D. Lirman, J.C. Hendee, and R.S. Nemeth. Hurricanes Benefit Bleached Corals. In *Proceedings of the National Academy of Sciences*, 2007.

T.R. McClanahan, N.A. Muthiga, and S. Mangi. Coral and Algal Changes After the 1998 Coral Bleaching: Interaction With Reef Management and Herbivores on Kenyan Reefs. *Coral Reefs*, 19:380–391, 2001.

T.R. McClanahan, M.J. Marnane, J.E. Cinner, and W.E. Kiene. A Comparison of Marine Protected Areas and Alternative Approaches to Coral-Reef Management. *Current Biology*, 16:1408–1413, 2006.

L.J. McCook. Macroalgae, Nutrients and Phase Shifts on Coral Reefs: Scientific Issues and Management Consequences for the Great Barrier Reef. *Coral Reefs*, 18:357–367, 1999.

L.J. McCook, J. Jompa, and G. Diaz Pulido. Competition Between Corals and Algae on Coral Reefs: a Review of Evidence and Mechanisms. *Coral Reefs*, 19: 400–417, 2001.

C.S. McFadden. A Comparative Demographic-Analysis of Clonal Reproduction in a Temperate Soft Coral. *Ecology*, 72:1849–1866, 1991.

J.W. McManus and J.F. Polsenberg. Coral-Algal Phase Shifts on Coral Reefs: Ecological and Environmental Aspects. *Progress in Oceanography*, 60:263–279, 2004.

J.W. McManus, L.A.B. Menez, K.N. Kesner-Reyes, S.G. Vergara, and M.C. Ablan. Coral Reef Fishing and Coral-Algal Phase Shifts: Implications for Global Reef Status. *Ices Journal Of Marine Science*, 57:572–578, 2000.

C.J.E. Metcalf, C.C. Horvitz, S. Tuljapurkar, and D.A. Clark. A Time to Grow and a Time to Die: a New Way to Analyze the Dynamics of Size, Light, Age and Death of Tropical Trees. *Ecology*, 90:2766–2778, 2009.

T.E.X. Miller, S.M. Louda, K.A. Rose, and J.O. Eckberg. Impacts of Insect Herbivory on Cactus Population Dynamics: Experimental Demography Across an Environmental Gradient. *Ecological Monographs*, 79:155–172, 2009.

K.A. Moloney. A Generalized Algorithm for Determining Category Size. *Oecologia*, 69:179–180, 1986.

G. Muller and C.F. D'Elia. Interactions Between Coral and Their Symbiotic Algae. *Life and Death of Coral Reefs*, pages 96–113, 1997.

P.J. Mumby and A.R. Harbourne. Marine Reserves Enhance the Recovery of Corals on Caribbean Reefs. *PLoS ONE*, 5:E8657, 2010.

P.J. Mumby, N.L. Foster, and E.A.G. Fahy. Patch Dynamics of Coral Reef Macroalgae under Chronic and Acute Disturbance. *Coral Reefs*, 24:681–692, 2005.

P.J. Mumby, C.P. Dahlgren, A.R. Harborne, C.V. Kappel, F. Micheli, D.R. Brumbaugh, K.E. Holmes, J.M. Mendes, K. Broad, J.N. Sanchirico, K. Buch, S. Box, R.W. Stoffle, and A.B. Gill. Fishing, Trophic Cascades, and the Process of Grazing on Coral Reefs. *Science*, 311:98–101, 2006a.

P.J. Mumby, J.D. Hedley, K. Zychaluk, A.R. Harborne, and P.G. Blackwell. Revisiting the Catastrophic Die-Off of the Urchin *Diadema antillarum* on Caribbean Coral Reefs: Fresh Insights on Resilience from a Simulation Model. *Ecological Modelling*, 196:131–148, 2006b.

P.J. Mumby, A. Hastings, and H.J. Edwards. Thresholds and the Resilience of Caribbean Coral Reefs. *Nature*, 450:98–101, 2007.

O. Naim, P. Chabanet, T. Done, C. Tourrand, and Y. Letourneur. Regeneration of a Reef Flat Ten Years After the Impact of the Cyclone Firinga (Reunion, SW Indian Ocean. *Proceedings 9th International Coral Reef Symposium,Bali, Indonesia*, 2000.

M.G. Neubert, M. Kot, and M.A. Lewis. Dispersal and Pattern-Formation in a Discrete-Time Predator-Prey Model. *Theoretical Population Biology*, 48:7–43, 1995.

C.J. Neumann, G.W. Cry, F.L. Caso, and B.R. Jarvinen. *Tropical Cyclones of the*

North Atlantic Ocean, 1871-1980. NOAA Special Publication, National Hurricane Center, 1985.

NOAA. NOAA: Why are Coral Reefs so Important?, August 2011. URL `http://www.celebrating200years.noaa.gov/foundations/coral/side.html`.

NOAA. How do tropical cyclones form?, July 2011. URL `http://www.aoml.noaa.gov/hrd/tcfaq/A15.html`.

M.M. Nugues and R.P.M. Bak. Differential Competitive Abilities Between Caribbena Coral Species and a Brown Alga: A Year of Experiments and A Long-Term Perspective. *Marine Ecology - Progress Series*, 315:75–86, 2006.

M. Nystrom, C. Folke, and F. Moberg. Coral Reef Disturbance and Resilience in a Human-Dominated Environment. *Trends in Ecology and Evolution*, 15:413–417, 2006.

T.G. O'Connor. The Influence of Rainfall and Grazing on the Demography of some African Savanna Grasses - A Matrix Modelling Approach. *Journal of Applied Ecology*, 30:119–132, 1993.

J.C. Ogden, R.A. Brown, and N. Salesky. Grazing by Echinoid *Diadema antillarum* Philippi - Formation of Halos Around West-Indian Patch Reefs. *Science*, 182:715–717, 1973.

K. Oouchi, J. Yoshimura, H. Yoshimura, R. Mizuta, S. Kusunoki, and A. Noda. Tropical Cyclone Climatology in a Global-Warming Climate as Simulated in a 20km-mesh Global Atmospheric Model: Frequency and Wind Intensity Analyses. *Journal of the Meteorological Society of Japan*, 84:259–276, 2006.

J.M. Pandolfi and J.B.C. Jackson. Broad-Scale Patterns in Pleistocene Coral Reef Communities for the Caribbean: Implications for Ecology and Management.

In *Geological Approaches to Coral Reef Ecology: Placing the Current Crisis in Histroical Context*, pages 201–236. Springer-Verlag, 2007.

J.M. Pandolfi, R.H. Bradbury, E. Sala, T.P. Hughes, K.A. Bjorndal, R.G. Cooke, D. McArdle, L. McClenachan, M.J.H. Newman, G. Paredes, R.R. Warner, and J.B.C. Jackson. Global Trajectories of the Long-Term Decline of Coral Reef Ecosystems. *Science*, 301:955–958, 2003.

J.M. Pandolfi, J.B.C. Jackson, N. Baron, R.H. Bradbury, H.M. Guzman, T.P. Hughes, C.V. Kappel, F. Micheli, J.C. Ogden, H.P. Possingham, and E. Sala. Are U.S. Coral Reef's on the Slippery Slope to Slime. *Science*, 307:1725–1726, 2005.

O. Perron. Jacobisher Kettenbruchalgorithmus. *Mathematische Annalen*, 64:1–76, 1907a.

O. Perron. Uber Matrizen. *Mathematische Annalen*, 64:248–263, 1907b.

P.S. Petraitis and S.R. Dudgeon. Detection of Alternative States in Marine Communities. *Journal of Experimental Biology and Ecology*, 300:343–371, 2004.

M.V. Price and P.A. Kelly. An Age-structured Demographic Model for the Endangered Stephens' Kangaroo Rat. *Conservation Biology*, 8:810–821, 1994.

S. Ramula and K. Lehtila. Matrix Dimensionality in Demographic Analyses of Plants: When to Use Smaller Matrices. *OIKOS*, 111:563–573, 2005.

S. Ramula, M. Rees, and Y.M. Buckley. Integral Projection Models Perform Better for Small Demographic Data Sets than Matrix Population Models: a Case Study of two Perennial Herbs. *Journal of Applied Ecology*, 46:1048–1053, 2009.

M. Rees and S. Ellner. Integral Projection Models for Populations in Temporally Varying Environments. *Ecological Monographs*, 79:575–594, 2009.

M. Rees and K.E. Rose. Evolution of Flowering Strategies in *Oenothera glazioviana*: an Integral Projection Model Approach. *Proceedings of the Royal Society of London Series B-Biological Sciences*, 269:1509–1515, 2002.

H. Renken, P.J. Mumby, I. Matsikis, and H.J. Edwards. Effects of Physical Environmental Conditions on the Patch Dynamics of *Dictyota pulchella* and *Lobophora variegata* on Caribbean Coral Reefs. *Marine Ecology Progress Series*, 403:63–74, 2010.

A.D. Rogers and D.d'A. Laffoley. *International Earth System Expert Workshop on Ocean Stresses and Impacts. Summary Report.* IPSO Oxford, 2011.

C.S. Rogers. Hurricanes and Coral Reefs: The Intermediate Disturbance Hypothesis Revisited. *Coral Reefs*, 12:127–137, 1993.

C.S. Rogers, T.H. Suchanek, and F.A. Pecora. Effects of Hurricanes David and Frederick (1979) on Shallow *acropora palmata* Reef Communities: St. Croix, US Virgin Islands. *Bulletin of Marine Science*, 32:532–548, 1979.

C.S. Rogers, L.N. McLain, and C.R. Tobias. Effects of Hurricane Hugo (1989) on a Coral Reef in St. John, USVI. *Marine Ecology Progress Series*, 78:189–199, 1991.

C.S. Rogers, V. Garrison, and R. Grober-Dunsmore. A Fishy Story about Hurricanes and Herbivory: Seven Years of Research on a Reef in St. John. *8th International Coral Reef Symposium*, 1:555–560, 1997.

K.E. Rose, M. Rees, and P.J. Grubb. Evolution in the Real World: Stochastic Variation and the Determinants of Fitness in *Carlina vulgaris. Evolution*, 56: 1416–1430, 2002.

K.E. Rose, S.M. Louda, and M. Rees. Demographic and Evolutionary Impacts of Native Insect Herbivores on *Cirsium canescens. Ecology*, 86:453–465, 2005.

D. Rosenblatt. On the Graphs and Asymptotic Forms of Finite Boolean Relation Matrices and Stochastic Matrices. *Naval Research Logistics Quarterly*, 4:151–167, 1957.

P.W. Sammarco. Effects of Grazing by *Diadema antillarum* Philippi (Echinodermata, Echinoidea) on Algal Diversity and Community Structure. *Journal of Experimental Marine Biology and Ecology*, 65:83–105, 1982.

M. Scheffer, S. Carpenter, J.A. Foley, C. Folke, and B. Walker. Catastrophic Shifts in Ecosystems. *Nature*, 413:591–596, 2001.

K. Shea and D. Kelly. Estimating Biocontrol Agent Impact with Matrix Models: *Carduus nutuns* in New Zealand. *Ecological Applications*, 8:824–832, 1998.

C.R.C Sheppard, A. Harris, and A.L.S. Sheppard. Archipelago-wide Coral Recovery Patterns Since 1998 in the Chagos Archipelago, Central Indian Ocean. *Marine Ecology Progress Series*, 362:109–117, 2008.

C.R.C. Sheppard, S.K. Davy, and G.M. Pilling. *The Biology of Coral Reefs*. Oxford University Press, Oxford, 2009.

E.A. Shinn. *Coral Reef Recovery in Florida and the Persian Gulf*. Environmental Conservation Department. Shell Oil Company, Houston, Texas, 1972.

R.H. Simpson and H. Riehl. *The Hurricane and its Impact*. Louisiana State University Press, Baton Rouge, 1981.

G.C. Smith and R.C. Trout. Using Leslie Matrices to Determine Wild Rabbit Population Growth and the Potential for Control. *Journal of Applied Ecology*, 31:223–230, 1994.

Y.I. Sorokin. *Coral Reef Ecology*. Springer-Verlag, Heidelberg, 1995.

A.F. Souza and F.R. Martins. Demography of the Clonal Palm *Geonoma brevispatha* in a Neotropical Swamp Forest. *Austral Ecology*, 31:869–881, 2006.

M.D. Spalding, C. Ravilious, and E.P. Green. *World Atlas of Coral Reefs*. University of Calafornia Press, 2001.

K.E. Stokes, J.M. Bullock, and A.R. Wakinson. Population Dynamics Across A Parapatric Range Boundary: *Ulex galli* and *Ulex minor*. *Journal of Ecology*, 92:142–155, 2004.

I. Stott, M. Franco, D. Carslake, S. Townley, and D. Hodgson. Boom or Bust? A Comparative Analysis of Transient Population Dynamics in Plants. *Journal of Ecology*, 98:302–311, 2010a.

I. Stott, S. Townley, D. Carslake, and D.J. Hodgson. On Reducibility and Ergodicity of Population Projection Matrix Models. *Methods in Ecology and Evolution*, 1:242–252, 2010b.

A.M. Szmant. Sexual Reproduction by the Caribbean Reef Corals *Montastraea annularis* and *M cavernosa*. *Marine Ecology - Progress Series*, 74:13–25, 1991.

A.M. Szmant. Nutrient Enrichment on Coral Reefs: Is it a Major Cause of Coral Reef Decline? *Estuaries*, 25:743–766, 2002.

B. Tenhumberg, A.J. Tyre, and R. Rebarber. Model Complexity Affects Transient Population Dynamics Following A Dispersal Event: A Case Study with Pea Aphids. *Ecology*, 90:1878–1890, 2009.

S. Townley and D. Hodgson. Predicting Transient Amplification in Perturbed Ecological Systems. *Journal of Applied Ecology*, 45:1836–1839, 2008.

S. Townley, D. Carslake, O. Kellie-Smith, D. McCarthy, and D. Hodgson. Predicting Transient Amplification in Perturbed Ecological Systems. *Journal of Applied Ecology*, 44:1243–1251, 2007.

E. Treml, M. Colgan, and M. Keevican. Hurricane Disturbance and Coral Reef Development: A Geographical Information System (GIS) Analysis of 501 Years of Hurricane Data from the Lesser Antilles. In *Proceedings of the Eigth International Coral Reef Symposium*, pages 541–546, 1997.

UNEP-WCMC. *In the Frontline: Shoreline Protection and Other Ecosystem Services from Mangroves and Coral Reefs*. UNEP-WCMC Cambridge, UK, 2006.

Scientific United Nations Educational and Cultural Organisation. Belize Barrier Reef Reserve System, August 2011. URL `http:\\www.whc.unesco.org/en/list/764`.

T. Valverde and J. Silvertown. Variation in the Demography of a Woodlan Understorey Herb (*Primula vulgaris*) Along the Forest Regeneration Cycle: Projection Matrix Analysis. *Journal of Ecology*, 86:545–562, 1998.

J. van der Meer. Choosing Category Size in a Stage Projection Matrix. *Oecologia*, 32:79–84, 1978.

P.J. Van Mantgem and N.L. Stephenson. The Accuracy of Matrix Population Model Projection for Coniferous Trees in the Sierra Nevada, California. *Journal of Ecology*, 93:737–747, 2005.

M.J.H. VanOppen and R.D. Gates. Conservation Genetics and the Resilience of Reef-Building Corals. *Molecular Ecology*, 15:3863–3883, 2006.

P.J. Webster, G.J. Holland, J.A. Curry, and H.R. Chang. Changes in Tropical Cyclone Number, Duration and Intensity in a Warming Environment. *Science*, 309:1844–1846, 2005.

P.J. Webster, G.J. Holland, J.A. Curry, and H.R. Chang. Response to Comment on changes in Tropical Cyclone Number, Duration and Intensity in a Warming Environment. *Science*, 311:1713c, 2006.

Wildlife Conservation Society. Glovers reef research station, November 2011. URL `http://programs.wcs.org/gloversreef/Background/tabid/206/Default.aspx`.

J.L. Williams and E.E. Crone. The Impact of Invasive Grasses on the Population Growth of *Anemone patens*, a Long-Lived Native Forb. *Ecology*, 87:3200–3208, 2009.

J.D. Woodley. The Effects of Hurricane Gilbert on Coral Reefs in the Discovery Bay. In *Assessment of the Economic Impacts of Hurricane Gilbert on Coastal and Marine Resources in Jamaica*, pages 77–80. Caribbean Environment Programme, United Nations Environment Program, 1989.

J.D. Woodley. The Incidence of Hurricanes on the North Coast of Jamaica Since 1870: Are the Classic Reef Descriptions Atypical? *Hydrobiologia*, 247:133–138, 1992.

J.D. Woodley, E.A. Chornesky, P.A. Clifford, J.B.C. Jackson, L.S. Kaufman, N. Knowlton, J.C. Lang, M.P. Pearson, J.W. Porter, M.C. Rooney, K.W. Rylaarsdam, V.J. Tunnifliffe, C.M. Wahle, J.L. Wulff, A.S.G. Curtis, M.D. Dallmeyer, B.J. Jupp, M.A.R. Koehl, K. Neigel, and E.M. Sides. Hurricane Allen's Impact on Jamaican Coral Reefs. *Science*, 214:749–755, 1981.

J.T. Wootton and D.A. Bell. A Metapopulation Model of the Peregrine Falcon in California - Viability and Management Strategies. *Ecological Applications*, 2: 307–321, 1992.

P.A. Zuidema, E. Jongejans, P.D. Chien, H.J. During, and F. Schieving. Integral Projection Models for Trees: A New Parametrization Method and a Validation of Model Output. *Journal of Ecology*, 98:345–355, 2010.